Terms and Conditions of Use of Digitised Theses from Trinity College Library Dublin

Copyright statement

All material supplied by Trinity College Library is protected by copyright (under the Copyright and Related Rights Act, 2000 as amended) and other relevant Intellectual Property Rights. By accessing and using a Digitised Thesis from Trinity College Library you acknowledge that all Intellectual Property Rights in any Works supplied are the sole and exclusive property of the copyright and/or other IPR holder. Specific copyright holders may not be explicitly identified. Use of materials from other sources within a thesis should not be construed as a claim over them.

A non-exclusive, non-transferable licence is hereby granted to those using or reproducing, in whole or in part, the material for valid purposes, providing the copyright owners are acknowledged using the normal conventions. Where specific permission to use material is required, this is identified and such permission must be sought from the copyright holder or agency cited.

Liability statement

By using a Digitised Thesis, I accept that Trinity College Dublin bears no legal responsibility for the accuracy, legality or comprehensiveness of materials contained within the thesis, and that Trinity College Dublin accepts no liability for indirect, consequential, or incidental, damages or losses arising from use of the thesis for whatever reason. Information located in a thesis may be subject to specific use constraints, details of which may not be explicitly described. It is the responsibility of potential and actual users to be aware of such constraints and to abide by them. By making use of material from a digitised thesis, you accept these copyright and disclaimer provisions. Where it is brought to the attention of Trinity College Library that there may be a breach of copyright or other restraint, it is the policy to withdraw or take down access to a thesis while the issue is being resolved.

Access Agreement

By using a Digitised Thesis from Trinity College Library you are bound by the following Terms & Conditions. Please read them carefully.

I have read and I understand the following statement: All material supplied via a Digitised Thesis from Trinity College Library is protected by copyright and other intellectual property rights, and duplication or sale of all or part of any of a thesis is not permitted, except that material may be duplicated by you for your research use or for educational purposes in electronic or print form providing the copyright owners are acknowledged using the normal conventions. You must obtain permission for any other use. Electronic or print copies may not be offered, whether for sale or otherwise to anyone. This copy has been supplied on the understanding that it is copyright material and that no quotation from the thesis may be published without proper acknowledgement.

Molecular Interactions in Obesity and Cancer

A dissertation submitted to the University of Dublin

for the degree of Doctor of Philosophy

by

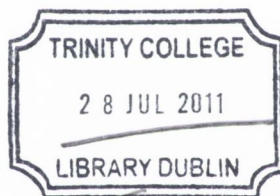## Emma Allott

Under the supervision of Dr. Graham Pidgeon

Departmental Head: Prof John V. Reynolds

Trinity College Dublin, October 2010

Department of Surgery

St James' Hospital
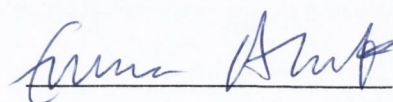
Trinity College Dublin

Declaration

I hereby declare that this thesis has not been submitted as an exercise for a degree at this or any other University and that it is entirely my own work except where otherwise acknowledged.

I agree that the Library may lend or copy this thesis upon request.

Emma Allott

October 2010

Summary

The incidence of overweight and obesity has reached pandemic proportions in modern society, affecting two thirds of the US and over half of the European population. Obesity is associated with increased morbidity and mortality in the form of elevated risk of cardiovascular disease, diabetes and many types of cancer. Overweight and obesity have been proposed to account for 14% of all cancer deaths in men and 20% in women in the US. Of all cancers, oesophageal adenocarcinoma (OAD) displays one of the strongest epidemiological links with obesity, making it an excellent model with which to study this association at a molecular level. OAD is an aggressive disease associated with early haematological and lymphatic dissemination. Incidence of this highly lethal cancer has risen by 50% in the last 15 years, mirroring the exponential rise in obesity. The overall aim of this thesis was to dissect the molecular pathways linking obesity with OAD and to determine if obesity could be linked to increased aggressiveness of this disease.

Microarray technology identified a pro-inflammatory, pro-angiogenic gene signature in the omentum of viscerally obese individuals. Visceral fat area (VFA), determined by computed tomography (CT), was found to be the strongest predictor of altered gene expression in visceral obesity. Multiplex Luminex technology identified a circulating pro-inflammatory phenotype common to visceral obesity, male sex and cancer mediated through reduction in levels of IL-4 and adiponectin and elevation in levels of leptin, IL-6, IL-8, MCP-1, IFNγ and VEGF. Altered levels of these adipokines were demonstrated to have functional effects on OAD cells with leptin increasing proliferation and adiponectin decreasing proliferation. Recent studies indicate that visceral obesity may share several hallmark pathways with cancer such as angiogenesis and inflammation. The distorted balance of these soluble mediators of angiogenesis and inflammation in visceral obesity could therefore represent important therapeutic targets, particularly in viscerally obese OAD patients.

Microarray based technology was used to examine the molecular effect of omental adipose tissue co-culture on OE33 OAD cells. Increased glycolytic flux and up regulation of the focal adhesion pathway, promoting cytoskeletal reorganisation and epithelial mesenchymal transition (EMT), culminated in an increased proliferative, migratory and invasive capacity of OAD. The expression of target genes, identified using this in vitro model, was subsequently examined in patient tumour biopsies. A novel association was demonstrated between visceral obesity and expression of genes involved in pathways of tumour invasion and metastasis,

matrix metalloproteinase 9 (MMP9) and plasminogen activator inhibitor 1 (PAI-1). Increased expression of MMP9 and PAI-1 and decreased expression of tumour suppressor p53 correlated with aggressive tumour biology and PAI-1 was found to be an independent prognostic marker in OAD. Increased expression of epithelial mesenchymal transition (EMT) regulator SNAI2 was associated with visceral obesity and was also identified as an independent prognostic factor in OAD. Expression of epithelial marker E-cadherin was decreased in visceral obesity however it did not correlate with expression of its transcriptional repressor, SNAI2, indicating that SNAI2 may exert its pro-tumour effect in OAD via E-cadherin independent pathways. Together these findings highlight a novel association between visceral obesity and pathways of tumour metastasis, particularly relevant in this aggressive cancer.

As clinical trials targeting MMP9 are ongoing in many cancer types, this key player in tumour metastasis was selected for examination at the protein level using tissue microarrays (TMAs). In agreement with results at the mRNA level, protein expression of MMP9 was found to be increased in viscerally obese patients. These preliminary results highlight a novel role for visceral obesity in up regulation of pro-tumour pathways characteristic of OAD. MMP9, PAI-1 and SNAI2 may be promising targets for the development of targeted therapies with the ultimate goal of stratified treatment of OAD patients with visceral obesity.

Acknowledgements

and chickpea lover, Niamh, what can I say.., what a brilliant few years of crazy student life… It was worth it just to meet such a great person to share the last few years with.

To my friends and family, you've all had to hear too much about the lab and about obesity and cancer, thank you for listening! To my parents Kathy and Norman, thank you for everything you've done for me and continue to do for me. I am very fortunate to have wonderful understanding and supportive parents like you. To Sven, thank you for being there for me always and especially for your support throughout the last few years, I am lucky to have you in my life.

Dedication

I dedicate this thesis to the memory of Liz who inspired me in many ways as a fellow scientist, eternal optimist, all round sports enthusiast and true friend.

List of Tables

List of Figures

xii

Abbreviations

ACM	adipose tissue conditioned medium
ADP	adenosine diphosphate
adj p	adjusted p value
ANOVA	analysis of variance
AP2	fatty acid binding protein
APS	ammonium persulfate
AR	adiponectin receptor
ATM	adipose tissue macrophages/ataxia telangiectasia mutated
ATP	adenosine triphosphate
ATP III	Adult Treatment Panel III
BCA	bicinhoninic acid
BCP	1-bromo-3-chloro-propane
BMI	body mass index
BO	Barrett's Oesophagus
BrdU	5'-bromo-2'-deoxyuridine
BSA	body surface area/bovine serum albumin
CCND1	cyclin D1
cDNA	complementary deoxyribonucleic acid
CDK4	cyclin dependant kinase 4
C/EBPα	CCAAT/enhancer binding protein α
COX-2	cyclooxygenase-2
CRC	colorectal carcinoma
CRT	chemoradiotherapy
CT	computed tomography
Ct	threshold cycle
CTDSPL	C-terminal domain RNA polymerase II polypeptide A (small phosphatase-like)
CXCL5	chemokine (C-X-C motif) ligand 5
CXCL7/PPBP	chemokine (C-X-C motif) ligand 7/pro-platelet basic protein
DAB	diaminobenzidine
DAG	diacylglycerol
DOCK1	dedicator of cytokinesis 1
DMEM	dulbecco's modified Eagles medium
DMSO	dimethyl sulfoxide

DNA	deoxyribonucleic acid
DTT	dithiothreitol
ECACC	European Collection of Cell Cultures
ECM	extracellular matrix
EDTA	ethylene-diamine tetra acetic acid
ELISA	enzyme-linked immunosorbent assay
EMT	epithelial mesenchymal transition
ES	enrichment score
EUS	endoscopic ultrasound
FACS	fluorescent-activated cell sorting
FCS	foetal calf serum
FDG-PET	fluoro-2-deoxyglucose positron emission tomography
FITC	fluorescein isothiocyanate
GORD	gastrointestinal reflux disease
GSEA	gene set enrichment analysis
HCS	high content screening
HDL	high density lipoprotein
HFD	high fat diet
HGF	hepatocyte growth factor
HRP	horseradish peroxidise
IBMX	3-isobutyl-1-methylxanthine
IDF	International Diabetes Federation
IHC	immunohistochemistry
IL	interleukin
KEGG	Kyoto Encyclopaedia of Genes and Genomes
LIMMA	Linear model in microarrays
logFC	log fold change
MetS	Metabolic Syndrome
NHNES	National Health and Nutrition Examination survey
NKT	natural killer T cells
NO	nitric oxide
NSAIDs	non steroidal anti-inflammatory drugs
ns	not signficant
NuGO	European Nutrigenomics Organisation
OAD	oesophageal adenocarcinoma

ObR	leptin receptor
PBS	phosphate buffered saline
PCR	polymerase chain reaction
PFA	paraformaldehyde
PI	propidium iodide
PVDF	polyvinylidene fluoride
PS	phosphotidylserine
qPCR	quantitative real time PCR
R	software environment for statistical computing
RIN	RNA integrity number
RIPA	radioimmunoprecipitation buffer
RNA	ribonucleic acid
ROS	reactive oxygen species
RPMI	Roswell Park Memorial Institute
RS	relative survival
RTPCR	reverse transcriptase polymerase chain reaction
SCC	oesophageal squamous cell carcinoma
SD	standard deviation
SEM	standard error of the mean
SFA	subcutaneous fat area
SGBS	Simpson-Golabi Behmel syndrome
SVF	stromal vascular fraction
TAE	tris-Acetate-EDTA
TBST	tris-buffered saline containing 0.1% Tween-20
TEMED	tetramethylethylenediamine
TMA	tissue microarray
TMB	tetramethylbenzidine
TNM	tumour-node-metastasis
VFA	visceral fat area
WC	waist circumference
WHR	waist hip ratio

Units

bp	base pairs
°C	degrees Celcius
g	grams
h	hours
µg	microgram
µl	microlitre
µM	micromolar
kDa	kilodaltons
kg	kilogram
hz	hertz
L	litre
M	molar
mA	milliamp
mg	milligram
ml	millilitre
mM	millimolar
n	number size
nM	nanomolar
ng	nanograms
rpm	revolutions per minute
U	units
w/v	weight per volume
v/v	volume per volume

Publications and Presentations

Publications

- ❖ Gilks, W.P., **Allott, E.H.**, Donohoe, G., Cummings, E., International Schizophrenia Consortium, Gill, M., Corvin, A.P., Morris, D.W. (2010) 'Replicated genetic evidence supports a role for HOMER2 in schizophrenia' *Neurosci Lett* Jan 14; 468(3): 229-33.

- ❖ Lysaght, J., Howard, J.M., McGarrigle, S., **Allott, E.H.**, Casey, R., Donohoe, C., Beddy, P., Ravi, N., Reynolds, J.V., Pidgeon, G.P. 'Utilisation of a unique bioresource for the molecular and immunological assessment of peripheral and visceral adipose tissue' (submitted to Cancer Letters)

- ❖ **Allott, E.H.**, Lysaght, J., Cathcart, M.C., Donohoe, C., Cummins, R., McGarrigle, S., Ravi, N., Kay, E., Reynolds, J., Pidgeon, G. 'MMP9 expression in oesophageal adenocarcinoma is up regulated with visceral obesity and correlates with poor tumour differentiation' (submitted to Molecular Cancer)

- ❖ **Allott, E.H.**, Lysaght, J., Ravi, N., Reynolds, J., Pidgeon, G. 'Characterisation and comparison of murine adipocyte model cell line 3T3-L1, human adipocyte cell strain SGBS and primary adipocytes isolated from human omentum' (in preparation)

- ❖ **Allott, E.H.**, Morine, M., Lysaght, J., Ravi, N., Roche, H.M., Reynolds, J., Pidgeon, G. 'Tumour expression of epithelial mesenchymal transition genes, PAI-1 and SNAI2, is elevated in obese oesophageal adenocarcinoma patients and predicts poor prognosis' (in preparation)

Oral presentations

- ❖ 'Tumour PAI-1 over expression correlates with visceral obesity and is a prognostic factor in oesophageal adenocarcinoma' (Plenary session, SARS, Ireland, Jan 2011)

- ❖ 'Omental adipose tissue increases the proliferative, migratory and invasive capacity of oesophageal adenocarcinoma via up regulation of MMP2, MMP9 and PAI-1 and down regulation of tumour suppressors ATM and p53' (Irish Association for Cancer Research, Ireland, March 2010)

- ❖ 'Co-culture of oesophageal tumour cells with adipocytes and adipose tissue regulates gene expression of pro-tumour pathways' (Sir Peter Freyer Surgical Symposium, Ireland, Sept 2009)

Poster presentations

- ❖ 'Omental adipose tissue increases the proliferative, migratory and invasive capacity of oesophageal adenocarcinoma via up regulation of focal adhesion and epithelial mesenchymal transition pathways' (American Association for Cancer Research, Washington D.C., 2010)

- ❖ 'Co-culture of oesophageal tumour cells with adipocytes and adipose tissue regulates gene expression of pro-tumour pathways' (American Association for Cancer Research, Denver, 2009; Institute of Molecular Medicine Annual meeting, Ireland, 2009)

- ❖ 'Adipose tissue and conditioned media protects oesophageal and colorectal tumour cells from chemotherapy induced death' (Keystone Symposium, Canada, 2009; Irish Association for Cancer Research, Ireland, 2008)

- ❖ 'Adipokine regulation of tumour cell survival in oesophageal and colorectal cancer cells' (All Ireland Cancer Conference, Ireland, 2008)

Awards and Scholarships

- ❖ 'Scholar in Training' award for poster presentation at American Association for Cancer Research (Washington D.C., April 2010)

- ❖ Travel award for oral presentation at Irish Association for Cancer Research (Ireland, March 2010)

- ❖ NCI Summer Curriculum in Cancer Prevention Scholar (Washington D.C., August 2009)

- ❖ Travel scholarship for poster presentation at Keystone Symposium (Canada, January 2009)

Table of Contents

1 General Introduction

1.1 Oesophageal cancer

1.1.1 Histological subtypes

Oesophageal cancer is one of the least studied and most deadly cancers worldwide (Enzinger and Mayer, 2003). More than 90% of oesophageal cancer can be divided into two histological subtypes, oesophageal adenocarcinoma (OAD) and oesophageal squamous cell carcinoma (SCC) (Daly et al., 2000). OAD arises from specialised intestinal glandular epithelium present at the junction of the oesophagus and the stomach. In certain cases, chronic gastrointestinal reflux (GORD) can give rise to the development of areas of specialised intestinal metaplasia (Barrett's oesophagus) and confers an increased risk of OAD. In contrast, SCC arises from the squamous epithelium and is localised in the upper two thirds of the oesophagus. SCC is related to nicotine and alcohol use (Enzinger and Mayer, 2003, Siewert et al., 2001).

1.1.2 Incidence and survival

Oesophageal cancer is the eighth most common cancer worldwide but the sixth most common cause of cancer related mortality, indicating the lethal nature of the disease (Ferlay et al., 2010). Overall incidence of oesophageal cancer has risen by 27% in Ireland in the last 15 years, however there is a substantial difference in profiles between histological subtypes (Ireland). Incidence of OAD has risen almost 50%, while incidence of SCC has dropped 4% in the last 15 years (Figure 1.1). These data underline the heterogeneous histology and aetiology of these subtypes (Siewert et al., 2001). Although five year relative survival (RS) is improving for both subtypes, it remains low, and therefore oesophageal cancer is one of the most fatal cancers (Lagergren, 2005). OAD RS has increased from 11.6% to 14.8% over the last 15 years while SCC RS have improved marginally more, from 11% to 16.3% (Ireland).
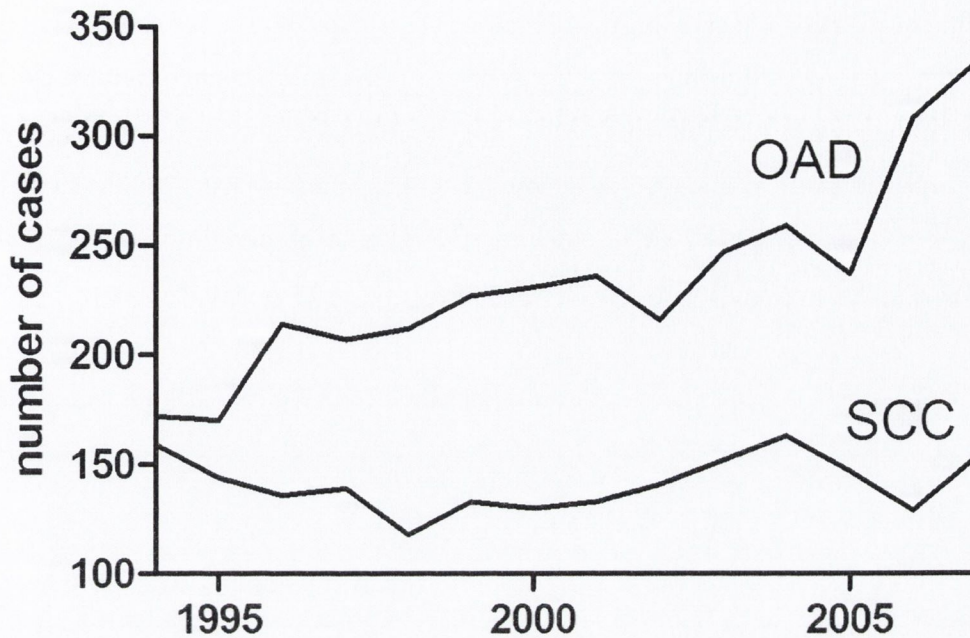
Figure 1.1: Number of newly diagnosed cases of oesophageal cancer in Ireland (National Cancer Registry Ireland 1994-2007) (OAD-oesophageal adenocarcinoma, SCC=oesophageal squamous cell carcinoma)

1.2 Oesophageal adenocarcinoma

1.2.1 Epidemiology

Although OAD remains a relatively rare form of cancer, incidence is rapidly increasing (Engel et al., 2003). Incidence of OAD in the USA overtook that of SCC in the mid 1990s, and this pattern is reflected in Europe (Heitmiller and Sharma, 1996). While SCC remains the most common subtype in Asia, the incidence of OAD is also beginning to rise there, potentially reflecting the Westernisation of this society (Fernandes et al., 2006, Shibata et al., 2008). In Ireland, OAD incidence and mortality are 1.2 to 3 times higher than the rest of EU and the USA (NCRI 2nd report, 1998-2000). There is a striking male to female predominance of OAD with incidence in males six fold higher than incidence in females. Ethnicity also plays a major role, and rates of OAD are fivefold higher in Caucasians than African Americans (Kubo and Corley, 2004). Caucasian males therefore have both the highest and fastest growing incidence of OAD (Kubo and Corley, 2002). As with most gastrointestinal cancers, age is associated with risk of OAD, and median age at diagnosis is 60 years (Lagergren, 2005).

1.2.2 Risk factors

The substantial increase in incidence of OAD could be attributable to several interrelated and modifiable risk factors. As shown in Table 1.1, separate risk factors are important for OAD and SCC. Only nicotine use is a shared risk factor between histological subtypes and this has been shown to play a greater role in SCC development (Enzinger and Mayer, 2003). It has been estimated that approximately 79% of OAD cases can be attributed to cigarette smoking, obesity, reflux symptoms and low intake of fruit and vegetables (Engel et al., 2003).

Table 1.1: Comparison of major risk factors for oesophageal cancer (adapted from Enzinger *et al*, 2003).

Table 1. Risk Factors for Esophageal Cancer.		
Risk Factor	Squamous-Cell Carcinoma	Adeno-carcinoma
Tobacco use	+++	++
Alcohol use	+++	—
Barrett's esophagus	—	++++
Weekly reflux symptoms	—	+++
Obesity	—	++

A single plus sign indicates an increase in the risk of less by a factor of less than two, two plus signs an increase by a factor of two to four, three plus signs an increase by a factor of four to eight, and four plus signs an increase by a factor greater than eight. A dash indicates no proven risk.

1.2.2.1 Reflux and Barrett's oesophagus

OAD is usually diagnosed late and over half of patients presenting with this disease have evidence of metastases and are therefore inoperable (Enzinger and Mayer, 2003). An improved understanding of pre-metaplastic precursors of OAD could thus be of great assistance both for early detection and treatment of this disease (Reid et al., 2010). The progression from gastrointestinal reflux disease (GORD) to the pre-malignant Barrett's oesophagus (BO) can give rise to OAD (Corley et al., 2007, Watanabe et al., 2007). Frequent and prolonged reflux of the acidic stomach contents into the distal oesophagus can lead to tissue damage and inflammation. Barrett's oesophagus results from the protective transformation of the normal stratified squamous epithelium of the oesophagus into columnar intestinal epithelium characteristic of the stomach lining, better equipped to withstand these acidic insults (Figure 1.2) (Flejou, 2005, Reid et al., 2010). Reflux disease increases the risk of

developing Barrett's oesophagus by approximately 1% (Reid et al., 2010) and patients with Barrett's oesophagus have 30 – 40 fold increased risk of developing OAD compared to the rest of the population (Ryan et al., 2008). However, up to 50% of individuals with OAD have no history of reflux disease (Farrow et al., 2000, Lagergren et al., 1999a) while over 95% have no previous history of Barrett's (Reid et al., 2010) suggesting the important contribution of other risk factors.
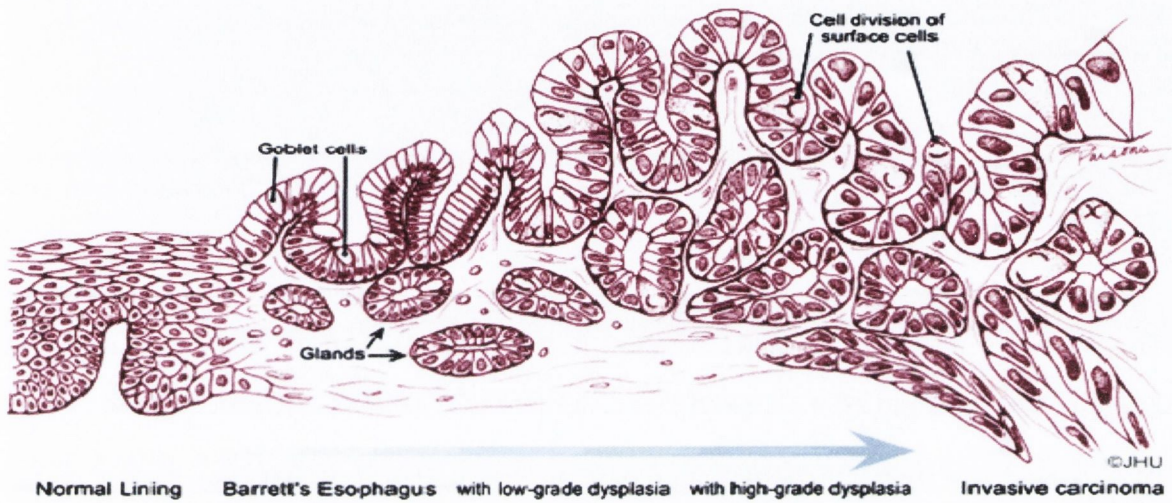
Figure 1.2: Pathological sequence of neoplastic transformation in oesophageal adenocarcinoma. Normal squamous epithelium acquires an intestinal metaplastic histology following prolonged exposure to bile acids (Barrett's oesophagus). This can give rise to dysplasia and eventually to invasive adenocarcinoma (taken from http://pathology2.jhu.edu/beweb/Definition.cfm).

1.2.2.2 Obesity

Obesity is an independent risk factor for OAD (Calle et al., 2003, Ryan et al., 2006, Lagergren et al., 1999b, Engel et al., 2003), and has been shown to increase OAD risk almost tenfold (Ryan et al., 2006). Adipose tissue is principally accumulated in two compartments, subcutaneous and central. Recently it has been suggested that centrally accumulated fat or visceral adipose tissue is more metabolically active than subcutaneous (Giorgino et al., 2005). There is an association of visceral obesity, independent of BMI, with GORD (Corley et al., 2007), Barrett's (Edelstein et al., 2007, Ryan et al., 2008) and OAD (Corley et al., 2008, Beddy et al., 2010), implying that an expanded mass of visceral adipose tissue could play a role at all stages in this sequence of events. It is intuitive that excess visceral adipose tissue could place extra mechanical pressure on the stomach thereby giving rise to increased reflux. However, studies have shown that adjustment for GORD only marginally reduces the risk conferred by obesity. It is thus likely that the substantial effect of obesity is mediated via molecular pathways (Corley

et al., 2008, Reid et al., 2010). Visceral obesity has been linked to carcinogenesis through metabolic abnormalities such as hyperinsulinaemia and hyperglycaemia (Renehan et al., 2006) and adipose tissue is an important site of sex steroid biosynthesis, also implicated in tumourigenesis (Roberts et al., 2009). Visceral obesity is associated with enhanced production of adipokines leading to the development of a chronic pro-inflammatory phenotype (Tilg and Moschen, 2006, Neels and Olefsky, 2006) which could in turn promote tumourigenesis (Colotta et al., 2009, Field et al., 2001). These molecular pathways are discussed in more detail in section 1.6 and 1.7.

1.2.2.3 Other risk factors

Cigarette smoking is associated with OAD risk (Anderson et al., 2007). Medication, diet and *Helicobacter pylori* infection are moderate modifiable protective factors in the development of OAD. Aspirin and other non steroidal anti-inflammatory drugs (NSAIDs) have been proposed to reduce the risk of OAD, although evidence is limited (Farrow et al., 1998). Low fruit and vegetable consumption is a moderate risk factor for OAD (Engel et al., 2003, Anderson et al., 2007). Reduced rates of *H. pylori* infection in the general population correlate with increased incidence of GORD, reflux oesophagitis and OAD (el-Serag and Sonnenberg, 1998, Anderson et al., 2008).

1.2.3 Clinical presentation

Once established, OAD can spread rapidly and at time of diagnosis approximately 50% of patients have evidence of metastasis and hence unresectable tumours (Enzinger and Mayer, 2003). Patients present most commonly with dysphagia (difficulty swallowing, 74%), weight loss (57.3%), GORD (20.5%), odynophagia (pain on swallowing food and liquids, 16.6%) and dyspnea (shortness of breath, 12.1%) (Daly et al., 2000).

1.2.4 Pathology and staging

Staging is carried out using a variety of techniques which include computed tomography (CT), endoscopic ultrasound (EUS), positron emission tomography (^{18}FDG-PET), laparoscopy and endoscopic mucosal resection (Murphy et al., 2008). Oesophageal adenocarcinoma is classified according to the 2002 American Joint Committee on Cancer tumour-node-metastasis (TNM) classification system (Greene, 2002). Tumours are classified by depth of tumour invasion (tumour (T) stage), presence or absence of lymph node involvement by metastatic disease (node (N) stage) and presence or absence of distant metastases (M stage) (Table 1.2) (Enzinger and Mayer, 2003). According to this classification system, 13 – 20% of patients have

stage I disease, 14 – 27% have stage IIA disease, 7 – 16% have stage IIB disease and 44 – 50% have stage III disease (Daly et al., 2000, Enzinger and Mayer, 2003). Upon complete removal of the tumour (R0 resection), 5 year survival is over 95% for stage 0 disease, 50 – 80% for stage I disease, 30 – 40% for stage IIA disease, 10 – 30% for stage IIB disease and 10 – 15% for stage III disease (summarised in Table 1.2) (Reed, 1999, Headrick et al., 2002, Pera et al., 1992). Patients with stage IV disease treated with palliative chemotherapy have an average survival of less than one year. A total of 35% of surgical resections for oesophageal cancer in Ireland are carried out at this centre in St. James's Hospital. Of patients presenting with oesophageal cancer 14% have stage I disease, 29% have stage II disease, 36% have stage III disease and 8% have stage IV disease (Six Year Cancer Audit Report, St James Hospital). At this institution, five year survival is over 75% for stage 0 disease, 70 – 75% for stage I disease, 25 – 30% for stage II disease and 15 – 20% for stage III and stage IV disease. Overall median survival for oesophageal cancer in this institution is 11 months and overall five year survival is 16% (Six Year Cancer Audit Report, St James Hospital), in line with the national average of 15.5% (National et al., 2001).

Table 1.2: TNM staging criteria (2002 American Joint Committee on Cancer tumour-node-metastasis (TNM) classification system) and associated five year survival rates (adapted from Enzinger *et al*, 2003).

Five-Year Survival Rates for Esophageal Carcinoma, According to the Tumor–Node–Metastasis Classification.				
Stage	Tumor	Node	Metastasis	5-Yr Survival
				%
0	Tis	N0	M0	>95
I	T1	N0	M0	50–80
IIA	T2-3	N0	M0	30–40
IIB	T1-2	N1	M0	10–30
III	T3	N1	M0	10–15
	T4	Any N	M0	
IVA	Any T	Any N	M1a	<5
IVB	Any T	Any N	M1b	<1

Primary tumour (T) is classified as follows: Tis=carcinoma in situ, T1=invasion of the lamina propria or submucosa, T2=invasion of the muscularis propria, T3=invasion of the adventitia, T4=invasion of adjacent structures. Regional lymph node metastases are classified as follows: N0=no regional lymph node metastases, N1=regional lymph node metastases. Distant metastases (M) are classified as follows: M0=no distant metastases, M1a=metastasis to cervical or celiac nodes, M1b=other distant metastases.

1.2.5　Treatment

Treatment for localised oesophageal adenocarcinoma involves transthoracic or transhiatal oesophagectomy to remove the tumour (Enzinger and Mayer, 2003). These surgical resection procedures involve laparatomy (incision in the abdominal wall to gain access to the abdominal cavity), dissection of the oesophagus and anastomosis in either the upper chest or neck, the final goal being R0 resection (complete removal of the tumour) and lymphadenectomy (Enzinger and Mayer, 2003). Five year survival of patients with resectable disease following oesophagectomy approaches 50%, indicating a need for multimodal therapy to increase these survival rates (Portale et al., 2006, Murphy et al., 2008). Although survival benefits are controversial, the standard of care for OAD today usually involves pre-operative neoadjuvant chemoradiotherapy followed by surgery (Murphy et al., 2008). Patients receive a standard regimen of chemoradiotherapy over the course of seven weeks and the tumour is re-staged at week 8. Surgery is carried out at week 9 if performance status of the patient has not deteriorated, if their neutrophil count is $>2 \times 10^6$/ml and if there is no local or systemic disease progression (Murphy et al., 2008, Walsh et al., 1996). Pre-operative neoadjuvant therapy consists of two courses of chemotherapy on week 1 and week 6 (5-fluorouracil: 15mg/kg body weight, cisplatin: 75 mg/m^2 body surface area) and a course of radiotherapy beginning concurrently with the first week of chemotherapy (40 Gy administered in 15 fractions over a three week period). Pre-operative chemoradiotherapy has been found to confer a significant survival advantage at three years compared to surgery alone (Walsh et al., 1996, Fiorica et al., 2004, Urschel and Vasan, 2003). Nonetheless OAD mortality remains high and study of molecular pathways involved is important in the development of novel targeted therapies.

1.2.6　Novel targeted therapies

Advances in the understanding of OAD biology and associated risk factors have led to the identification of molecular targets (Table 1.3) and subsequent development of targeted preventative therapies and treatments. Proton pump inhibitors (PPIs) are administered to normalise stomach pH and thus reduce the damaging effects of acid reflux, yet their effectiveness in controlling Barrett's oesophagus is controversial (Peters and Fitzgerald, 2007). The use of anti-oxidants is under investigation as a preventative therapy. A diet rich in fruit and vegetables and vitamins C and E is protective in development of OAD (Gonzalez et al., 2006, Bollschweiler et al., 2002). Curcumin is a yellow polyphenol found in turmeric, synthesised by plants to protect against reactive oxygen species damage. Its role as an anti-oxidant, anti-inflammatory and anti-carcinogenic agent in OAD is currently under investigation, and is thought to act through a number of pathways including repression of the

pro-inflammatory transcription factor NF-κB (Peters and Fitzgerald, 2007, Lambert et al., 2005). With inflammation a key step in the sequence from GORD to Barrett's to OAD, the chemoprotective use of anti-inflammatory drugs has been examined. A meta-analysis suggested a protective association of aspirin and other non steroidal anti-inflammatory drugs (NSAIDs) with both histological subtypes of oesophageal cancer (Corley et al., 2003). COX-2 is an important rate-limiting enzyme in prostaglandin production, the target pathway of NSAIDs, and is often over expressed in both Barrett's oesophagus and oesophageal adenocarcinoma (Syrigos et al., 2008). A specific COX-2 inhibitor Celecoxib is currently on trial in oesophageal cancer although possible cardiovascular toxicity is a concern (Syrigos et al., 2008).

Epidermal growth factor receptor tyrosine kinases EGFR and ErbB2 (HER2/neu) are over expressed in many cancers including OAD, with EGFR associated with advanced tumour stage, lymph node metastasis and poorer patient survival (Wang et al., 2007). Cetuximab is an anti-EGFR monoclonal antibody currently used in colorectal and head and neck carcinoma (Cunningham et al., 2004, Karamouzis et al., 2007). A Phase II trial found that cetuximab can be safely administered with chemoradiotherapy in oesophageal cancer (Safran et al., 2008). Trastuzumab (Herceptin) is an anti-ErbB2/HER2 monoclonal antibody that can be safely incorporated into the chemoradiotherapy regimen for oesophageal cancer without increased toxicity (Safran et al., 2007). Gefitinib, a receptor tyrosine kinase (RTK) inhibitor, has shown promising results in Phase II and Phase III trials in non small cell lung cancer, especially in a subgroup of patients with EGFR mutations (Peters and Fitzgerald, 2007). In oesophageal cancer, a Phase II trial of gefitinib has been shown to have a clinical response rate of 11%, and relatively mild associated toxicity. Subsequent microarray analysis in this study showed that gefitinib treatment down regulated expression of oncogenes associated with tumour progression including caspase 8 (Ferry et al., 2007).

Vascular endothelial growth factor (VEGFA) is up regulated in Barrett's oesophagus and OAD, with the characteristic salmon pink colour of Barrett's attributable to enhanced vascularisation of the tissue (Kleespies et al., 2004). Anti-VEGF monoclonal antibody Bevacizumab (Avastin®) binds with high affinity to VEGFA, preventing it binding to its receptors and thereby inhibiting its angiogenic activity (Syrigos et al., 2008). Bevacizumab has been approved by the US Food and Drug Administration for first line therapy in colorectal (Hurwitz et al., 2004) and non small cell lung carcinoma (Sandler et al., 2006). Preliminary results from trials in oesophageal cancer

are promising with 26.6% of patients achieving a partial response to therapy. Confirmation of these results in ongoing trials is eagerly anticipated (Syrigos et al., 2008).

Matrix metalloproteinases (MMPs) play an important role in extracellular matrix degradation, vital for tumour invasion and metastasis (Belotti et al., 2003). Two orally administered MMP inhibitors have recently been developed, Marimastat and Prinomastat, however preliminary clinical trials have demonstrated limited success. Although patients treated with Marimastat showed significantly increased survival, this drug was associated with high musculoskeletal toxicity (Bramhall et al., 2002), while Prinomastat was found to give rise to unexpected thrombo-embolic events, necessitating early closure of the trial (Heath et al., 2006). Advances in understanding of molecular pathways in oesophageal cancer have led to identification of some promising novel molecular targets (Table 1.3). The development of targeted preventative therapies and treatments could limit the incidence and improve the poor survival rates associated with OAD.

Table 1.3: Molecular targets and their pathogenic roles in oesophageal cancer (adapted from Syrigos *et al*, 2008).

Role	Molecular targets
1. Cell-growth regulation	ErbB receptors family (EGFR, HER2/ neu)
2. Stimulation of angiogenesis	Vascular endothelial growth factor (VEGF-A)
3. Regulation of inflammatory response	Cyclooxygenase-2 (COX-2)
4. Regulation of metastatic potential	Matrix metalloproteinases (MMP)
5. Apoptosis regulation	Transcriptional nuclear factor kappa-b (NK-Kb)

1.3 Obesity

'To lengthen thy life, lessen thy meals'

Benjamin Franklin, Poor Richard's Almanack, 1737

1.3.1 Epidemiology

Obesity is defined by the accumulation of excess adipose tissue and is associated with increased morbidity and mortality in the form of increased risk of cardiovascular disease, stroke, hypertension, metabolic syndrome, type II diabetes mellitus, osteoarthritis, sleep apnoea, gall bladder disease and many types of cancer (Must et al., 1999, Field et al., 2001, Guh et al., 2009). It is traditionally classified by body mass index (BMI) (kg/m^2). Overweight corresponds to a BMI of between 25 and 30, while obesity corresponds to a BMI greater than 30 (Table 1.4).

Table 1.4: Classification of obesity status by body mass index (BMI) (taken from Donohoe *et al*, 2010).

	BMI (kg/m^2)
Underweight	$\leq 18{\cdot}5$
Normal weight	$18{\cdot}5-25$
Overweight	$25-30$
Obese class I	$30-35$
Obese class II	$35-40$
Obese class III	≥ 40

In Europe, 56% of adult males and 53% adult females are overweight with 14% and 23%, respectively, classified as obese (WHO report 2007). In the United States these figures are even higher with approximately two thirds of the adult population overweight, and one third of these obese (National Health and Nutrition Examination Survey (NHNES) 2007 – 2008). It is clear that obesity is becoming a worldwide pandemic with rates doubling in the United States over the last 30 years (Ogden et al., 2006)(National Health and Nutrition Examination Survey (1971-74 to 2003-06)) and tripling in Europe over the same time period (WHO report 2007). With rates of overweight and obesity now merely 5% lower than the US (SLAN 2007), Ireland is no exception. A comparison between the North/South Food Consumption survey conducted in 1999 and the SLAN 2007 survey shows that while incidence of overweight have remained approximately the same, rates of obesity have risen by 5% (SLAN 2007). Two out of three Irish

adults are now overweight while almost one in four adults are classified as obese (SLAN 2007). Obesity in women is the major contributor to this rise, with incidence of obesity in females increasing 7% between 1999 and 2007, while incidence in males has remained roughly the same over this same time period (SLAN 2007).

At least one in 13 deaths in the European Union (EU) is estimated to be attributable to overweight and obesity (Banegas et al., 2003, Allender and Rayner, 2007) and of these deaths 60 – 70% are due to cardiovascular disease and 20% are due to cancer (Banegas et al., 2003). The Million Women Study in the United Kingdom (Reeves et al., 2007) found that overweight and obesity are responsible for 5% of all cancers among post-menopausal women. A study conducted in the United States in 2003 found that males with BMI ≥ 35 had a 1.23 relative risk of developing all types of cancer, while women with a BMI ≥ 40 had a 1.62 relative risk of developing all types of cancer, and that overweight and obesity could account for 14% of all cancer deaths in men and 20% in women in the United States (Calle et al., 2003). If the current obesity trends were to continue all US adults would be overweight or obese by 2048 and total health care costs attributable to excess weight would double every decade (Wang et al., 2008). With this terrifying possibility on the horizon, there is an absolute necessity to understand the molecular basis of the association of obesity with increased morbidity and mortality.

1.3.2 Adipose tissue depots and measuring obesity

Fat depots differ in size, function and contribution to pathological states and adipose tissue is therefore a heterogeneous organ (Tchkonia et al., 2007, Perrini et al., 2008). It is now known that accumulation of visceral fat is more detrimental to health than overall obesity indicating the pathophysiological importance of adipose tissue distribution (Despres, 2001). Gene expression data suggests that different fat depots are essentially 'mini organs', with different developmental, adipogenesis and metabolic gene expression profiles suggesting distinct developmental origins (Tchkonia et al., 2007). There are also acquired differences between depots: obesity is associated with increased adipocyte necrosis (Strissel et al., 2007) and preferential macrophage infiltration into visceral adipose tissue (Cancello et al., 2006). Visceral adiposity is associated with male sex (Misra and Vikram, 2003), and male sex in turn is more strongly associated with obesity related morbidities than female sex (Ryan et al., 2006). Visceral adiposity is a stronger predictor of related morbidity and mortality than overall obesity (Gesta et al., 2006, Giorgino et al., 2005). This important finding is reflected in the International Diabetes Foundation (IDF) definition of the Metabolic Syndrome, a cluster of

metabolic abnormalities leading to increased incidence of Type II Diabetes and related disorders (Federation, 2006) (described in section 1.3.3, below).

BMI is a measure of overall adiposity and therefore does not take into consideration either composition of body mass or distribution of adipose tissue (Hu, 2007). As adipose tissue distribution has been shown to be of great importance with visceral adiposity linked to increased development of obesity related morbidities and mortalities, BMI may not be the ideal measure of obesity (Hu, 2007, Wajchenberg, 2000). This finding may serve to amplify the current obesity pandemic as incidence of visceral adiposity is far higher than incidence of overall adiposity. While less than 25% of adults in Ireland are classified as obese by BMI, over 60% of adults are classified as obese by waist circumference, a surrogate measure of visceral obesity (SLAN 2007). There are a number of ways to measure visceral obesity (Hu, 2007). The cross sectional surface area of the visceral fat depot is the measured by computed tomography (CT) between lumbar vertebrae L3 and L4 to give visceral fat area (VFA) (cm^2), the current gold standard measurement of visceral adiposity (Figure 1.3) (Beddy et al., 2010).
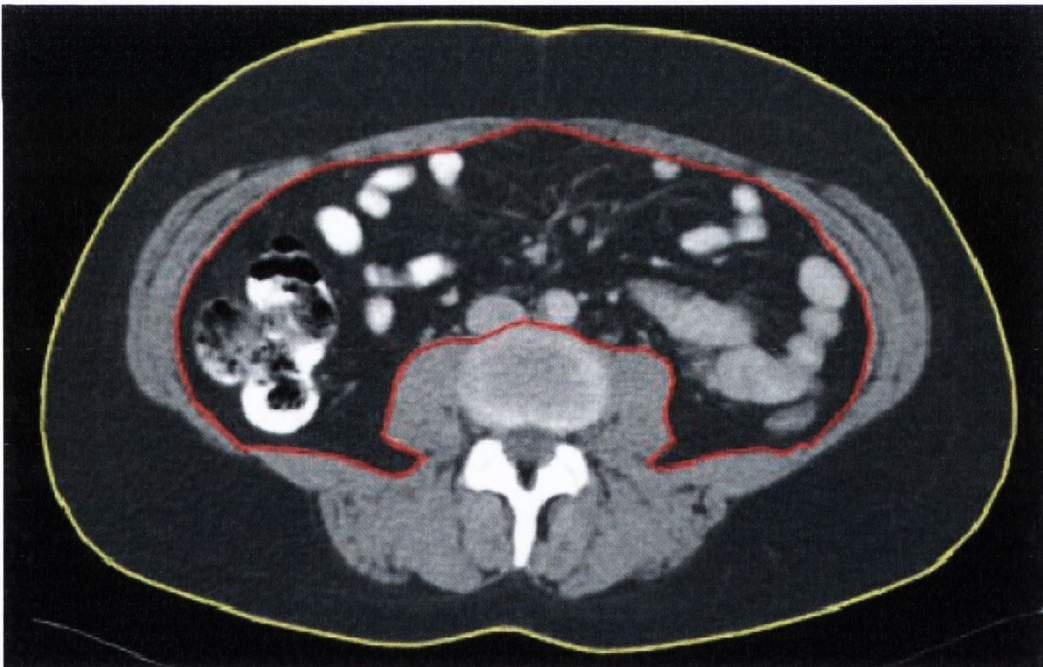
Figure 1.3: Total fat area is the area inside the yellow line drawn around the skin surface; visceral fat area (VFA) is the area inside the red line drawn around the inner layer of the abdominal wall musculature; subcutaneous fat area (SFA) is VFA subtracted from total fat area (taken from Beddy *et al*, 2010).

When the technology and expertise required to measure VFA is not available, waist circumference is a simple yet reliable measure of visceral obesity and correlates well with VFA

(Klein et al., 2007, Valsamakis et al., 2004). Although WC requires only a tape measure and therefore appears to be a straightforward technique, it is challenging to standardise between patients and different studies have measured at different locations (e.g. at the level of the umbilicus, at the midpoint between the lower rib and iliac crest) (Hu, 2007). Waist hip ratio (WHR) introduces another variable as it is a measure of both increased visceral fat and decreased gluteofemoral fat and thus its interpretation may be more complicated (Hu, 2007). A study comparing BMI, WHR and WC found that WC was the best surrogate measure of CT defined visceral obesity (Onat et al., 2004). WC was found to correlate better with cardiovascular disease than WHR, further underlining the superiority of this measurement (Pouliot et al., 1994). These data suggest that while VFA is the ultimate measure of visceral adiposity (Beddy et al., 2010) WC is an acceptable surrogate, although care is needed to standardise between patients. While the International Diabetes Federation (IDF) cut-off of 94 cm in men and 80 cm in women is widely used to define visceral obesity (Federation, 2006), there is no widely accepted VFA cut-off value currently in use. Several have recently been proposed: in a Turkish population, cardiovascular disease was found to correlate with VFA > 140 cm^2 in men and > 120 cm^2 in women (Onat et al., 2004) while in a Western population, VFA > 131 cm^2 in males was associated with increased cardiovascular risk (Hunter et al., 1994). A similar study, also in a Western population, found a VFA > 130 cm^2 in both males and females was associated with increased risk of Type II Diabetes and cardiovascular disease (Despres and Lamarche, 1993). With the recent recognition of the important contribution of visceral adiposity to the obesity pandemic and associated disease (Giorgino et al., 2005), it is vital to define VFA cut-off values that can be brought into widespread use, standardising this measurement and allowing accurate comparison between studies.

1.3.3   Obesity and the metabolic syndrome

The Metabolic Syndrome (MetS) is the term used to describe a cluster of metabolic abnormalities leading to increased incidence of related disorders such as cardiovascular disease (Gami et al., 2007) and Type II Diabetes Mellitus (Ford et al., 2005). There have been a number of definitions of MetS over the years (National et al., 2001, Federation, 2006, Alberti et al., 2005) and the population prevalence of the disorder depends on the definition used (Donohoe et al., 2010). The International Diabetes Federation (IDF) is the most recent and increases the prevalence of MetS by approximately 20% compared with the older Adult Treatment Panel III (ATP III) definition (Ford et al., 2005, Donohoe et al., 2010, National et al., 2001). The IDF definition requires presence of visceral obesity defined by a waist circumference of >80 cm in females and >94 cm in males, plus two or more of the following

metabolic abnormalities: raised triglycerides, reduced HDL-cholesterol, raised blood pressure and raised plasma glucose (Table 1.5) (Federation, 2006). This definition therefore underlines the important contribution of visceral adipose tissue in obesity related disorders.

Table 1.5: International Diabetes Federation definition of Metabolic Syndrome (Federation, 2006)

Visceral obesity (measured by waist circumference)	
Plus any two of the following:	
Raised triglycerides	≥1.7 mmol/L Or specific treatment for this condition
Reduced HDL-cholesterol	<1.03 mmol/L in males <1.29 mmol/L in females Or specific treatment for this condition
Raised blood pressure	Systolic ≥130 mmHg or diastolic ≥85 mmHg Or treatment of previously diagnosed hypertension
Raised plasma glucose	Fasting plasma glucose ≥5.6 mmol/L Or previously diagnosed with Type II Diabetes

(HDL=high density lipoprotein)

1.3.4   Adipose tissue: a dynamic, multi-functional endocrine organ.

Adipose tissue has long been considered merely a triglyceride reservoir with roles in energy storage, mechanical support and insulation (Rosen and MacDougald, 2006, Otero et al., 2005). This view began to change dramatically upon discovery of the genetically obese mouse (Figure 1.4) (Ingalls et al., 1950), cloning of the gene responsible, *ob*, and identification of its product, leptin (Zhang et al., 1994). Mutation of the recessive *ob* gene results in a phenotype characterised by leptin deficiency, hyperphagia, insulin resistance, reproductive dysfunction and early onset morbid obesity in mouse models. Daily injections of leptin increase energy expenditure and reduce food intake and body fat while maintaining lean muscle mass and euglycaemia and restoring reproductive function (Zhang et al., 1994). Mutation of the leptin receptor gives rise to the *db/db* mouse and the *fa/fa* rat with the same phenotype (Chua et al., 1996). While mutation of leptin and leptin receptors are causative of the obesity phenotype in the obese mouse model, these genotypes are highly unusual in humans where molecular pathways controlling metabolism are much more complex (Otero et al., 2005).
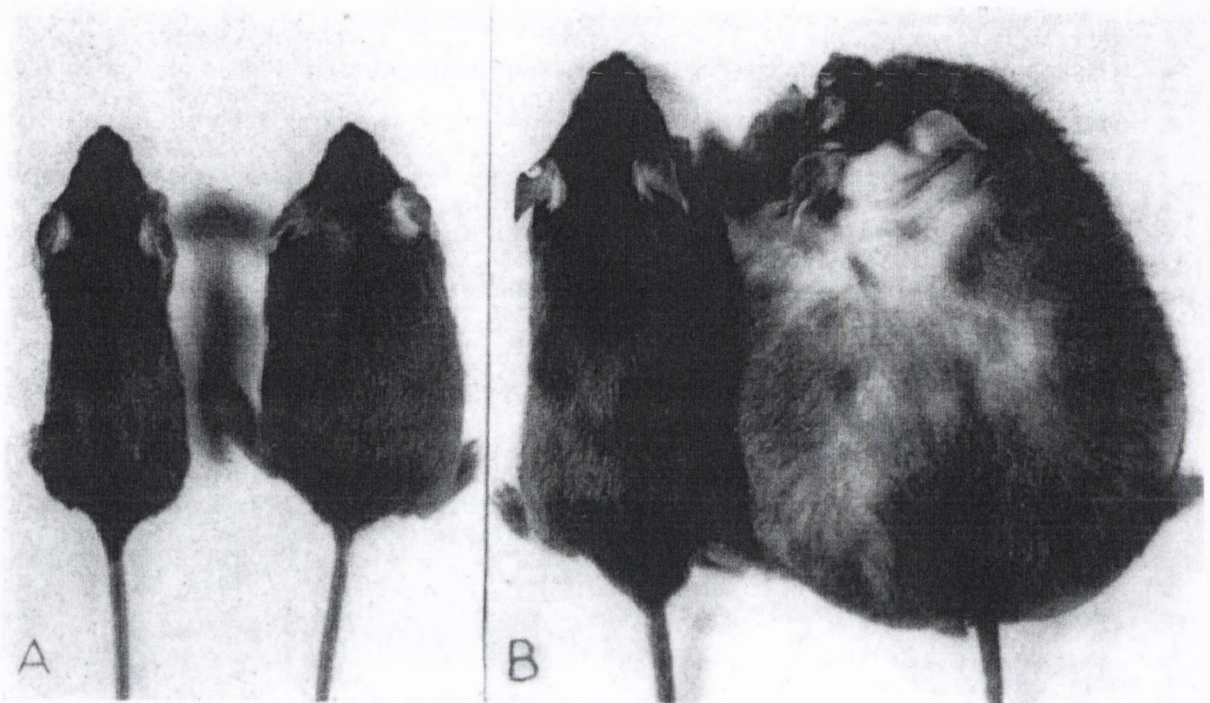
Figure 1.4: The discovery of the *ob/ob* mouse model (taken from Ingalls *et al*, 1950). A shows a normal weight and obese mouse at 21 days of age, B shows a normal weight and obese mouse at 10 months of age.

1.3.4.1 Leptin

In humans, leptin is produced in proportion to the size of adipose tissue depots and signals repletion of energy stores to the hypothalmus (Fruhbeck, 2006). Levels are increased in obesity and are higher in women than in men (Schaffler et al., 2007), with oestrogen increasing leptin levels (Castracane et al., 1998) and testosterone decreasing leptin levels (Blum et al., 1997). In addition to its role as a satiety factor, leptin is involved in the development of insulin resistance, a key component of obesity related morbidity and mortality (Renehan et al., 2006). Insulin resistance is common in obesity and results in a compensatory increase in production of this circulating growth factor (Roberts et al., 2009). Hyperinsulinaemia, characterised by chronically elevated levels of insulin and insulin resistance, is associated with elevated leptin levels (Segal et al., 1996, MacDougald et al., 1995). Leptin belongs to the IL-6 superfamily of Type I cytokines along with IL-2, IL-4, oncostatin M and IL-12 (Zhang et al., 1997) which bind and activate Type I cytokine receptors. This receptor superfamily, lacking endogenous kinase activity, signal through JAKs (Janus kinases) and STATs (signal transducers and activators of transcription) (Fruhbeck, 2006) to play a role in a wide variety of biological processes including reproduction (Holness et al., 1999),

growth (Ogunwobi and Beales, 2008b), angiogenesis (Roberts et al., 2009) and wound healing (Frank et al., 2000). Leptin also has an important role in modulating the immune system, through induction of pro-inflammatory cytokines such as TNFα and IL-1β (Lord et al., 1998, Fruhbeck, 2006). Hence, like other members of the Type I cytokine superfamily, leptin is functionally pleiotropic and the leptin receptor ObR is ubiquitously expressed (Fruhbeck, 2006). Five alternatively spliced isoforms of the receptor have been identified to date, designated ObRa, ObRb, ObRc, ObRd, ObRe (Wang et al., 1996), and these can be divided into three classes: short, long and secreted. The long isoform ObRb/ObR$_{long}$, is expressed at high levels in the hypothalamus and is the sole receptor to contain all the signalling motifs necessary for JAK STAT signal transduction. It is therefore thought to be the most functionally relevant isoform (Fruhbeck, 2006). Mutations in this receptor are responsible for the *db/db* mouse and *fa/fa* rat obese phenotypes, indicating that this receptor is crucial for leptin signalling (Chua et al., 1996). ObRa, ObRc, ObRd and ObRf are short isoforms missing some or all of the motifs present in ObRb and thus signalling either weakly or not at all (Friedman and Halaas, 1998). The short leptin receptor isoforms could play a role in uptake of leptin from the cerebrospinal fluid into the brain (Hileman et al., 2002), while the soluble form of the receptor, ObRe, has been proposed to act as the major binding protein involved in modulation of circulating leptin bio-availability (Lammert et al., 2001).

1.3.4.2 Adiponectin

Adiponectin is an abundant adipocyte-specific protein first identified over 10 years ago (Hu et al., 1996). In direct contrast with leptin, adiponectin is negatively correlated with obesity and plays an important role in maintaining insulin sensitivity. Exogenous administration of adiponectin improves insulin sensitivity in mouse models (Yamauchi et al., 2001), while hyperinsulinaemia decreases serum adiponectin (Kelesidis et al., 2006). Adiponectin is made up of a globular carboxyl terminal domain and a collagenous amino terminal domain and circulates in a range of multimeric conformations (Galic, S 2010). Adiponectin is mainly present in serum as a trimer or hexamer of low molecular weight (LMW) and as a larger multimeric structure of high molecular weight (HMW) (Figure 1.5). A shortened globular fragment can also be found at low concentrations in serum (Kadowaki and Yamauchi, 2005). The proportion of HMW to total adiponectin has been shown to be the best indicator of insulin sensitivity, indicating that this is the active form (Pajvani et al., 2004, Kobayashi et al., 2004). Adiponectin levels are lower in men than women (Cnop et al., 2003) and circulating levels are decreased by testosterone (Kelesidis et al., 2006).
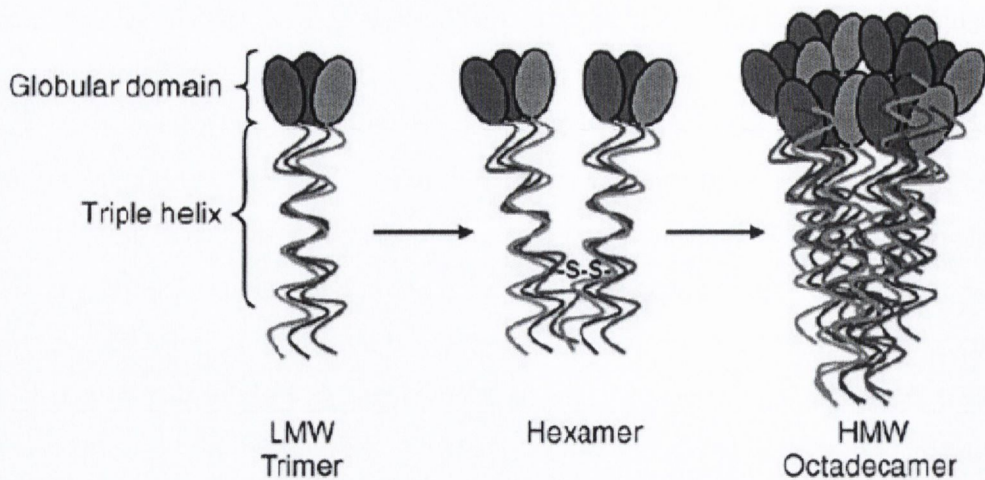
Figure 1.5: Representation of adiponectin trimeric, hexameric and octadecameric isoforms (taken from Galic *et al*, 2010). The location of the disulfide bond responsible for trimer association is shown in the hexamer isoform.

Two receptors for adiponectin have been identified, AR1 and AR2, binding globular and full length adiponectin, respectively (Yamauchi et al., 2003). AR1 has the highest affinity for globular adiponectin and although this receptor is ubiquitous, it is expressed predominantly in skeletal muscle. AR2 has intermediate affinity for both globular and full length adiponectin and is predominantly expressed in the liver (Goldstein and Scalia, 2004, Kadowaki and Yamauchi, 2005). The pivotal discoveries of these adipose-derived soluble factors or adipokines, leptin and adiponectin, has led to the recognition of adipose tissue as a dynamic, multi-functional endocrine organ (Otero et al., 2005).

1.3.4.3   Pro-inflammatory adipokines

Around the same time as the discovery of leptin, TNFα was found to be expressed in human adipose tissue at elevated levels in obesity (Kern et al., 1995). TNFα was found to be a negative regulator of the insulin pathway, identifying for the first time a mechanistic link between obesity and insulin resistance (Ulsyal 1997). It is now known that TNFα is produced mainly by adipose tissue macrophages (ATM) (Weisberg et al., 2003). In addition to TNFα, ATMs secrete a host of pro-inflammatory cytokines including IL-1 and IL-6 (Wellen and Hotamisligil, 2003). Approximately two thirds of circulating IL-6 is produced by the stromal vascular fraction (SVF) (including macrophages, endothelial cells, fibroblasts) of white adipose tissue (Mohamed-Ali et al., 1997). IL-6 levels are raised in obesity and Type II Diabetes (Lazar, 2005) and IL-6 contributes to insulin resistance through inhibition of the insulin signalling pathway (Galic et al., 2010). Visfatin, an adipokine highly enriched in visceral adipose tissue, was originally identified as an insulin mimetic in mice (Fukuhara et al., 2005) but its role is less clear in

humans (Rasouli and Kern, 2008). Resistin was first identified as a novel adipocyte specific transcript in mice and was named for its deleterious effect on glucose tolerance and its role in development of insulin resistance (Steppan et al., 2001, Kim et al., 2001, Holcomb et al., 2000). While expressed by adipocytes in mice, it is expressed by macrophages in humans (Patel et al., 2003). While resistin has been demonstrated to be important in mouse models, its function has not been well characterised in humans and serum concentrations are not found to be universally elevated in obesity and insulin resistance (Galic et al., 2010, Sentinelli et al., 2002). Retinol binding protein 4 (RBP4) was identified as an adipokine with elevated levels found in an insulin resistant GLUT4 knockout mouse model (Yang et al., 2005). Administration of RBP4 to lean mice resulted in development of insulin resistance while RBP4 knockout mice were protected from the development of high fat diet induced insulin resistance (Yang et al., 2005). This adipokine has also been investigated in humans, with insulin resistance correlating with a high level of circulating RBP4 (Graham, T.E. 2006). Adipsin, identical to complement factor D, is expressed at high levels in adipose tissue and correlates negatively with obesity status (White et al., 1992). These discoveries have provided foundation for the identification of a host of other adipokines, of which over 100 have been characterised to date (Roberts et al., 2009). There is now enormous interest in adipose tissue as a significant mediator of inflammatory and immune responses via adipokine production and the delicate balance of these pro and anti-inflammatory mediators could be an important mechanism of obesity pathogenesis (Neels and Olefsky, 2006).

1.3.5 The paradigm of obesity induced inflammation

It is now clear that cancer can arise from a background of sub-clinical, chronic inflammation (Colotta et al., 2009, Szlosarek et al., 2006). More recently it has been found that this state of persistent, unresolved inflammation is mirrored in obesity and could contribute to the pathogenesis of excess adipose tissue (Weisberg et al., 2003). As a result of these observations there has been much recent interest in characterisation of adipokines, soluble mediators of inflammation produced by adipose tissue (Galic et al., 2010, Roberts et al., 2009). While leptin and adiponectin are produced chiefly by adipocytes, many other pro-inflammatory adipokines are produced by cells of the stromal vascular fraction (SVF) comprising pre-adipocytes, fibroblasts, endothelial cells and immune cells (Kahn and Flier, 2000). It has been established that immune cells infiltrate preferentially into omental adipose tissue, indicating the importance of this depot in the development of the pro-inflammatory phenotype characteristic of obesity (Kintscher et al., 2008, Xu et al., 2003, Neels and Olefsky, 2006).

1.3.5.1 Adipose tissue macrophages

In an environment of caloric excess, adipose tissue can expand in two ways: by increasing adipocyte size through increased triglyceride storage (hypertrophy), and by increasing adipocyte number (hyperplasia) (Halberg et al., 2009, Huber et al., 2007, Boivin et al., 2007). Both methods of adipose tissue expansion can give rise to the development of a hypoxic, oxygen deficient environment as *de novo* angiogenesis fails to keep pace with the expanding adipose tissue (Halberg et al., 2009). Adipocyte necrosis, a pathological hallmark of obesity, can lead to the infiltration of scavenging macrophages (Rasouli and Kern, 2008, Cinti et al., 2005). It has been reported that 90% of macrophages are localised in adipose tissue in a syncytium, an enlarged multinucleated cell surrounding necrosing adipocytes, referred to as a 'crown like structure' (Figure 1.6) (Cinti et al., 2005). The rapid and widespread development of crown like structures in obesity places a huge inflammatory burden on the surrounding adipose tissue (Rasouli and Kern, 2008). Oxygen deficit and resulting tissue damage therefore triggers the production of pro-inflammatory and pro-angiogenic adipokines including VEGFA, IL-6, leptin and MCP-1. These molecules can recruit more immune cells into the damaged tissue and allow neo-vascularisation to occur to promote tissue re-oxygenation and repair (Halberg et al., 2009).
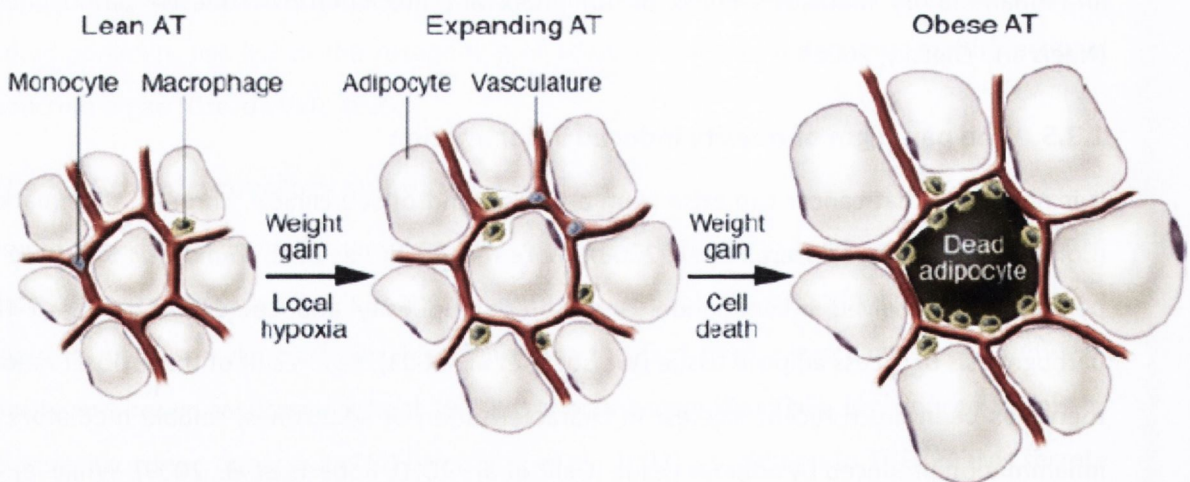
Figure 1.6: Adipose tissue expansion during weight gain leads to recruitment of macrophages through a variety of signals which may include local hypoxia. These macrophages predominantly localise around dead adipocytes (taken from Neels *et al*, 2006).

Monocyte chemoattractant protein 1 (MCP-1/CCL2) is a potent chemokine produced in large amounts by adipose tissue macrophages (ATMs) in obese adipose tissue. Monocytes, circulating precursors of macrophages with no phagocytotic ability, can be found circulating

inert in the bloodstream. In response to chemokine signalling, they can extravasate through the walls of the blood vessel into the damaged or infected tissue, where they become activated macrophages to carry out normal damage repair (Figure 1.7) (Duffield, 2003). In addition to its role in this normal healing response, over expression of MCP-1 can lead to insulin resistance through suppression of insulin-stimulated glucose uptake, and this has been demonstrated in 3T3-L1 adipocytes (Sartipy and Loskutoff, 2003). Over expression of MCP-1 in transgenic mice was associated with increased numbers of ATMs, increased TNFα and IL-6 production and insulin resistance (Kamei et al., 2006). On the other hand, mice with deletions of MCP-1 and its receptor CCR2 have decreased macrophage infiltration, a diminished pro-inflammatory state, improved insulin sensitivity and increased adiponectin concentrations (Weisberg et al., 2006). Together these data suggest that MCP-1, increased in obesity, plays an important role in ATM infiltration, insulin resistance and development of obesity related disease.
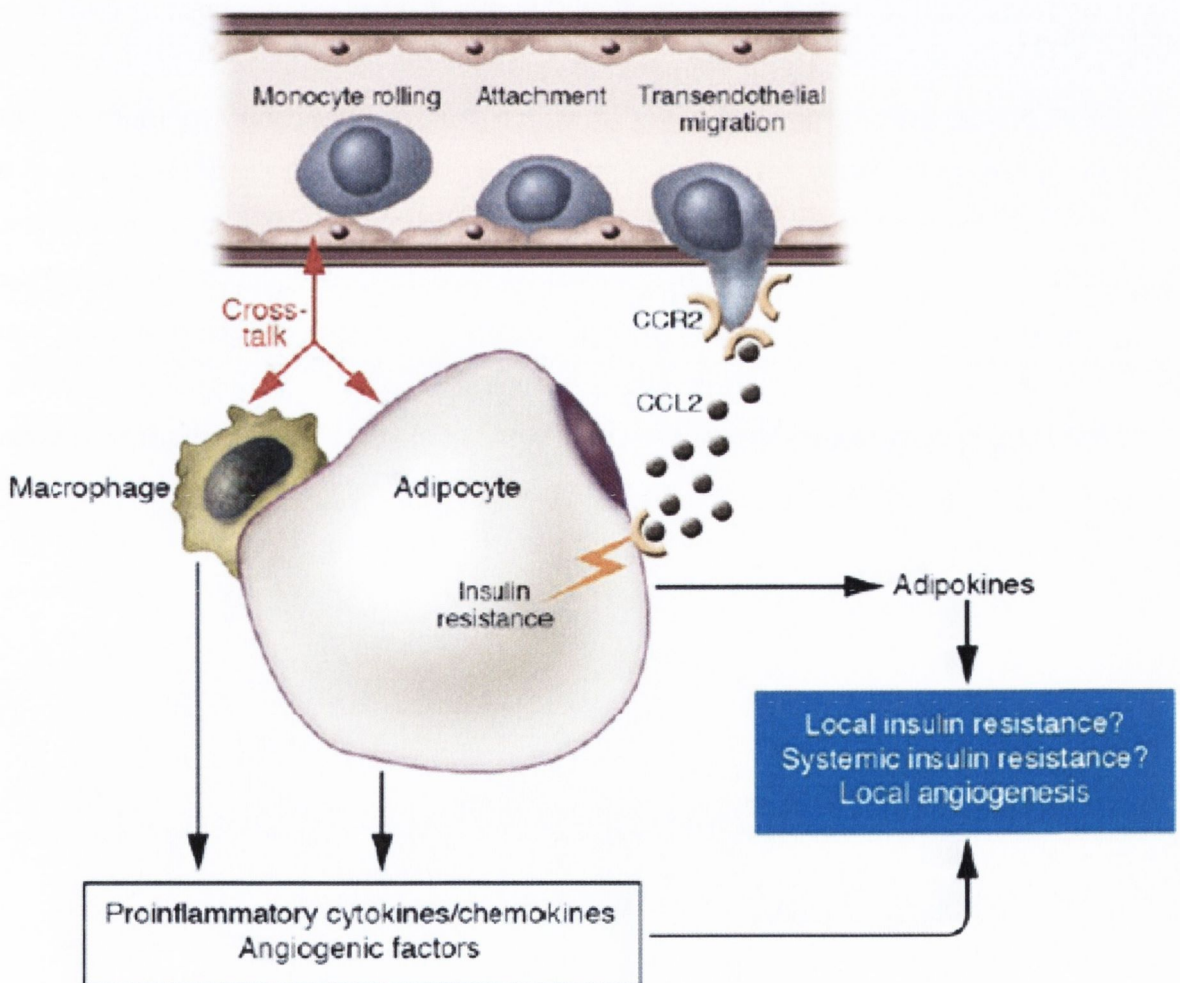
Figure 1.7: Monocyte adhesion occurs after initial rolling and attachment to activated endothelial cells. These monocytes then extravasate through the endothelial cell layer and differentiate into macrophages. MCP-1 (CCL-2) and its receptor CCR2 play an important role in this process (taken from Neels *et al*, 2006).

Under normal circumstances the inflammatory response is typically transient and is quickly resolved following tissue repair. However in pathological processes such as obesity and cancer, it has been proposed that a chronic sub-clinical level of inflammation persists, destroying tissue architecture and causing organ dysfunction (Cinti et al., 2005). In addition to increased numbers of ATMs in obesity (Weisberg et al., 2003), there is also evidence to suggest that the activation state of these macrophages is altered. Resident ATMs in normal weight are predominantly M2 polarised and thus produce low levels of pro-inflammatory mediators. Conversely, obesity is associated with an infiltrating population of pro-inflammatory M1 ATMs (Lumeng et al., 2007, Strissel et al., 2007). M1 or classical activation of macrophages is induced by hypoxia and by T_H1 pro-inflammatory cytokines such as IFNγ (Figure 1.8) present in visceral obesity (Strissel et al., 2007). M1 macrophages produce a variety of pro-inflammatory cytokines including TNFα, IL-6 and IL-12 and reactive oxygen species are generated following activation of inducible nitric oxide synthase (iNOS) to produce nitric oxide (NO) (Duffield, 2003). Alterative activation, M2 polarisation, is induced by T_H2 anti-inflammatory cytokines IL-4 and IL-13. M2 macrophages produce an anti-inflammatory response, secreting IL-4, IL-10 and IL-13 and suppressing production of pro-inflammatory cytokines and ROS (Gordon, 2003). Normal immune responses are characterised by a delicate balance of M1 and M2 macrophages. Both types are necessary for normal tissue damage repair and healing and a deficiency of either type can lead to a pathological response (Duffield, 2003). In obesity there is a switch in this fine balance to favour M1 polarisation, resulting in the creation of a pro-inflammatory phenotype (Lumeng et al., 2007). Infiltration and M1 activation of ATMs in visceral obesity is proposed to be a necessary step in the development of insulin resistance and Type II Diabetes (Lumeng et al., 2007) and therefore could play an important role in tumourigenesis.
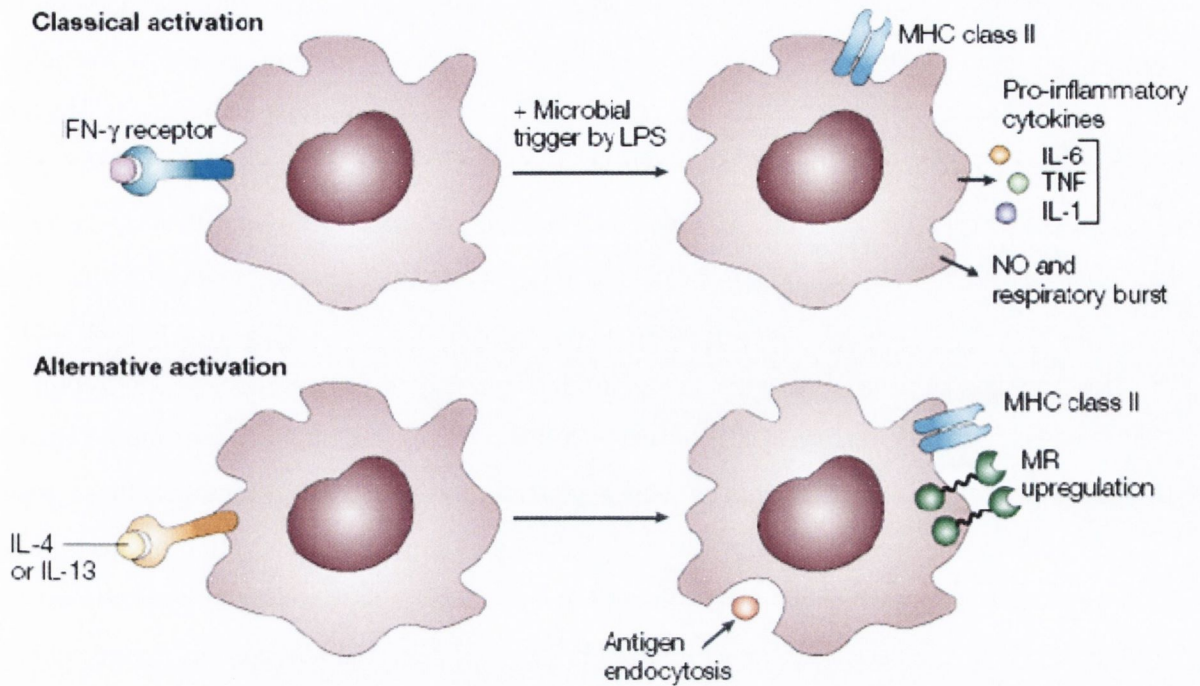
Figure 1.8: Classical activation is mediated by a priming stimulus by T$_H$1 cytokine IFN-γ, followed by a microbial trigger (e.g. lipopolysaccharide (LPS)). Alternative activation is mediated by T$_H$2 cytokines interleukin (IL) -4 and IL-8, acting through a common receptor (taken from Gordon *et al*, 2003).

1.3.5.2 Other adipose tissue infiltrating immune cells

In addition to the established role of ATMs, there is increasing evidence for the contribution of T lymphocytes, natural killer T (NKT) cells and mast cells to obesity induced adipose tissue inflammation (Anderson et al., 2010). Increased numbers of T lymphocytes have been reported in obese mouse models (Rocha et al., 2008, Wu et al., 2007). Infiltration of CD4$^+$, IFN-γ-producing T lymphocytes has been shown to be an early event during the development of insulin resistance in a mouse model of high fat diet (HFD) induced obesity, preceding the recruitment of monocytes (Kintscher et al., 2008). T$_H$1 cytokine IFN-γ was found to induce SGBS pre-adipocyte production of MCP-1 (Kintscher et al., 2008), a key chemokine in recruitment and classical activation of ATMs. Obese mice deficient in IFN-γ had decreased mRNA expression of pro-inflammatory cytokine TNF-α and chemokine MCP-1, decreased adipose tissue inflammation and improved glucose tolerance (Rocha et al., 2008). These data indicate the importance of the pro-inflammatory T$_H$1 cytokine IFN-γ in obesity induced inflammation. Infiltration of T lymphocytes has also been demonstrated in human adipose tissue, with increased mRNA expression of regulated on activation, normal T cell expressed and secreted (RANTES) and its receptor CCR5 in visceral adipose tissue in obese individuals (Wu et al., 2007). These findings suggest a key role for T$_H$1 polarised, IFN-γ producing T

lymphocytes in the orchestration of adipose tissue inflammatory processes. In addition to T lymphocytes, the presence of natural killer T (NKT) cells has been demonstrated in the adipose tissue of mice (Caspar-Bauguil et al., 2005). NKT cells are innate-like T lymphocytes which can produce a mixture of T_H1 and T_H2 cytokines such as IFN-γ and IL-4 (Caspar-Bauguil et al., 2005). A β2-microglobulin knockout mouse model lacking NKT cells was found to have decreased macrophage infiltration and improved glucose tolerance relative to the control mouse model following HFD induced obesity. Additionally, activation of NKT cells by administration of glycosphingolipid exacerbated glucose intolerance, increased macrophage infiltration and increased gene expression of T_H1 cytokine IFN-γ and chemokine MCP-1 in the adipose tissue of a mouse model of HFD induced obesity (Ohmura et al., 2010). Together these results demonstrate the importance of NKT cells in the recruitment and activation of macrophages and development of insulin resistance. A recent study has reported infiltration of mast cells prior to the appearance of macrophages in human adipose tissue with increased numbers found in the adipose tissue of obese individuals (Liu et al., 2009). Mast cells function mainly in allergic responses but have recently been demonstrated to play a role in obesity related diseases such as atherosclerosis (Sun et al., 2007) and may be important mediators of diet induced obesity and glucose intolerance via production of pro-inflammatory cytokines IL-6 and IFN-γ (Liu et al., 2009). Collectively, these recent studies provide evidence for the contribution of a variety of immune cells including macrophages, T lymphocytes, NKT cells and mast cells to the chronic inflammatory environment present in visceral obesity.

1.3.6 Models of Obesity

Adipose tissue consists of mature adipocytes surrounded by a stromal vascular fraction (SVF) composed of multiple different cell types. These include pre-adipocytes, endothelial cells, pericytes, fibroblasts, mesenchymal stem cells and immune cells (Kahn and Flier, 2000, Christiaens and Lijnen, 2010). In order to study this complex disorder, it may be of use to simplify the experimental system, focussing solely on one cell type at a time. *In vitro* cell culture is therefore an indispensable tool of scientific research, enabling the analysis of individual factors or pathways of interest under controlled conditions (Fischer-Posovszky et al., 2008). Ideally *in vitro* work would be carried out in individual populations of primary cells of interest; however there are a number of limitations concerning use of human material. This has led many research groups to rely on immortalised cell lines for *in vitro* studies (Fischer-Posovszky et al., 2008). Primary adipocytes are unpredictably variable between individuals due to a wide variety of factors including race, age, sex, genetic and lifestyle differences, weight differences, disease status, medication, type and length of surgery and site of sample harvest.

In addition, isolated primary cells can have a limited life span *in vitro* and the quantity of available tissue can sometimes be restricted. A cell line, on the other hand, can provide an unlimited supply of homogenous material (Wabitsch et al., 2001, Fischer-Posovszky et al., 2008, Rosenow et al., 2010).

The murine adipocyte cell lines 3T3-L1 and 3T3-F442A have been widely used to date and therefore are well characterised (Bour et al., 2007). Greater clinical relevance would be derived from working with a human model and to this end a human pre-adipocyte cell strain, SGBS, was established (Wabitsch et al., 2001). SGBS are derived from the stromal vascular fraction (SVF) of subcutaneous adipose tissue of an infant with Simpson-Golabi Behmel syndrome (SGBS), a rare X-linked disorder characterised by pre and post natal overgrowth (MIM 312870) (Wabitsch et al., 2001). 3T3-L1 and 3T3-F442A are mouse embryonic fibroblasts developed through clonal isolation to create an immortalised pre-adipocyte cell line (Rosen and MacDougald, 2006). 3T3 adipogenesis follows a well defined sequence of events marked by alterations in gene expression of early adipogenic transcription factors including CCAAT/enhancer binding protein α (C/EBPα), sterol regulatory element binding protein 1c (SREBP 1c) and peroxisome proliferator-activated receptor γ (PPARγ) (Rosen and MacDougald, 2006). These transcription factors induce expression of terminal adipocyte differentiation genes including adipocyte fatty acid binding protein (AP2), glucose transporter 4 (GLUT4), lipoprotein lipase (LPL), glyceraldehyde-3-phosphate dehydrogenase (GAPDH) and leptin, required for adipocyte function (MacDougald and Lane, 1995). Although SGBS adipogenesis is relatively less well described, similar changes in gene expression throughout the process of differentiation have been demonstrated (Wabitsch et al., 2001).

A growing number of comparative studies outline numerous species differences, alterations in patterns of cell growth, differential expression of splice variants of key proteins and altered adipokine expression between human and murine models (Newell et al., 2006, Wood et al., 2003, Bodles et al., 2006). 3T3-L1 and 3T3-F442A adipocytes undergo mitotic clonal expansion followed by growth arrest in the early stages of differentiation, while this process is absent both in SGBS and in primary human pre-adipocytes (Newell et al., 2006). It is not yet well understood if this difference arises due to *in vivo* clonal expansion of human pre-adipocytes prior to isolation, or alternatively that progression through the S phase of the cell cycle may be sufficient for human pre-adipocyte differentiation (Rosen and MacDougald, 2006, Newell et al., 2006). In either case, it is perhaps a significant characteristic of human adipogenesis.

Although the gene expression profile of adipogenesis is generally similar between 3T3 and SGBS, there are marked differences in several important factors. GLUT12, although expressed in mice is not expressed by 3T3-L1 cell line, while it is expressed by both primary human adipocytes and the SGBS cell line (Wood et al., 2003). Fasting induced adipose factor (FIAF), a novel adipokine identified in 2000 (Kersten et al., 2000), is produced by both SGBS and human white adipose tissue in native form, while only the truncated form is produced by 3T3-L1 (Mandard et al., 2004). 3T3-F442A and SGBS express different ratios of adiponectin isoforms in response to treatment with pioglitazone, indicating potential differences in insulin sensitivity and inflammatory phenotypes (Bodles et al., 2006). These data indicate that the human SGBS model may be more clinically relevant for the study of human obesity and disease. Once differentiated, SGBS have been shown to behave both functionally and biochemically like mature human adipocytes (Fischer-Posovszky et al., 2008).

The majority of adipokines to date have been identified using both *in vitro* and *in vivo* murine models, and differences commonly exist in humans with regard to expression, alternative splicing and function of these proteins (Galic et al., 2010, Rasouli and Kern, 2008). The scarcity of clinically relevant cell line models has therefore hindered obesity research to date and the human SGBS pre-adipocyte cell strain could represent an important new tool in the study of obesity (Fischer-Posovszky et al., 2008). A recent proteomic screen of SGBS uncovered a range of previously uncharacterised adipocyte secreted proteins, demonstrating the successful use of the SGBS model in novel adipokine discovery (Rosenow et al., 2010).

While the use of *in vitro* systems has simplified experimental systems and enabled characterisation of both the adipocyte differentiation process and the adipocyte secretome (Rosen and MacDougald, 2006, Rosenow et al., 2010), a number of disadvantages also exist (Perrini et al., 2008). Firstly, the adipocyte cell line lacks the important influence of the microenvironment, shown to play a key role in the development of the pro-inflammatory state characteristic of visceral obesity and crucial for the development of related diseases, including cancer (Weisberg et al., 2003, Colotta et al., 2009). Secondly, it has been shown that adipocytes differentiated *in vitro* retain the characteristics of the adipose tissue depot from which they were isolated (Tchkonia et al., 2006, Perrini et al., 2008). This observation must be taken into account when studying the subcutaneous derived SGBS model in the context of visceral obesity related disease. It therefore remains to be further investigated if

subcutaneous derived SBGS could present a clinically relevant model for the study of visceral obesity related disease.

1.4 Epidemiology of obesity and cancer

Obesity has recently been linked to increased incidence of an ever-growing list of cancers including postmenopausal breast, endometrial, kidney, colorectal, oesophageal adenocarcinoma, multiple myeloma, leukaemia, non-Hodgkin's lymphoma, pancreatic and ovarian (Reeves et al., 2007, Field et al., 2001, Guh et al., 2009). In males, the association between OAD and increased bodyweight has been shown by meta-analysis to be the strongest (RR 1.52, p<0.0001) (Figure 1.9), while in females OAD ranks third after endometrial and gallbladder carcinoma (RR 1.51, p<0.0001) (Figure 1.10). A strong inverse relationship exists between SCC and obesity in both males (RR 0.71, p<0.0001) (Figure 1.9) and females (RR 0.57, p<0.0001) (Figure 1.10) (Renehan et al., 2008). Obesity has also been linked to increased mortality following development of cancer (Calle et al., 2003) and this association has been shown in breast (Carmichael, 2006, Dal Maso et al., 2008), colorectal (Dignam et al., 2006, Haydon et al., 2006), endometrial (von Gruenigen et al., 2006), ovarian (Kjaerbye-Thygesen et al., 2006) and prostate cancer (Gong et al., 2007). Obesity could therefore contribute both to increased cancer incidence and also to increased tumour progression. While the epidemiological link is well documented, an increased understanding of the underlying molecular mechanisms responsible is now imperative.

Cancer site and type	Number of studies	RR (95% CI)	p	I^2
Oesophageal adenocarcinoma	5	1·52 (1·33–1·74)	<0·0001	24%
Thyroid	4	1·33 (1·04–1·70)	0·02	77%
Colon	22	1·24 (1·20–1·28)	<0·0001	21%
Renal	11	1·24 (1·15–1·34)	<0·0001	37%
Liver	4	1·24 (0·95–1·62)	0·12	83%
Malignant melanoma	6	1·17 (1·05–1·30)	0·004	44%
Multiple myeloma	7	1·11 (1·05–1·18)	<0·0001	7%
Rectum	18	1·09 (1·06–1·12)	<0·0001	3%
Gallbladder	4	1·09 (0·99–1·21)	0·12	0%
Leukaemia	7	1·08 (1·02–1·14)	0·009	0%
Pancreas	12	1·07 (0·93–1·23)	0·33	70%
Non-Hodgkin lymphoma	6	1·06 (1·03–1·09)	<0·0001	0%
Prostate	27	1·03 (1·00–1·07)	0·11	73%
Gastric	8	0·97 (0·88–1·06)	0·49	35%
Lung	11	0·76 (0·70–0·83)	<0·0001	63%
Oesophageal squamous	3	0·71 (0·60–0·85)	<0·0001	49%

Risk ratio (per 5 kg/m² increase)

Figure 1.9: Cancer and BMI in men (taken from Renehan et al 2007). The I^2 statistic measures the degree of heterogeneity between studies where I^2 values of 25%, 50%, and 75% correspond to cut-off points of low, medium and high heterogeneity, respectively.

Cancer site and type	Number of studies	RR (95% CI)	p	I^2
Endometrium	19	1·59 (1·50–1·68)	<0·0001	77%
Gallbladder	2	1·59 (1·02–2·47)	0·04	67%
Oesophageal adenocarcinoma	3	1·51 (1·31–1·74)	<0·0001	0%
Renal	12	1·34 (1·25–1·43)	<0·0001	45%
Leukaemia	7	1·17 (1·04–1·32)	0·01	80%
Thyroid	3	1·14 (1·06–1·23)	0·001	5%
Postmenopausal breast	31	1·12 (1·08–1·16)	<0·0001	64%
Pancreas	11	1·12 (1·02–1·22)	0·01	43%
Multiple myeloma	6	1·11 (1·07–1·15)	<0·0001	0%
Colon	19	1·09 (1·05–1·13)	<0·0001	39%
Non-Hodgkin lymphoma	7	1·07 (1·00–1·14)	0·05	47%
Liver	1	1·07 (0·55–2·08)		
Gastric	5	1·04 (0·90–1·20)	0·56	4%
Ovarian	13	1·03 (0·99–1·08)	0·30	55%
Rectum	14	1·02 (1·00–1·05)	0·26	0%
Malignant melanoma	5	0·96 (0·92–1·01)	0·05	0%
Premenopausal breast	20	0·92 (0·88–0·97)	0·001	39%
Lung	6	0·80 (0·66–0·97)	0·03	84%
Oesophageal squamous	2	0·57 (0·47–0·69)	<0·00 01	60%

Risk ratio (per 5 kg/m² increase)

Figure 1.10: Cancer and BMI in women (taken from Renehan et al 2007). The I^2 statistic measures the degree of heterogeneity between studies where I^2 values of 25%, 50%, and 75% correspond to cut-off points of low, medium and high heterogeneity, respectively.

28

1.5   Obesity and cancer treatment

Obesity is associated with increased mortality in many cancers (Calle et al., 2003). A BMI > 30 was found to confer an 11% increased risk of cancer recurrence and overall mortality in colon cancer (Meyerhardt et al., 2003). In breast cancer, obese patients were found to present with a higher pathological tumour stage than their normal weight counterparts (Litton et al., 2008). A number of factors may contribute to the association of obesity with increased cancer mortality including increased disease recurrence (Kroenke et al., 2005, Dignam et al., 2006), increased wound healing complications (El-Tamer et al., 2007), delay in cancer diagnosis due to lower screening rates (Maruthur et al., 2009a) and poorer response to therapy (Litton et al., 2008). Breast cancer detection has been demonstrated to be lower in obese women. A meta-analysis found that mammography screening rates were 20% lower in class III morbidly obese women (BMI > 40) (Maruthur et al., 2009a). Another meta-analysis found an inverse relationship between cervical cancer screening rates and obesity (Maruthur et al., 2009b). Lower screening rates of obese individuals could contribute to delayed diagnosis, leading to presentation of these patients with more clinically advanced tumours (Maruthur et al., 2009a). In addition, inadequate neoadjuvant chemotherapy dosing in obese breast cancer patients could contribute to poorer outcome in these patients (Griggs et al., 2005). The doses of most chemotherapy drugs are calculated by body surface area (BSA) and are often reduced in obese patients with a BSA > 2 m^2 due to overdosing concerns (van der Sijs and Guchelaar, 2002, Griggs et al., 2005). Many large studies indicate that the beneficial impact of neoadjuvant chemotherapy is diminished when full doses of therapy are not given (Griggs et al., 2005) and therefore sub-optimal dosing could contribute to increased cancer mortality in obese patients. Overweight and obese breast cancer patients were found to be significantly less likely to obtain a complete pathological response to neoadjuvant therapy than normal weight patients (Litton et al., 2008). This could be due in part to sub-optimal dosing. Also, excess body weight has also been linked to altered clearance of cytotoxic drugs (Rodvold et al., 1988, Litton et al., 2008), potentially via a number of mechanisms including altered levels of circulating growth factors, hormones and cytokines (described in section 1.6). Response to radiotherapy may also be adversely affected by obesity (Carmichael and Bates, 2004, King et al., 2009). While molecular factors have not yet been investigated, obesity may be associated with technical difficulties in applying the adequate radiation dose to the correct area; this has been suggested in breast (Carmichael and Bates, 2004) and prostate cancer (King et al., 2009). Identification of the factors associated with poorer response to CRT in obesity could therefore

lead to reassessment of current CRT regimens and guide the development of individualised patient treatment.

1.6   Candidate molecular mechanisms linking obesity and cancer

Several mechanisms of obesity related pathogenesis have been proposed to date. It is well established that visceral obesity has a pronounced effect on levels of circulating growth factors (including insulin and IGF), sex hormones (including oestrogen and androgens) and cytokines (including leptin and adiponectin) (Donohoe et al., 2010, Renehan et al., 2006). Insulin resistance and compensatory hyperinsulinaemia are common metabolic disorders in visceral obesity (Roberts et al., 2009, Federation, 2006) and are associated with increased incidence of OAD (Neale et al., 2009, Watanabe et al., 2007). Treatment with the anti-diabetic drug metformin decreases insulin and glucose levels, increases insulin sensitivity and reduces cancer risk in diabetic patients (Evans et al., 2005, Gonzalez-Angulo and Meric-Bernstam, 2010). This drug is currently in clinical trials in a group of 1000 breast cancer patients (Cazzaniga et al., 2009). Hyperinsulinaemia has been linked to increased circulating amounts of bioactive, bio-available insulin like growth factor 1 (IGF-1) through decreased expression of IGF binding proteins 1 and 2 (IGFBP1, 2) (Donohoe et al., 2010, Renehan et al., 2006). Together these growth factors exert both mitogenic and anti-apoptotic effects, creating an environment favourable for tumourigenesis (Renehan et al., 2006) and elevated IGF-1 has been linked to prostate and premenopausal breast cancer (Renehan et al., 2004). Chronic hyperinsulinaemia can lead to reduction in circulating levels of sex hormone binding globulin (SHBG), increasing levels of bio-available oestrogen to produce both mitogenic and mutagenic effects in oestrogen responsive tissues (Donohoe et al., 2010, Calle and Kaaks, 2004, Roberts et al., 2009). Sex specific differences in circulating levels of androgens have been proposed to be responsible for the association of male sex with OAD and higher levels of testosterone have been demonstrated in OAD patients (Awan et al., 2007).

Reliance of tumour cells on glycolysis even in the presence of oxygen is a phenomenon termed the Warburg effect, a fundamental hallmark of cancer providing the basis for the widely used 2-[^{18}F] fluoro-2-deoxyglucose positron emission tomography (FDG-PET) molecular imaging of tumours including OAD (Kelloff, G.J., 2005). Molecular imaging of glucose metabolism by FDG-PET has been shown to be a feasible measure of neoadjuvant response in OAD (Roedl et al., 2009), demonstrating that glycolytic flux is linked to tumour response to therapy. Glycolysis has been found to be up regulated in Barrett's oesophagus relative to normal squamous oesophagus (van Baal et al., 2006) indicating that this may be an important biochemical

transformation in the sequence of progression from Barrett's to OAD. In terms of ATP production glycolysis is far less efficient than oxidative phosphorylation and so tumour cells must compete for limited nutrients through enhanced glycolytic pathway flux (Kelloff, G.J., 2005, Vander Heiden 2010). As tumour cells are adapted to outcompete their normal neighbours for nutrients, chronic hyperglycaemia characteristic of visceral obesity could specifically fuel tumour growth. Enhanced production of lactate as the end metabolite of this pathway increases the pH of the tumour microenvironment, eradicating normal cells, expanding margins of the neoplasic area (Kellenberger et al., 2010) and promoting increased tumour invasion (Martinez-Zaguilan et al., 1996). This adaptation of tumour cells to exploit obesity related hyperglycaemia could be targeted in a therapeutic manner in to reduce tumour aggressiveness in viscerally obese cancer patients.

1.7 Visceral obesity can modulate the hallmarks of OAD

A seminal contribution to the understanding of mechanisms involved in cancer biology came with the identification of six essential changes to cell physiology both necessary and sufficient to give rise to carcinoma development. These hallmarks of cancer were proposed to be self sufficiency in growth signals, insensitivity to anti-growth signals, evasion of apoptosis, limitless replicative potential, sustained angiogenesis and tissue invasion and metastasis (Figure 1.11) (Hanahan and Weinberg, 2000). More recently, a state of 'smouldering' chronic sub-clinical inflammation has been identified as a seventh hallmark of cancer (Colotta et al., 2009). Obesity is now established to be a major risk factor for both cancer initiation and progression, giving rise to increased cancer incidence and increased cancer mortality (Calle et al., 2003). The molecular mechanisms behind these associations are not yet fully understood, but there are preliminary indications that obesity may share several hallmarks with cancer such as *de novo* angiogenesis (Christiaens and Lijnen, 2010) and a chronic state of inflammation (Xu et al., 2003). Uncovering the mechanisms of interaction in visceral obesity and cancer could identify shared pathways as potential preventative and therapeutic targets. This strategy may be particularly relevant in shared pathways which are up regulated by the cluster of metabolic abnormalities characteristic of viscerally obese individuals (Federation, 2006).
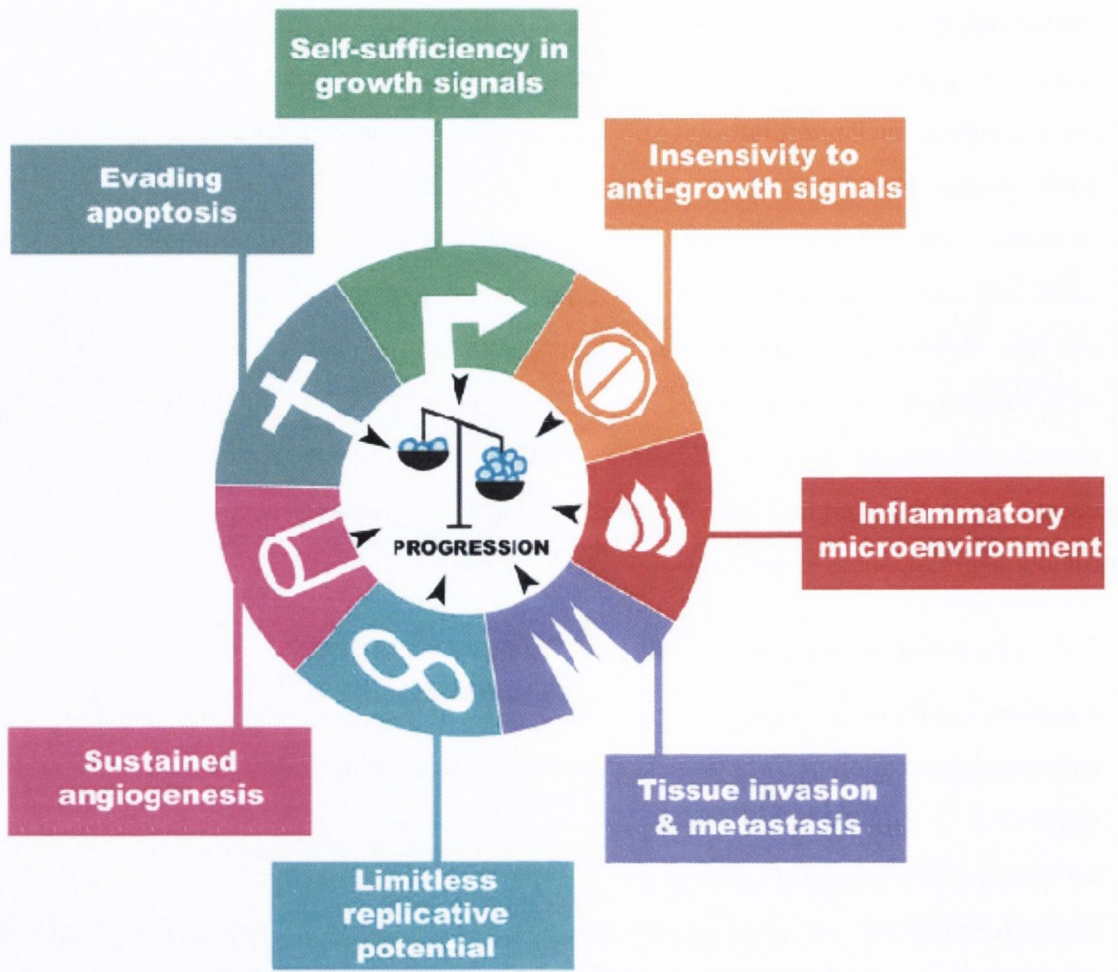
Figure 1.11: The hallmarks of cancer (taken from Colotta et al 2009).

1.7.1   Self-sufficiency in growth signals

Tumours respond to exogenous growth signals by expressing appropriate receptors for circulating growth factors, hormones and cytokines (Lagarde et al., 2007). Tumour production of growth signals, over expression of relevant receptors and constitutive activation of these receptors can remove tumour dependence on exogenous signals and lead to self-sufficient proliferation (Lagarde et al., 2007). Several genes have been shown to be prognostic indicators in OAD. Cyclin D1 (CCND1) is an oncogene involved in cell cycle regulation (Lagarde et al., 2007) and CCND1 amplification and nuclear localisation has been associated with OAD survival (Bani-Hani et al., 2000, Miller et al., 2003). Another pathway demonstrated to be of great importance in OAD is epidermal growth factor (EGF) and transforming growth factor alpha (TGFα) binding to the EGF receptor tyrosine kinase (EGFR) family to increase cell proliferation (Spano et al., 2005). EGFR and related ErbB2 (HER2/neu) genes are commonly amplified in OAD, with frequencies of 8% and 22%, respectively (Miller et al., 2003). EGFR over expression is associated with advanced tumour stage, lymph node metastasis and poorer patient survival in many cancers including OAD (Wang et al., 2007). Cetuximab, trastuzumab and gefitinib are inhibitors targeted against the EGFR family currently under investigation in the treatment of many cancers including OAD (Peters and Fitzgerald, 2007, Safran et al., 2007).

Visceral obesity and insulin resistance are associated with elevated levels of leptin (Segal et al., 1996). Leptin has been demonstrated to act as a growth factor *in vitro*, stimulating growth of breast cancer, Barrett's oesophagus and OAD cell lines (Hu et al., 2002, Ogunwobi and Beales, 2008b, Somasundar et al., 2003, Ogunwobi et al., 2006). A bidirectional synergistic effect has been observed between leptin and IGF-1 *in vitro* and together these growth factors have been demonstrated to induce transactivation of the EGFR (Saxena et al., 2008). MMP activity is necessary for EGFR transactivation (Prenzel et al., 1999) and MMP inhibitors prevent leptin and IGF-1 induced tyrosine phosphorylation of EGFR (Saxena et al., 2008) in addition to inhibiting the proliferative effects of leptin in OAD cell lines (Ogunwobi and Beales, 2008b). In patients, primary or treatment induced resistance to EGFR targeted cancer therapy is frequent (Fiorio et al., 2008). The development of novel treatments to target the leptin pathway could therefore be useful, especially in the treatment of resistant tumours (Fiorio et al., 2008). Targeted treatment of the leptin pathway would be particularly relevant in obese patients with elevated circulating levels of leptin and IGF-1.

1.7.2 Insensitivity to anti-growth signals

In addition to acquiring self-sufficiency in growth signals, successful tumour cells must also evade anti-growth signals (Hanahan and Weinberg, 2000). One mechanism by which this is achieved is through down regulation, loss or mutation of relevant receptor or downstream signalling protein expression in tumour cells. For example, transforming growth factor- β (TGF-β), a cytokine produced by adipose tissue (Trayhurn and Wood, 2004), plays an important role in many cancers as a negative growth factor and tumour suppressor (Lagarde et al., 2007). The TGF-β signalling cascade is frequently mutated in gastrointestinal malignancies (Onwuegbusi et al., 2006). Barrett's oesophagus is associated with inactivation of TGF-β signalling molecule SMAD4 (Onwuegbusi et al., 2006) and OAD is associated with loss of functional TGF-β receptor expression (Lagarde et al., 2007).

Visceral obesity and insulin resistance are associated with decreased serum levels of anti-inflammatory adipokine adiponectin (Arita et al., 1999). Reduced levels of adiponectin have also been linked to gastric (Ishikawa et al., 2005), breast (Miyoshi et al., 2003), endometrial (Petridou et al., 2003) and prostate cancer (Goktas et al., 2005). Adiponectin has been demonstrated to exert anti-proliferative effects *in vitro*, inhibiting leptin induced growth of OAD cell lines (Ogunwobi and Beales, 2008a). Expression of both AR1 and AR2 have been shown to be down regulated in gastric cancer, suggesting tumour cell evasion of the anti-proliferative effects of adiponectin signalling (Otani et al., 2010). However similar studies in colon, breast and OAD have yielded conflicting results, indicating that more work needs to be carried out in this area (Howard et al., 2010, Takahata et al., 2007, Yoneda et al., 2008).

1.7.3 Evasion of apoptosis

The ability of a tumour to expand in size is not solely linked to the rate of proliferation but is also dependent on rate of programmed cell death, or apoptosis (Hanahan and Weinberg, 2000). Tumour suppressor p53 lies at the hub of a vast signalling network involved in the maintenance of genomic stability and its importance is well established in protection against carcinogenesis (Harris and Levine, 2005). Under normal conditions p53 is marked for ubiquitin-mediated degradation by negative inhibitor MDM2 and in response to acute damage is stabilised through inhibition of its interaction with MDM2 (Whibley et al., 2009). The p53 network is activated in response a variety of cellular insults including DNA damage, over expression of oncogenes and hypoxia (Vogelstein et al., 2000). Tumour suppressor ataxia telangiectasia mutated (ATM) detects double stranded breaks in DNA and activates p53 by phosphorylation. This pathway triggers cell cycle arrest and subsequent senescence or

apoptosis of cells harbouring potentially oncogenic alterations (Vogelstein et al., 2000). Deregulation of the p53 network is a universal hallmark of cancer and loss of function mutations in this tumour suppressor occur in over 50% of cancers (Vogelstein et al., 2000). Mutations in p53 were found in approximately half of OAD patients (Madani et al., 2010, Schneider et al., 2000) and were significantly associated with p53 over expression, poorer tumour differentiation and poorer patient survival (Madani et al., 2010). Tumour suppressor p53 has also been linked to cellular metabolism. Loss of p53 function is associated with reduced oxygen consumption and the switch to anaerobic glycolysis characteristic of tumour cells (Matoba et al., 2006, Vousden and Lane, 2007). This data indicates that p53 expression may be an important mediator of altered cellular metabolism in obesity.

Adiponectin has been shown to induce apoptosis in endothelial cells *in vitro* through cascade activation of caspase-3, -8, and -9. In addition, adiponectin administration in a fibrosarcoma mouse model was demonstrated to cause tumour cell apoptosis (Brakenhielm et al., 2004). The anti-apoptotic effects of leptin have been demonstrated in the oesophageal adenocarcinoma (Ogunwobi et al., 2006) and colon cancer cell lines (Ogunwobi and Beales, 2007). In addition, leptin has been demonstrated *in vitro* to synergistically enhance the anti-apoptotic effects of acid treatment, mimicking exposure of cells to acid reflux (Beales and Ogunwobi, 2007). The altered metabolic state present in obesity is characterised by an increase in levels of anti-apoptotic leptin (Otero et al., 2005) and a concurrent decrease in levels of pro-apoptotic adiponectin (Yamauchi et al., 2001). Altered levels of these circulating adipokines could therefore exert a protective effect on the growing tumour.

1.7.4 Limitless replicative potential

Normal cells undergo a finite number of replications before entering senescence (Hanahan and Weinberg, 2000). Telomerase is a reverse transcriptase that specifically synthesises telomeric DNA, lengthening the ends of chromosomes and thus extending the life span of the cell. Normal cells do not express telomerase and therefore exhibit a progressive shortening of their telomeres with each round of division. Eventually this results in degradation of chromosome ends and can give rise to aberrant fusion, triggering cell senescence (Shay and Bacchetti, 1997). Reactivation of telomerase in tumour cells is required to overcome replicative senescence (Kyo et al., 1999) and approximately 90% of tumour cells express active telomerase (Shay and Bacchetti, 1997, Gertler et al., 2008). In OAD, there is a significant increase in telomerase expression relative to normal oesophagus (Shammas et al., 2008, Gertler et al., 2008), and expression is significantly correlated with prognosis (Gertler et al.,

2008). Treatment with telomerase inhibitors has been shown to inhibit OAD growth both *in vitro* and *in vivo* (Shammas et al., 2008) and this pathway could therefore represent a novel therapeutic strategy in the treatment of this cancer. Telomerase inhibitor Imetelstat (GRN163L) has been demonstrated to reduce tumour proliferation and metastasis in a xenograft breast cancer model and could present a promising candidate for clinical trials (Hochreiter et al., 2006).

The transcription of human telomerase reverse transcriptase (hTERT) has been recently demonstrated to be regulated by a number of obesity related factors. Levels of leptin, IGF-1 and oestrogen are elevated in obesity (Roberts et al., 2009, Fruhbeck, 2006) and these factors can mediate the activation of hTERT via their respective signalling pathways (Kyo et al., 1999, Wetterau et al., 2003, Ren et al., 2010). STAT3 is a transcription factor involved in cytokine and growth factor signalling, frequently over expressed in cancer. STAT3 has been demonstrated to be involved in regulation of hTERT transcription (Konnikova et al., 2005) and it has been suggested that oestrogen and leptin can function synergistically to increase STAT3 phosphorylation thus up regulating hTERT expression (Gao et al., 2007). Oestrogen, IGF-1 and leptin could therefore be attractive therapeutic targets to reduce telomerase activation and induce tumour senescence in viscerally obese OAD patients.

1.7.5 Sustained angiogenesis

The establishment of new blood vessels by *de novo* angiogenesis is a prerequisite process for development, progression and dissemination of malignant tumours (Hanahan and Weinberg, 2000). Vascular endothelial growth factor (VEGFA) is a potent inducer of angiogenesis that stimulates endothelial cell proliferation and invasion into the extracellular matrix to form new vasculature. VEGFA signalling is induced by hypoxia, a characteristic hallmark of a rapidly expanding tumour that outgrows its blood supply (Bergers et al., 2000). VEGFA is up regulated early in the sequence of progression from Barrett's oesophagus to OAD, contributing to early onset local tumour spread and metastasis to distant organs (Kleespies et al., 2004, Griffiths et al., 2007). VEGFA therefore could represent an attractive therapeutic target and preliminary results from ongoing clinical trials in oesophageal cancer are promising (Syrigos et al., 2008).

The process of angiogenesis has been well characterised in tumourigenesis and is recently proposed to be of great importance during adipose tissue expansion in visceral obesity (Trayhurn et al., 2008). Unlike most other tissues, adipose tissue displays great plasticity, expanding and reducing in size throughout the lifespan of the individual according to energy

abundance (Christiaens and Lijnen, 2010). Adipose tissue is an extensively vascularised organ with each adipocyte surrounded by at least one capillary (Lijnen, 2008). In order for adipose tissue to expand while maintaining a steady supply of oxygen and nutrients, the rate of angiogenesis must parallel the rate of tissue growth. Analogous to tumour growth in cancer, adipose tissue expansion in obesity is therefore tightly associated with the process of angiogenesis. Adipose tissue produces a wide variety of pro-angiogenic factors including the major angiogenic factor VEGFA together with many others including hepatocyte growth factor (HGF), fibroblast growth factor (FGF), platelet-derived growth factor (PDGF)-β, leptin, angiopoietin (ang)-1 and 2, transforming growth factor (TGF)-β, tissue necrosis factor (TNF)-α, tissue factor (TF), plasminogen activator inhibitor (PAI)-1 and matrix metalloproteinases (MMPs) (Christiaens and Lijnen, 2010). The levels of many of these adipokines are increased in obesity including VEGFA (Silha et al., 2005), TGF-β (Samad et al., 1997), leptin (Segal et al., 1996), TNF-α (Katsuki et al., 1998), TF (Samad et al., 1998), PAI-1 (Ma et al., 2004) and MMPs (Catalan et al., 2009). These adipokines can act to increase the expression of potent angiogenic factors. For example, leptin has been demonstrated to up regulate VEGFA expression through Jak/STAT signalling thereby inducing aggregation of endothelial cells and tube formation *in vitro* (Sierra-Honigmann et al., 1998, Suganami et al., 2004). The development of a hypoxic environment in both obesity and cancer leads to increased immune cell infiltration (Trayhurn et al., 2008, Colotta et al., 2009). ATM production of matrix degrading proteinases and pro-angiogenic cytokines implicates these immune cells in ECM remodelling and angiogenesis, necessary for adipose tissue expansion (Huber et al., 2007, Strissel et al., 2007). The development of a hypoxic environment in visceral obesity could therefore contribute to the creation of a milieu favourable for sustained angiogenesis through increased production of proteolytic factors and pro-angiogenic adipokines (Christiaens and Lijnen, 2010, Trayhurn et al., 2008). Pro-angiogenic pathways could present potential targets for therapeutic interventions to inhibit processes of sustained angiogenesis in OAD, particularly in viscerally obese patients.

1.7.6 Tissue invasion and metastasis

Oesophageal adenocarcinoma is an aggressive disease associated with a poor five year survival of merely 15% (National Cancer Registry Ireland, 2000-2005). This is due in part to the early lymphatic and haematogenous dissemination associated with this disease (Lagarde et al., 2007) implying that pathways involved in tumour invasion and metastasis are of particular significance. Tumour metastasis accounts for up to 90% of cancer mortality (Hanahan and Weinberg, 2000) and therefore the increased understanding of these pathways is of utmost

importance. Proteolytic cleavage and degradation of the extracellular matrix, carried out by matrix metalloproteinases (MMPs) and serine proteases, is necessary for both the establishment of a new blood supply and tumour metastasis (Liotta et al., 1991, Ludwig, 2005). MMP2 and MMP9 are members of the gelatinase family of matrix metalloproteinases which degrade type IV collagen, the principle component of the basement membrane (Liotta et al., 1991, Ludwig, 2005, Turpeenniemi-Hujanen, 2005). MMP2 and MMP9 knockout mice have decreased incidence of metastasis following tumour cell implantation (Itoh et al., 1999, Itoh et al., 1998), demonstrating the importance of these MMPs in tumour invasion and metastasis. The role of MMPs as prognostic factors in OAD has not yet been established, however they have been linked to poor prognosis in many obesity related cancers including breast (Sternlicht et al., 2006, Harbeck et al., 2004), rectal (Langenskiold et al., 2009, Angenete et al., 2009) and colorectal carcinoma (Sakakibara et al., 2005). In addition, there is a recently established role for MMP protease activity in leptin mediated transactivation of the EGFR pathway (Ogunwobi and Beales, 2008b, Saxena et al., 2008) which has been linked to advanced tumour stage, lymph node metastasis and survival in OAD (Wang et al., 2007). Levels of MMP2 and MMP9 are elevated in visceral adipose tissue in obesity (Catalan et al., 2009) and decreased in response to treatment with insulin sensitising pioglitazone (Unal et al., 2010) and diet induced weight loss (Madsen et al., 2009). It has been shown that leptin signalling can induce MMP2 activation via p38 MAP Kinase signalling (Schram et al., 2010). The leptin signalling pathway could therefore present a therapeutic target to reduce MMP levels, particularly relevant in viscerally obese patients with elevated levels of leptin.

There is accumulating evidence for an important role of the plasminogen system and serine proteases in tumour invasion and metastasis. Plasminogen activator inhibitor 1 (SerpinE1/PAI-1) is a serine protease inhibitor which, through inhibition of various plasminogen activator isoforms, prevents plasminogen cleavage to form plasmin. Plasmin is involved in ECM degradation and activation of growth hormones and MMP zymogens including MMP2 and MMP9 and is negatively associated with patient survival (Festuccia et al., 1998, Durand et al., 2004). Thus it is counter-intuitive that elevated levels of its inhibitor, PAI-1, is associated with enhanced tumour invasion and metastasis (Duffy and Duggan, 2004, Liotta et al., 1991). Separate from its role in inhibition of the plasmin pathway, PAI-1 has been shown to modulate cell adhesion through altered binding of the cell to ECM protein vitronectin (Brooks et al., 2000). Treatment of a fibrosarcoma cell line with PAI-1 induces a dose dependant decrease in vitronectin binding and a corresponding increase in migratory and invasive capacity and these

effects are blocked by an antibody against PAI-1 (Brooks et al., 2000). PAI-1 therefore could support tumour metastasis by promoting tumour cell detachment from the ECM, thereby allowing tumour cell migration. While elevated PAI-1 has been linked to breast cancer, the role of PAI-1 in OAD has not yet been well studied (Duffy and Duggan, 2004). PAI-1 has been proposed to have a direct role in obesity and insulin resistance. Mice deficient in PAI-1 have reduced adipose tissue mass, insulin resistance and hyperglycaemia (Ma et al., 2004). Treatment with a PAI-1 inhibitor not only reduced serum triglyceride levels in an APC deficient colorectal cancer mouse model, but reduced the number of intestinal polyps (Mutoh et al., 2008). These findings support a potential role for modulation of levels of PAI-1 activity in the treatment of cancer. PAI-1 inhibition could be particularly relevant in viscerally obese patients with high circulating levels of PAI-1.

Following ECM degradation, metastasis requires movement of tumour cells through the basement membrane and epithelium into the blood stream and lymphatic system (Turpeenniemi-Hujanen, 2005). For this to occur, tumour cells must acquire a migratory phenotype which involves altered expression of cell adhesion molecules and reorganisation of the cytoskeleton in a process known as epithelial mesenchymal transition (EMT) (Alves et al., 2009). Integrin mediated signalling plays an integral (hence the name) role in attachment of the cytoskeleton to the extracellular matrix through the formation of focal adhesion complexes. The focal adhesion complex interacts with the cytoplasmic tail of the activated integrin cluster triggering downstream signalling events to initiate cytoskeletal reorganisation and ECM remodelling, required for angiogenesis, epithelial mesenchymal transition (EMT), migration and invasion to occur (Zhao and Guan, 2009). One of the key features of EMT is down regulation of cell adhesion molecule E-cadherin, and transcription factor Slug has been identified as an important repressor of E-cadherin expression (Alves et al., 2009). OAD cell lines over expressing Slug were found to have increased expression of mesenchymal markers vimentin and fibronectin and decreased expression of epithelial marker E-cadherin, indicating a gain in motility (Jethwa et al., 2008). These changes corresponded to a functional effect with Slug over expression linked to increased OAD cell proliferation and invasion *in vitro* (Zhang et al., 2010). Increased Slug expression together with nuclear localisation of this transcription factor has been observed in the progression from Barrett's oesophagus to OAD, and these changes correlated with decreased E-cadherin expression (Jethwa et al., 2008). Slug is expressed in adipose tissue and is required for adipogenesis (Perez-Mancera et al., 2007). Slug over expressing mice display adipocyte hypertrophy while adipose tissue mass is reduced in

Slug deficient mice (Perez-Mancera et al., 2007). Slug may therefore represent a common pathway in obesity and cancer and could be a novel therapeutic target in OAD, particularly in obese individuals.

1.7.7   Inflammatory microenvironment

Approximately 15% of the global cancer burden is linked to infectious agents and resulting inflammation (Balkwill and Mantovani, 2001). Cancers associated with infectious agents and subsequent inflammation include gastric cancer (linked to *Helicobacter pylori* infection), cervical carcinoma (linked to human papillomavirus infection) and hepatic carcinoma (linked to Hepatitis B and C infection) (Balkwill and Mantovani, 2001). The use of non-steroidal anti-inflammatory drugs (NSAIDs) such as aspirin has been linked to decreased risk of gastrointestinal cancers (Langman et al., 2000). This association of inflammation and cancer is particularly evident in OAD where chronic inflammation resulting from prolonged GORD predisposes to Barrett's oesophagus and OAD (Flejou, 2005). A stepwise increase in pro-inflammatory cytokine IL-1β and chemokine IL-8 has been demonstrated in the progression of normal oesophagus to Barrett's oesophagus to OAD (O'Riordan et al., 2005) and levels of pro-inflammatory IL-6 have also been found to be elevated in Barrett's oesophagus (Dvorakova et al., 2004). These pro-inflammatory cytokines induced in GORD damaged tissue are proposed to mediate their effects through activation of transcription factors NF-κB and STAT3, expressed at higher levels in Barrett's oesophagus (O'Riordan et al., 2005, Dvorakova et al., 2004). Inhibition of pro-inflammatory cytokine signalling may present a therapeutic target in the sequence of progression from normal oesophagus to Barrett's to OAD.

Nuclear factor (NF)-κB is a transcription factor with a central role in the regulation of genes involved in inflammation and carcinogenesis such as iNOS and COX-2 (Babar et al., 2010, Kyrgidis et al., 2005). Under normal circumstances NF-κB is held inactive in the cytoplasm, bound to its inhibitor IκB. Pro-inflammatory cytokines including TNFα and IL-1 activate NF-κB through release from its inhibitor IκB thereby allowing translocation to the nucleus where it exerts an anti-apoptotic effect (Lagarde et al., 2007). There is a step-wise up regulation of NF-κB expression in the sequence of progression from normal oesophagus to Barrett's oesophagus to OAD, and expression correlates with patient response to neoadjuvant therapy (Abdel-Latif et al., 2004). COX-2 is an important rate-limiting enzyme in prostaglandin production, the target pathway of NSAIDs, frequently over expressed in both Barrett's oesophagus and OAD (Syrigos et al., 2008). The specific COX-2 inhibitor celecoxib inhibits NF-

κB activation leading to the down regulation of COX-2 in non-small cell lung carcinoma (Shishodia et al., 2004).

Key features of cancer related inflammation include infiltration of macrophages and immune cells, production of pro-inflammatory cytokines and tumour remodelling and angiogenesis (Colotta et al., 2009). The development of hypoxia, linked with both malignant tumour growth (Balkwill and Mantovani, 2001) and adipose tissue expansion (Trayhurn et al., 2008), is strongly associated with these processes (Colotta et al., 2009). Therefore visceral obesity may play an important role in cancer related inflammation. It is now established that visceral obesity is associated with an adipose tissue infiltration of pro-inflammatory immune cells such as macrophages and T lymphocytes (Weisberg et al., 2003, Xu et al., 2003). In addition, these infiltrating immune cells have been shown to be classically activated and produce pro-inflammatory cytokines and chemokines (Lumeng et al., 2007). It has been suggested that the resulting chronic inflammatory phenotype could not only be characteristic of visceral adiposity (Wellen and Hotamisligil, 2005) but also of cancer (Mantovani et al., 2008). The pro-inflammatory phenotype characteristic of visceral obesity could therefore be an important contributing factor to the newly established association between chronic inflammation and cancer (Colotta et al., 2009).

1.8 Aims and objectives

1.8.1 General aim

Obesity is linked both to increased cancer incidence and increased cancer mortality (Calle et al., 2003). Of all cancers, OAD displays one of the strongest links with obesity (Renehan et al., 2008) and so presents an ideal model with which to study this association. The overall aim of this thesis is to dissect the molecular pathways linking obesity and OAD and to determine if obesity could be linked to increased aggressiveness of this disease.

1.8.2 Specific objectives

The overall aim of this thesis will be investigated by a) identification of a pro-tumour gene expression signature present in visceral adipose tissue of OAD patients, b) identification of an adipokine profile associated with both visceral obesity and male sex and c) identification of a gene signature characteristic of OAD which is altered in visceral obesity. In addition, standard measurements of obesity BMI, WC and VFA will be assessed to determine which measure is the strongest predictor of visceral obesity related pathology. Finally, this work will evaluate the clinical relevance of the newly established human adipocyte cell strain SGBS for *in vitro* studies of obesity and cancer. The identified candidate pathways linking visceral obesity and OAD will be examined in OAD biopsies with respect to obesity status, tumour stage and survival. This will allow dissection of the complex role of obesity in the process of tumour initiation and promotion. The knowledge obtained from this series of experiments will assist in the understanding of this obesity associated cancer and in the development of novel therapeutic strategies in its prevention and treatment.

2 Material and Methods

2.1 Reagents

All laboratory chemicals and reagents were purchased from Sigma Chemical Company (MO, USA) unless otherwise stated, and prepared and stored according to manufacturer's instructions. Solid reagents were weighed using a Scout Pro electronic balance (Ohaus Corporation, NJ) or an Explorer Pro fine electronic balance (Ohaus Corporation, NJ), and made up using double distilled water, unless otherwise stated. The pH of solutions was measured using a pH 211 microprocessor pH metre (Hanna instruments, RI, USA), calibrated with buffers at pH 4, pH 7 and pH 10. Solutions were autoclaved prior to use and stored at room temperature unless otherwise stated. Gilson pipettes were used to transfer liquid volumes up to 1 ml (Gilson S.A., France), electronic pipette aids (Drummond, PA, USA) and disposable Pasteur pipettes (Starstedt Ltd., Wexford, Ireland) were used for volumes greater than 1 ml and graduated cylinders were used for volumes in excess of 10 ml.

2.2 Cell culture

All cell culture medium was purchased from Lonza (Basel, Switzerland) and all cell culture plastics were purchased from Starstedt Ltd. (Wexford, Ireland) unless otherwise indicated. All cells lines were purchased from the European Collection of Cell Cultures (ECACC, Wiltshire, England, UK) with the exception of the SGBS which were a kind gift from Dr Martin Wabitsch (University of Ulm, Ulm, Germany). Cell culture was carried out in a dedicated cell culture room which was regularly cleaned and sterilised. Cell culture was carried out in a Grade II laminar hood using aseptic technique while wearing a clean lab coat with elasticised cuffs and disposable latex gloves. The cabinet was cleaned with 70% (v/v) ethanol before and after each use and all reagents, medium and plastics taken inside the cabinet were also cleaned in this manner.

2.2.1 Oesophageal cancer cell lines

Cell lines derived from oesophageal adenocarcinoma (OE33 and OE19) were maintained in Roswell Park Memorial Institute (RPMI) 1640 medium supplemented with penicillin (50 Units/ml), streptomycin (50 Units/ml) and 10% foetal calf serum (FCS). Cell lines were incubated in 25 cm^2 or 75 cm^2 flasks in a humidified atmosphere at 37 °C and 5% CO_2.

2.2.2 Adipocyte cell lines

The 3T3-L1 adipocyte cell line was maintained in Dulbecco's modified Eagle medium (DMEM) medium supplemented with penicillin (50 Units/ml), streptomycin (50 Units/ml) and 10% FCS and incubated in a humidified atmosphere at 37 °C and 5% CO_2. The Simpson-Golabi-Behmel

syndrome (SGBS) cell strain was maintained in DMEM/F12 supplemented with biotin (8×10^{-3} mg/ml), pantothenate (4×10^{-3} mg/ml), penicillin (50 Units/ml), streptomycin (50 Units/ml) and non heat-inactivated 10% FCS in a humidified atmosphere at 37 ° C and 5% CO_2.

2.2.3 Cell subculture

Cell lines were examined daily using an inverted phase contrast Nikon microscope (Nikon Corporation, Tokyo, Japan) and subcultured upon reaching 80 – 90% confluency. Growth medium was decanted and cells were washed in phosphate buffered saline (PBS) to remove residual medium. 1 ml trypsin ethylene-diamine tetra acetic acid (EDTA) (0.05% (w/v) trypsin, 0.02% (w/v) EDTA) was added to the flask and incubated at 37 °C for several minutes or until the cells detached from the surface. 10 ml of complete medium (containing 10% FCS) was then added to inactivate the trypsin and cells were seeded at appropriate densities into new flasks.

2.2.4 Preparation of frozen stocks

Frozen stocks were prepared from cell lines growing in the exponential phase and at 70 – 80% confluency. Cells were trypsinised as described above (section 2.2.3) and 10 ml maintenance medium was added to inactivate the trypsin. Cells were centrifuged at $180 \times g$ for 3 minutes, the supernatant decanted, and pelleted cells were resuspended in FCS containing 5% dimethyl sulfoxide (DMSO). The cell suspension was divided into 750 µl aliquots and cryovials were quickly transferred to a 'Mr Frosty' freezing container (Thermo Fischer Scientific, Leicestershire, UK). The 'Mr Frosty' contains isopropanol which slowly lowers the temperature of the cells by approximately 1 °C/minute, required for successful cell cryopreservation and recovery. Cyrovials were placed in a – 80 °C freezer for short term storage or under liquid nitrogen for long term storage.

2.2.5 Reconstitution of frozen cells

Frozen stocks were thawed rapidly at 37 °C, added to 5 ml of appropriate maintenance medium and centrifuged at $180 \times g$ for 3 minutes. The cell pellet was resuspended in 5 ml maintenance medium, transferred to a 25 cm^2 flask and incubated overnight at 37 °C and 5% CO_2. Medium was replaced the following day to remove any dead cells and cell subculture was continued as described (section 2.2.3).

2.2.6 Cell counting

Cell counting was carried out using a Bright Line haemocytometer (Hausser Scientific, PA, USA). Cells were trypsinised as described (section 2.2.3), added to 10 ml maintenance medium and centrifuged at $180 \times g$ for 3 minutes. The supernatant was decanted and the cell pellet

resuspended by repeated pipetting in 1 ml maintenance medium. 20 µl of the cell suspension was added to 180 µl trypan blue (0.4% w/v) solution and allowed to sit at room temperature for one minute. Viable cells were unstained due to their active exclusion of trypan blue, whereas dead cells were stained blue, due to their disrupted membranes. 20 µl of this cell suspension was added to the counting chamber of the haemocytometer and the number of viable cells in each of the four corners of the grid was counted. The number of cells per ml was calculated using the following equation:

$$(total\ number\ of\ cells/4) \times 10^4 \times 10\ (dilution\ factor) = no.\ cells/ml$$

2.2.7 Mycoplasma testing

Upon receipt of each new cell line, and every six months thereafter, cells were tested for mycoplasma infection using the MycoAlert™ mycoplasma detection system (Cambrex BioScience, Rockland, ME, USA). Mycoplasmal enzymes react with the MycoAlert™ substrate resulting in the conversion of ADP to ATP. The level of ATP in the sample before and after the addition of the substrate therefore indicates whether the sample is contaminated with mycoplasma. Cell lines to be tested were passaged twice in antibiotic free medium before a 1 ml sample of supernatant was taken. The supernatant sample was centrifuged at 180 × g for 3 minutes to pellet floating cells and 100 µl of supernatant was transferred to a luminescence compatible plate. 100 µl of MycoAlert™ reagent was added and incubated for 5 minutes before a one second intergrated reading ('Reading A') was taken on a luminometer (Wallac Victor 2 1420, PerkinElmer, Ballymount, Dublin). 100 µl of MycoAlert™ substrate was then added to the sample and incubated for 10 minutes before a second reading ('Reading B') was taken. A 'Reading B': 'Reading A' ratio <1 indicated that cells were free of mycoplasma and all cell lines remained clear of mycoplasma infection throughout the course of this work (representative test results shown in Appendix I).

2.3 Adipose tissue biobank

An adipose tissue biobank was established in the Department of Surgery in July 2007 and standard operating procedures were optimised from a previously published study (Alvarez-Llamas et al., 2007).

2.3.1 Patient recruitment and classification

Patients (>40 years old) undergoing resective surgery for oesophageal adenocarcinoma, oesophageal squamous cell carcinoma and colorectal carcinoma, in addition to non cancer patients undergoing surgery for laparoscopic Nissan fundoplication, cholecystectomy and

hernia repair, were recruited to the adipose tissue biobank. All recruited patients gave informed consent for use of their adipose tissue in this study, and the study obtained ethical approval from St James' Hospital Ethical Review Board. Patients were separated into viscerally obese and non obese categories using a waist circumference cut off measurement of 94 cm for males and 80 cm for females, as specified by the International Diabetes Federation (IDF). Waist circumference was measured at the midpoint between superior iliac crest and subcostal margin; height and weight were recorded and used to determine body mass index (BMI) while computed tomography (CT) at the L3 - L4 intervertebral space was used to calculate visceral, subcutaneous and total fat area. A fasting serum sample was taken prior to surgery and fasting glucose, high density lipoprotein (HDL) and triglyceride levels were measured by the hospital biochemistry lab. Patients were then separated into categories of those with and those without Metabolic Syndrome (MetS) according to the latest IDF definition (Alberti et al., 2005), summarised in the table below.

Table 2.1: Criteria for Metabolic Syndrome defined by IDF (Federation, 2006).

Visceral obesity (measured by waist circumference)	
Plus any **two** of the following:	
Raised triglycerides	≥1.7 mmol/L Or specific treatment for this condition
Reduced HDL-cholesterol	<1.03 mmol/L in males <1.29 mmol/L in females Or specific treatment for this condition
Raised blood pressure	Systolic ≥130 mmHg or diastolic ≥85 mmHg Or treatment of previously diagnosed hypertension
Raised plasma glucose	Fasting plasma glucose ≥5.6 mmol/L Or previously diagnosed with Type II Diabetes

2.3.2   Biobanking

Two 3 ml fasting blood samples were taken in serum blood collection tubes on the morning of surgery. The samples were centrifuged at 750 × g for 10 minutes to separate the serum which was then stored at − 80 °C. An omental and a subcutaneous adipose tissue specimen were excised at the beginning of the surgical procedure and immediately transported in sterile

transport buffer (glucose (0.1%), gentamycin (0.05 mg/ml) in PBS) for processing in a Grade II laminar air flow cabinet. A thumbnail sized sample of both subcutaneous and omental adipose tissue was preserved in 10% paraformaldehyde for future immunohistochemical analysis. The remaining adipose tissue was minced with a scissors and washed with sterile PBS. Aliquots of 300 mg of tissue was placed in separate cryovials, snap frozen in liquid nitrogen and stored at − 80 °C for RNA extraction, while the remainder was cultured to produce adipose conditioned medium (ACM). This was carried out as follows: in a tissue culture dish, aliquots of 5 g of minced adipose tissue were incubated in 10 ml serum free M199 medium (containing 0.05 mg/ml gentamycin) for 72 hours at 37 °C and 5% CO_2. ACM was then filtered (BD Biosciences, Bedford, MA, USA) to remove adipose tissue fragments and the supernatant was stored at − 80 °C.

2.3.3   Adipose tissue digestion

10 g omental adipose tissue was digested in 10 ml collagenase buffer (Krebs Ringer bicarbonate buffer (118 mM NaCl, 24.8 mM $NaHCO_3$, 1.2 mM KH_2PO_4, 4.8 mM KCl, 1.25 mM $CaCl_2$, 1.2 mM $MgSO_4$, 10 mM HEPES) (pH 7.4), 4% bovine serum albumin (BSA), 2 mg/ml Type II collagenase) at 180 rpm for one hour at 37 °C. Digested tissue was passed through a 500 μm filter (BD Biosciences, Bedford, MA, USA) to remove undigested fragments, and centrifuged at 180 × g for 3 minutes. The floating layer of adipocytes was washed with 10 ml wash buffer (Krebs Ringer bicarbonate buffer pH 7.4, 1% BSA) and the pelleted stromal vascular fraction (SVF) was cleared of red blood corpuscles by the addition of 2 ml ammonium chloride (0.87% w/v) for 1 minute at room temperature. 10 ml PBS was added and the sample was centrifuged at 200 × g for 3 minutes. The supernatant was decanted and the pellet was resuspended in TriReagent (Molecular Research Center, Montgomery Road, OH, USA) and stored at − 80 °C for RNA extraction.

2.3.4   Ceiling culture of adipocytes

Adipocytes were set up in a ceiling culture as previously described (Zhang et al., 2000) for RNA extraction, examination of morphology, conditioned medium and co-culture experiments.

For RNA extraction and examination of adipocyte morphology, 1×10^7 adipocytes were placed in a T25 tissue culture flask which was completely filled with DMEM/F12 medium (containing penicillin (50 Units/ml), streptomycin (50 Units/ml) and 10% FCS). The flask was inverted to allow adipocytes to float and adhere to the culture surface, and incubated for 72 hours at 37 °C and 5% CO_2. The medium was then decanted and the culture surface gently rinsed with

sterile PBS to remove any cell debris and lipid droplets, and RNA was extracted using Qiagen RNeasy Lipid kit (Qiagen Inc., CA, USA) (described in section 2.6.3). Alternatively, Oil Red O staining was carried out to visualise morphology (described in section 2.5.2).

For co-culture experiments and to generate adipocyte conditioned medium, adipocytes were seeded at 2.5×10^5 cells per well in a six well plate in serum free M199 medium (containing 0.05 mg/ml gentamycin). A 24 × 24 mm coverslip (Menzel-Gläser, Braunschweig, Germany) was carefully floated on the surface of each well to create an attachment surface for the adipocytes and the plate was incubated for 72 hours at 37 °C and 5% CO_2. Adipocyte conditioned medium was collected and stored at − 80 °C and the coverslip with attached adipocytes was used for co-culture experiments (described in section 2.3.6).

2.3.5 Co-culture of SGBS with tumour cells

Following overnight incubation in serum-depleted medium (containing 0.5% FCS); OE33 were seeded into 12 well Costar® Transwell® plates (Corning Incorporated, NY, USA) at a dilution of 5×10^4 cells per insert. Inserts were placed into wells containing 2.5×10^5 pre-differentiated SGBS, differentiated SGBS and 2 ml control M199 medium, for 24 hours. The 0.4 µm pore size of the Transwell® insert creates a non-contact co-culture system, allowing diffusion of medium containing cytokines, adipokines and growth factors, but no cell contact. RNA was extracted from tumour cells using Qiagen RNeasy kit (Qiagen Inc., CA, USA) (section 2.6.1) and used for Human Cancer Profiler and Affymetrix arrays (described in sections 2.6.11, 2.6.12).

2.3.6 Co-culture of adipose tissue and adipocytes with tumour cells

Following overnight incubation in serum-depleted medium (containing 0.5% FCS); tumour cells were seeded into 12 well Costar® Transwell® plates (Corning Incorporated, NY, USA) at a dilution of 5×10^4 cells per insert. Inserts were placed into wells containing 1 g adipose tissue fragments in 2 ml adipose conditioned medium, a shattered coverslip with attached adipocytes in 2 ml adipocyte conditioned medium or 2 ml control M199 medium, for 24 hours. The 0.4 µm pore size of the Transwell® insert creates a non-contact co-culture system, allowing diffusion of medium containing cytokines, adipokines and growth factors, but no cell contact. RNA was extracted from tumour cells using Qiagen RNeasy kit (Qiagen Inc., CA, USA) (section 2.6.1) and used for Human Cancer Profiler and Affymetrix arrays (described in sections 2.6.11, 2.6.12), while the supernatant was collected and stored at − 80 ° C.
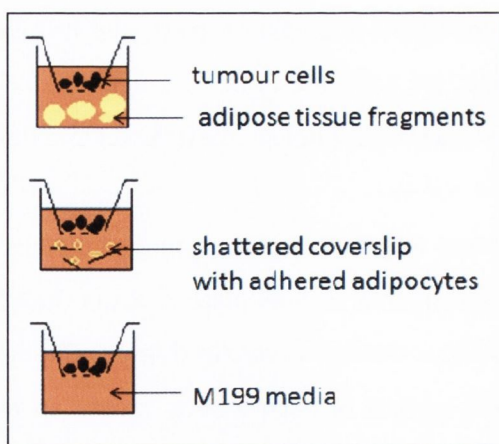
Figure 2.1: Diagram illustrating the co-culture setup. Tumour cells are present in the insert while adipose tissue fragments or adipocytes are present in the well in adipose conditioned medium or adipocyte conditioned medium, respectively.

For validation of Human Cancer Profiler and Affymetrix arrays, a 6 well plate co-culture set-up was used. Tumour cells were seeded at a dilution of 1.5×10^5 cells/well and allowed to adhere for a minimum of 6 hours before serum starving (medium containing 0.5% FCS) overnight. The following day, 1 g of adipose tissue fragments in 2 ml adipose conditioned medium, a coverslip with attached adipocytes in 2 ml adipocyte conditioned medium (2 ml conditioned medium was first added to the well and the coverslip was then gently floated on the surface) or 2 ml control M199 medium was added to wells and the plate was incubated at 37 °C and 5% CO_2 for 24 hours. RNA was extracted from tumour cells using the TriReagent protocol (section 2.6.2) and supernatant was stored at − 80 °C.
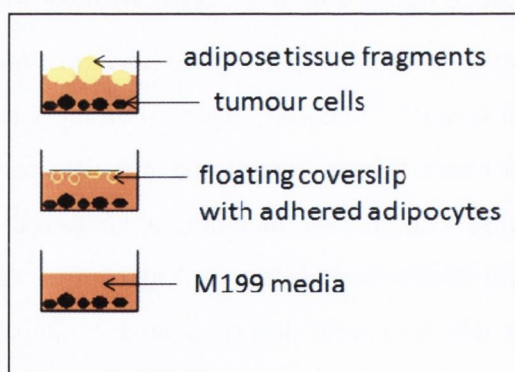
Figure 2.2: Diagram illustrating cartoon images of the co-culture setup. Tumour cells are adhered to the well while adipose tissue fragments or adipocytes are present in the well in adipose conditioned medium or adipocyte conditioned medium, respectively.

2.3.7 Culture of tumour cell lines with ACM

For validation of Human Cancer Profiler and Affymetrix arrays, a 6 well plate culture set-up was used. Tumour cells were seeded at a dilution of 1.5×10^5 cells/well and allowed to adhere for a minimum of 6 hours before serum starving (medium containing 0.5% FCS) overnight. The following day 2 ml adipose conditioned medium or 2 ml control M199 medium was added to wells and the plate was incubated at 37 °C and 5% CO_2 for 24 hours. RNA was extracted from tumour cells using the TriReagent protocol (section 2.6.2) and supernatant was stored at $-$ 80 °C.

2.4 Adipocyte cell line differentiation

2.4.1 3T3-L1 differentiation

Differentiation was induced in 3T3-L1 as described by the ECACC at two days post confluency by the addition of the maintenance medium supplemented with insulin (0.01 mg/ml), dexamethasone (1 µM) and 3-isobutyl-1-methylxanthine (IBMX, 500 µM) for 4 days, followed by maintenance medium containing insulin (0.01 mg/ml) only for a further 2 days. This medium was subsequently replaced by the maintenance medium alone which was changed every 2 days until cells were fully differentiated by day 8.

2.4.2 SGBS differentiation

Differentiation was induced in SGBS at 80% confluency by the addition of serum free maintenance medium containing transferrin (0.01 mg/ml), insulin (0.2 µg/ml), cortisol (0.1 µM), thyroid hormone (0.2 nM), dexamethasone (0.3 µM), IBMX (500 µM) and rosiglitazone (2 µM) for 4 days. Following this, the medium was replaced with serum free maintenance medium containing only transferrin (0.01 mg/ml), insulin (0.2 µg/ml), cortisol (0.1 µM), thyroid hormone (0.2 nM) until cells were fully differentiated by day 14.

2.5 Assessment of adipocyte differentiation

2.5.1 Adipocyte gene expression

RNA was collected every second day throughout the process of differentiation until adipocytes were fully differentiated and expression levels of differentiation specific genes were investigated as described in section 2.6.9.1.

2.5.2 Oil red O staining

Cells were morphologically assessed for differentiation by staining with Oil Red O, a red lysochrome (fat soluble dye). All steps were carried out at room temperature. Cells were fixed

with 4% paraformaldehyde (PFA) for 30 minutes, and PFA was disposed of into an appropriate waste container. Cells were washed gently three times with PBS and incubated with 60% isopropanol for 5 minutes. A 3 mg/ml stock solution of Oil Red O was prepared in 99% isopropanol and a working solution was prepared by mixing 3 parts stock solution with 2 parts deionised water. The working solution was allowed to sit at room temperature for 10 minutes and was then filtered through a 0.8 μm filter (Millipore, Watford, UK), before being added to the cells and incubated for 5 minutes. Cells were gently rinsed three times with PBS and photographed using an inverted phase contrast microscope with camera (Olympus Corporation, Tokyo, Japan).

2.5.3 Adipocyte functional assays

2.5.3.1 Glycerol-3-phosphate dehydrogenase (GPDH) enzyme activity assay

A commercially available GPDH activity assay kit (B-Bridge International Inc., CA, USA) was used to assess enzyme activity in 3T3-L1, SGBS and primary human adipocytes. A measure of lipogenesis in adipocytes, GPDH reduces dihydroxyacetone phosphate (DHAP) to glycerol-3-phosphate using the co-enzyme nicotinamide adenine dinucleotide (NAD). When exogenous DHAP and NADH are added to the test sample, the resulting decrease in NADH concentration, proportional to the amount of GPDH present, is measured on an Alpha Fluor Plus spectrophotometer (Tescan Trading AG, Switzerland).

$$\text{Dihydroxyacetone phosphate} \xrightarrow[\text{GPDH}]{\text{NADH} \quad \text{NAD}} \text{Glycerol-6-phosphate}$$
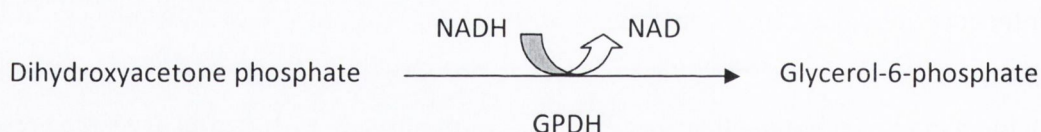
Cells were seeded at a density of 1×10^5 cells/well in a 24 well plate in maintenance medium. Upon reaching 70-80% confluency (SGBS) or 2 days post confluency (3T3-L1), differentiation was initiated by adding the appropriate differentiation cocktail for the required length of time (described in section 2.4). Primary human omental adipocytes were prepared by digestion of omental adipose tissue to obtain a purified adipocyte fraction (described in section 2.3.3). Protein from adipocytes was then extracted using radioimmunoprecipitation (RIPA) lysis buffer (described in section 2.7.2). The cell lysate was passed through a 29 gauge needle (BD Micro-Fine, NJ, USA) to shear insoluble proteins and centrifuged at $180 \times g$ for 5 minutes at 4 °C to pellet any remaining insoluble debris. The cleared supernatant was added to an equal volume of substrate solution and change in optical density was measured in triplicate using an Alpha

Fluor Plus spectrophotometer (Tescan Trading AG, Switzerland) at 340 nm at 30 second intervals for 10 minutes in order to determine the rate of GPDH enzyme activity. Enzyme activity was normalised to protein concentration of each sample, determined by BCA assay (described in section 2.7.3).

2.5.3.2 Glucose assay

Glucose concentration in the adipocyte supernatant was measured using the commercially available QuantiChrom^{TM} Glucose Assay Kit (BioAssay Systems, CA, USA). Adipocyte cell lines were seeded at 2×10^5 cells in a 25 cm^2 flask in complete maintenance medium. Upon reaching 70-80% confluency (SGBS) or 2 days post confluency (3T3-L1), differentiation was initiated by adding the appropriate differentiation cocktail for the required length of time (described in section 2.4). Primary adipocytes were prepared in a 25 cm^2 flask (described in section 2.3.4). 5 µl of sample supernatant was added to 500 µl Reagent (BioAssay Systems, CA, USA) and mixed well by vortexing. A standard curve was prepared by serial dilutions of glucose standard (BioAssay Systems, CA, USA) in sterile distilled water. Standards and samples were heated in a boiling water bath for 8 minutes and cooled on ice for 4 minutes. 200 µl of each standard and sample was added in duplicate to a 96 well plate and the optical density was read at 620 nm on an Alpha Fluor Plus spectrophotometer (Tescan Trading AG, Switzerland). Glucose concentrations were determined by interpolation from the standard curve, and normalised to protein concentration in the sample, as determined by BCA assay (section 2.7.3).

2.6 Investigation of RNA expression

2.6.1 RNA isolation from tumour tissue and cell lines using Qiagen RNeasy kit

Tumour biopsies from oesophageal adenocarcinoma and oesophageal squamous cell carcinoma were immediately taken from fresh tumour tissue following surgical resection. The biopsy was incubated overnight at 4 °C in RNAlater (Qiagen Inc., CA, USA) which was decanted the following day and the tumour tissue was stored at − 80 °C until RNA extraction. RNA was extracted using Qiagen RNeasy Mini kit (Qiagen Inc., CA, USA). A 20 mg piece of tumour was homogenised in 600 µl Buffer RLT using a Qiagen TissueLyser (Retsch GmbH & Co., Haan, Germany) at 800 rpm for 6 minutes with one 5 mm stainless steel bead (Qiagen Inc., CA, USA) added to each sample to aid homogenisation. The bead was removed and samples were centrifuged at 12,000 × g for 3 minutes at 4 °C, and supernatant was transferred to a new tube by pipetting. 600 µl of ethanol (70% v/v) was added to the supernatant, mixed immediately by pipetting and transferred in volumes of 700 µl to an RNeasy spin column placed in a 2 ml collection tube. The spin column was centrifuged at 12,000 × g for 15 seconds and the flow

through was discarded. The spin column was washed by first applying 700 µl buffer RW1, then 500 µl buffer RPE with centrifugation at 12,000 × g for 15 seconds at room temperature between each step. A final wash step in 500 µl buffer RPE was centrifuged for 2 minutes in order to dry the membrane and ensure no ethanol was carried over. RNA was eluted in 60 µl of RNase free water by centrifugation for 1 minute at 12,000 × g at room temperature.

For Human Cancer Pathway Profiler Arrays and Affymetrix arrays, RNA was isolated from OE33 tumour cells using Qiagen RNeasy kit as described, omitting the homogenisation step.

2.6.2   RNA isolation from tumour cell lines using TriReagent method

RNA to be used for reverse transcriptase PCR and quantitative real time PCR was isolated from tumour cell lines using the TriReagent method. RNA was isolated from tumour cell lines (OE33, OE19, HCT-15, SW480) using 1 ml TriReagent (Molecular Research Center, Montgomery Road, OH, USA), containing a mixture of guanidine thiocyanate and phenol in a monophasic solution. Samples lysed in TriReagent were stored at − 80 °C until RNA extraction. Total RNA was isolated as follows: samples were thawed and stored at room temperature for 5 minutes following which 100 µl BCP was added. Samples were then vortexed vigorously for 15 seconds and allowed to stand at room temperature for 15 minutes. Following centrifugation at 12,000 × g at 4 °C for 15 minutes, the upper aqueous phase was carefully removed to a new tube, and subsequent steps were carried out at room temperature. 500 µl isopropanol was added and the tube incubated for 10 minutes followed by centrifugation at 12,000 × g for 8 minutes. The supernatant was decanted and the pellet washed in 1 ml ethanol (75% v/v) by brief vortexing followed by centrifugation at 12,000 × g for 5 minutes. The ethanol was decanted and the pellet allowed to air dry for 3-5 minutes. The pellet was resuspended in 60 µl RNase free water.

2.6.3   Isolation of RNA from adipose tissue and adipocytes

RNA was isolated from adipose tissue using the Qiagen RNeasy Lipid Mini kit (Qiagen Inc., CA, USA). A 150 mg piece of adipose tissue was homogenised in 1 ml Qiazol using a Qiagen TissueLyser (Retsch GmbH & Co., Haan, Germany) at 800 rpm for 6 minutes with one 5 mm stainless steel bead (Qiagen Inc., CA, USA) added to each sample to aid homogenisation. The bead was removed and samples were centrifuged at 12,000 × g for 10 minutes at 4 °C, and supernatant was transferred to a new tube by pipetting. The homogenate was allowed to sit at room temperature for 5 minutes to allow complete dissociation of the nucleoprotein complexes. 100 µl of 1-bromo-3-chloro-propane (BCP) was added and the tube was vortexed

vigorously for 15 seconds. The tube was again allowed to sit for 2-3 minutes at room temperature to allow phase separation to begin. The tube was then centrifuged at 12,000 × g for 15 minutes at 4 °C. The upper aqueous phase containing RNA was carefully transferred to a new tube and one volume of ethanol (70% v/v) was added. The sample was then applied to the RNeasy Mini spin column in volumes of 700 µl and centrifuged at 12,000 × g for 15 seconds. The spin column was washed by first applying 700 µl buffer RW1, then 500 µl buffer RPE with centrifugation at 12,000 × g for 15 seconds at room temperature between each step. A final wash step in 500 µl buffer RPE was centrifuged for 2 minutes in order to dry the membrane and ensure no ethanol was carried over. RNA was eluted in 60 µl of RNase free water by centrifugation for 1 minute at 12,000 × g at room temperature.

2.6.4   RNA quantification and purity analysis

RNA quantification was determined spectrophotometrically, using a Nanodrop 1000 spectrophotometer (version 3.1.0, Nanodrop technologies, DE, USA). 1 µl RNase free water was used to blank the instrument. 1 µl of each sample of isolated RNA was loaded onto the instrument and concentration was measured in ng/µl. 260:280 and 260:230 purity ratios were also recorded. A 260:280 ratio greater than 1.65 was indicative of a relatively pure RNA yield, while a 260:230 ratio greater than 1.7 indicated that the sample was free of phenol contamination.

2.6.5   RNA integrity analysis

RNA integrity was assessed using Agilent 2100 Bioanalyser, a 'lab-on-a-chip' micro-fluidics based platform. This technology uses pressure to apply an even and controlled distribution of the gel through a network of channels etched onto the surface of a small chip, to which the RNA samples are added. An electrophoretic trace of the RNA sample is produced, including any degradation products which may be present, in order to generate an RNA integrity number (RIN). 2 µl of RNA ladder and 2 µl of each RNA sample were denatured at 72 ° C for 2 minutes and immediately placed on ice. The chip was prepared by evenly distributing a gel-dye mix onto the surface of the chip using pressure, following which 1 µl of ladder and 1 µl of each sample were placed in the appropriate wells on the chip surface. The chip was vortexed at 2,400 rpm for 1 minute and read on the Agilent 2100 Bioanalyser within 5 minutes of preparation. A RIN > 6.7 was required for RNA samples to be used for Affymetrix array technology.

2.6.6 cDNA synthesis

All reverse transcription reagents were purchased from Invitrogen (Invitrogen Corporation, CA, USA). cDNA was made by adding random primers (0.5 µg/µl) to 1 µg total RNA and heating the sample to 70 ° C for 10 minutes in order to denature the RNA. A master mix containing reverse transcription components was then added to each sample containing: RNaseOUT recombinant ribonuclease inhibitor (1 Unit/µl), dNTPs (10 mM, prepared as a 1:1:1:1 ratio of dATP, dTTP, dCTP, dGTP), dithiothreitol (DTT) (0.01 mM) and Superscript III reverse trancriptase (200 Units/µl) in 5× First Strand reaction buffer (250 mM Tris-HCl (pH 7.5), 100 mM KCl, 15 mM MgCl$_2$) and this mixture was incubated at 37 ° C for 1 hour. The resulting cDNA was stored at − 20 ° C and 1 µl of cDNA template was used to investigate gene expression.

Table 2.2: Reagents and volumes used in cDNA synthesis

Reagent	Volume (1 ×) (µl)
Random primers	1
1 µg RNA + RNase free H$_2$O	10
Heated for 10 mins at 70 °C then following mix added:	
5 × First Strand Reaction buffer	4
DTT	2
RNase free H$_2$O	1
dNTPs	0.5
RNase out	0.5
Superscript	0.5
Total volume:	**20**

For Human Cancer Profiler Array, cDNA synthesis was generated using the First Strand cDNA synthesis kit (Super Array Bioscience Corporation, Frederick, MD, USA). 200 ng of each RNA sample was combined with 1 µl of random primers in a sterile PCR tube and made up to a final volume of 10 µl with RNase free water. The contents were vortexed briefly and centrifuged before being placed in a thermal cycler at 70 °C for 3 minutes, followed by 37 °C for 10 minutes. 10 µl reverse transcription cocktail (4 µl of 5 × RT-Buffer, 4 µl RNase free water, 1 µl RNase inhibitor, 1 µl reverse transcriptase) was added to each sample, briefly vortexed and centrifuged before incubating at 37 °C for one hour. Samples were then heated to 95 °C for 5

minutes to degrade the RNA and deactivate the reverse transcriptase. 80 µl of RNase free water was added to each sample and mixed well to give a final volume of 100 µl. Samples were stored at − 20 °C overnight and run on arrays the following day (described in section 2.6.11).

2.6.7 Reverse transcriptase polymerase chain reaction (RTPCR)

cDNA was used as a template for polymerase chain reaction (PCR). The following PCR master mix was added to each sample: GoTaq®Green Master Mix (2× GoTaq® Reaction buffer (pH 8.5), 400 µM dATP, 400 µM dGTP, 400 µM dCTP, 400 µM dTTP, 3 mM $MgCl_2$, GoTaq® DNA polymerase) (Promega, WI, UK), forward primer (20 µM), reverse primer (20 µM) and RNase free water. 1 µl cDNA was used per reaction and a non template control was included for each primer set by replacing cDNA with 1 µl RNase free water. Template DNA was denatured at 94 °C for 5 minutes, and each cycle consisted of primer annealing (55-62 °C for 1 minute, optimised for each target) and extension (72 °C for 1 minute). This was followed by an elongation step to complete the amplification cycle (72 °C for 5 minutes).

Table 2.3: Reagents and volumes used in RTPCR

Reagent	Volume (1 ×) (µl)
GoTaq® Master Mix	10
Forward primer	1
Reverse primer	1
RNase free water	7
cDNA	1
Total volume	**20**

All reverse transcriptase primers were purchased in lyophilised form from Operon (Eurofins MWG Operon, Ebersberg, Germany) and rehydrated to a stock concentration of 400 µM in RNase free water. Primer sequences, annealing temperatures and number of amplification cycles used in each PCR are outlined in the table below.

Table 2.4: Reverse transcriptase PCR sequences

Gene	Sequence	cycle no.	annealing temp. (°C)
Adipo R1	Fw 5'-CGGTGGAACTGGCTGAACTG-3'	30	55
	Rv 5'-CCGCACCTCCTCCTCTTCTT-3'		
Adipo R2	Fw 5'-ACGGAGTTGGCACTCAC-3'	30	55
	Rv 5'-GCCATCGTCTTGTACCTCAC-3'		
Adiponectin	Fw 5'-CTATGATGGCTCCACTGGTA-3'	35	55
	Rv 5'-GAGCATAGCCTTGTCCTTCT-3'		
Adipsin	Fw 5'-GGTCACCCAAGCAACAAAGT-3'	35	55
	Rv 5'-CCTCCTGCGTTCAAGTCATC-3'		
β-actin	Fw 5'-GACGAGGCCCAGAGCAAGAGCG-3'	30	55
	Rv 5'-TCAGGCAGCATAGCTCTCCAGGG-3'		
GAPDH	Fw 5'-GCAGGGAGACAAAAGGG-3'	35	55
	Rv 5'-TGCCAGCCCCAGCGTCAAAG-3'		
GLUT4	Fw 5'-CATCCTGATGACTGTGGCTC-3'	35	57
	Rv 5'-TCTCATCTGGCCCTAAATACT-3'		
Leptin	Fw 5'-GACCTTGGACAGCCTGGGGG-3'	35	62
	Rv 5'-CTGTGCCCATCCAAAAAGTCC-3'		
ObR$_{long}$	Fw 5'-CCAGAAACGTTTCAGCATCT-3'	35	55
	Rv 5'-CAAAAGCACACCACTCTCTC-3'		
ObR$_{short}$	Fw 5'-GAAGGAGTGGGAAAACCAAAG-3'	35	55
	Rv 5'-CCACCATATGTTAACTCTCAG-3'		
PPARγ	Fw 5'-TCTCTCCGTAATGGAAGACC-3'	35	55
	Rv 5'- GCATTATGAGCATCCCCAC-3'		
Resistin	Fw 5'-ATGAAAGCTCTCTGTCTCCTCC-3'	35	55
	Rv 5'-TCAGGGCTGCACACGACAGC-3'		
Visfatin	Fw 5'-AAGAGACTGCTGGCATAGGA-3'	35	55
	Rv 5'-ACCACAGATACAGGCACTGA-3'		

2.6.8 Agarose gel electrophoresis

Agarose gels were prepared in Tris-Acetate-EDTA (TAE) buffer (40 mM Tris HCl (pH 8.3), 20 mM acetic acid, 1 mM EDTA). A 1.4% agarose solution was heated in a microwave for several minutes to allow the agarose to dissolve. It was allowed to cool to approximately 55 °C before adding SYBR® safe DNA gel stain (10,000 × concentrate in DMSO, Invitrogen Corporation, CA,

USA) to a final concentration of 1 μg/ml. The solution was poured into a gel tray to a depth of 3-5 mm and allowed to set.

The DNA samples, containing loading buffer present in the GoTaq ® reagent, were loaded along with a 100 base pair DNA ladder (Promega Corporation, Madison, WI, USA). Electrophoresis of the DNA samples was carried out at 100 volts in an EC-360 Maxicell gel system (EC Apparatus Corp., FL, USA), using 1 × TAE as a running buffer. The bands were visualised and photographed under UV light using a BioSpectrum Imaging System (Ultra Violet Products, Cambridge, UK).

2.6.9 Quantitative real time PCR (qPCR)

Quantitative PCR was used to quantify expression of mRNA in samples relative to the 18S ribosomal RNA endogenous control. This was carried out using a probe based and an intercalation based method. The probe method works as follows: sequence specific probes are labelled with a fluorescent reporter molecule at the 5' end, and a fluorescence quencher molecule at the 3' end. The close proximity of the reporter to the quencher prevents detection of fluorescence. Upon transcription, the 5'-3' exonuclease activity of the Taq polymerase removes the quencher molecule and allows fluorescence emission, detected following laser excitation of the sample. The intercalation based method uses SYBR Green; a fluorescent dye that intercalates with newly synthesised double stranded DNA. Using either method, an increase in expression of the gene product is proportional to the amount of fluorescence in the sample.

All reagents were purchased from ABI Biosystems (CA, USA). A master mix containing forward and reverse primer, probe (if applicable) and Taqman® Gene Expression Master Mix or SYBR Green was added to 1 μl cDNA template (described in section 2.6.6) (see table below). A final volume of 20 μl was pipetted into a well of a MicroAmp™ Optical 96 well reaction plate (ABI Biosystems, CA, USA) and real time PCR was performed on the ABI Prism 7500 (ABI Biosystems, CA, USA) real-time thermal cycler. The plate was heated to 95 °C for 15 minutes, followed by 40 cycles of 95 °C for 15 seconds and 60 °C for one minute. The threshold cycle (Ct) for each well was calculated using the instrument software and data analysis was carried out using a Microsoft Excel-based data analysis template. Data analysis was based on the ΔΔCt method with raw data normalised by the 18S housekeeping genes included on the plate.

Table 2.5: Reagents and volumes used for qPCR.

Reagent	ABI primer/probe	Metabion	SYBR Green
Master Mix	10	10	10
Forward primer	⎫	1.4	1.75
Reverse primer	⎬ 1	1.4	1.75
Probe	⎭	1.4	-
RNase free water	8	4.8	5.5
cDNA	1	1	1
Final volume	20	20	20

2.6.9.1 Adipocyte differentiation

Real time quantitative qPCR was carried out in SGBS and primary human adipocytes with inventoried primers for GLUT4 (Hs00168966_m1), AP2 (Hs00609791_m1), PPARγ2 (Hs01115512_m1), LPL (Hs01012571_m1) and leptin (Hs00174877_m1) (Applied Biosystems, CA, USA).

Table 2.6: Murine qPCR primer sequences used to track 3T3-L1 differentiation.

Gene	Primer sequence
GLUT4	Fw: 5'-GGGGCGCCGGACGCTCCA-3', Rv: 5'-TGGCCCTAAATACTCAAG-3'
AP2	Fw: 5'-AACACCGAGATTTCCTT-3', Rv: 5'-ACACATTCCACCACCAG-3'
PPARγ2	Fw: 5'-CTCCTATTGACCCAGAAAGCGA-3', Rv: 5'-GTGGAGATGCAGGCTCCACTT-3'
GAPDH	Fw: 5'-CAAGGTCATCCATGACAACTTTG-3', Rv: 5'- GGCCATCCACAGTCTTCTGG-3'
LPL	Fw: 5'-AGGACCCCTGAAGACAC-3', Rv: 5'-GGCACCCAACTCTCATA-3'
Leptin	Fw: 5'- ATCTCCGAGACCTCCTCCATCT, Rv: 5'- TGCAGGCCACTGGTCTGA-3' probe: 5'- FAM-CTGGCCTTCTCCAAGAGCTGCTCCC-TAMRA-3'

2.6.9.2 Human Cancer Profiler and Affymetrix array validations

Real time qPCR was carried out to validate the Human Cancer Profiler Array and to investigate selected gene targets in patient tumour biopsies.

Table 2.7: Primer sequences used to validate Human Cancer Profiler Array.

Gene	Primer sequence
MMP9	Fw: 5'-CGCTGGGCTTAGATCATTCC-3'
	Rv: 5'-GTGCCGGATGCCATTCAC-3'
	Probe: 5'-Fam-CCGGAGGCGCTCATGTACCCTATG-Tamra-3'
MMP2	Fw: 5'-ACTGTGACGCCACGTGACA-3'
	Rv: 5'-CGTATACCGCATCAATCTTTTCC-3'
	Probe: 5'-Fam-CCCCTGCTGGTGGCCACATTCT-Tamra-3'
PAI-1	Fw: 5'-GCCATGGAACAAGGATGAGATC-3'
	Rv: 5'-GCCCTGGACCAGCTTCAGA-3'
	Probe: 5'-Fam-CCACAGACGCGATCTTCGTCCAGC-Tamra-3'
TP53	Fw: 5'-TGGGACAGCCAAGTCTGTGA-3'
	Rv: 5'-GGCCAGTTGGCAAAACATCT-3'
	Probe: 5'-Fam-TTGCACGTACTCCCCTGCCCTCAAC-Tamra-3'

Real time quantitative qPCR was carried out to validate Affymetrix arrays and investigate selected gene targets in patient tumour biopsies using inventoried primers for SEMA4B (Hs00384240_m1), ITGA3 (Hs00233722_m1), S100A8 (Hs00374263_m1), LAMC2 (Hs01043711_m1), SNAI2 (Hs00161904_m1), CTDSPL (Hs00965660_m1), CXCL5 (Hs00171085_m1), PPBP (Hs00234077_m1), LAMB3 (Hs00165078_m1), VEGFA (Hs00900055_m1) and E-cadherin (Hs01023894_m1) (Applied Biosystems, CA, USA).

2.6.10 Human endogenous control qPCR array

Changes in the expression profile of a panel of housekeeping genes were examined between pre-differentiated SGBS (day 0) and differentiated SGBS (day 14) using Taqman Express Plate Endogenous Control (Applied Biosystems, CA, USA). A complete list of genes investigated can be found in Appendix V.

SGBS cell strain was differentiated according to standard protocols (as described in section 2.4.2) and RNA was extracted from day 0 and day 14 SGBS (as described in section 2.6.3). cDNA synthesis was carried out as described in section 2.6.6. Each well of the qPCR array was reconstituted with a mix containing Taqman gene expression Master Mix (Applied Biosystems, CA, USA) and 500 ng cDNA to a final volume of 20 µl. The PCR array was tightly sealed using optical thin wall 8-cap strips (Applied Biosystems, CA, USA) and real time PCR detection was performed on an ABI Prism 7500 (ABI Biosystems, CA, USA) real-time thermal cycler. The plate was heated to 95 °C for 15 minutes, followed by 40 cycles of 95 °C for 15 seconds and 60 °C for one minute. The threshold cycle (Ct) for each well was calculated using the instrument software SDS 2.3 and data analysis was carried out using a Microsoft Excel-based data analysis template. Data analysis was based on the ΔΔCt method with raw data normalised by 18S ribosomal subunit, included on the plate.

2.6.11 Human Cancer Pathway Finder arrays

Changes in the expression profile of a panel of genes representative of molecular pathways of tumourigenesis were examined using RT^2 Profiler™ Human Cancer Pathway Finder PCR Array technology (Super Array Bioscience Corporation, Frederick, MD, USA). This array is based on a 96 well plate format, containing primer sets for 84 genes involved in six biological pathways of tumourigenesis: apoptosis, cell cycle, angiogenesis, invasion and metastasis, signal transduction and adhesion, as previously described (Hanahan and Weinberg, 2000). Five housekeeping genes were included to normalise the data and two negative controls were included to estimate the level of DNA contamination in the PCR system. Genes measured by this array are listed in Appendix V.

Samples were prepared for loading onto the RT-PCR array by adding 1225 µl 2 × SuperArray PCR master mix and 1127 µl RNase free water to 98 µl of the diluted cDNA synthesis reaction to give a final volume of 2450 µl. 25 µl of reaction mix was added to each well except the non template control, to which the same mix was added with RNase free water instead of cDNA. The PCR array was tightly sealed using optical thin wall 8-cap strips (Super Array Bioscience Corporation, Frederick, MD, USA) and real time PCR detection was performed on an ABI Prism 7500 (ABI Biosystems, CA, USA) real-time thermal cycler. The plate was heated to 95 °C for 15 minutes, followed by 40 cycles of 95 °C for 15 seconds and 60 °C for one minute. The threshold cycle (Ct) for each well was calculated using the instrument software SDS 2.3 and data analysis was carried out using a Microsoft Excel-based data analysis template. Data analysis was based

on the ΔΔCt method with raw data normalised by the housekeeping genes included on the plate. Fold-changes in gene expression observed in the RT-PCR array analysis were validated using quantitative reverse transcription qPCR, using the protocols previously described in section 2.6.9.2. Gene changes were only reported if the transcript was amplified before 35 cycles in either the test sample (for up regulated genes) or the control sample (for down regulated genes).

2.6.12 Affymetrix arrays

The Affymetrix Human Genome U133 Plus 2.0 Array was custom-designed by the European Nutrigenomics Organisation (NuGO) to include a selection of nutrition and obesity related genes. This is one of the most comprehensive arrays to date, covering approximately two thirds of the human genome (www.affymetrix.com).

RNA was extracted from adipose tissue and tumour cell lines using the appropriate Qiagen RNeasy kit (described in section 2.6.1). RNA purity was assessed using Nanodrop 1000 spectrophotometer (version 3.1.0, Nanodrop technologies, DE, USA) (described in section 2.6.4) and RNA integrity was assessed using Bioanalyser (Agilent Technologies, Inc) (described in section 2.6.5). The RNA integrity number (RIN) was < 6 and the 260/280 ratio < 1.65 for all RNA samples. A volume of 5 µg of RNA (with a concentration range of 100 – 500 ng/µl) was sent to Service XS (Leiden, The Netherlands) to run Affymetrix arrays.

Statistical analysis was carried out in collaboration with Ms Melissa Morine (Nutrigenomics Research Group, University College Dublin) using predefined scripts and flexible programming with the R software environment for statistical computing. R function 'linear model in microarrays' (LIMMA) was used to select significantly altered single genes while gene set enrichment analysis (GSEA) was used to examine changed pathway expression.

2.6.12.1 Affymetrix array quality control

It is imperative to the success of a microarray experiment that sufficient quality control checks are carried out after each stage of the hybridisation and analysis process. All RNA samples processed on Affymetrix microarrays had an RNA integrity number (RIN) >6.7, and a 260/280 ratio greater than 1.65 (Bioanalyser and Nanodrop results listed in Appendix). These quality control parameters were investigated on site before sending samples to Service XS, and again by Service XS upon receipt of the samples.

Prior to data analysis, a number of necessary quality control measures were carried out; first by Service XS prior to release of the data, and again by us upon receipt of the data. Variability in microarray data can be introduced by differences in the array manufacturing process, by variation in sample labelling and hybridisation processes and by variation in the quantification of spot intensities. These potentially confounding sources of variability must be controlled for before analysis is carried out. Normalisation between array chips was conducted and overall signal intensity was found to be similar between arrays (Appendix V). GAPDH and actin were used as internal control genes, and these genes were detected using both 3' and 5' probes. A high 3'/5' ratio indicates degraded or inefficiently transcribed RNA and we found all arrays to fall within standard range (Appendix V). The absence of technical faults between chips was verified by analysis of distribution of intensity across the chip surface through examination of positive and negative border elements (Appendix V). Finally, an overall array intensity correlation was carried out to identify possible outlier arrays. All arrays passed these quality control tests and we therefore included all samples in bioinformatic analysis. All Affymetrix analysis was carried out using predefined scripts and flexible programming with the R software environment for statistical computing.

2.6.12.2 Affymetrix microarray analysis

Levels of individual transcripts significantly altered between groups were selected using LIMMA (linear models in microarray), from the R library of functions, using p values adjusted for multiple testing. The more tests carried out (over 16,000 in this case), the more stringent the adjustment of the p value. Therefore, in order to find a greater number of significantly altered transcripts, the number of tests carried out was reduced by omitting the transcripts which were less interesting. This can be carried out in one of two ways; by using an intensity filter to remove all genes below certain signal intensity, or by using a variance filter to remove genes with close to zero variance between treatment and control. Although microarray technology is excellent for high throughput experiments, it is relatively weak at picking up low intensity signals, so using an intensity filter may introduce further bias against low expression transcripts. By removing genes in the lowest 10% of variance using a variance filter, the number of transcripts tested was decreased, thus reducing the extent of multiple testing and false positive results. Altered transcripts were ranked by log fold change (logFC) and researched using the NCBI website (http://www.ncbi.nlm.nih.gov/sites/entrez?db=PubMed) to establish biological function and to examine previous publications.

Gene set enrichment analysis (GSEA) was utilised to discover altered pathways in the study; this method was previously developed by a group examining skeletal muscle in Type II Diabetes (Mootha et al., 2003). First, individual gene alterations were ranked by log fold change (logFC) to create a gene list using linear models in microarray (LIMMA) predefined script (R). The null hypothesis, H_j, assumed that there was no difference between groups (culture with adipose tissue or adipocytes and culture with control medium), while the alternative hypothesis, $\hat{H}_j$, proposed that gene alterations were associated with the group label i.e. culture with adipose tissue or culture with adipocytes. The association was then measured by a non-parametric, running sum statistic called the enrichment score (ES); this calculates the number of genes in a pathway or co regulated gene set which are close to the top of the single gene list (i.e. have a large logFC). Pathway ES is high when many members of the pathway appear at the top of the single gene ranked list. The difference in the mean between the adipose tissue/adipocyte and control groups is calculated and called T_{obs}. Permutation analysis, which also adjusts for multiple testing, is then carried out; the samples are shuffled and randomly reassigned to groups, and the mean difference recalculated each time. This is carried out approximately 1,000 times. If T_{obs} is contained outside the centre 95% of the other random permutations, the null hypothesis at $p < 0.05$ can be rejected and the pathway deemed significantly altered. For example: if a pathway is given a p value of 0.029, this means that out of 1000 permutations, 29 permutations of the pathway had a score greater than that achieved using the actual diagnostic groups. The top five pathways, ranked by the adjusted p value for bidirectional enrichment, were selected for further investigation.

The Kyoto Encyclopaedia of Genes and Genomes (KEGG) database was used to visualise individual transcript alterations within biological pathways. Alterations in individual transcript expression and of overall pathway regulation were then validated at mRNA, protein and functional levels.

2.7 Western blotting

2.7.1 Sample preparation

OE33 and OE19 were seeded into a T75 flask and allowed to reach 70% confluency. Cells were serum starved overnight in medium containing 0.5% FCS and cultured with 5 g minced adipose tissue in 10 ml ACM. Following 24 hours, adipose tissue and ACM was discarded and protein was extracted as described below.

2.7.2 Protein extraction

Cells were washed three times in PBS and lysed by addition of 100 µl ice-cold RIPA lysis buffer (50 mM Tris-HCl pH 7.4, 150 mM NaCl, 1 mM EDTA, 1% Triton 100×, 1% sodium doxycholate, 0.1% SDS, 1 mM PMSF, 1 mM protein inhibitor cocktail (5 µg/ml aprotinin, 5 µg/ml leupeptin)). Cells were incubated on ice for 5 minutes and the resulting cell lysate was collected using a cell scraper. Insoluble protein was sheared using a 29 gauge needle (BD Micro-Fine, NJ, USA) and the sample was centrifuged at 4,000 × g for 2 minutes to pellet any remaining insoluble fraction, the supernatant was stored at − 20 °C.

2.7.3 Protein quantification

Protein quantification was carried out using the commercially available Pierce Bicinchoninic (BCA) Protein Assay Kit (Thermo Scientific, IL, USA). In the presence of protein, Cu^{2+} is oxidised to Cu^+ which reacts with the reagent under alkaline conditions to yield a coloured product. A standard curve was prepared using the supplied stock solution of bovine serum albumin (BSA) (2000 µg/ml) of 1000 µg/ml, 800 µg/ml, 600 µg/ml, 400 µg/ml, 200 µg/ml, 100 µg/ml, 50 µg/ml and 0 µg/ml. 10 µl of each standard concentration and of each sample was added to a 96-well plate in triplicate. A 50:1 solution was prepared of BCA Reagent A (Na_2CO_3, $NaHCO_3$, bicinchoninic acid, $Na_2C_4H_4O_6$ (sodium tartrate) in 0.1 M NaOH) and BCA Reagent B (containing 4% $CuSO_4$) and 200 µl was added to each well of the 96-well plate which was then incubated at 37 °C for 30 minutes. The absorbance of each well was read on an Alpha Fluor Plus spectrophotometer (Tecan Trading AG, Switzerland) at 490 nm and protein concentrations were determined by interpolation from the standard curve of known concentrations of BSA.

2.7.4 Denaturing polyacrylamide gel (SDS-Page)

A 12% SDS-Page gel was used for resolution of proteins smaller than 100 kDa while an 8% SDS-Page gel was used for resolution of proteins larger than 100 kDa. A 12% separating gel was prepared as follows for a 30 ml gel mould: 9.2 ml 30% acrylamide:bisacrylamide (37.5:1), 4.5 ml 1.875 M Tris HCl (pH 8.8), 8.3 ml water, 176 µl 10% (w/v) SDS, 120 µl 10% (w/v) fresh ammonium persulfate (APS), 10 µl N,N,N',N'-tetramethylethylenediamine (TEMED). An 8% separating gel was prepared as follows for a 30 ml gel mould: 6.13 ml 30% acrylamide:bisacrylamide (37.5:1), 4.5 ml 1.875 M Tris HCl (pH 8.8), 10.3 ml water, 176 µl 10% (w/v) SDS, 120 µl 10% (w/v) fresh ammonium persulfate (APS), 10 µl N,N,N',N'-tetramethylethylenediamine (TEMED). The solution was gently mixed and the gels were cast between upright glass plates (Bio-Rad Laboratories, Hercules, CA, USA). 70% ethanol was gently layered on top of the gels to exclude air and aid polymerisation; this was removed once

polymerisation occurred. A 5% (w/v) stacking gel was prepared containing 1 ml 30% (w/v) acrylamide:bisacrylamide (37.5:1), 2 ml 0.6 M Tris HCl (pH 6.8), 6 ml water, 100 µl 10% (w/v) SDS, 150 µl 10% (w/v) fresh APS, 10 µl TEMED. The stacking gel was added to the top of the polymerised gel and a 12-well comb was inserted before allowing the gel to set.

2.7.5   Protein electrophoresis and transfer

Protein samples were diluted to a final volume of 30 µl with 2 × Laemmli buffer (2 ml Tris HCl pH 6.8, 5 ml 10% (w/v) SDS, 1 ml 2-β-mercaptoethanol, 2 ml glycerol, 0.05 g (w/v) bromophenol blue) and denatured by heating to 95 °C for 10 minutes. Samples were separated by electrophoresis at 50 mA per gel in electrode buffer (50 mM Trizma base, 384 mM glycine, 0.1% (w/v) SDS) for 90 minutes, or until the dye front reached the bottom of the gel. 10 µl of a tri-chrom pre-stained protein marker (Pierce, Rockford, IL, USA) was also loaded onto each gel and all gels were run in duplicate. Separated proteins were transferred onto polyvinylidene fluoride (PVDF) membrane (Pall Corp., Pensacola, FL, USA) using a semi-dry transfer apparatus (Sigma Chemical Company, MO, USA). PVDF membrane was pre-activated in 100% methanol for one minute. The transfer apparatus was covered in cold transfer buffer (0.15 M glycine, 20 mM Tris, 0.1% (w/v) SDS, 20% (v/v) methanol). PVDF and Whatman filter paper (Whatman Laboratory Division, Maidstone, Kent, UK) were soaked in transfer buffer before transfer. Polyacrylamide gels were placed in the transfer apparatus on top of the PVDF membrane in a sandwich of double layered 3 mm Whatman filter paper. Bubbles were carefully removed from between layers and proteins were transferred for 2 hours at 225 mA and maximum voltage.

2.7.6   Antibody probing of membranes

Following the transfer of proteins, membranes were blocked with 5% (w/v) non-fat dry milk (Marvel) which was reconstituted in Tris-buffered saline (25 mM Tris HCl (pH 7.6), 150 mM NaCl) containing 0.1% Tween-20 (TBST) on a shaker (Bibby Sterilin Ltd., Staffordshire, UK) for one hour at room temperature. The membrane was then incubated in the primary antibody, diluted in 5% (w/v) Marvel in TBST on a shaker overnight at 4 °C. Membranes were washed three times for 5 minutes each in TBST before incubation in horseradish peroxidise (HRP) conjugated secondary antibody (1:2,000 dilution in TBST) (Dako, Glostrup, Denmark) for one hour on a shaker at room temperature. Six further 5 minute washes in TBST were then carried out. The Supersignal West Pico Chemiluminescent substrate kit (Pierce, Rockford, IL, USA) was then used to detect bound antibody complexes. Working reagent was prepared just prior to use by mixing two solutions in equal volumes and adding to the membrane for 1 minute. Membranes were then exposed to scientific X-Ray film (Fuji Photo Film Co. Ltd., Tokyo, Japan),

which was developed using a medical film processor (Agfa-Gevaert, Mortsel, Belgium). Exposure times ranged from 1 minute to 30 minutes, depending on the signal intensity.

Table 2.8: Antibodies used in Western blotting

Antibody	Supplier	Isotype	Type	Block	Primary Ab
PAI-1	R&D systems	goat	polyclonal	5% Marvel 1 hour, RT	1/500 o/n, 4 °C
TP53	Cell signaling	rabbit	polyclonal	5% Marvel 1 hour, RT	1/1000 o/n, 4 °C
MMP9	Millipore	mouse	monoclonal	5 % BSA 1 hour, RT	1/500 o/n, 4 °C
LAM γ2	Millipore	mouse	monoclonal	5 % BSA 1 hour, RT	1/500 1 hour, RT
FAK	Millipore	mouse	monoclonal	3% Marvel 1 hour, RT	1/000 o/n, 4 °C
Src	Millipore	mouse	monoclonal	3% Marvel 1 hour, RT	1/1000 o/n, 4 °C
β-actin	Calbiochem	mouse	monoclonal	5% Marvel 1 hour, RT	1/20,000 1 hour, RT

2.7.7 Stripping of probed membranes

Membranes were stripped of antibody complexes for re-probing using Restore Western Blot stripping buffer (Pierce, Rockford, IL, USA). The membrane was placed in 10 ml stripping buffer on a shaker at room temperature for 15 minutes, followed by three 5 minute washes with TBST.

2.7.8 Densitometry

Densitometric analysis was carried out using TINA (version 4.0) software (Raytest, Straubenhardt, Germany). Values were represented as a ratio of sample band intensity to that of the corresponding β-actin control.

2.7.9 Zymography

Zymography is an SDS-Page based technique to investigate MMP activity. In this study gelatinase activity of MMP2 and MMP9 was measured using commercially available gelatin containing SDS-Page gels (Bio-Rad Laboratories, Hercules, CA, USA). Size separation of MMP isoforms followed by protein renaturation allows visualisation of bands corresponding to the molecular weight of both pro- and active MMPs.

Samples were prepared and protein was extracted as for Western analysis. One part protein sample was mixed with two parts zymogram sample buffer (Bio-Rad Laboratories, Hercules, CA, USA). This sample was not heated to denature the protein, as the proteolytic activity of the protein was to be measured. Samples were separated by electrophoresis at 50 mA per gel in electrode buffer (50 mM Trizma base, 384 mM glycine, 0.1% (w/v) SDS) for 90 minutes, or until the dye front reached the bottom of the gel. 10 µl of a tri-chrom pre-stained protein marker (Pierce, Rockford, IL, USA) was also loaded onto each gel and Collagenase F (5 µg/ml in zymogram sample buffer) was loaded as a positive control (Sigma). The gels were equilibrated in zymogram renaturation buffer (0.25% Triton × 100, distilled water) for 30 minutes at room temperature with gentle agitation and then incubated in zymogram renaturation buffer at 37 °C overnight. The gels were stained with Coomassie Blue R-250 (Sigma) (0.5% w/v in 40% methanol, 10% acetic acid, 50% distilled water) for one hour. Gels were then destained with destaining solution (40% methanol, 10% acetic acid, 50% distilled water) until areas of protease activity were clearly visible against the dark blue background.

2.8 Millipore Milliplex MAP Technology

Milliplex MAP assays (Millipore, Watford, UK) are based on Luminex ×Map technology, allowing multiplex detection of proteins from a single biological sample. The technology is based on the coating of microspheres or beads with capture antibodies of interest, to which the sample is then added. The use of multiple conjugated beads allows multiple readouts from the same sample, thus conserving valuable biological specimens. Adipose tissue conditioned medium (ACM) samples were tested on the Human Cytokine and Human Adipokine panels (analytes listed in Appendix II) by Millipore. Milliplex Map results were validated using ELISA, described below.

2.9 Randox Evidence Investigator

The Randox Evidence Investigator multiplex technology enables the detection of a panel of 12 cytokines simultaneously (analytes listed in Appendix II) using biochip array technology. A

volume of 100 μl of adipose tissue conditioned medium (ACM) or serum was added the biochip. Cytokines present in the sample bind to immobilised ligands on the biochip and are detected using chemiluminescent immunoassays. A charge coupled device camera detects the light signal and advanced image processing software compares each signal to a calibration curve.

2.10 ELISA

Enzyme-linked immunosorbent assay (ELISA) assays (R&D systems, Inc., MN, USA) were used to determine cytokine and adipokine concentrations in adipose conditioned medium (ACM) and serum. The ELISA plate was coated with 50 μl capture antibody overnight at 4 °C, and washed three times in PBS (with 0.05% Tween 20). Samples were diluted to appropriate concentrations in 1% BSA, as determined by optimisation steps and 50 μl of sample was applied to each well in triplicate with the exception of blanks which contained only 1% BSA. A serial dilution was made from the standard supplied and 50 μl of each concentration were applied to the plate in triplicate. Samples were incubated at 4 °C overnight and the plate was washed three times in PBS (with 0.05% Tween 20). 50 μl of detection antibody was added and the plate incubated at room temperature for two hours followed by five washes in PBS Tween 20 (0.05%). A 50 μl volume of streptavidin-HRP (1/200 dilution in 1% BSA) was added to each well and incubated for 20 minutes at room temperature. 50 μl of substrate tetramethylbenzidine (TMB) was added to each well and covered with tinfoil until the colour developed (2-15 minutes). 50 μl H_2SO_4 was added to each well to stop the reaction and the plate was read immediately at 450 nm using an Alpha Fluor Plus spectrophotometer (Tescan Trading AG, Switzerland). Protein concentrations were determined by interpolating from a standard curve of known concentrations (Appendix II).

Table 2.9: Antibodies used in ELISA

ELISA	Capture antibody	Top standard	Detection antibody
Leptin	4 µg/ml	2,000 pg/ml	12.5 ng/ml
Adiponectin	2 µg/ml	4,000 pg/ml	2 µg/ml
IL-6	2 µg/ml	600 pg/ml	200 ng/ml
IL-8	4 µg/ml	2,000 pg/ml	20 ng/ml
MCP-1	1 µg/ml	1,000 pg/ml	100 ng/ml
VEGFA	1 µg/ml	2,000 pg/ml	100 ng/ml
IFG-γ	4 µg/ml	1,000 pg/ml	50 ng/ml

2.11 FACS analysis of integrin expression

Cells were seeded at a dilution of 2×10^5 cells per well in a 12 well plate and allowed to adhere for a minimum of 6 hours. They were serum starved overnight (maintenance medium containing 0.5% FCS) and treated the following day with ACM from two viscerally obese and two non obese male OAD patients or control M199 medium for a period of 24 and 48 hours. Cells were set up on different days so that all time-points could be measured on the flow cytometer on the same day. Supernatants were collected and transferred to 5 ml flow tubes (BD Biosciences, Bedford, MA, USA) and adherent cells were lifted using EDTA (0.02% w/v), which was incubated with cells for 15 minutes and added to tubes containing the respective supernatant. Cells were pelleted at $180 \times g$ for 3 minutes and the supernatant discarded. 1 ml FACS buffer (0.1% sodium azide, 2% FCS in PBS) was added to each tube, vortexed for a few seconds, and centrifuged at $180 \times g$ for 3 minutes. The supernatant was discarded and 1 ml blocking buffer (50% FCS, 50% FACS buffer) was added to each tube and incubated at room temperature for 5 minutes. 1 ml FACS buffer was added and tubes centrifuged at $180 \times g$ for 3 minutes. Supernatant was discarded and an appropriated volume of antibody (detailed in table below) was added to appropriate tubes. Samples were vortexed to resuspend cells and incubated in the dark for 20 minutes at 4 °C. 1 ml FACS buffer was added to each tube, vortexed and centrifuged at $180 \times g$ for 3 minutes. Cells were resuspended in 300 µl FACS buffer and integrin subunit levels were measured using a FACSCalibur flow cytometer (BD Biosciences, Bedford, MA, USA). 10,000 events were collected per sample from a live cell gate.

Data analysis was carried out using Cell Quest software (BD Biosciences, Bedford, MA, USA) by a trained user of the instrument, Dr Joanne Lysaght. Integrin expression in ACM treated cells was expressed relative to untreated cells from three independent experiments.

Table 2.10: Antibodies used in FACS

Antibody	Conjugation	Volume per sample	Supplier
ITGA3 (CD49c)	PE	5 µl	BD Pharmingen
ITGA5 (CD49e)	PE	5 µl	BD Pharmingen
ITGA6 (CD49f)	PE	1 µl	ebiosciences

2.12 High Content Screening analysis of focal adhesion pathway

OE33 cells were seeded at a dilution of 4×10^3 cells per well in maintenance medium in 96 well plates and allowed to adhere for a minimum of 6 hours. They were then serum starved (medium containing 0.5% FCS) overnight. The following day they were incubated with 100 µl of the ACM and control M199 medium for a period of 24 hours. Cells were fixed with 4% paraformaldehyde for 30 minutes at room temperature and washed three times with PBS.

For FAK staining, cells were blocked and permeabilised for 1 hour at room temperature with 5% goat serum (100 µl goat serum, 2 ml PBS, 0.5% Triton ×100). For phosphopaxillin staining, cells were permeabilised by the addition of 100 µl of ice-cold methanol for 5 minutes in the freezer, prior to the blocking step. Blocking serum was removed by flicking and tapping the plate. A volume of 100 µl of primary antibody (anti phospho-paxillin (Tyr 118) (Millipore) 1/50, anti FAK (Millipore) 1/100) was added to each well in triplicate in antibody dilution buffer (0.4 g BSA, 40 ml PBS, 0.1% Triton ×100). Following overnight incubation at 4 °C, wells were washed three times with PBS. A volume of 100 µl of secondary antibody (containing secondary antibody (green) (1/1000), Hoechst nuclear stain (blue) (1/500) and phalloidin cytoskeleton stain (red) (1/2000)) was added to each well. Following two hours incubation at room temperature in the dark, cells were washed 2 times with 100 µl of PBS, the PBS was replaced and cells were immediately analysed on the InCell analyser 1000.

2.13 Lactate assay

Co-culture supernatants were assayed for lactate concentration using a commercially available lactate assay kit (BioVision, CA, USA). This kit measures L(+)-lactate concentration in biological samples such as cell culture supernatants. The lactate standard was diluted to 1 nmol/μl by mixing 10 μl of Lactate Standard (Biovision) with 990 μl Lactate Assay Buffer (BioVision). A serial dilution was carried out to generate a standard curve of 0, 2, 3, 4, 6, 8, 10 nmol/well of L-(+)-lactate standard. A volume of 1 μl sample in 50 μl Lactate Assay Buffer (BioVision) was added to each well in triplicate. A volume of 50 μl Reaction mix (46 μl Lactate Assay Mix, 2 μl Lactate probe, 2 μl Lactate Enzyme Mix) was added to each well and mixed well. The reaction was incubated for 30 minutes at room temperature in the dark. The absorbance was measured at 570 nm using an Alpha Fluor Plus spectrophotometer (Tescan Trading AG, Switzerland). Protein concentrations were determined by interpolating from a standard curve of known concentrations (Appendix II).

2.14 Immunohistochemistry

Resected tumour from OAD patients was fixed in 10% formalin overnight and embedded in paraffin wax on a Leica EG 1140H embedder (Laboratory Instruments and Supplies, Dublin, Ireland). Tissue sections 5 μm in thickness were cut from tissue microarray blocks using a Microm HM325 microtome (Thermo Fisher Scientific, IL, USA) and floated onto Superfrost Plus poly-L-lysine coated glass slides (Thermo Fisher Scientific, IL, USA). Cut sections were baked overnight at 37 °C in a tissue-drying oven (Binder, Tuttlingen, Germany) and processed immediately.

2.14.1 Immunohistochemical full face staining

MMP9 (Millipore) was optimised on full face sections before staining tissue microarrays (TMAs). Antigen retrieval was carried out using Trilogy™ (Cell Marque™ Corporation, Rocklin, CA, USA) which combines three pre-treatment steps: deparaffinisation, rehydration and unmasking. Slides were incubated in Trilogy™ (1/20 dilution in distilled water) in a Princess DYB350 programmable pressure cooker on low pressure for 10 minutes. Vectastain Elite kits (Vector Labs, Burlingame, CA, USA) were used for all immunohistochemical staining. Tissue sections were incubated in 3% H_2O_2 in methanol for 30 minutes to quench endogenous peroxidase activity. The sections were then washed three times for 5 minutes each in phosphate buffered saline (PBS) and blocked for 30 minutes with diluted normal serum from the animal in which the secondary antibody was raised. The slides were then incubated in primary antibody (MMP9: 1/100, 1/500, 1/1000) overnight at 4 °C and then washed three

73

times for 5 minutes each in PBS. The sections were incubated for 30 minutes in a 1:400 dilution of biotinylated secondary antibody and then washed again three times for 5 minutes each in PBS. They were then incubated for 30 minutes in avidin-biotin complex reagent. Following this, the sections were washed three times for 5 minutes each in PBS and incubated for 2-15 minutes (depending on the level of protein expression in the tissue) in the dark in diaminobenzidine (DAB) peroxidase solution. The sections were rinsed in tap water and counterstained in Harris's haemytoxylin for 30 seconds. The slides were placed in a PBS bath for 5 minutes and subsequently rinsed in gently running tap water for 5 minutes. The slides were then dipped in two separate baths of 100% methanol (up and down 10 times) and two separate baths of xylene (up and down 10 times) before being transferred to a separate container of xylene for at least 4 hours. Coverslips (VWR International, West Chester, PA, USA) were mounted onto the slides using DPX mountant (B.D.H. Ltd., Poole, Dorset, UK) and left to dry in a fume hood. Images were taken using Image Pro-Plus 4.1 software (Media Cybernetics, Gelichen, Germany).

2.14.2 Tissue microarray staining

Sections 4 µm in thickness were cut from tissue microarray (TMA) blocks using a Microm HM325 microtome (Thermo Fisher Scientific, IL, USA) and floated onto Superfrost Plus slides (Thermo Fisher Scientific, IL, USA). Cut sections were baked at 37°C overnight and stored at 4°C. All staining was carried out on a Bond III automated immunostainer (Leica Microsystems, Wetzlar, Germany) in collaboration with Dr Robert Cummins at Beaumont Hospital, Dublin 9. Sections were loaded onto the system and automated staining was carried out according to the appropriate protocol. Slides were deparaffinised and antigen retrieval was carried out for a length of time previously optimised for the antibody (see table below). ER1 is a sodium citrate based antigen retrieval solution (pH 6.0) and the section is incubated at 100°C in the solution for the required length of time. The appropriately diluted primary antibody (see table below) was added to the sections for 20 minutes. Antibody binding was detected using diaminobenzidine (DAB) solution and sections were then counterstained lightly with haematoxylin. Coverslips (VWR International, West Chester, PA, USA) were mounted onto the slides using DPX mountant (B.D.H. Ltd., Poole, Dorset, UK) and left to dry in a fume hood. Images were taken using Image Pro-Plus 4.1 software (Media Cybernetics, Gelichen, Germany).

74

Table 2.11: Antibodies used for TMA immunostaining.

Antibody	Supplier	Type	Control	Pre-treatment	Dilution
VEGF	Millipore	Polyclonal	Placenta	ER1 20 mins	1/500
MMP-9	Millipore	Monoclonal	TAC[1]	ER1 10 mins	1/2000

[1]TAC is a composite positive control block consisting of a piece of tonsil, normal appendix and carcinoma tissue.

2.14.3 Immunohistochemical staining quantification

Tissue microarrays were graded independently by three individuals. Intensity of staining was graded on a scale from 0 to 3. A score of 0 corresponded to no staining, a score of 1 to weak staining, a score of 2 to moderate staining and a score of 3 to strong staining. Percentage of tumour cells stained was graded in quartiles of 0%, 25%, 50%, 75% and 100%. The average grade for each patient was calculated by multiplication of the intensity score by the percentage of tumour score. This value was averaged over the three cores present on the TMA for each patient. The final grade was calculated by averaging the grades from each of the three independent individuals. Statistical analysis was carried out as described in section 2.20.

2.15 BrdU cell proliferation assay

Cells were seeded at a dilution of 5×10^3 cells per well in appropriate maintenance medium in 96 well plates and allowed to adhere for a minimum of 6 hours. They were then serum starved (medium containing 0.5% FCS) overnight. The following day they were incubated with 100 µl of ACM or the required treatment (Table 11) for a period of 24 or 48 hours and cell proliferation was assessed using BrdU cell proliferation ELISA (Roche Diagnostics Ltd., Sussex, UK). The pyrimidine analogue BrdU (5-bromo-2'-deoxyuridine) is incorporated in the place of thymine in the newly synthesised DNA of proliferating cells, and is bound by the BrdU anti-POD antibody. The antibody complexes are then detected by a subsequent substrate reaction.

BrdU label (1/1000 dilution in appropriate cell culture medium) was added to each well (except no BrdU label control) for 3 hours at 37 °C, following which the medium was tapped and flicked off. Cells were fixed by adding 200 µl of fixative solution (Roche Diagnostics Ltd., Sussex, UK) for 30 minutes at room temperature. 100 µl anti-BrdU-POD (mouse monoclonal antibody, peroxidase conjugated) was added to each well and the plate was incubated for 90 minutes at room temperature. Cells were then washed in PBS and 100 µl of substrate solution

was added to each well. The plate was incubated at room temperature for 5 – 10 minutes or until colour was sufficient for photometric detection. 25 µl H_2SO_4 was then added to stop the reaction and the plate absorbance was read at 450 nm on an Alpha Fluor Plus spectrophotometer (Tescan Trading AG, Switzerland). Wells containing cells but no BrdU label were used to subtract background absorbances and percentage increase/decrease in proliferation was calculated relative to untreated cells.

Table 2.12: Adipokine concentrations for dose response proliferation curves in oesophageal adenocarcinoma cell lines.

Adipokine	Dose response concentrations					
Leptin (µM)	0	1	10	100	500	
Adiponectin (µM)	0	100	500	1000	5000	
VEGFA (ng/ml)	0	0.1	1	10	100	1000

2.16 Cell migration assay

Migration assays were carried out using the QCM Chemotaxis 96 well Cell Migration assay (Millipore, Watford, UK). The assay is performed in a 96 well plate, each well containing a chamber lined with an 8 µm pore size polycarbonate membrane. Non-migratory cells cannot move through these pores while cells with migratory properties can migrate through the porous membrane and cling to the bottom of the chamber. These migratory cells are dislodged following incubation in Detachment Buffer, lysed and detected with a fluorescent dye.

The assay was performed in a Grade II laminar hood. Adipose conditioned medium (ACM) from viscerally obese (n=15) and non obese (n=14) male oesophageal adenocarcinoma patients, and control M199 medium was placed into the feeder wells beneath the chambers in triplicate. OE33 cells were serum starved (medium containing 0.5% FCS) overnight, trypinised and seeded at a dilution of 5×10^4 cells per chamber. Following an incubation period of 24 hours, non-migratory cells which had remained in the chamber were flicked and tapped off. The chambers were rinsed by placing the plate into a feeder tray of PBS for one minute. The PBS was replaced by Cell Detachment Solution and the chamber plate was incubated in this solution for 30 minutes at 37 °C. Cells were dislodged by gently tilting the chamber plate back and forth several times during the incubation period. A lysis buffer containing fluorescent dye

was made up for all samples by diluting CyQuant GR fluorescent Dye 1:75 with 4× Lysis Buffer. 50 µl of this solution was added to each well of the feeder tray containing the cells which had invaded or migrated through the membrane. The tray was incubated at room temperature for 15 minutes and 150 µl of this mixture was transferred to a fluorescence compatible plate and the proportion of cells which had migrated/invaded through the membrane was determined using a fluorimeter (Wallac Victor 2 1420, PerkinElmer, Ballymount, Dublin) at the 485 nm/535 nm filter set. Control wells, containing all components but no cells, were used as blanks and these fluorescence values were subtracted for all other values in order to interpret the data. Results were calculated as a percentage increase in migratory or invasive capacity relative to untreated cells.

2.17 Cell invasion assay

Migration assays were carried out using the QCM 96 well Cell Invasion assay, respectively (Millipore, Watford, UK). This assay is performed in a 96 well plate, each well containing a chamber lined with an 8 µm pore size polycarbonate membrane. The membrane pores are occluded by a thin coating of ECMatrix (extracellular matrix), blocking non-invasive cells from moving through. Cells with invasive properties, on the other hand, can move through the ECM layer and porous membrane and cling to the bottom of the chamber. These invasive cells are dislodged following incubation in Detachment Buffer, lysed and detected with a fluorescent dye.

The assay was performed in a Grade II laminar hood. 100 µl of prewarmed serum free medium was added to the chambers of the invasion assay and incubated at room temperature for 90 minutes to rehydrate the ECM. Adipose conditioned medium (ACM) from viscerally obese (n=15) and non obese (n=14) male oesophageal adenocarcinoma patients, and control M199 medium was placed into the feeder wells beneath the chambers in triplicate. OE33 cells were grown to 70% confluency and serum starved (medium containing 0.5% FCS) overnight. They were then trypinised and seeded at a dilution of 1×10^5 cells per chamber for the invasion assays, respectively. Following an incubation period of 24 hours, non-invasive cells which had remained in the chamber were flicked and tapped off and the assay was continued as described in section 2.17.

2.18 Annexin-V-FITC/Propidium Iodide Apoptosis Assay

One of the early events in apoptosis is translocation of phosphotidylserine (PS) from the inner to the outer leaflet of the plasma membrane, detected in this assay by binding of anticoagulant protein Annexin V to exposed PS. Propidium iodide (PI) intercalates with double stranded DNA, only accessed after the cell membrane has lost integrity following apoptosis or necrosis. The combination of Annexin V-FITC and PI stain allows for the differentiation of early apoptotic cells (Annexin V-FITC positive), late apoptotic and/or necrotic cells (Annexin V-FITC and PI positive) and viable cells (unstained).

Cells were seeded into 12 well plates at a dilution of 1.5×10^4 cells per well and allowed to adhere for a minimum of 6 hours before serum starvation (medium containing 0.5% FCS) overnight. Cells were then treated with increasing concentrations of cisplatin (1 µM, 10 µM, 100 µM, 1 mM) in the presence or absence of adipose conditioned medium (ACM) for a period of 24 and 48 hours. Control wells contained ACM or M199 medium alone. Cells were set up on different days so that all time-points could be measured on the flow cytometer on the same day. Supernatants were collected and transferred to 5 ml flow tubes (BD Biosciences, Bedford, MA, USA) and adherent cells were trypsinised at 37 °C until they lifted off the plate surface. The trypsin was deactivated by the addition of maintenance medium (containing 10% FCS), and the cell suspension was added to the tubes containing the respective supernatant. Cells were pelleted at $180 \times g$ for 3 minutes and the supernatant discarded. The pellet was resuspended in 2 ml 1× Binding Buffer (Biosource International, CA, USA), vortexed briefly, and centrifuged at $180 \times g$ for 3 minutes. The supernatant was again discarded and the cell pellet resuspended in 100 µl of 1× binding buffer. 3 µl of Annexin V (IQ Products, Gronigen, The Netherlands) was added to all samples except no stain and PI only controls. The tubes were briefly vortexed to resuspend the cell pellet and the incubated in the dark at 4 °C for 20 minutes. 1 ml 1× binding buffer was added, the tubes were again briefly vortexed, and then centrifuged at $180 \times g$ for 3 minutes. The supernatant was discarded and the cell pellet resuspended in 250 µl of 1× binding buffer. Immediately before acquiring, 250 µl of PI (1:4000 dilution of 1 mg/ml stock in 1× binding buffer, Invitrogen Corporation, CA, USA) was added to all samples except no stain and Annexin V only controls. Tubes were vortexed and apoptosis levels were measured using a FACSCalibur flow cytometer (BD Biosciences, Bedford, MA, USA). 10,000 events were collected for each sample using a gate to exclude cellular debris. Data analysis was carried out using Cell Quest software (BD Biosciences, Bedford, MA, USA) by a trained user of the instrument, Dr Joanne Lysaght. The x axis (FL1) of the dot plot represents

the log Annexin V-FITC fluorescence, while the Y axis (FL2) represents the log PI fluorescence. The percentage of apoptosis in treated cells was expressed relative to untreated control cells from three independent experiments.

2.19 Statistical analysis

Statistical analysis was computed using GraphPad Prism 5 software. All data are expressed as mean ± SEM. SEM is calculated as the SD of the original sample divided by the square root of the sample size. Student's t-tests were used to compare the means of two groups. In cases where data were paired (i.e. tumour/normal matched samples from the same patient or patient samples with age-matched controls), a paired t-test was used for statistical analysis. Otherwise, the unpaired t-test was used. Data analysis was performed by one way analysis of variance (ANOVA), where the number of groups in the experiment was three or more. A post hoc test was necessary following ANOVA in order to determine which groups were significantly different to each other. Post test analysis was carried out by Tukey multiple comparisons test where sample groups were unpaired. When sample groups were paired, post test analysis was carried out by Bonferroni multiple comparisons test. These post hoc tests assume Gaussian distribution of the sample population. In cases where the distribution was not Gaussian, the Mann-Whitney test was used to examine statistical significance between unpaired groups of data. Kaplan-Meiers curves were generated for survival analysis. In order to carry out the analysis, data were split into two groups: median survival ≥ median value and median survival < median value. The resulting two sets of data were used to generate survival curves. Statistical analysis was carried out by the Gehan-Breslow-Wilcoxon test. For all statistical analysis, a probability of (p) of ≤ 0.05 was considered to represent a significant difference between groups. All Affymetrix microarray analysis was carried out in collaboration with a bioinformatician Ms Melissa Morine (under Prof Helen Roche, Nutrigenomics Research Group, UCD) and is described in section 2.6.12.2.

3 Pathways involved in inflammation, angiogenesis and cell signalling are up regulated in the omentum of viscerally obese oesophageal adenocarcinoma patients.

3.1   Introduction

Obesity, defined as the accumulation of excess adipose tissue, is strongly associated with increased morbidity and mortality (Calle et al., 1999; Flegal et al., 2005). Visceral adiposity in particular is a key risk factor for cardiovascular disease, stroke, hypertension, metabolic syndrome, type II diabetes mellitus, osteoarthritis, sleep apnoea and gall bladder disease (Guh et al., 2009; Must et al., 1999). More recently obesity has been linked to increased cancer incidence and mortality (Calle et al., 2003; Calle et al., 1999; Field et al., 2001). Rates of obesity have now reached pandemic proportions with two thirds of US adults overweight and one third obese (National Health and Nutrition Examination Survey (NHNES) 2007 – 2008). Rates of overweight and obesity in Ireland are currently 5% lower than the US but increasing rapidly (SLAN, 2007). The incidence of worldwide obesity is increasing at an exponential rate (Ogden et al., 2006; SLAN, 2007) and an enhanced understanding of the underlying molecular mechanisms responsible for the myriad of obesity related disorders and diseases is now imperative.

A wide range of cell types in adipose tissue are potential contributors to the pathogenesis of excess adiposity and these include mature adipocytes, pre-adipocytes, endothelial cells, fibroblasts and immune cells (Kahn and Flier, 2000). *In vitro* cell culture is therefore an indispensable tool of obesity research enabling the analysis of these individual cell types, their secreted factors and signalling pathways under controlled conditions (Fischer-Posovszky et al., 2008). Primary cells are unpredictably variable between individuals, the quantity of available material is usually limited and isolated primary cells have a limited life span *in vitro* (Fischer-Posovszky et al., 2008; Wabitsch et al., 2001). For these reasons, many research groups choose to rely on immortalised cell lines for *in vitro* studies of adipogenesis and obesity related disease. 3T3-L1 and 3T3-F442A are murine embryonic fibroblasts developed through clonal isolation which differentiate spontaneously when exposed to a standard differentiation inducing hormone cocktail (Rosen and MacDougald, 2006). 3T3 adipogenesis has been widely studied and follows a well defined sequence of events marked by early alterations in gene expression of adipogenic transcription factors including CCAAT/enhancer binding protein α (C/EBPα), sterol regulatory element binding protein 1c (SREBP 1c) and peroxisome proliferator-activated receptor γ (PPARγ) (Rosen and MacDougald, 2006). These transcription factors are responsible for the induction of adipocyte fatty acid binding protein (AP2), glucose transporter 4 (GLUT4), lipoprotein lipase (LPL), glyceraldehyde-3-phosphate dehydrogenase (GAPDH) and leptin (MacDougald and Lane, 1995). Expression of these adipocyte specific

genes are necessary for adipocyte function and they are involved in protein secretion, lipid synthesis, glucose transport and insulin sensitivity (Rosen and MacDougald, 2006; Wabitsch et al., 2001).

The murine adipocyte cell lines 3T3-L1 and 3T3-F442A are both well characterised and widely used (Bour et al., 2007). However in studies of human disease, greater clinical relevance would be derived from working with a human model and to this end a human pre-adipocyte cell strain, SGBS, has been established (Wabitsch et al., 2001). SGBS are derived from the stromal vascular fraction (SVF) of subcutaneous adipose tissue of an infant with Simpson-Golabi Behmel syndrome (SGBS), a rare X-linked congenital overgrowth syndrome (Wabitsch et al., 2001). SGBS adipogenesis follows a similar pattern of adipocyte differentiation specific gene expression to that of the well characterised 3T3 (Wabitsch et al., 2001). One difference worth noting is that 3T3-L1 and 3T3-F442A adipocytes undergo mitotic clonal expansion followed by growth arrest in the early stages of differentiation, while this process is absent both in SGBS and in primary human pre-adipocytes indicating a fundamental difference between species (Newell et al., 2006). It has been demonstrated that SGBS are similar to primary human adipocytes regarding glucose transporter expression (Wood et al., 2003), expression of adipokine splice variants (Kersten et al., 2000; Mandard et al., 2004) and ratio of adiponectin isoform expression (Bodles et al., 2006). These initial studies indicate that SGBS may be a relevant model for the study of human obesity related disease and SGBS have been shown, once differentiated, to behave functionally like mature human adipocytes (Fischer-Posovszky et al., 2008). This series of experiments aimed to compare morphology, differentiation specific gene expression and biochemical function between SGBS and primary human omental adipocytes with reference to the well characterised and widely used 3T3-L1 model. Obesity has an important role in cancer initiation and progression (Calle et al., 2003) and this study aimed to identify a clinically relevant experimental model of adipocyte biology within this context.

In parallel, microarray technology was used to identify pro-tumour pathways up regulated in the omentum of viscerally obese oesophageal adenocarcinoma patients. Obesity is a complex disorder involving deregulation of multiple gene networks (Morine et al., 2008). Microarray technology is ideally suited to the challenge of delineating these networks as it enables the quantitative and reproducible analysis of thousands of transcripts simultaneously (Lipshutz et al., 1999). Microarray technology has been widely used in obesity research and studies to date have examined differences between subcutaneous and omental adipose tissue depots (Linder et al., 2004), subcutaneous adipose tissue in obesity (Henegar et al., 2008) and omental

adipose tissue in obesity (Gomez-Ambrosi et al., 2004). Visceral adiposity is a stronger predictor of related morbidity and mortality than overall obesity (Gesta et al., 2006; Giorgino et al., 2005) and this important finding is reflected in the International Diabetes Foundation (IDF) definition of the Metabolic Syndrome (Federation, 2006). One possible weakness of published microarray studies is the classification of patients using BMI, a measure of overall obesity (Gomez-Ambrosi et al., 2004). This is the first large scale microarray study to date to examine altered omental adipose tissue gene expression in visceral obesity, as defined by visceral fat area using computed tomography.

3.2   Aims and objectives

The overall aims of this chapter were:

1. To evaluate the clinical relevance of the SGBS adipocyte cell strain as an experimental model in the study of obesity related human disease.

2. To identify a gene expression signature in human omentum of viscerally obese OAD patients which could contribute to obesity related pathology.

Specific objectives:

- Comparison of morphology, differentiation specific gene expression and biochemical function between human SGBS and primary human adipocytes, with reference to the well established and widely used 3T3-L1 adipocytes.

- Microarray analysis of omental adipose tissue from viscerally obese and non obese male oesophageal adenocarcinoma patients.

3.3 Results

3.3.1 SGBS and 3T3-L1 pre-adipocytes undergo morphological changes during the process of differentiation.

Murine 3T3-L1 and human SGBS pre-adipocytes were differentiated according to standard protocols (as described in section 2.4) and morphology was examined by Oil Red O staining (as described in section 2.5.2). Differentiation was initiated at two days post confluency in 3T3-L1, and at 70% confluency in SGBS, according to published standard protocols (Fischer-Posovszky et al., 2008; Moloney et al., 2007). The process of differentiation was carried out for standard, previously published lengths of time: eight days for 3T3-L1 (Moloney et al., 2007) and 14 days for SGBS (Fischer-Posovszky et al., 2008; Wabitsch et al., 2001). In order to investigate whether differentiation over a longer time period could induce further morphological changes, 3T3-L1 were differentiated for 14 days and SGBS for 21 days, one week longer than standard established protocols.

Pre-adipocytes accumulated lipid droplets over the course of differentiation, beginning at day four in 3T3-L1 and at day six in SGBS. Differentiation efficiency was similar between 3T3-L1 and SGBS models with 90% - 95% of cells accumulating lipid by day eight and day 14, respectively, as assessed by manual counting (Figure 3.1). The degree of confluency over the course of differentiation was much greater in 3T3-L1 compared with SGBS, highlighting a potentially important difference between these models. Not only was differentiation initiated at a higher confluency in 3T3-L1, according to published protocols (Moloney et al., 2007; Wabitsch et al., 2001), but this cell line also undergoes clonal expansion in the early stages of differentiation (Newell et al., 2006). Primary adipocyte morphology was characterised by a single central lipid vesicle while both 3T3-L1 and SGBS accumulated multiple smaller lipid droplets. An increase in lipid droplet size together with a decrease in number of lipid droplets occurred in both models in the final stages of differentiation, however this change was particularly pronounced in SGBS (Figure 3.1). SGBS were therefore morphologically similar to primary adipocytes with respect to lipid droplet size and number (Figure 3.2).
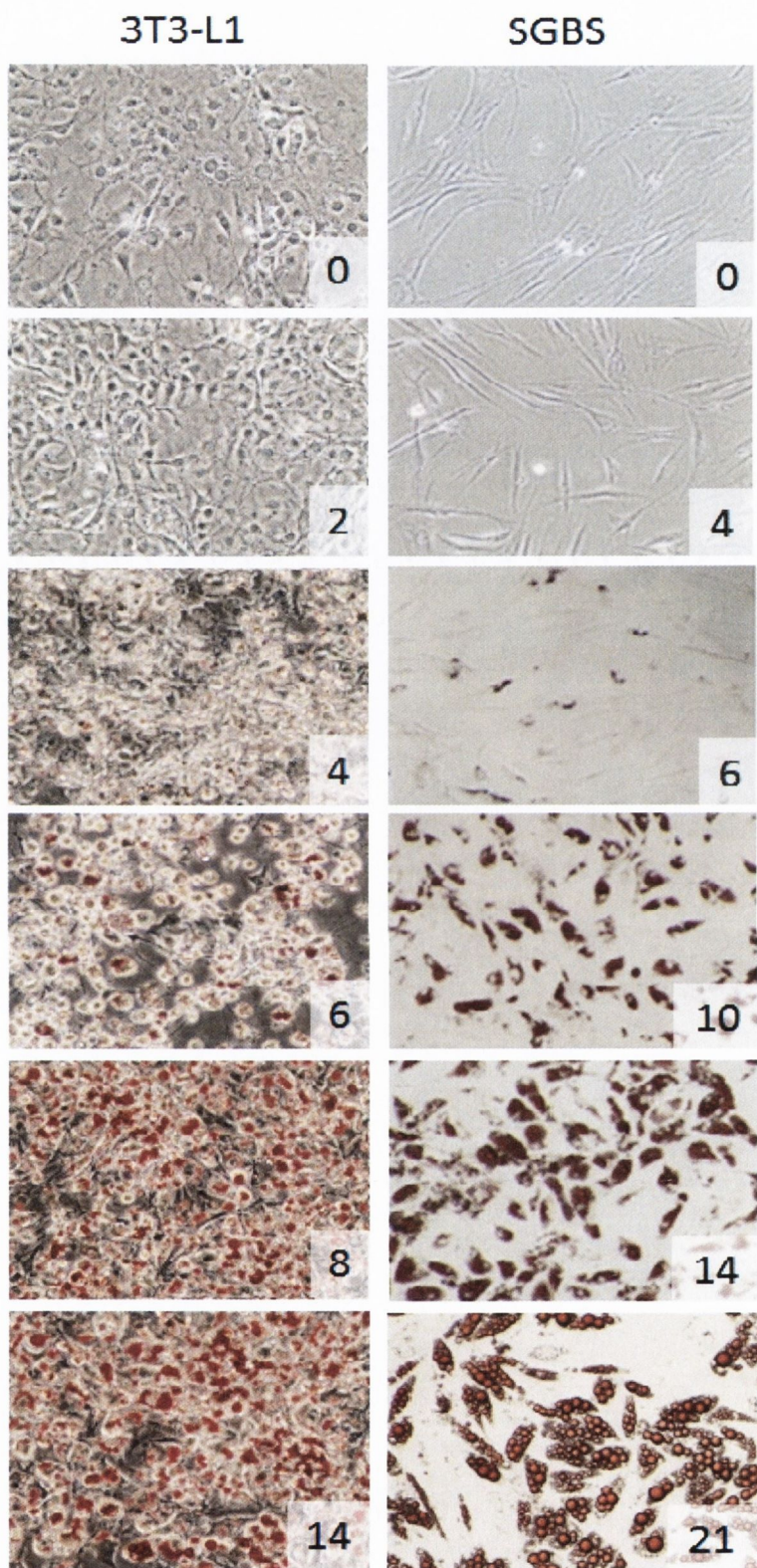
Figure 3.1: Morphological changes in adipocyte cell lines 3T3-L1 and SGBS at regular intervals throughout the process of differentiation. Lipid droplets were stained red with Oil Red O at days 0, 2, 4, 6, 8 and 14 (3T3-L1) and at days 0, 4, 6, 10, 14 and 21 (SGBS) following initiation of differentiation at day 0 using standard protocols. Photographs were taken at 10X magnification.
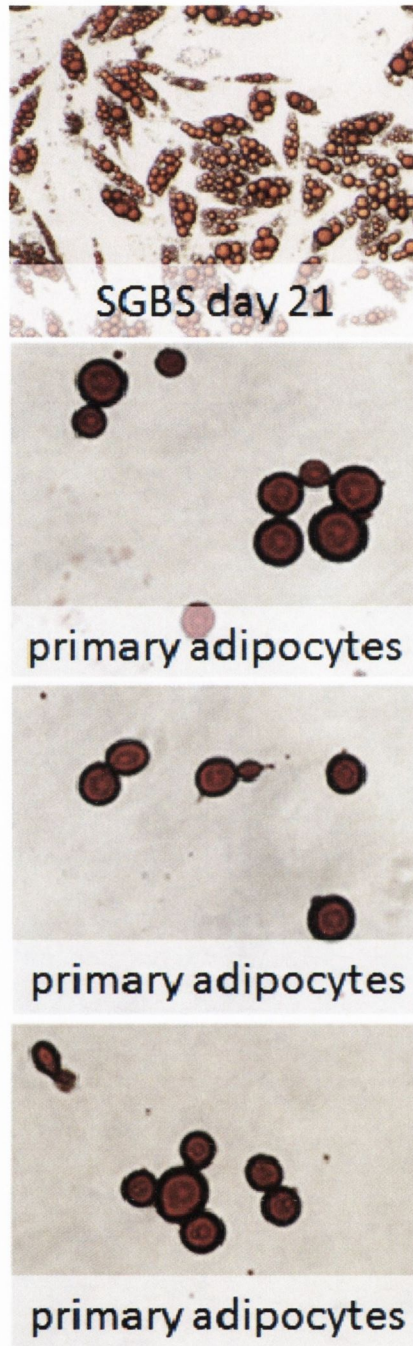
Figure 3.2: Mature primary adipocytes isolated from human omentum of viscerally obese oesophageal adenocarcinoma patients (n=3) were ceiling cultured for 72 hours before lipid droplets were stained with Oil Red O. SGBS adipocytes at day 21 of differentiation were included in this panel for purposes of comparison. Photographs were taken at 10X magnification.

3.3.2 Expression of adipocyte genes is induced upon adipocyte differentiation.

During the process of differentiation, expression of genes involved in adipocyte specific protein secretion, lipid synthesis, glucose transport and insulin sensitivity are induced in 3T3-L1 and SGBS cells (Rosen and MacDougald, 2006; Wabitsch et al., 2001). Key transcription factor and master regulator of differentiation peroxisome proliferator-activated receptor γ (PPARγ) is necessary in the initiation of this process. PPARγ, in combination with several other important transcription factors, induces expression of genes necessary for adipocyte function and these include leptin, glucose transporter 4 (GLUT4), lipoprotein lipase (LPL), adipocyte protein 2/fatty acid binding protein 4 (AP2/FABP4) and glyceraldehyde-3-phosphate dehydrogenase (GAPDH). A direct comparison of expression of this differentiation specific panel of genes was carried out in murine 3T3-L1 and human SGBS by quantitative qPCR (as described in section 2.6.9).

Expression of adipogenic transcription factor PPARγ was induced 8 fold in SGBS and 28 fold in 3T3-L1 (Figure 3.3). Expression of adipocyte function genes leptin, glucose transporter 4 (GLUT4), lipoprotein lipase (LPL), and adipocyte protein 2/fatty acid binding protein 4 (AP2/FABP4) were induced to varying degrees during both 3T3-L1 and SGBS differentiation, however fold changes were most pronounced in SGBS (Figure 3.3). Leptin was induced over 200,000 fold in SGBS but merely 5 fold in 3T3-L1. Leptin expression in differentiated SGBS adipocytes was significantly higher than in 3T3-L1 adipocytes (p<0.01). GLUT4 was induced 30,000 fold in SGBS and 7000 fold in 3T3-L1. LPL was induced almost 700,000 in SGBS but only 15 fold in 3T3-L1. AP2 was induced 50,000 fold in SGBS and 8000 fold in 3T3-L1. As these adipocyte specific gene expression changes are required for basic adipocyte function, this finding suggests SGBS may be a superior model in this regard. On the other hand, 3T3-L1 may be a better model for the study of early regulation of adipocyte differentiation as PPARγ, a master regulator of this process, is induced more strongly in this model.

There is some evidence for altered expression of commonly used housekeeping genes during the process of adipocyte differentiation (Hurtado del Pozo et al., 2010). Expression of GAPDH remained the same throughout SGBS differentiation, indicating that it is a suitable housekeeping gene in this cell line (Figure 3.3). As previously published (Alexander et al., 1985), GAPDH expression was found to fluctuate throughout 3T3-L1 differentiation, suggesting it may not be suitable as an endogenous control in the 3T3-L1 cell line.
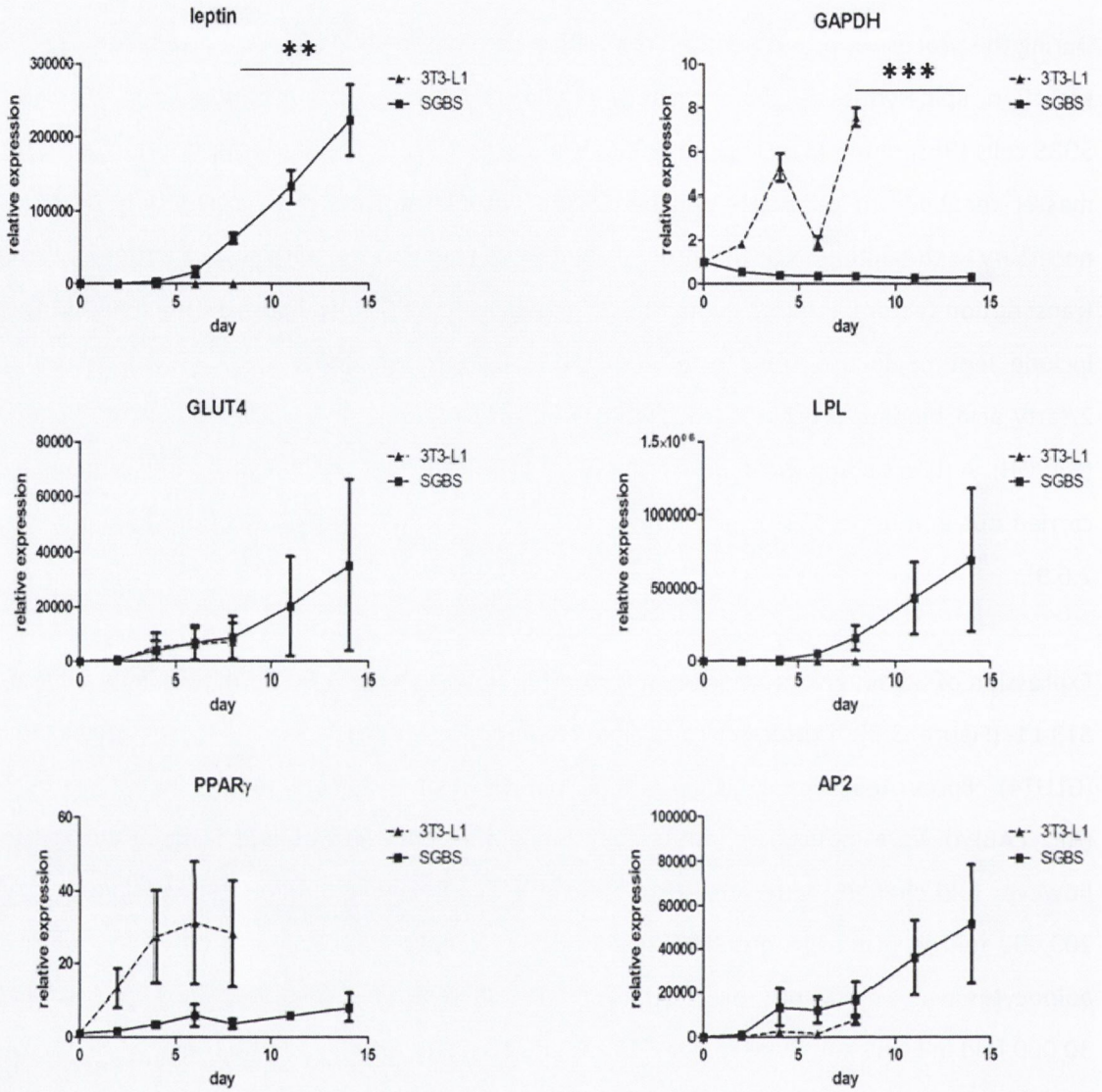
Figure 3.3: Gene expression throughout differentiation was measured by real time qPCR at day 0, 2, 4, 6 and 8 (3T3-L1) and at day 0, 2, 4, 6, 8 and 14 (SGBS). 18S was used as an endogenous control and calibrator for this assay. Data points are the mean values of three independent experiments ± SEM. Statistical analysis was carried out using unpaired t tests between day 8 3T3-L1 and day 14 SGBS expression (**p<0.01, ***p<0.0001).

3.3.3   Gene expression in primary omental adipocytes is similar to SGBS adipocytes.

Levels of expression of adipocyte differentiation specific genes were compared between SGBS and primary human adipocytes. SGBS were differentiated according to standard protocols for 14 days (as described in section 2.4.2). Adipocytes were isolated from omental adipose tissue collected from male OAD patients, classified into groups of viscerally obese (n=15) or non obese (n=9) by waist circumference (as described in section 2.3.3). BMI (p<0.0001), WC (p<0.001) and VFA (p<0.05) were significantly different between patient groups (Table 3.1). Expression of differentiation specific genes leptin, GLUT4, PPARγ, LPL and AP2 were compared in primary human adipocytes from viscerally obese (n=15) and normal weight (n=9) OAD patients by qPCR, using 18S as an endogenous control. Levels of gene expression were then compared between primary human adipocytes and differentiated SGBS by qPCR, using 18S as an endogenous control (as described in section 2.6.9).

Table 3.1: Anthropometric details for patients included in adipocyte gene expression study.

	non obese	obese
No. subjects	9	15
Sex (male), n (%)	7 (78)	12 (80)
Age at surgery, mean (range)	65 (58-76)	63 (49-75)
Waist circumference (cm), mean (range)	88 (83-93) **	103 (84-116)
BMI (kg/m²), mean (range)	24 (22-26) ***	30 (25-36)
VFA (cm²), mean (range)	121 (51-178) *	214 (68-329)
metabolic syndrome, n (%)	0 (0)	11 (73)
neo-adjuvant therapy, n (%)	6 (67)	4 (27)

Patients were categorised using the IDF defined waist circumference cut-off of 94 cm. Statistical analysis was carried out using student's t-test (*p<0.05, **p<0.001, ***p<0.0001). BMI=body mass index (kg/m^2), VFA=visceral fat area (cm^2)

GLUT4 expression was down regulated twofold in omental adipocytes from viscerally obese relative to normal weight patients (p<0.05) (Figure 3.4), and expression was significantly correlated with waist circumference (r^2=0.23, p<0.05) (Figure 3.5). Decreased GLUT4 expression is a marker of reduced insulin sensitivity, a common metabolic disorder in viscerally obese patients (Renehan et al., 2006). There was increased expression of master regulator of adipocyte differentiation, PPARγ, in omental adipocytes from viscerally obese patients.

However this trend did not reach statistical significance and did not correlate with obesity measured by WC (r^2=0.0001, p=ns). Leptin expression was increased fivefold in viscerally obese relative to non obese patients. This result did not reach statistical significance, possibly due to large inter-patient variability in factors influencing leptin production such as adipocyte size, levels of circulating sex hormones and insulin sensitivity (Castracane et al., 1998; Segal et al., 1996). There was a near significant correlation of leptin mRNA levels with WC, indicating that this measure of obesity may be a good predictor of adipocyte leptin expression (r^2=0.13, p<0.1). Expression of LPL and AP2 was unchanged with patient obesity status (Figure 3.4).

Leptin levels in primary human adipocytes were twofold higher in normal weight and 11 fold higher in viscerally obese patients compared to differentiated SGBS (Figure 3.4). Leptin expression is an indicator of adipocyte function and metabolic health and is affected by a wide variety of physiological factors such as circulating levels of insulin, glucose, cytokines and sex hormones (Castracane et al., 1998; Segal et al., 1996). It therefore follows that leptin levels in cell lines cultured away from their physiological system are decreased compared to adipocytes freshly isolated from adipose tissue, and this effect is particularly evident in visceral obesity where leptin levels are high (MacDougald and Lane, 1995). GLUT4 and PPARγ expression was twofold higher while LPL and AP2 expression was three fold higher in subcutaneous derived SGBS compared to primary omental adipocytes (Figure 3.4). It has been previously published that the expression levels of these genes are increased in human subcutaneous relative to visceral adipose tissue (Perrini et al., 2008; Veilleux et al., 2009; Walker et al., 2008). These results indicate that while the morphology, gene expression profile and function of SGBS adipocytes is similar to that of primary human adipocytes; inherent differences between adipose tissue depots must be taken into account when studying subcutaneous derived SGBS adipocytes in the context of visceral obesity.
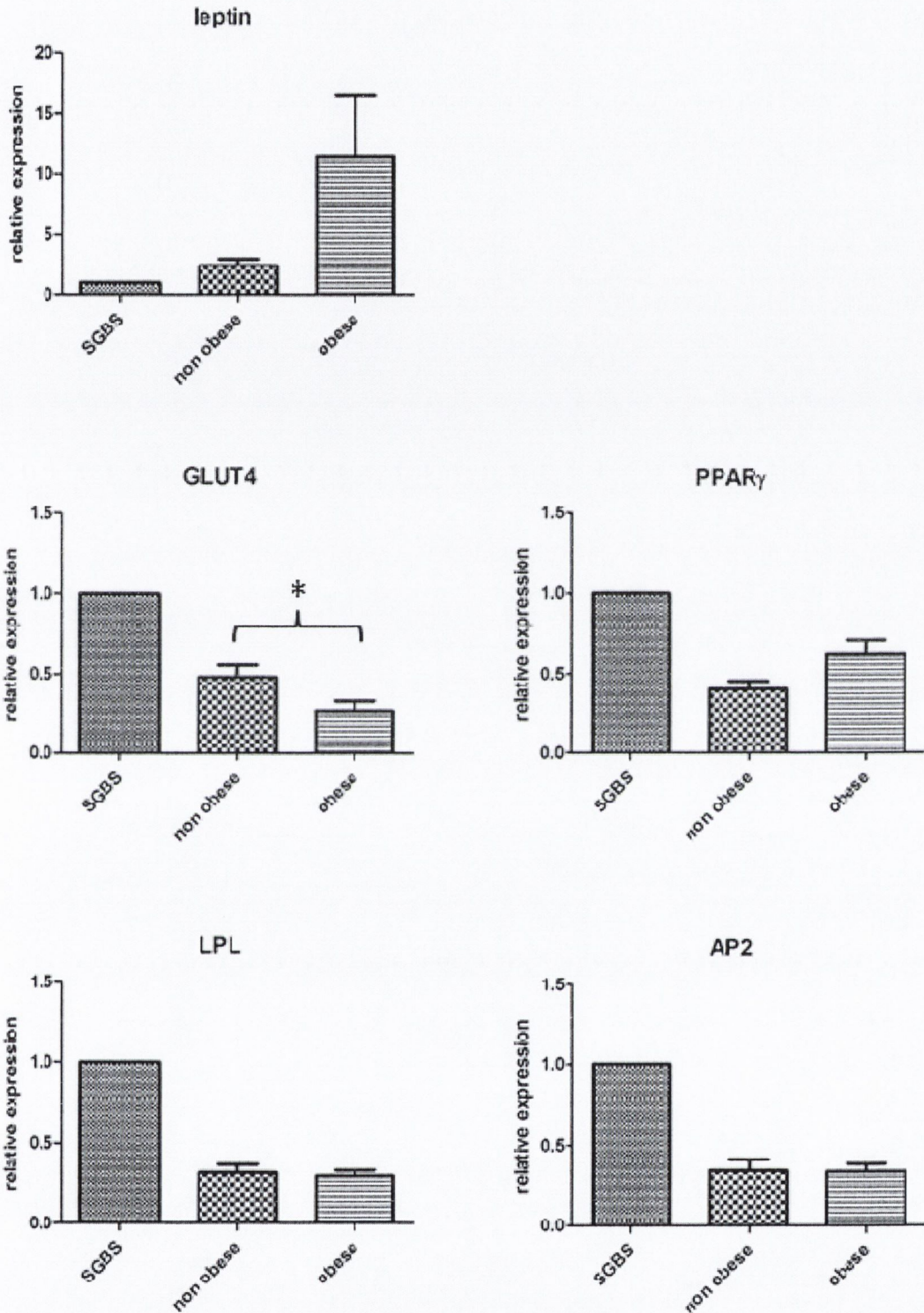
Figure 3.4: Gene expression in primary mature adipocytes isolated from omental adipose tissue from obese (n=15) and non obese (n=9) oesophageal adenocarcinoma patients. Visceral obesity was defined by a waist circumference of < 94 cm in males and < 80 cm in females. Expression is relative to differentiated SGBS (day 14) gene expression and data are expressed as mean ± SEM. Statistical analysis was performed using an unpaired student's t-test (*p<0.05).
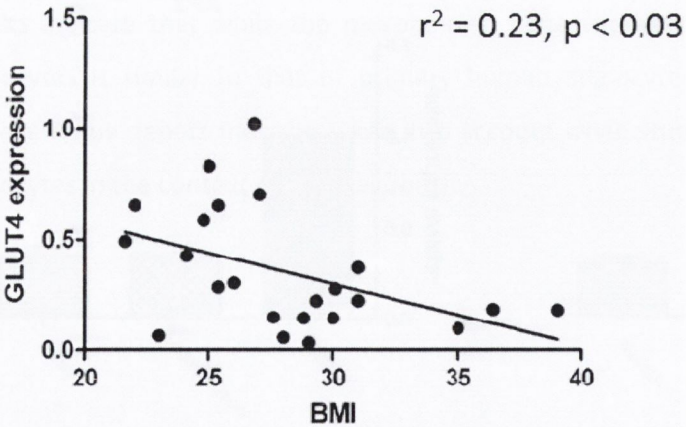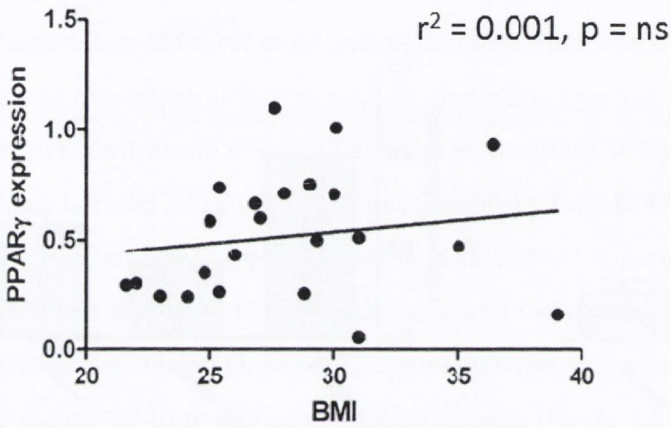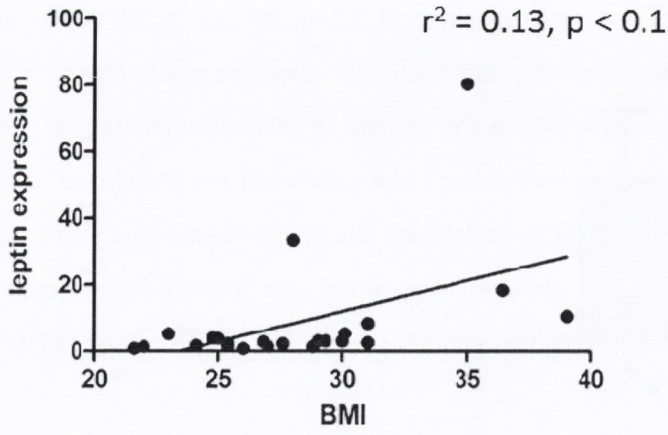
Figure 3.5: Correlation of leptin, PPARγ and GLUT4 expression with visceral obesity, defined by waist circumference of < 94 cm in males and < 80 cm in females. Gene expression was analysed in primary omental adipocytes isolated from viscerally obese (n=16) and non obese (n=9) oesophageal adenocarcinoma patients. Statistical analysis was performed using linear regression analysis.

3.3.4 Biochemical function is similar between SGBS and primary omental adipocytes.

Measures of adipocyte function were compared between murine 3T3-L1, human SGBS and primary human adipocytes. Glycerol-3-phosphate dehydrogenase (GPDH) enzyme activity is required to catalyse the reversible reaction between dihydroxyacetone phosphate and glycerol-3-phosphate. This reaction is necessary for triglyceride synthesis and is strongly induced upon adipocyte differentiation (Wabitsch et al., 2001). GPDH activity (Units) was measured in differentiated murine 3T3-L1, human SGBS and primary human adipocytes and normalised to amount of protein (mg) present in the sample (as described in section 2.7.3). Glucose concentration is used as a clinical measure of adipocyte function and increased levels may indicate insulin resistance (Federation, 2006). Glucose concentration (μM) was measured in supernatants of differentiated murine 3T3-L1, human SGBS and primary human adipocytes and normalised to amount of protein (mg) present in the sample (as described in section 2.7.3).

There was no difference in GPDH enzyme activity between primary human adipocytes (1.3×10^{-2} U/mg protein) and differentiated SGBS (1.5×10^{-2} U/mg), indicating similar levels of triglyceride synthesis between these models (Figure 3.5). However, GPDH activity was found to be significantly higher in murine 3T3-L1 (2.8×10^{-2} U/mg, p<0.0001). SGBS therefore display a greater degree of similarity with primary human adipocytes regarding triglyceride formation compared with 3T3-L1. There was no difference in glucose concentration in the supernatant of primary human adipocytes (88 μM), SGBS (81 μM) or 3T3-L1 (91 μM), indicating similar adipocyte function with respect to glucose uptake (Figure 3.6).

In summary, similar adipocyte morphology and size was observed between human SGBS and primary human adipocytes. Gene expression analysis showed a similar range of expression of genes critical for adipocyte function in human SGBS and primary human adipocytes. Functional data showed no significant differences in GPDH activity or glucose production between human SGBS and primary human adipocytes. Together these findings demonstrate a similarity between SGBS and primary human adipocytes with respect to adipocyte morphology, gene expression and biochemical function. With the majority of *in vitro* studies to date carried out in 3T3 adipocytes; these data indicate that SGBS adipocytes may provide a superior pre-clinical model for the study of multiple obesity related disease states.
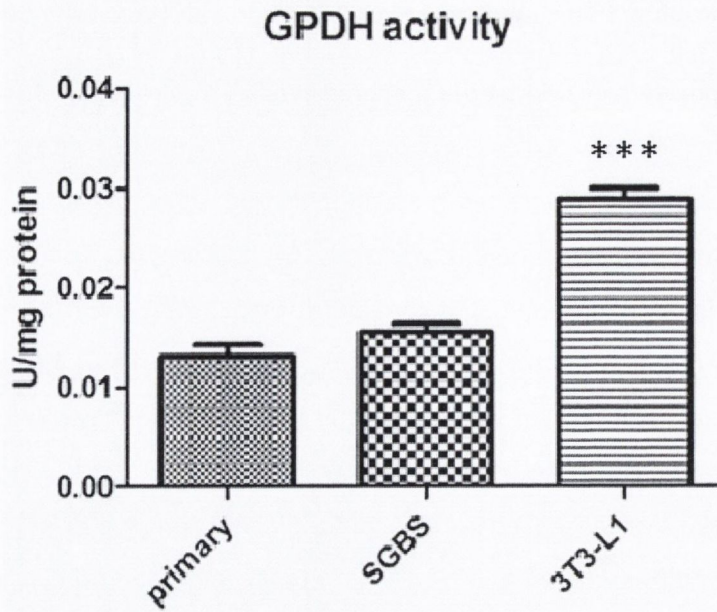
GPDH activity

Figure 3.6: Glycerol-3-phosphate dehydrogenase (GPDH) enzyme activity of primary, SGBS and 3T3L1 adipocytes. Adipocyte cell lines were differentiated under standard conditions (n=3) and mature primary adipocytes (n=3) were isolated from whole omental adipose tissue and ceiling cultured for 72 hours. GPDH enzymatic activity was determined by colorimetric assay. Data are expressed as mean ± SEM. Statistical analysis was performed using an ANOVA (one way analysis of variance) with Tukey's multiple comparisons post test (***p<0.0001).
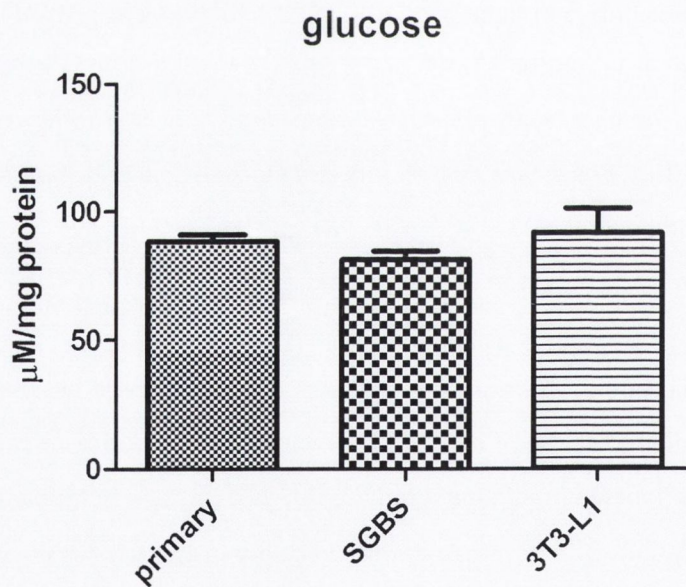
glucose

Figure 3.7: Glucose production was measured in cell culture medium of primary, SGBS and 3T3-L1 adipocytes using a colorimetric assay. Data are expressed as mean ± SEM of three independent repeats. Statistical analysis was performed using an ANOVA (one way analysis of variance) with Tukey's multiple comparisons post test.

3.3.5 Expression of housekeeping genes is altered during SGBS differentiation.

As SGBS were found to be a relevant adipocyte model in terms of morphology, gene expression and function, this cell line was selected for subsequent experiments. The process of adipocyte differentiation has been shown to be accompanied by alterations in the expression of some commonly used housekeeping genes (Hurtado del Pozo et al., 2010; Spiegelman and Farmer, 1982). This process involves morphological conversion of the fibroblast-like pre-adipocyte into a spherical adipocyte, triggered by alterations in the cytoskeleton. 3T3-L1 adipocyte differentiation has been found to be accompanied by altered expression of cytoskeletal genes actin and tubulin, commonly used as housekeeping genes (Spiegelman and Farmer, 1982). In order to guarantee correct interpretation of gene expression studies in the SGBS model, it is necessary to select an endogenous control with unchanged expression over the course of differentiation (Hurtado del Pozo et al., 2010; Spiegelman and Farmer, 1982). To our knowledge, no study to date has examined housekeeping gene expression over the course SGBS differentiation.

The expression of 28 commonly used housekeeping genes was measured using a commercially available Taqman express endogenous control qPCR array, employing 18S as a calibrator (Applied Biosystems) (as described in section 2.6.10) (A complete gene list can be found in Appendix V). Of this panel, 11 genes were down regulated by twofold or more (HPRT1, GUSB, HMBS, IPO8, TFRC, YWHAZ, POLR2A, CDKN1B, PES1, RPS17) and three genes up regulated (ABL1, ELF1, RPL37A) by twofold or more in differentiated relative to pre-differentiated SGBS (Table 3.2). These data indicate that these 14 genes would be the least suitable to use as housekeeping genes in the study of SGBS adipocyte differentiation. The expression of the remaining 14 genes (GAP-DH, ACTB, B2M, PGK1, RPLPO, UBC, PPIA, CDKN1A, GADD45A, PUM1, PSMC4, EIF2B1, MRPL19, POP4, CASC3) were altered by less than twofold. In particular, expression of GAP-DH, PGK1, PUM1, PSMC4 and EIF2B4 remained almost constant (with fold changes of 0.8, 0.9, 1.1, 1, 1.1 fold, respectively), indicating that these genes would be the most suitable for use as housekeeping genes in tracking SGBS differentiation (Table 3.2). The ribosomal subunit 18S was used as an endogenous control for qPCR studies and the use of this housekeeping gene in SGBS adipocytes has been previously published (Bour et al., 2007).

Table 3.2: Expression of common housekeeping genes was investigated in pre-differentiated (day 0) and differentiated SGBS (day 14) in order to identify an appropriate endogenous control for adipocyte differentiation. Genes which were up or down regulated by greater than twofold in differentiated SGBS relative to pre-differentiated SGBS are highlighted in red and blue, respectively. 18S was used as a calibrator for this assay.

gene	fold change	gene	fold change
GAP-DH	0.8	CDKN1A	0.6
HPRT1	0.4	CDKN1B	0.4
GUSB	0.1	GADD45A	1.4
ACTB	0.7	PUM1	1.1
B2M	1.2	PSMC4	1.0
HMBS	0.5	EIF2B1	1.1
IPO8	0.4	PES1	0.5
PGK1	0.9	ABL1	3.5
RPLP0	1.7	ELF1	2.6
TFRC	0.2	MRPL19	1.4
UBC	1.3	POP4	1.9
YWHAZ	0.2	RPL37A	2.4
PPIA	1.4	RPS17	0.1
POLR2A	0.4	CASC3	1.2

(GAP-DH=glyceraldehydes-3-phosphate dehydrogenase, HPRT1=hypoxanthine phosphoribosyltransfer-ase 1, GUSB=glucuronidase, beta, ACTB=actin, beta, B2M=beta-2-microglobulin, HMBS=hydroxymethylbilane synthase, IPO8=importin 8, PGK1=phosphoglycerate kinase 1, RPLP0=ribosomal protein, large, P0, TFRC=transferrin receptor (p90, CD71), UBC=ubiquitin C, YWHAZ=tyrosine 3-monooxygenase, PPIA=peptidylprolyl isomerase A, POLR2A=polymerase II polypeptide A, CDKN1A=cyclin-dependent kinase inhibitor 1A (p21), CDKN1B=cyclin-dependent kinase inhibitor 1B (p27), GADD45A= growth arrest and DNA-damage-inducible, alpha, PUM1=pumilio homolog 1, PSMC4=proteasome (prosome, macropain) 26S subunit, ATPase, 4, EIF2B1=eukaryotic translation initiation factor 2B, subunit 1 alpha, PES1=pescadillo homolog 1, ABL1=v-abl Abelson murine leukemia viral oncogene homolog 1, ELF1=E74-like factor 1, MRPL19=mitchondrially encoded ATP synthase 6, POP4= processing of precursor 4, ribonuclease P, RPL37A=ribosomal protein L37a, RPS17=ribosomal protein S17, CASC3=cancer susceptibility candidate 3)

3.3.6 Gene expression in omental adipose tissue of oesophageal adenocarcinoma patients is altered with visceral obesity status.

Complex disease processes such as obesity involve deregulation of multiple gene networks and microarray technology is well suited to the challenge of dissecting multiple pathways through enabling the simultaneous, reproducible and quantitative analysis of thousands of transcripts (Lipshutz et al., 1999). Microarray analysis was used to examine alterations in gene expression in omental adipose tissue isolated from viscerally obese (n=6) and non obese (n=6) male oesophageal adenocarcinoma patients using the Affymetrix Human Genome U133 Plus 2.0 Array. This array is one of the most comprehensive to date, covering approximately two thirds of the human genome (www.affymetrix.com). The arrays used in this project were custom-designed by the European Nutrigenomics Organisation (NuGO) to include a range of nutrition and obesity related genes. RNA was extracted from omental adipose tissue, assessed for purity and integrity and run on Affymetrix arrays with Service XS (Leiden, The Netherlands) (as described in sections 2.6.3, 2.6.4, 2.6.5, 2.6.12, respectively). Data were analysed in collaboration with bioinformatician Ms. Melissa Morine (Prof. Helen Roche, Nutrigenomics Research Group, Conway Institute, UCD) using predefined scripts and flexible programming with the R software environment for statistical computing (described in section 2.6.12.2).

3.3.6.1 Affymetrix array quality control

The purity and integrity of RNA samples was measured by Nanodrop and Agilent Bioanalyser, respectively (as described in section 2.6.4 and 2.6.5), before sending samples to Service XS and by Service XS prior to running the arrays. Upon receipt of the Affymetrix data from Service XS, a number of quality control measures were carried out using statistical environment, R (as described in section 2.6.12). All arrays passed these quality control tests (results shown in Appendix V) and all samples were therefore included in the bioinformatic analysis.

3.3.6.2 Affymetrix array analysis

A variance filter was used to remove genes in the lowest 10% of variance between viscerally obese and non obese patients. Levels of individual transcripts significantly altered between these groups were selected using LIMMA (linear models in microarray) from the R library of functions, with p values adjusted for multiple testing (as described in section 2.6.12.2). Gene set enrichment analysis (GSEA) was used to discover altered pathways in response to culture with adipose tissue (as described in section 2.6.12.2).

3.3.6.3 Visceral fat area predicts an altered gene expression signature in omentum.

Of the total number of genes analysed, 58-60% of transcripts were detectable in adipose tissue, a relatively high number when compared with previous adipose tissue microarray studies (Gomez-Ambrosi et al., 2004). This study strength may be attributable to the use of custom-designed microarrays including a range of nutrition and obesity related genes expressed by adipose tissue.

When binned measurements of BMI, WC, VFA and SFA values were examined (i.e. obese = 1, non obese = 0) there were no significant gene changes (adj $p<0.05$) in the omentum of obese versus non obese patients (Table 3.4). However when unbinned values were used there were 49 significant gene changes associated with VFA, two significant gene changes associated with SFA, two significant gene changes associated with BMI and one significant gene alteration associated with WC (adj $p<0.05$) (Table 3.4). Visceral obesity measured by VFA was therefore associated with the greatest number of gene changes in omental adipose tissue. This finding provides evidence that VFA is the strongest predictor of gene alterations in obesity and thus subsequent pathway analysis was conducted using this measure of visceral obesity. Neoadjuvant therapy was not associated with any significant gene expression changes in omentum (Table 3.4).

Sphingolipid metabolism and dorso-ventral axis formation were the only two significantly up regulated pathways in omentum in visceral obesity (adj $p<0.03$, adj $p<0.04$, respectively). Although not significantly up regulated, the chronic myeloid leukaemia pathway was the top ranked bidirectionally enriched pathway (adj $p<0.04$) (Figure 3.8). Pathways including VEGF signalling, mismatch repair and sex hormone metabolism were also significantly bi-directionally enriched (adj $p<0.05$) however these pathways were altered to a lesser extent (Figure 3.8). The Kyoto Encyclopaedia of Genes and Genomes (KEGG) database was used to visualise individual transcript alterations within sphingolipid metabolism, dorso-ventral axis formation and chronic myeloid leukaemia (as described in section 2.6.12.2) (Figure 3.8).

Table 3.3: Anthropometric information on patients (n=12) for Affymetrix microarray.

	non obese	obese
No. subjects	6	6
Sex (male), n (%)	6 (100)	6 (100)
Diagnosis	OAD	OAD
Age at surgery, mean (range)	64.5 (48-80)	58 (49-63)
Waist circumference, mean (range)	83 (76-89)	107 (98-130)**
BMI, mean (range)	22.5 (21-25)	30.3 (25-39)*
VFA (cm^3), mean (range)	79.6 (18-149)	210 (121-298)**
SFA (cm^3), mean (range)	82.6 (40-109)	278 (146-478)**
HDL, mean (range)	1.26 (0.6-1.64)	1.04 (0.6-1.8)
Trig, mean (range)	0.8 (0.4-1.6))	1.1 (0.6-1.4)
Fasting glucose, mean (range)	4.8 (3.2-5.7)	5.3 (4.7-6.6)
Metabolic syndrome, n (%)	0 (0)	2 (33.3)
Neoadjuvant therapy, n (%)	2 (33.3)	3 (50)

Groups were selected using the International Diabetes Federation (IDF) cutoff of WC>94 cm to define presence of visceral obesity. Obesity status is represented as mean ±SEM. Statistical analysis was performed using student's t test (*p<0.05, **p<0.01)WC=waist circumference, BMI=body mass index, VFA=visceral fat area, SFA=subcutaneous fat area, HDL=high density lipoprotein, Trig=triglycerides

Table 3.4: Gene expression alterations in omental adipose tissue in obesity using different measures of obesity status.

Independent parameter	Genes changed (adjusted p <0.05)	Genes changed (raw p <0.05)
BMI (binned)	0	811
BMI	2	1256
WC (binned)	0	337
WC	1	1078
Visceral fat (binned)	0	821
Visceral fat	49	1426
Superficial fat (binned)	0	530
Superficial fat	2	1164
Neoadjuvant therapy	0	474

(BMI=body mass index, WC=waist circumference)
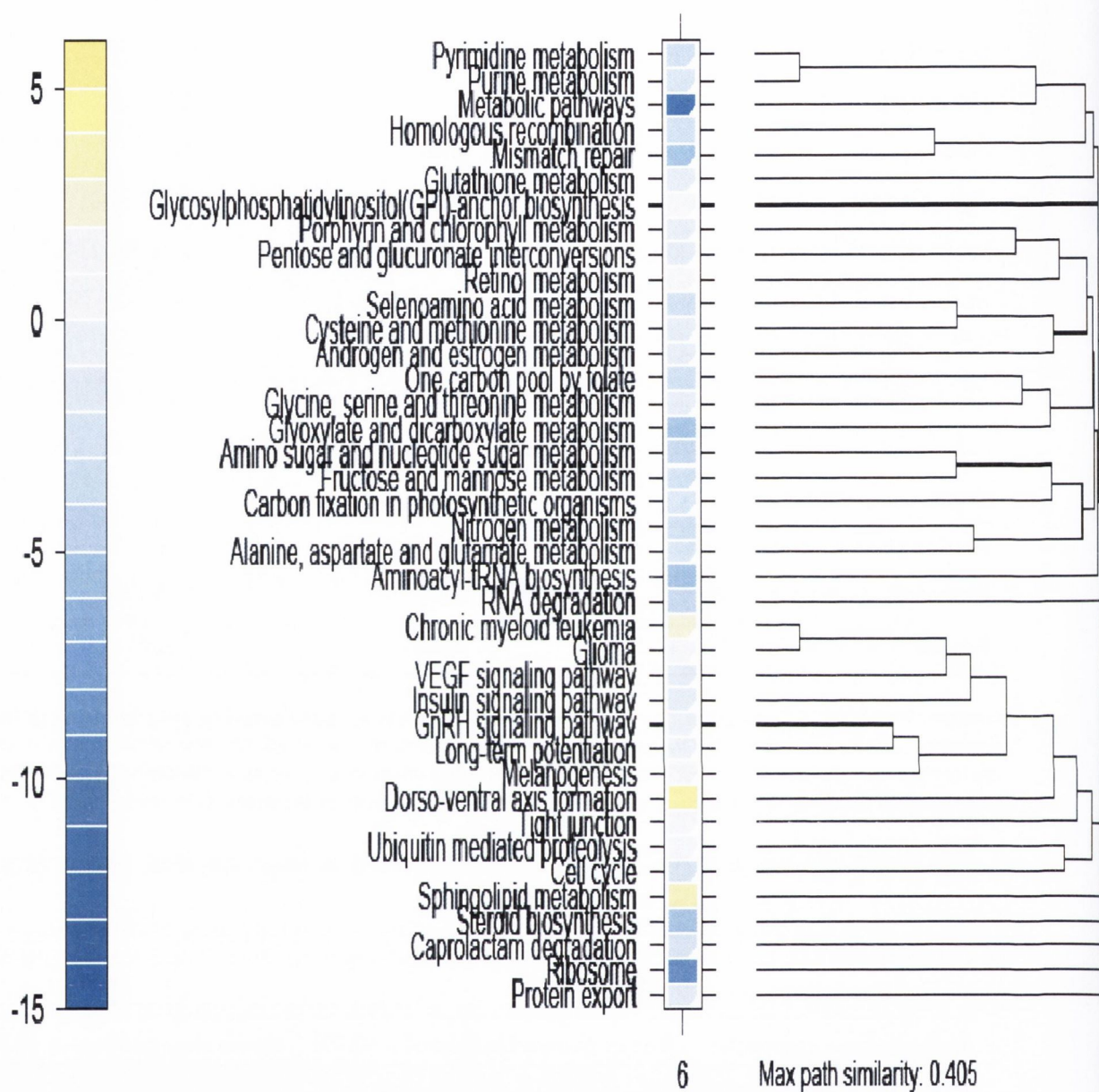
Figure 3.8: Pathway alterations (KEGG) in omental adipose tissue from viscerally obese oesophageal adenocarcinoma patients categorised by VFA (unbinned). Filled boxes represent unidirectional pathway alterations while partly filled boxes represent bidirectional enrichment. Yellow boxes represent up regulated pathways while blue boxes represent down regulated pathways.

3.3.6.4 The dorso-ventral signalling pathway is up regulated in the omentum of viscerally obese patients.

Dorso-ventral axis formation comprises several key pathways in vertebrate development (Miele et al., 2006) and this network of pathways was found to be significantly up regulated in the omentum of viscerally obese patients (adj p<0.05). Notch signalling determines cell fate through cell-cell contact, mediated by the binding of notch receptors to a variety of membrane bound ligands on neighbouring cells (Yin et al., 2010). Notch3 receptor was significantly up regulated in omentum of viscerally obese patients (adj p<0.05) (Figure 3.10). In humans, notch3 has been shown to be induced by hypoxia and is involved in *de novo* vascularisation (Liu et al., 2010). Also with roles in angiogenesis and ECM remodelling, transcription factors v-ets erythroblastosis virus E26 homologue 1 (ETS1), homologue 2 (ETS2) and ETS variant 6 (ETV6) were up regulated in this study via a significant up regulation in the expression of mitogen-activated protein (MAP) kinase kinase (MAP2K1/MEK1) (adj p<0.05) (Figure 3.9). Angiogenesis is a crucial process necessary for the supply of oxygen and nutrients to expanding adipose tissue in obesity and these pathways are possible mechanisms by which angiogenesis is up regulated in obesity (Christiaens and Lijnen, 2010). In addition to their role in angiogenesis, ETS and ETV transcription factors are a family of proto-oncogenes demonstrated to be markers of poor prognosis in breast cancer (Lincoln and Bove, 2005). They have been linked to tumourigenesis through a variety of mechanisms including telomerase induction (Dwyer et al., 2007), *de novo* angiogenesis (Lincoln and Bove, 2005) and regulation of tumour associated macrophage induced inflammation (Zabuawala et al., 2010). These data therefore outline one of many possible mechanisms by which excess visceral adiposity may give rise to *de novo* angiogenesis and activation of proto-oncogenes in the expanded omentum.
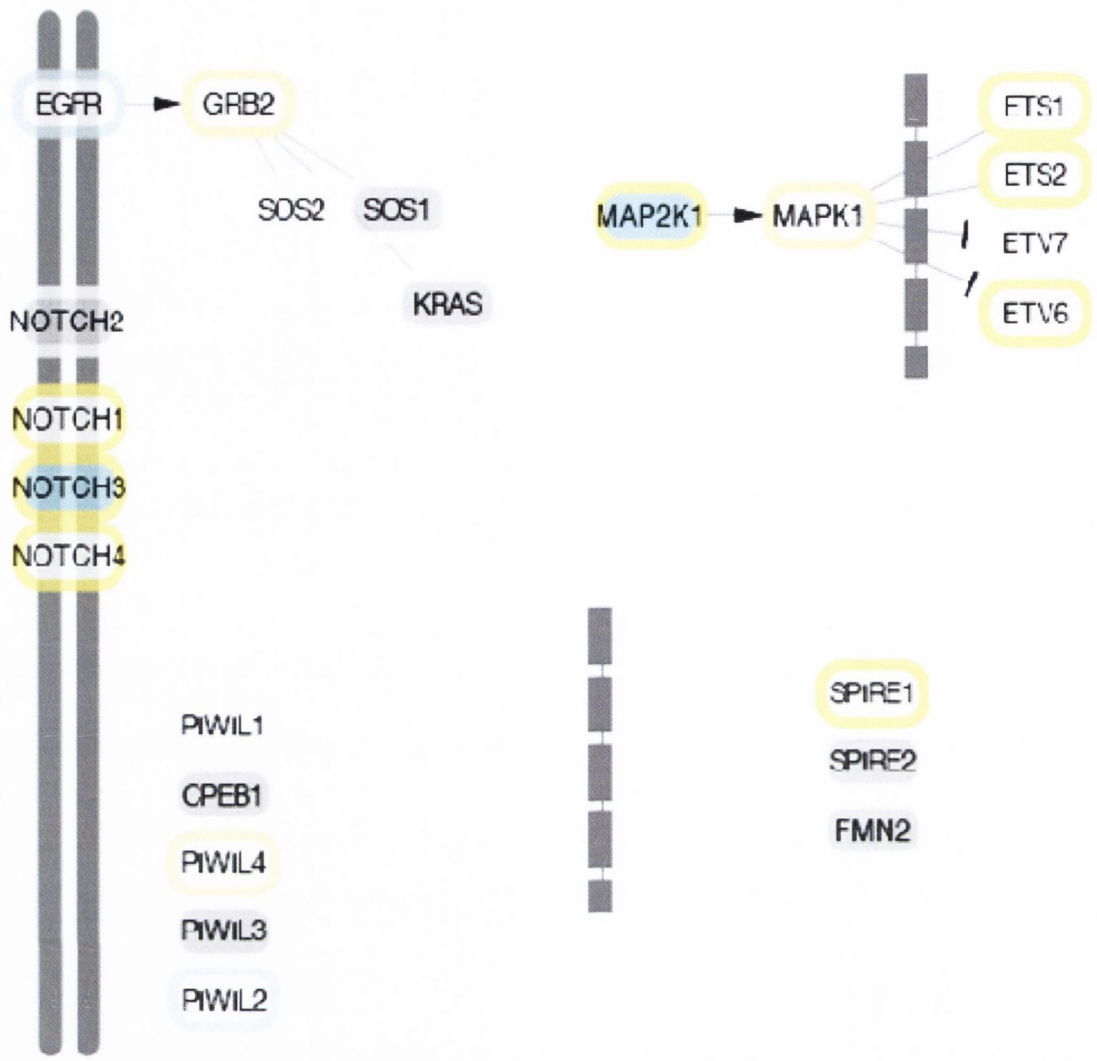
Figure 3.9: Dorso-ventral signalling pathway adapted from KEGG by Melissa Morine. Blue borders represent down regulated genes, while yellow borders represent up regulated genes. Intensity of blue/yellow shading represents the degree of transcript fold change. Light blue filled nodes represent a significant alteration (adj p<0.05). Grey nodes represent transcripts either not detected or removed by the variance filter.

3.3.6.5 Sphingolipid metabolism is altered in omentum from viscerally obesity individuals.

Sphingolipids are a family of glycoproteins previously demonstrated to be selectively up regulated by circulating factors associated with increased adiposity and metabolic deregulation. Although comprising a relatively minor proportion of total lipid, they are proposed to play an important pathological role in obesity related disorders (Holland and Summers, 2008).

All three splice variants of phosphatidic acid phosphatise type 2A (PAP2A) were significantly up regulated in omental adipose tissue from viscerally obese OAD patients (adj $p<0.05$) (Figure 3.11). PAP2A is an integral membrane protein which catalyses the hydrolysis of phosphatidic acid (PA) to generate diacylglycerol (DAG) (Ishida et al., 2007). DAG may then be either converted to free fatty acids (FFA) by phospholipases or back to PA by DAG kinase (Roberts and Morris, 2000). All three splice variants of acid ceramidase (ASAH1) were significantly up regulated in omental adipose tissue from viscerally obese OAD patients (adj $p<0.05$) (Figure 3.10). ASAH1 catalyses the conversion of ceramide to sphingosine, a sphingolipid with multiple roles in regulation of the actin cytoskeleton, endocytosis, cell cycle and apoptosis (Smith et al., 2000). Degenerative spermatocyte homologue 1 (DEGS1) is a lipid desaturase, involved in insertion of double bonds into saturated fatty acids (Cadena et al., 1997). DEGS1 was significantly up regulated in omentum of viscerally obese OAD patients (adj $p<0.05$). Lysosomal sialidase 1 (NEU1) was significantly down regulated in omentum of viscerally obese OAD patients (adj $p<0.05$). Autosomal recessive mutation of NEU1 results in the lysosome storage disorder sialidosis (Seyrantepe et al., 2003). Down regulation of NEU1 therefore implies metabolic deregulation of adipose tissue in visceral obesity.

The balance of sphingolipid metabolite levels is tightly regulated by enzymes including PAP, ASAH1 and DEGS1. Deregulation of this dynamic yet delicate balance of sphingolipid metabolism and degradation can contribute to metabolic disease (Holland and Summers, 2008) and has been linked to breast cancer development and response to therapy (Ruckhaberle et al., 2009).
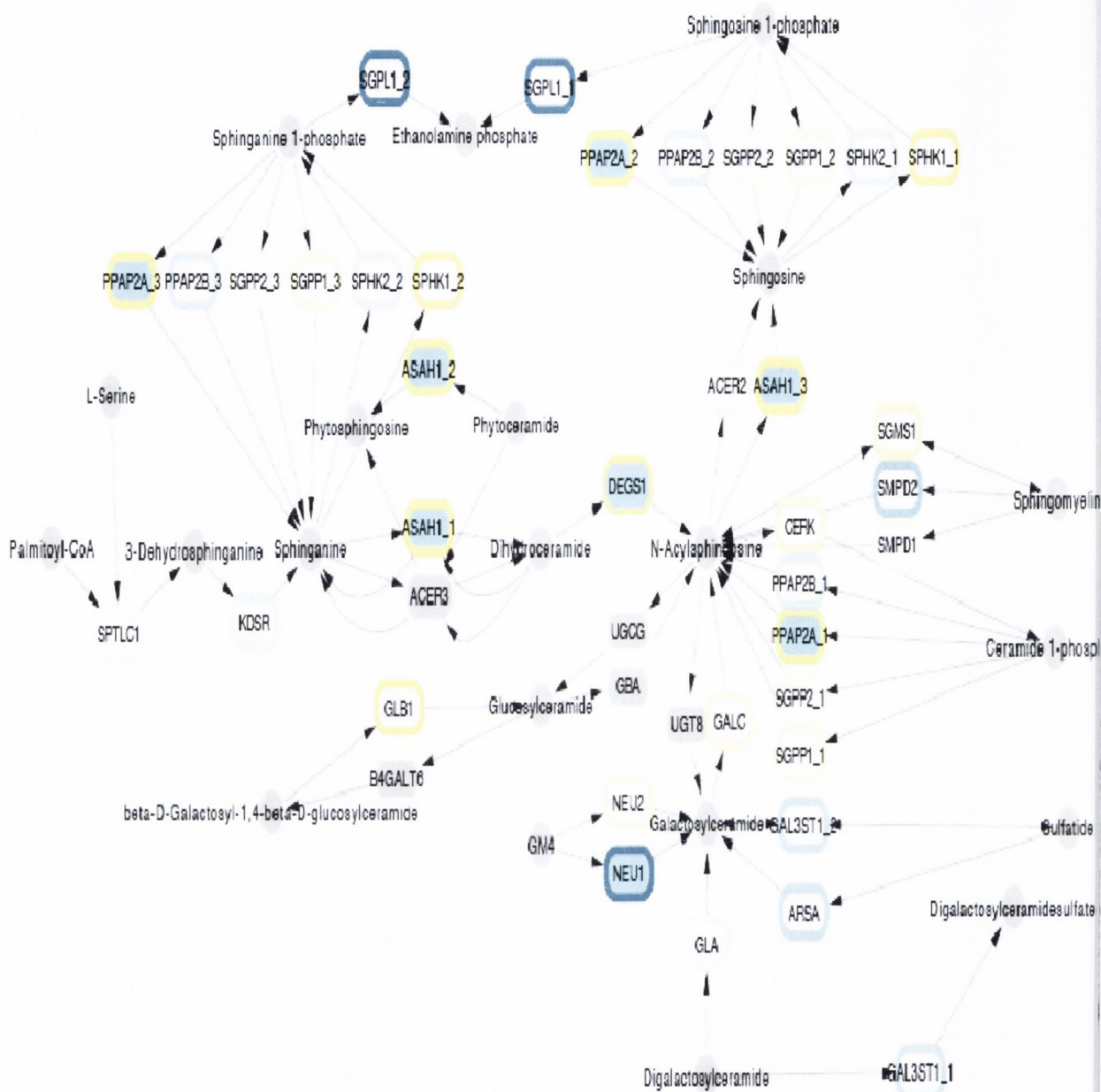
Figure 3.10: Sphingolipid pathway adapted from KEGG by Ms Melissa Morine. Blue borders represent down regulated genes while yellow borders represent up regulated genes. Intensity of blue/yellow shading represents the degree of transcript fold change. Light blue filled nodes represent a significant alteration (adj p<0.05). Grey nodes represent transcripts either not detected or removed by the variance filter.

3.3.6.6 Components of the chronic myeloid leukaemia pathway are altered in omentum from viscerally obese individuals.

The KEGG chronic myeloid leukaemia (CML) pathway is a combination of MAPK, p53 and TGF-β signalling pathways collectively controlling apoptosis, cell cycle and proliferation (Figure 3.10). Alterations in this KEGG pathway are therefore associated with multiple disease processes including obesity and cancer. The CML pathway was significantly bidirectionally enriched in the omentum of viscerally obese OAD patients (adj p<0.05). Mitogen-activated protein (MAP) kinase kinase (MAP2K1/MEK1) was significantly up regulated (adj p<0.05) in omentum from viscerally obese OAD patients. Phosphoinositide-3-kinase (PI3K), regulatory subunit 3 (PIK3R3) and protein tyrosine phosphatase non-receptor 11 (PTPN11) were also significantly up regulated (adj p<0.05) in omental adipose tissue from viscerally obese patients. The MAPK, PI3K and PTP families of signalling proteins are involved in regulation of a variety of cellular processes such as survival, proliferation, differentiation, cell cycle, transcriptional regulation and development (Cohen, 1992). The transforming growth factor β (TGF-β) pathway also plays an important role in cellular proliferation (Korpal and Kang, 2010). TGF-βR2 was found to be significantly up regulated (adj p<0.05) while its ligand TGF-β3 was significantly down regulated (adj p<0.05) in omentum from viscerally obese OAD patients.

Regulators of G1/S phase cell cycle progression cyclin D1 (CCND1) and cyclin dependant kinase 4 (CDK4) were significantly up and down regulated, respectively (adj p<0.05). Nuclear factor NFκB is a transcription factor involved in pathways of inflammation, and is inhibited by IκB proteins (Sakamoto et al., 2010). IκB inhibitor IKBKB triggers degradation of IκB, thus de-inhibiting NFκB. IKBKB was significantly up regulated (adj p<0.05) in omentum from viscerally obese OAD patients, indicating increased activity of the pro-inflammatory NFκB transcription factor. Cytokine signalling commonly occurs through signal transducer and activator of transcription (STAT) to trigger a diverse range of biological processes including immune response and inflammation (Fruhbeck, 2006). STAT5B was significantly up regulated (adj p<0.05) in omental adipose tissue from viscerally obese OAD patients.

Although pathways involved in chronic myeloid leukaemia are extremely diverse, there appears to be an overall up regulation in pathways involved in cellular survival and proliferation in visceral obesity via MAPK, PTP and PI3K signalling. Inflammatory pathways may also be over activated in the omentum of viscerally obese patients through up regulation of STAT signalling and increased degradation of the NFκB inhibitor, IκB.

Figure 3.11: Chronic myeloid leukaemia pathway adapted by Melissa Morine from KEGG. Blue borders represent down regulated genes while yellow borders represent up regulated genes. Intensity of blue/yellow shading represents the degree of transcript fold change. Light blue filled nodes represent a significant alteration (adj p<0.05). Grey nodes represent transcripts either not detected or removed by the variance filter.

3.3.6.7 Expression of leptin and GLUT4 correlate with visceral fat area.

Leptin and GLUT4 expression in whole omental adipose tissue correlated positively (r^2 = 0.56, p<0.005) and negatively (r^2 = 0.58, p<0.004), respectively, with visceral fat area (Figure 3.13). There was no relationship between PPARγ and visceral adiposity (r^2 = 0.12, p<0.3). AP2 belonged to the 10% of genes least altered in visceral obesity and was therefore removed by the variance filter. These data from whole omental tissue validate the previous finding that expression of leptin and GLUT4 correlate significantly with visceral obesity status, measured by waist circumference, in adipocytes (results section 3.3.5). Validation of this result is intuitive, as in adipose tissue both leptin and GLUT4 are solely expressed by adipocytes (Fruhbeck, 2006; Veilleux et al., 2009).
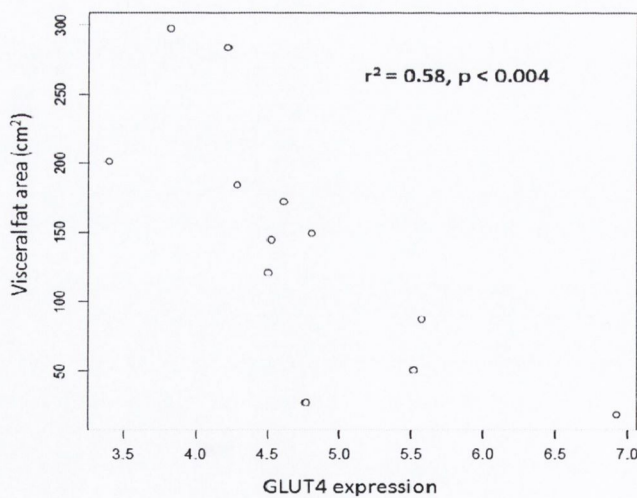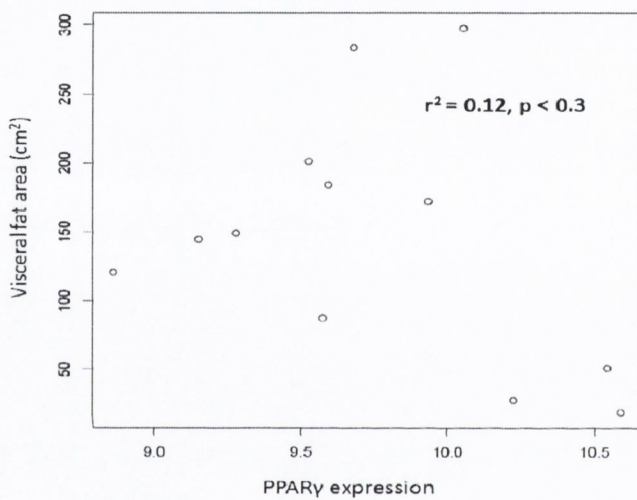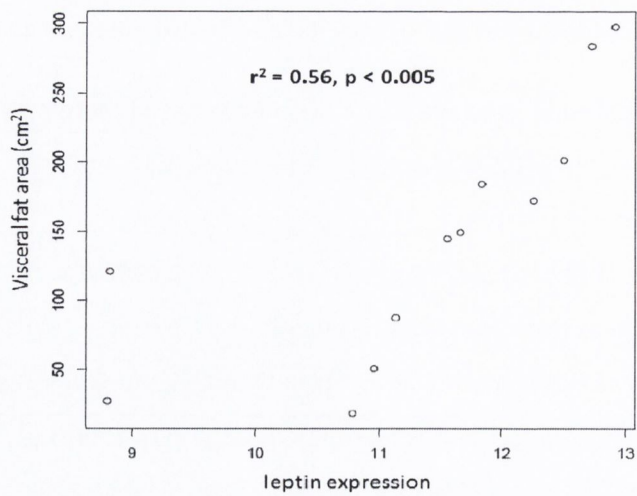
Figure 3.12: Correlation of leptin, PPARγ and GLUT4 expression with visceral obesity status, defined by visceral fat area. Affymetrix microarray analysis was carried out in the omentum of viscerally obese (n=6) and non obese (n=6) oesophageal adenocarcinoma patients. Statistical analysis was carried out using linear regression analysis.

3.4   Discussion

The incidence of obesity is growing at an alarming rate in Western society (Ogden et al., 2006), bringing with it increasing incidence of many obesity related illnesses including a wide range of cancers (Banegas et al., 2003; Calle et al., 2003). An *in vitro* model of obesity is required; although the 3T3-L1 adipocyte cell line is a validated model it may be of greater clinical relevance to work with the newly established human SGBS adipocyte cell strain (Wabitsch et al., 2001). While differences exist regarding the degree of mitotic clonal expansion (Newell et al., 2006), length of the differentiation process and expression of several adipocyte specific proteins (Bodles et al., 2006; Kersten et al., 2000; Mandard et al., 2004; Wood et al., 2003), it was found that both human and murine models undergo comparable morphological and gene expression changes throughout the process of adipogenesis. While neither 3T3-L1 nor SGBS differentiation produced the single expanded lipid vesicle typical of primary adipocytes, SGBS was closer to this morphology with fewer, larger lipid droplets compared with 3T3-L1. Gene expression of leptin, LPL, GLUT4, AP2 and PPARγ was induced in 3T3-L1 and SGBS over the course of differentiation, as has been previously published (Fischer-Posovszky et al., 2008; Rosen and MacDougald, 2006). GAPDH levels in SGBS remained constant throughout the course of differentiation, also in agreement with current literature (Fischer-Posovszky et al., 2008). Expression of early adipocyte transcription factor PPARγ was induced to a greater extent in 3T3-L1, and this could indicate that 3T3-L1 may be a good model for the study of early adipocyte differentiation and genetic regulation of this process. Expression of terminal adipocyte differentiation genes were induced to a greater extent in SGBS and were similar to levels in primary human adipocytes, indicating the relevance of this model in the study of human adipocyte biology. This was most notable in the case of leptin, a key marker of adipocyte function and insulin sensitivity with both endocrine and immune functions (Otero et al., 2005) and LPL, a key regulator of lipid deposition (Zechner et al., 2000). Leptin was found to correlate with obesity status in patients, with human adipocytes producing and releasing leptin in proportion to their state of differentiation and size (Wabitsch et al., 1996). Leptin levels in normal weight patients were found to be similar to SGBS adipocytes. It has been previously observed that leptin levels are higher in adipocytes isolated from adipose tissue compared to adipocyte cell lines and this could be due to the contribution of the tissue microenvironment, absent in the *in vitro* system (MacDougald et al., 1995). In addition GPDH activity and glucose production in SGBS was similar to primary adipocytes. SGBS could therefore provide a clinically relevant *in vitro* model of adipogenesis as they are similar to human primary adipocytes in terms of morphology, induction of adipocyte specific gene

expression and function. Additionally, it can be argued that the SGBS pre-adipocyte cell strain have the added advantage of undergoing the process of differentiation in a serum free culture system, while 3T3-L1 require the presence of serum to differentiate. A serum free system removes this significant environmental variable (Fischer-Posovszky et al., 2008).

A potential drawback of using SGBS as a model system is that this cell strain is derived from subcutaneous adipose tissue, and there is currently no omental derived human adipocyte cell line widely available. Levels of LPL, GLUT4, AP2 and PPARγ have all been shown to be higher in the subcutaneous relative to the omental adipose tissue depot (Sewter et al., 2002; Tchkonia et al., 2006; Veilleux et al., 2009; Walker et al., 2008) and SGBS expression of these adipocyte specific genes reflected these findings indicating that SGBS are indeed more characteristic of subcutaneous adipocytes. Given recent research highlighting the differences in adipocyte biology from different adipose tissue depots (Tchkonia et al., 2002), and the more recent identification of the visceral depot as the biggest contributor to obesity related morbidity and mortality (Corley et al., 2007; Mathieu et al., 2010; Schelbert, 2009), a possible shortcoming of the SGBS model is its subcutaneous origin.

There is some evidence for altered expression of commonly used housekeeping genes during the process of adipocyte differentiation (Hurtado del Pozo et al., 2010; Spiegelman and Farmer, 1982). In agreement with previously published data, GAPDH was found to remain unchanged throughout SGBS differentiation (Fischer-Posovszky et al., 2008). Housekeeping genes IPO8 and HPRT1 have been previously used in the study of both 3T3-L1 and primary adipocyte differentiation (Hurtado del Pozo et al., 2010; Zhou et al., 2010). In this study however they were down regulated over twofold and therefore were deemed unsuitable for use as housekeeping genes. This finding highlights the need for careful validation of individual housekeeping genes in each cell line before they are judged a reliable endogenous control. Ribosomal subunit 18S was used to calibrate the housekeeping gene array and as an endogenous control in subsequent adipocyte differentiation studies, and it has been widely reported that this gene is a suitable candidate for this purpose (Bour et al., 2007; Bujalska et al., 2002; Park et al., 2009).

Microarray technology was used to assess which measure of obesity was most predictive of altered gene expression in omentum. The majority of previously published studies have relied on BMI, a measure of overall adiposity, to categorise patients (Gomez-Ambrosi et al., 2004; Henegar et al., 2008; Linder et al., 2004; MacLaren et al., 2008; Walewski et al.). In this study,

four different measures of obesity were assessed; body mass index (BMI), waist circumference (WC), visceral fat area (VFA) and subcutaneous fat area (SFA). VFA was the strongest predictor of gene expression alterations in omentum. This finding not only substantiates the previously established role of visceral adiposity in obesity related morbidity and mortality (Giorgino et al., 2005), but highlights the superior nature of VFA as a measurement of visceral adiposity. In addition, the larger range of VFA measurements (18 cm^2 - 298 cm^2) compared to WC measurements (76 cm - 130 cm) makes VFA more suitable for use in correlation studies.

Previous studies examining gene expression alterations in adipose tissue in obesity discovered up regulation of pro-inflammatory pathways (Henegar et al., 2008), down regulation of lipolysis pathways (Gomez-Ambrosi et al., 2004) and deregulation of insulin signalling (MacLaren et al., 2008). This study examining altered gene expression in adipose tissue in visceral obesity found up regulation of the notch signalling pathway, up regulation of sphingolipid metabolism and up regulation of central signalling pathways involved in the regulation of apoptosis, cell cycle and proliferation. Notch is a highly conserved developmental pathway with roles in determination of cell fate, tissue patterning and morphogenesis. It has more recently been discovered to play a role in the progression of many types of cancer including those of the gastrointestinal tract (Katoh, 2007). The significant up regulation of notch3 in the omentum of viscerally obese OAD patients could contribute to increased tumour progression, contributing to a mechanistic explanation for the association of visceral obesity with cancer mortality (Calle et al., 2003). Gamma-secretase is an inhibitor of notch signalling and its therapeutic potential is currently being investigated in breast cancer in Phase I clinical trials (Yin et al., 2010). Inhibition of the notch signalling pathway could be particularly relevant in viscerally obese cancer patients, where this pathway is up regulated. Sphingolipid metabolism was also found to be highly up regulated in adipose tissue of viscerally obese oesophageal adenocarcinoma patients. Sphingolipids are lipid signalling components of the plasma membrane induced by circulating factors associated with obesity and may play an important pathogenic role in metabolic disorders (Holland and Summers, 2008). Sphingolipid metabolism is up regulated in liver and skeletal muscle in mice and rats fed a high fat diet (Aerts et al., 2007) and in skeletal muscle in human obesity (Adams et al., 2004). Pharmacological lowering of glycosphingolipids in obese mice improves insulin sensitivity and reduces adipose tissue inflammation (van Eijk et al., 2009). PAI-1 and MCP-1 levels are reduced upon inhibition of sphingolipid synthesis (Yang et al., 2009a) and inhibition of PAI-1 resulted in decreased sphingolipid metabolism in mice (Shah et al., 2008). Pro-inflammatory adipokines MCP-1 and PAI-1 are therefore possible mediators of sphingolipid induced pathogenesis.

Pathways involved in sphingolipid metabolism were significantly up regulated with increasing VFA in omental adipose tissue of oesophageal adenocarcinoma patients, mediating the development of adipose tissue inflammation. Finally, recent developments in treatment of gastrointestinal cancers have focussed on targeting of epidermal growth factor receptors EGFR and ErbB2 using inhibitors such as cetuximab, trastuzumab and gefitinib, with some success (Ferry et al., 2007; Safran et al., 2008). The major pathways targeted by these receptors are the MAPK, PI3K and STAT signalling pathways and individual components belonging to all these pathways were significantly up regulated in the omentum of viscerally obese OAD patients. These pathways may therefore offer potential downstream targets of EGFR for the development of new obesity related targeted therapies in gastrointestinal cancer.

The deregulation of metabolic pathways in visceral obesity have been demonstrated to contribute to increased tumourigenesis (Calle et al., 2003). In this study inflammation, angiogenesis and cell signalling were found to be enhanced in omental adipose tissue in visceral obesity. These pathways have previously been shown to be fundamental in the process of carcinogenesis (Colotta et al., 2009; Hanahan and Weinberg, 2000). These findings therefore provide mechanistic evidence for the association between visceral obesity and cancer and highlight the human SGBS cell strain as an appropriate model with which to study this relationship.

4 Visceral obesity and male sex are independently associated with increased production of inflammatory mediators.

4.1   Introduction

Adipose tissue, originally thought to be an inert energy storage site, is now recognised to play an important role in the immune system and inflammation (Das, 2001; Rosen and MacDougald, 2006). Recently, as the current global obesity pandemic shows no sign of abating (Team, 2005), a great deal of interest has been focussed on this multifunctional endocrine organ. An excess accumulation of adipose tissue, particularly visceral adipose tissue (Giorgino et al., 2005), has been linked with an increasing number of associated co-morbidities including many types of cancer (Calle et al., 1999; Guh et al., 2009). Three interconnected mechanisms of obesity pathogenesis have been proposed to date: insulin and insulin like growth factor (IGF) axis, circulating levels of sex hormones and adipokine signalling (Donohoe et al., 2010; Renehan et al., 2006).

Insulin and IGF-1 are elevated in obesity, and insulin resistance is a common metabolic disorder of viscerally obese individuals (Roberts et al., 2009). Compensatory hyperinsulinaemia is characterised by chronically elevated insulin levels and decreased expression of IGF binding proteins 1 and 2 (IGFBP1, 2), resulting in increased circulating amounts of bioactive, bioavailable IGF-1 (Donohoe et al., 2010; Renehan et al., 2006). Together, these growth factors exert both mitogenic and anti-apoptotic effects, creating an environment favourable for tumourigenesis (Renehan et al., 2006). Hyperinsulinaemia has been linked to increased incidence of several cancers, including colorectal carcinoma (Argiles and Lopez-Soriano, 2001; Trevisan et al., 2001). Chronic hyperinsulinaemia can lead to reduction in the amount of circulating sex hormone binding globulin (SHBG) (Roberts et al., 2009). This event increases levels of bio-available oestrogen, producing both mitogenic and mutagenic effects in oestrogen responsive tissues (Calle and Kaaks, 2004; Donohoe et al., 2010; Roberts et al., 2009).

Visceral obesity is associated with an infiltration of T lymphocytes and macrophages into omental adipose tissue, producing soluble mediators of inflammation in the form of cytokines, chemokines and adipokines (Kintscher et al., 2008; Weisberg et al., 2003; Xu et al., 2003). The low levels of resident immune cells in adipose tissue from normal weight individuals are predominantly T_H2 T lymphocytes and M2 macrophages. These immune cells exert a predominantly anti-inflammatory effect on tissue microenvironment through production of IL-4, IL-10 and IL-13 (Duffield, 2003). Adipose tissue hypoxia (Trayhurn et al., 2008) and elevated levels of pro-inflammatory IFNγ in visceral obesity (Strissel et al., 2007) can trigger a

phenotypic switch, favouring classical, pro-inflammatory T_H1 polarisation of infiltrating T lymphocytes and M1 polarisation of infiltrating macrophages (Lumeng et al., 2007). Classically activated immune cells produce pro-inflammatory cytokines IFNγ, TNFα, IL-6 and IL-12 (Duffield, 2003; Kintscher et al., 2008) and levels of these cytokines have been demonstrated to be elevated in obesity (Fantuzzi, 2005). Increased circulating leptin and decreased adiponectin levels are also characteristic of visceral obesity and are linked to development of insulin resistance and related disorders (Tilg and Moschen, 2006). Raised levels of resistin and visfatin are associated with obesity and linked to insulin resistance (Fukuhara et al., 2005; Steppan et al., 2001). Adipsin, on the other hand, has insulin sensitising effects and levels have been found to be decreased in obesity (White et al., 1992). Together these mediators contribute to a state of chronic low grade inflammation characteristic of visceral adiposity, an important mechanism of insulin resistance and development of the Metabolic Syndrome (Federation, 2006; Wellen and Hotamisligil, 2005). An analogous state of 'smouldering' sub-clinical chronic inflammation has also been linked to tumourigenesis (Mantovani et al., 2008). It therefore follows that this pro-inflammatory phenotype present in obesity could be an important contributing factor to the well established epidemiological association between excess adiposity and cancer (Calle et al., 1999).

Hyperinsulinaemia related proliferative, mutagenic and anti-apoptotic effects (Renehan et al., 2006) combined with a state of chronic inflammation induced by an altered cytokine, chemokine and adipokine environment (Xu et al., 2003) could provide some mechanistic clarification as to how visceral obesity creates an environment favourable for tumour initiation and progression (Calle et al., 2003). Precise details of molecular pathways and roles of specific adipocytokines need to be fully elucidated in order to identify possible preventative strategies and therapeutic targets for the control of obesity related cancers.

4.2   Aims and objectives

The aim of this chapter was twofold; firstly, to investigate adipokine expression in adipose tissue and serum, and secondly, to determine functional effects of the adipose tissue 'secretome' on oesophageal adenocarcinoma cell lines.

Specific objectives

- To examine alterations in adipokine levels in ACM with respect to obesity, cancer, male sex and location of adipose tissue depots.

- To investigate cytokine, chemokine and adipokine expression in serum of matched patients.
- To test the functional effect of ACM on proliferation and apoptosis of oesophageal adenocarcinoma cell lines.

4.3 Results

4.3.1 Adipokine levels in conditioned medium from omental adipose tissue are altered in viscerally obese relative to normal weight OAD patients and in omental relative to subcutaneous adipose tissue.

Visceral obesity is associated with a state of chronic low grade inflammation (Weisberg et al., 2003; Xu et al., 2003). In this section, multiplex screening assays were utilised in order to identify mediators of inflammation which may be altered in visceral obesity. Milliplex panels of 20 cytokines, chemokines and adipokines (leptin, adiponectin, HGF, NGF, total PAI-1, GM-CSF, resistin, MCP-1, TNFα, IFNγ, IL-1β, IL-2, IL-4, IL-5, IL-6, IL-7, IL-8, IL-10, IL-12 and IL-13) were tested in ACM from viscerally obese (n=15) and non obese (n=15) male OAD patients, categorised by WC (Table 4.1). ACM was prepared from omental adipose tissue of these patients (as described in section 2.4.2) and analysed Milliplex MAP Luminex technology, by Millipore (described in section 2.8) (Appendix II). There were no significant differences between obese and non obese groups with respect to age at surgery or administration of neoadjuvant therapy however, as expected, groups differed significantly across all measures of obesity (BMI, WC, VFA) (p<0.0001) and fasting glucose levels (p<0.05) (Table 4.1).

The Milliplex panels provided a preliminary indication of adipokine expression in the omental adipose tissue of obese and non obese individuals. Of the 20 analytes tested, the levels of five adipokines were altered in the ACM prepared from adipose tissue from viscerally obese patients (Table 4.2). The anti-inflammatory adipokine adiponectin and the T_H2 adipokine IL-4 were found to be significantly reduced in ACM from viscerally obese patients (p<0.0001 and p<0.01, respectively), and these adipokines are involved in inhibition of pro-tumour T_H1 responses (Colotta et al., 2009; Duffield, 2003). However, pro-inflammatory T_H1 adipokines IL-6, IL-8 and MCP-1 were also significantly reduced in ACM from viscerally obese patients (p<0.0001) (Table 4.2). This result was both counter-intuitive and in direct conflict with published findings (Kim et al., 2006; Tilg and Moschen, 2006) and could highlight limitations in biobank standard operating procedures used for the preparation of ACM. A weight of 5 g minced adipose tissue from viscerally obese and non obese patients is cultured in 10 ml medium to produce ACM (as described in section 2.4.2). Although this protocol enables standardisation between patients, it does not reflect the extra bulk of adipose tissue present in viscerally obese patients. This shortcoming must be taken into account when interpreting cytokine levels in the ACM. Therefore, the measurement of circulating levels of adipokines, cytokines and chemokines in serum may be a more representative analysis of the patient's pro-inflammatory profile *in vivo*.

Table 4.1: Anthropometric details for patients included in Randox Evidence Invesigator and Milliplex MAP Luminex screen.

	non obese	obese
No. subjects	15	15
Diagnosis	OAD	OAD
Sex (male), n (%)	15 (100)	15 (100)
Age at surgery, mean (range)	61 (43-87)	63 (44-84)
Waist circumference, mean (range)	90 (76-93)	114 (96-130)***
BMI, mean (range)	23 (21-25)	30 (25-39)***
VFA, mean (range)	137 (18-318)	255 (121-384)***
HDL, mean (range)	1.16 (0.58-1.6)	1.14 (0.6-2.2)
Trig, mean (range)	1.2 (0.36-3)	1.5 (0.59-2.7)
Fasting glucose, mean (range)	5 (3.2-5.8)	5.9 (4.7-11.6)*
Metabolic syndrome, n (%)	0 (0)	13 (77)
Neoadjuvant therapy, n (%)	7 (39)	7 (41)

Patients were categorised using the IDF defined waist circumference cut-off of 94 cm. Statistical analysis was carried out using an unpaired student's t-test (*$p<0.05$, ***$p<0.0001$). (BMI=body mass index (cm/kg^2), VFA=visceral fat area (cm^3), HDL=high density lipoprotein (mmol/L), Trig=triglycerides (mmol/L))

Table 4.2: Adipokine levels (pg/ml) in adipose conditioned medium (ACM) measured using Milliplex MAP Luminex technology in male age matched viscerally obese (n=15) and non obese (n=15) oesophageal adenocarcinoma patients.

	Non Obese	Obese	p value
Leptin	51641 (8246)	49351 (11422)	0.8720
Adiponectin	1079000 (76963)	664300 (46642)	0.0001
HGF	42323 (5765)	43317 (3832)	0.8869
NGF	292.7 (34.78)	200.0 (36.26)	0.0756
PAI-1 (total)	50275 (9165)	36645 (15235)	0.4497
GM-CSF	134.5 (73.41)	194.8 (96.28)	0.6225
resistin	4815 (1712)	2405 (1244)	0.2644
MCP-1	4746 (89.16)	4071 (58.12)	0.0001
TNF-α	10.21 (3.259)	26.96 (20.56)	0.4280
IFN-γ	20.06 (2.133)	18.89 (1.122)	0.6331
IL-1β	64.30 (35.88)	35.33 (24.95)	0.5128
IL-2	1.179 (0.3248)	0.6853 (0.1234)	0.1662
IL-4	2.830 (0.2010)	1.993 (0.1925)	0.0055
IL-5	50.37 (13.59)	60.04 (33.87)	0.7930
IL-6	8615 (68.44)	7970 (73.66)	0.0001
IL-7	81.21 (8.323)	84.33 (8.896)	0.7994
IL-8	4848 (106.6)	4079 (77.58)	0.0001
IL-10	519.7 (111.6)	493.1 (84.02)	0.8504
IL-12 (p70)	3.779 (0.5088)	3.222 (0.2048)	0.2949
IL-13	3.119 (0.7230)	3.071 (1.155)	0.9705

Waist circumference was used to define obesity status. Data are expressed as mean ± SEM. Statistical analysis was performed using an unpaired student's t-test.

Due to the contradictory results observed using the Milliplex screen, it was decided to proceed by screening ACM and serum using Randox Evidence Investigator technology. A panel of 12 cytokines, chemokines and adipokines (IL-1α, IL-1β, IL-2, IL-4, IL-6, IL-8, IL-10, EGF, IFN-γ, MCP-1, VEGF, TNFα) was analysed in ACM derived from omental and subcutaneous adipose tissue, and in matched serum in an identical cohort of male OAD patients (Table 4.1). This was conducted on site, using Randox Evidence Investigator biochip array technology (Randox Laboratories Ltd., UK) (described in section 2.9). However, this technology did not enable a

quantifiable expression in ACM of three of the most abundant cytokines, IL-6, IL-8 and MCP-1. A single dilution of sample was applied to the multiplex arrays, and the level was cut at the top standard (IL-6: 900 pg/ml, IL-8: 3000 pg/ml and MCP-1: 900 pg/ml) (Appendix II). Despite this, the Randox panel provided a preliminary indication of adipokine expression in omental and subcutaneous adipose tissue and corresponding circulating levels in serum. VEGF, IL-6, IL-8 and MCP-1 were the most abundant adipokines in ACM. While this assay did not allow for quantifiable expression of IL-6, IL-8 or MCP-1 between adipose tissue depots, it could be determined that VEGF levels were higher in visceral compared to subcutaneous adipose tissue.

The Milliplex screen indicated an alteration in the equilibrium of pro- and anti-inflammatory adipokines in visceral obesity. Reduced levels of anti-inflammatory adipokines could act to reduce anti-tumour immunity, supporting tumourigenesis. The maintenance of a critical balance of pro and anti inflammatory adipokines is necessary for normal immune system function and the alteration of this balance in visceral obesity could therefore trigger a pathological response (Duffield, 2003). The Randox screen indicated an elevated expression of VEGF in the visceral relative to the subcutaneous adipose tissue depot. This finding indicates a potentially important role for VEGF in visceral obesity associated pathogenesis.
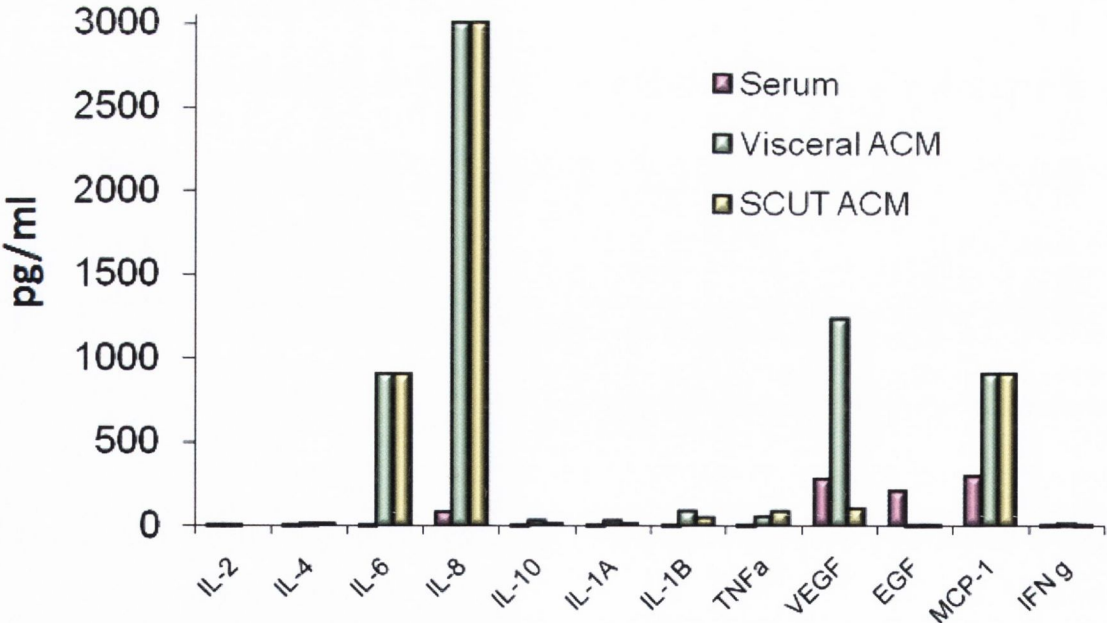
Figure 4.1: Randox screen of ACM using the cytokine and growth factor multiplex biochip immunoassay on matched serum and ACM, generated from subcutaneous and visceral adipose tissue from male OAD patients (n=30). Vascular endothelial growth factor (VEGF), monocyte chemotactic protein-1 (MCP-1), interleukin-6 (IL-6) and IL-8 were the most abundant cytokines and chemokines produced in ACM.

4.3.2 Validation of adipokine screens in an independent cohort of viscerally obese and non obese patients.

Based on the MAP Luminex and Randox Evidence Investigator results, a selection of seven cytokines, chemokines and adipokines of interest (leptin, adiponectin, IL-6, IL-8, MCP-1, IFNγ and VEGF) were chosen for validation by ELISA (as described in section 2.10) in an independent cohort of ACM and serum from viscerally obese (n=40) and non obese patients (n=31) (Table 4.3). Patient groups were selected by WC and all measures of obesity (p<0.0001) and measures of metabolic syndrome (p<0.05) were significantly different between obese and non obese patients. There was no difference in sex or administration of neoadjuvant therapy between obese and non obese patient groups (Table 4.3).

Anti-inflammatory adipokine adiponectin was found to be significantly decreased in ACM from viscerally obese patients (p<0.05), validating the results of the initial adipokine screen. Decreased adiponectin levels have been demonstrated to play an important role in development of insulin resistance and associated pathogenic processes of visceral obesity (Kelesidis et al., 2006). There was no change in levels of pro-inflammatory adipokines leptin, IL-6, IL-8, MCP-1, VEGF or IFNγ between viscerally obese and non obese patients (Table 4.4). This result therefore failed to validate the initial adipokine screen which showed a significant decrease in levels of these pro-inflammatory adipokines in ACM of viscerally obese patients. This data draws attention to the danger of obtaining spurious results from a size restricted cohort, and highlights the importance of validations in a larger, independent cohort. The results obtained from the independent cohort using the more robust technique of ELISA were in accordance with previously published work (Kim et al., 2006; Tilg and Moschen, 2006).

Levels of leptin, adiponectin, IL-6, IL-8, MCP-1, VEGF and IFNγ were subsequently investigated in the systemic circulation of patients using matched serum samples (Table 4.5). Circulating concentrations may be more reflective of *in vivo* levels of pro-inflammatory mediators as they account for the presence of a greater bulk of adipose tissue in viscerally obese individuals. Leptin and VEGF levels were found to be significantly enhanced (p<0.01 and p<0.05, respectively) while adiponectin levels were significantly reduced (p<0.05) in the serum of viscerally obese patients. While IL-6 and MCP-1 levels were also increased in obesity this result did not reach statistical significance. This may be due to low variation in WC measurements accounted for by the lack of morbidly obese patients in this cohort. There was no significant difference in levels of serum IFNγ between viscerally obese and non obese patients (Table 4.5). Together these data indicate that levels of serum cytokines, chemokines and adipokines may

be more strongly associated with visceral obesity than levels of adipose tissue secreted adipokines.

Table 4.3: Anthropometric details for patients selected for validations of Milliplex MAP data.

	non obese	obese
No. subjects	31	40
Sex (male), n (%)	15 (48)	22 (55)
Age at surgery, mean (range)	63 (30-86)	64 (41-84)
Waist circumference, mean (range)	79 (50-93)	101 (82-114) ***
BMI, mean (range)	23 (17-27)	30 (22-40) ***
HDL, mean (range)	1.4 (0.6-2.2)	1.2 (0.6-2.6) *
Trig, mean (range)	1.2 (0.5-3.7)	1.6 (0.7-4.9) *
Fasting glucose, mean (range)	5 (3.2-5.9)	6 (4.3-15.9) *
Metabolic syndrome, n (%)	0 (0)	27 (68)
Neoadjuvant therapy, n (%)	9 (29)	11 (28)

Patients were divided into viscerally obese (n=40) and non obese (n=31) groups by waist circumference (80 cm for women and 94 cm for men). Statistical analysis was carried out using an unpaired student's t-test (*p<0.05, ***p<0.0001). (BMI=body mass index (cm/kg^2), VFA=visceral fat area (cm^3), HDL=high density lipoprotein (mmol/L), Trig=triglycerides (mmol/L))

Table 4.4: Validations of adipokine levels (pg/ml) in adipose conditioned medium (ACM) measured by ELISA in a group of viscerally obese (n=40) and non obese (n=31) patients.

	Non Obese	Obese	p value
Leptin	116616 (30720)	98253 (21060)	0.6219
Adiponectin	417135 (34923)	309499 (33611)	0.0326
IL-6	190791 (26554)	186148 (21448)	0.8910
IL-8	198081 (28832)	198404 (22835)	0.9929
MCP-1	106182 (21616)	96091 (15820)	0.7011
VEGF	1468 (164.6)	1376 (185.2)	0.7149
IFN-γ	79.0 (44.17)	14.95 (5.327)	0.1719

Data are expressed as mean ± SEM and statistical analysis was performed using an unpaired student's t-test.

Table 4.5: Validations of adipokine levels (pg/ml) in serum measured by ELISA in a group of viscerally obese (n=40) and non obese (n=31) patients.

	Non Obese	Obese	p value
Leptin	11261 (1853)	25091 (3672)	0.0094
Adiponectin	5338000 (569272)	3775000 (300496)	0.0107
IL-6	14.03 (4.089)	43.10 (18.73)	0.2286
IL-8	34.52 (8.486)	41.71 (17.59)	0.7464
MCP-1	75.03 (9.947)	101.9 (15.29)	0.1897
VEGF	62 (18)	104 (21)	0.0431
IFN-γ	292.3 (187.4)	235.2 (109.5)	0.7778

Data are expressed as mean ± SEM and statistical analysis was performed using an unpaired student's t-test.

4.3.3 Omental adipose tissue expresses higher levels of pro-inflammatory adipokines relative to subcutaneous adipose tissue.

Levels of leptin, adiponectin, IL-6, IL-8, MCP-1 and VEGF, found to be altered in viscerally obese patients, were examined in omental and subcutaneous adipose tissue in a cohort of cancer patients (n=30). ACM was prepared from both the omental and subcutaneous depots of these patients (as described in section 2.4.2) and adipokine expression was measured by ELISA (as described in section 2.10).

There was no difference in levels of pro-inflammatory adipokines leptin, adiponectin, IL-8 or MCP-1 between omental and subcutaneous adipose tissue depots. However expression of pro-inflammatory T_H1 adipokine, IL-6, and pro-angiogenic factor, VEGF, were significantly elevated in omental relative to subcutaneous adipose tissue ($p<0.01$ and $p<0.0001$, respectively) (Figure 4.2). Hypoxia is a strong inducer of VEGF (Halberg et al., 2009) and elevated levels of VEGF in omentum provide evidence for the preferential development of a hypoxic environment in visceral adipose tissue (Trayhurn et al., 2008). Together these data highlight the importance of the enlarged visceral adipose tissue depot in the establishment of a pro-angiogenic and pro-inflammatory environment linked with insulin resistance and obesity related disease (Halberg et al., 2009).
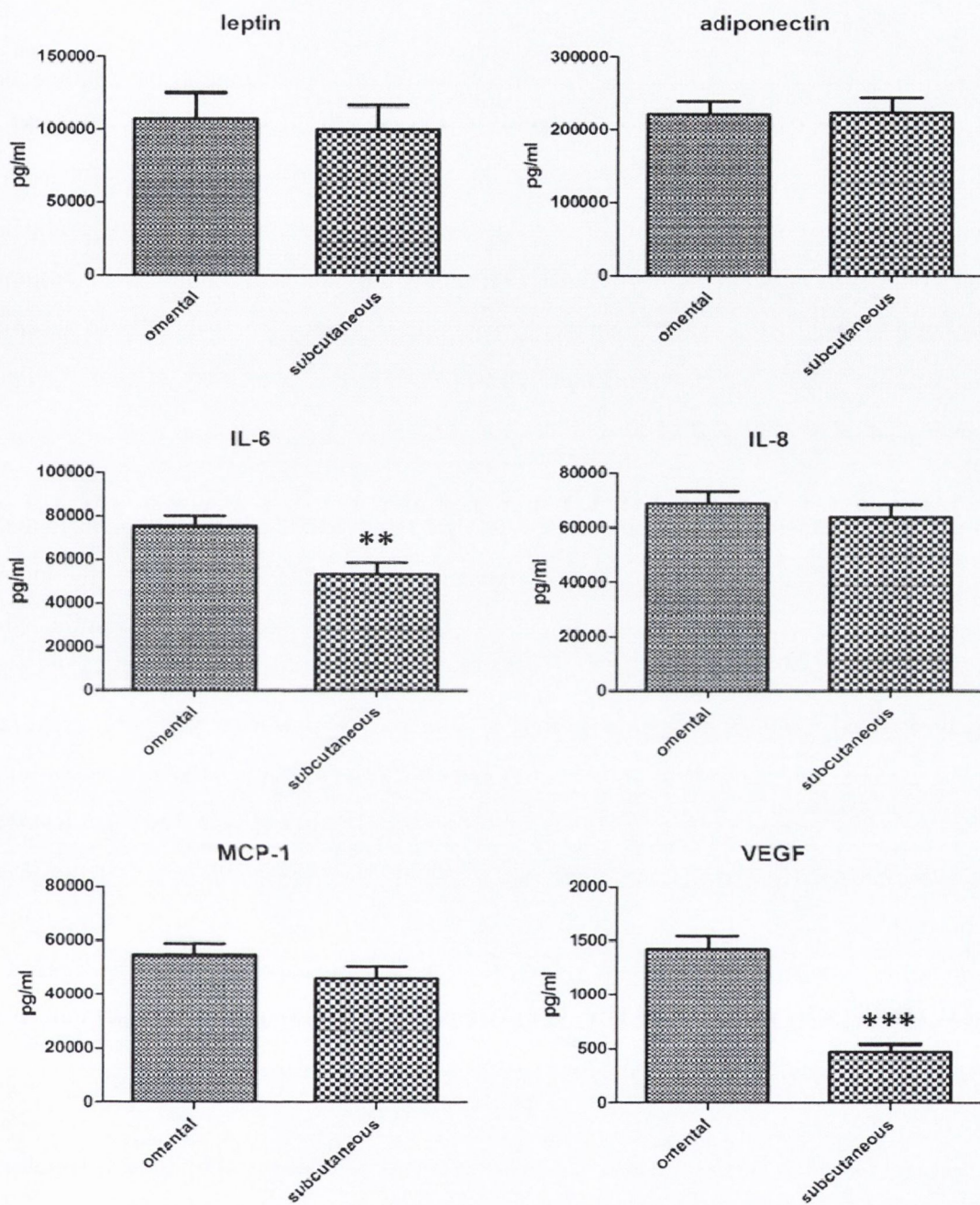
Figure 4.2: Adipocytokine levels (pg/ml) were altered in adipose conditioned medium from matched omental and subcutaneous adipose tissue (n=30). Data are expressed as mean ± SEM and statistical analysis was performed using an unpaired student's t-test (**$p<0.01$, ***$p<0.0001$).

4.3.4 Male sex is independently associated with higher levels of pro-inflammatory cytokines, chemokines and adipokines.

Cytokines, chemokines and adipokines found to be altered in visceral obesity (adiponectin, IL-6, IL-8 and MCP-1) were measured by ELISA (as described in section 2.10) in a cohort of male (n=27) and female (n=22) patients. While there was no difference in age, BMI, metabolic syndrome factors or metabolic syndrome status between sexes, males had significantly higher WC compared with females (p<0.0001), reflecting the tendency of males to accumulate omental adipose tissue in the abdominal cavity and the tendency of females to accumulate subcutaneous adipose tissue (Misra and Vikram, 2003). BMI, a measure of overall adiposity, was the same between sexes (Table 4.6).

Levels of pro-inflammatory adipokines IL-6 (p<0.0001), IL-8 (p<0.0001) and MCP-1 (p<0.0005) and levels of the anti-inflammatory adipokine adiponectin were significantly increased (p<0.0001) in ACM of male patients (Table 4.7). Levels of IL-8 were also significantly higher in male serum (p<0.0001), while there was no significant difference in serum IL-6 or MCP-1 levels between male and female patients (Table 4.8). There is little information to date on the role of male sex hormones in IL-8 regulation, however initial studies have demonstrated IL-8 production by prostate cancer cell lines in response to treatment with androgen (Gannon et al., 2010). While there was an elevated level of adiponectin in ACM in male patients, levels of serum adiponectin were lower in male relative to female patients, although this did not reach significance. Adiponectin levels are altered by sex hormones and circulating androgens have been shown to decrease serum adiponectin levels in men (Nishizawa et al., 2002) which could account for this somewhat conflicting result.

These data identify an association of male sex with a pro-inflammatory phenotype, potentially due to the characteristic male storage of excess adipose tissue in the abdominal cavity. A pro-angiogenic and pro-inflammatory phenotype is characteristic of the visceral adipose tissue depot, evidenced by significantly increased levels of IL-6 and VEGF in this depot (section 4.3.3). Together these results outline potential molecular mechanisms responsible for the association of male sex with increased incidence of obesity related disease, including OAD (Ryan et al., 2006).

Table 4.6: Anthropometric details for patients grouped by male (n=45) and female (n=40) sex.

	female	male
No. subjects	22	27
Age at surgery, mean (range)	64 (41-83)	63 (30-84)
Waist circumference, mean (range)	87 (66-107)	98 (80-114) ***
BMI, mean (range)	26 (17-40)	27 (22-36)
HDL, mean (range)	1.36 (0.58-2.55)	1.24 (0.63-2.44)
Trig, mean (range)	1.49 (0.49-4.9)	1.4 (0.64-3.67)
Fasting glucose, mean (range)	5.44 (4.3-9.8)	5.63 (3.2-15.9)
Metabolic syndrome, n (%)	14 (41)	14 (38)
Neoadjuvant therapy, n (%)	0 (0)	0 (0)

Statistical analysis was carried out using an unpaired student's t-test (***p<0.0001). (BMI=body mass index (cm/kg^2), VFA=visceral fat area (cm^3), HDL=high density lipoprotein (mmol/L), Trig=triglycerides (mmol/L))

Table 4.7: Adipokine levels (pg/ml) in adipose conditioned medium (ACM) measured by ELISA in male (n=27) and female (n=22) patients.

	Female	Male	*p value*
Adiponectin	211630 (17931)	440844 (43053)	*0.0001*
MCP-1	56995 (5486)	160988 (27670)	*0.0005*
IL-6	76814 (5028)	246184 (25568)	*0.0001*
IL-8	70252 (4681)	286400 (26842)	*0.0001*

Data are expressed as mean ± SEM and statistical analysis was performed using an unpaired student's t-test.

Table 4.8: Adipokine levels (pg/ml) in serum measured by ELISA in male (n=27) and female (n=22) patients.

	Female	Male	*p value*
Adiponectin	5459000 (563873)	3957000 (549459)	*0.0639*
MCP-1	75.16 (8.13)	78.17 (8.618)	*0.8007*
IL-6	23.59 (12.39)	15.62 (5.159)	*0.5230*
IL-8	11.32 (2.026)	56.06 (9.386)	*0.0001*

Data are expressed as mean ± SEM and statistical analysis was performed using an unpaired student's t-test.

4.3.5 Adipokine levels in conditioned medium from omental adipose tissue are altered in cancer relative to non cancer patients.

A panel of 20 adipokines (leptin, adiponectin, HGF, NGF, total PAI-1, GM-CSF, resistin, MCP-1, TNFα, IFNγ, IL-1β, IL-2, IL-4, IL-5, IL-6, IL-7, IL-8, IL-10, IL-12 and IL-13) was tested in OAD patients (n=30) and non cancer patients undergoing surgical procedures for laparoscopic Nissen fundoplication, cholecystectomy and hernia repair (n=5). ACM was prepared from the omental adipose tissue of these patients (as described in section 2.4.2) and analysed using Milliplex MAP Luminex technology, by Milliplex (described in section 2.8). There were no significant differences between measures of obesity or metabolic syndrome factors between groups. However non cancer patients underwent surgery only while 47% of cancer patients received neoadjuvant therapy prior to surgery (Table 4.9). To avoid the potentially confounding influence of neoadjuvant therapy, cancer patients undergoing surgery only were analysed separately.

Of the panel of adipokines screened, the levels of four adipokines were significantly altered in cancer patients. Cancer patients had significantly higher levels of pro-inflammatory T_H1 adipokines IFNγ ($p < 0.05$), IL-6 ($p < 0.01$), IL-8 ($p < 0.0001$) and MCP-1 ($p < 0.01$) (Figure 4.9). This effect was less pronounced in cancer patients undergoing surgery only, implying that neoadjuvant therapy can affect adipokine production. However, IL-6, IL-8 and MCP-1 remained significantly higher in cancer relative to non cancer patients following adjustment for neoadjuvant therapy ($p < 0.05$, $p < 0.01$, $p < 0.02$, respectively), and IFNγ was near significant ($p < 0.07$). Elevated expression of pro-inflammatory adipokines in cancer patients could serve to fuel pathways in tumour growth and metastasis (Colotta et al., 2009; Ruffell et al., 2010).

Table 4.9: Anthropometric details for patients included in Milliplex MAP Luminex screen of 20 cytokines and adipokines.

	non cancer	*cancer*
No. subjects	5	30
Sex (male), n (%)	5 (100)	30 (100)
Age at surgery, mean (range)	54 (43-72)	64 (44-87)
Waist circumference, mean (range)	96 (80-114)	98 (76-130)
BMI, mean (range)	27 (24-31)	26 (21-39)
VFA, mean (range)	292 (286-303)	188 (18-384)
HDL, mean (range)	1.39 (0.69-2.2)	1.12 (0.58-1.83)
Trig, mean (range)	1.69 (1.17-2.46)	1.5 (0.36-6.84)
Fasting glucose, mean (range)	5.4 (5.1-5.6)	5.5 (3.2-11.6)
Metabolic syndrome, n (%)	2 (40)	11 (37)
Neoadjuvant therapy, n (%)	0 (0)	14 (47)

Patients were divided into cancer and non cancer groups. Statistical analysis was carried out using student's t-test. (BMI=body mass index (cm/kg^2), VFA=visceral fat area (cm^3), HDL=high density lipoprotein (mmol/L), Trig=triglycerides (mmol/L))

Table 4.10: Adipokine levels (pg/ml) in adipose conditioned medium (ACM) measured using Milliplex MAP Luminex technology in male age matched cancer (n=30) and non cancer (n=5) oesophageal adenocarcinoma patients.

	Non Cancer	All Cancer	p value	Cancer - neo	p value
Leptin	110736 (85839)	50496 (6925)	0.1089	53794 (8561)	0.2766
Adiponectin	656510 (156455)	871717 (58638)	0.1794	947143 (104474)	0.1621
HGF	39829 (13795)	42820 (3402)	0.7646	47871 (4812)	0.4869
NGF	186.7 (68.04)	246.3 (26.14)	0.3982	214.8 (33.72)	0.6897
PAI-1 (total)	21765 (5802)	43460 (8826)	0.3838	31688 (6743)	0.4633
GM-CSF	30.02 (13.19)	164.7 (59.75)	0.3704	129.8 (80.74)	0.4789
resistin	2242 (1394)	3610 (1063)	0.6143	1949 (525.5)	0.8088
MCP-1	3195 (744.3)	4408 (81.64)	0.0013	4468 (122.7)	0.0178
TNF-α	5.840 (1.654)	18.58 (10.34)	0.6228	9.426 (3.572)	0.5681
IFN-γ	13.04 (2.886)	19.47 (1.189)	0.0488	20.88 (2.085)	0.0612
IL-1β	4.292 (0.6257)	49.81 (21.64)	0.4024	31.20 (21.01)	0.4472
IL-2	0.580 (0.1509)	0.9323 (0.1768)	0.4312	1.237 (0.3712)	0.3024
IL-4	2.049 (0.2505)	2.411 (0.1573)	0.4205	2.269 (0.2118)	0.5995
IL-5	66.47 (45.14)	55.21 (17.95)	0.8145	71.83 (37.74)	0.9377
IL-6	6298 (1435)	8292 (77.66)	0.0014	8356 (140.1)	0.0318
IL-7	84.71 (17.11)	82.77 (5.992)	0.9055	86.34 (10.57)	0.9362
IL-8	2937 (723.5)	4463 (96.35)	0.0002	4536 (181.4)	0.0072
IL-10	231.8 (117.4)	506.4 (68.67)	0.1282	552.1 (119.2)	0.1524
IL-12 (p70)	3.558 (0.696)	3.481 (0.2606)	0.9178	3.643 (0.4176)	0.9210
IL-13	2.190 (0.5461)	3.099 (0.6283)	0.5832	3.851 (1.251)	0.4699

Data are expressed as mean ± SEM. Statistical analysis was performed using an unpaired student's t-test. (All cancer=cancer patients undergoing surgery only and cancer patients undergoing neoadjuvant therapy and surgery, cancer-neo=cancer patients undergoing surgery only)

4.3.6 Validation of Milliplex MAP Luminex data in an independent cohort of cancer and non cancer patients.

A selection of seven cytokines, chemokines and adipokines of interest (leptin, adiponectin, IL-6, IL-8, MCP-1, IFNγ and VEGF) were chosen for validation by ELISA (as described in section 2.10) in ACM from an independent cohort of cancer (OAD) (n=16) and non cancer patients (n=5) (Table 4.13). There were no differences in obesity status, metabolic syndrome factors or metabolic syndrome status between cancer and non cancer groups. Non cancer patients were significantly younger (p<0.01) than cancer patients (Table 4.13). A number of potentially confounding factors were taken into consideration. Males were found to have an increased pro-inflammatory profile compared with females with increased levels of IL-8 in serum (p<0.0001) and increased levels of IL-6 (p<0.0001), IL-8 (p<0.0001) and MCP-1 (p<0.0005) in ACM (results section 4.3.4). Therefore, subsequent analysis was carried out in males only. Patients who received neoadjuvant therapy prior to surgery had significantly higher levels of leptin and IL-6 in ACM (p<0.02), together with increased leptin levels in serum (p<0.05), compared to those who had surgery only (Tables 4.11, 4.12). Subsequent analysis was therefore carried out in patients who underwent surgery only.

Table 4.11: Adipokine levels in ACM (pg/ml) measured by ELISA in a cohort of patients who received neoadjuvant therapy (n=20) prior to surgery, and who had surgery only (n=43).

	Surgery only	Surgery + neoadj	*p value*
Leptin	84203 (14421)	187214 (55784)	*0.0148*
Adiponectin	440844 (43053)	497446 (57788)	*0.4319*
IL-6	243015 (28026)	346543 (24439)	*0.0137*
IL-8	286400 (26842)	346908 (20857)	*0.1309*
MCP-1	160988 (27670)	177877 (37697)	*0.3555*
VEGF	1366 (129.4)	1608 (327.6)	*0.4221*
IFN-γ	21.74 (1.541)	18.11 (10.31)	*0.7456*

Data are expressed as mean ± SEM and statistical analysis was performed using an unpaired student's t-test.

Table 4.12: Adipokine levels (pg/ml) in serum measured by ELISA in a cohort of patients who received neoadjuvant therapy (n=20) prior to surgery, and who had surgery only (n=43).

	Surgery only	Surgery + neoadj	p value
Leptin	16225 (2144)	31017 (9722)	*0.0270*
Adiponectin	3957000 (549459)	2948000 (464523)	*0.2407*
IL-6	15.62 (5.159)	61.0 (51.57)	*0.1988*
IL-8	56.06 (9.386)	106.3 (75.37)	*0.3299*
MCP-1	78.17 (8.618)	139.1 (40.48)	*0.0891*
VEGF	260.2 (35.45)	373.3 (164.0)	*0.2915*
IFN-γ	309.7 (129.4)	137.4 (109.4)	*0.4475*

Data are expressed as mean ± SEM and statistical analysis was performed using an unpaired student's t-test.

Anthropometric details for male OAD patients who underwent surgery only are listed in Table 4.13. In ACM, levels of pro-inflammatory T_H1 adipokines IL-6, IL-8 and IFNγ were increased in cancer patients, however these changes did not reach statistical significance. There was no difference in levels of leptin, adiponectin, MCP-1 or VEGF in ACM between cancer and non cancer patients (Table 4.14). In serum, there was a significant elevation in levels of IL-6 ($p<0.05$) and IL-8 ($p<0.03$) in cancer patients. There was also a decrease in anti-inflammatory adiponectin levels together with an increase in pro-angiogenic VEGF and pro-inflammatory T_H1 adipokine IFNγ, however these changes did not reach statistical significance. Serum leptin and MCP-1 levels were similar between cancer and non cancer patients (Table 4.15). The pro-inflammatory phenotype resulting from elevated levels of these pro-inflammatory mediators has recently been identified to be a hallmark of cancer and could be linked to increased tumour growth and metastasis (Colotta et al., 2009).

Table 4.13: Anthropometric details for patients selected for validations of Milliplex MAP data. All patients received surgery only.

	non cancer	cancer
No. subjects	5	16
Sex (male), n (%)	5 (100)	16 (100)
Age at surgery, mean (range)	52 (44-61)	68.5 (49-86) **
Waist circumference, mean (range)	95.8 (80-114)	97.4 (86-113)
BMI, mean (range)	26.6 (23.8-30.6)	25.8 (22-35)
HDL, mean (range)	1.37 (0.69-2.16)	1.18 (0.7-2.4)
Trig, mean (range)	1.5 (0.5-2.5)	1.4 (0.5-4.9)
Fasting glucose, mean (range)	5.9 (4.6-8.9)	5.5 (3.2-15.9)
Metabolic syndrome, n (%)	2 (40)	8 (50)

Patients were divided into cancer (n=16) and non cancer (n=5) groups. Statistical analysis was carried out using student's t-test. (BMI=body mass index (cm/kg^2), VFA=visceral fat area (cm^3), HDL=high density lipoprotein (mmol/L), Trig=triglycerides (mmol/L))

Table 4.14: Validations of adipokine levels (pg/ml) in adipose conditioned medium (ACM) measured by ELISA in cancer (n=16) and non cancer (n=5) patients.

	Non Cancer	Cancer	p value
Leptin	77434 (25344)	88369 (18042)	0.7227
Adiponectin	352001 (80700)	412357 (49738)	0.2463
IL-6	180704 (57573)	266646 (27397)	0.1572
IL-8	206989 (50152)	311216 (29645)	0.0989
MCP-1	50271 (10067)	60838 (6489)	0.3669
VEGF	1199 (165.2)	1469 (181.6)	0.3239
IFN-γ	20.93 (1.737)	83.96 (67.8)	0.6024

Data are expressed as mean ± SEM and statistical analysis was performed using an unpaired student's t-test.

Table 4.15: Validations of adipokine levels (pg/ml) in serum measured by ELISA in cancer (n=16) and non cancer (n=5) patients.

	Non Cancer	Cancer	p value
Leptin	19558 (2801)	15398 (2984)	0.3661
Adiponectin	4694000 (1015000)	3326000 (514717)	0.2214
IL-6	4.862 (1.403)	25.62 (9.221)	0.0419
IL-8	30.59 (8.633)	71.35 (11.87)	0.0298
MCP-1	74.41 (18.37)	79.93 (9.957)	0.7734
VEGF	200.2 (59.21)	285.3 (41.3)	0.2417
IFN-γ	26.83 (4.629)	380.5 (152.8)	0.3007

Data are expressed as mean ± SEM and statistical analysis was performed using an unpaired student's t-test.

In summary, a circulating pro-inflammatory phenotype was associated with visceral obesity (Tables 4.4, 4.5). Visceral adipose tissue produced greater levels of pro-inflammatory adipokines than subcutaneous adipose tissue (Figure 4.2). Male sex, associated with preferential accumulation of visceral adipose tissue, was associated with increased levels of pro-inflammatory cytokines, chemokines and adipokines (Tables 4.7, 4.8). These results highlight the potential importance of leptin, IL-6, IL-8, MCP-1, VEGF and IFNγ as major pro-inflammatory and pro-tumour mediators and the importance of adiponectin and IL-4 as major anti-inflammatory and anti-tumour factors. An alteration in the balance of these key adipokines was found to be associated with visceral obesity, male sex and cancer. Together these data contribute to the delineation of molecular mechanisms responsible for the epidemiological link between visceral obesity, male sex and OAD (Beddy et al., 2010; Kubo and Corley, 2002).

4.3.7 Oesophageal adenocarcinoma OE33 and OE19 cell lines express adipokines and their receptors.

Visceral obesity, male sex and cancer were found to be associated with a circulating pro-inflammatory profile. It was subsequently investigated whether OE33 and OE19 oesophageal adenocarcinoma cells were capable of responding to these paracrine signals by expressing relevant adipokine receptors. It was also investigated whether OE33 and OE19 could express adipokines themselves, indicating a potential for autocrine signalling. Cell lines were cultured in full serum (10% FCS) medium or serum depleted (0.5% FCS) medium for 24 hours before RNA was extracted (as described in section 2.6.2). Gene expression was investigated using RT-PCR (as described in section 2.6.7) and expression was quantified using densitometric analysis (as described in section 2.7.8). Two oesophageal adenocarcinoma cell lines, OE33 and OE19, were examined to investigate whether this was a cell specific effect, or characteristic of multiple OAD cell lines.

OE33 and OE19 expressed detectable mRNA levels of visfatin, resistin and adipsin. A very low basal expression of leptin was detectable in OE33 and undetectable in OE19. Expression of adiponectin was undetected in both OE33 and OE19 cell lines. There was no change in adipokine expression in response to 24 hour serum starvation, carried out to mimic the hypoxic, nutrient depleted tumour microenvironment (Figure 4.3). While leptin and adiponectin are adipocyte specific, resistin is expressed in adipocytes, muscle, pancreas and macrophages (Tilg and Moschen, 2006), adipsin is expressed in adipose tissue and macrophages (White et al., 1992) and visfatin is ubiquitously expressed (Kitani et al., 2003). These data indicate that OAD cell lines have the capability to express mRNA levels of adipose tissue specific leptin and adipsin in addition to the more ubiquitously expressed adipokines visfatin and resistin. In full serum medium, both OE33 and OE19 expressed leptin receptor ObR and adiponectin receptors AR1 and AR2. In OE33, levels of these receptors were induced upon serum starvation with ObR and AR1 undergoing a 1.3 fold up regulation and AR2 undergoing a 3.2 fold up regulation, following densitometric analysis (Figure 4.4). In OE19, levels of these receptors were unchanged following serum starvation. In OE33, expression of the functional form of the leptin receptor ObR$_{long}$ was undetectable in full serum medium however was induced upon serum starvation. In OE19 however, ObR$_{long}$ was undetectable both in full serum medium and following serum starvation. These data demonstrate that mRNA expression of leptin and adiponectin receptors can be induced in OAD cell lines in response to nutrient

depletion in the microenvironment (Figure 4.4). A hypoxic, nutrient starved tumour therefore may have increased capacity to respond to increased circulating levels of leptin in obesity.
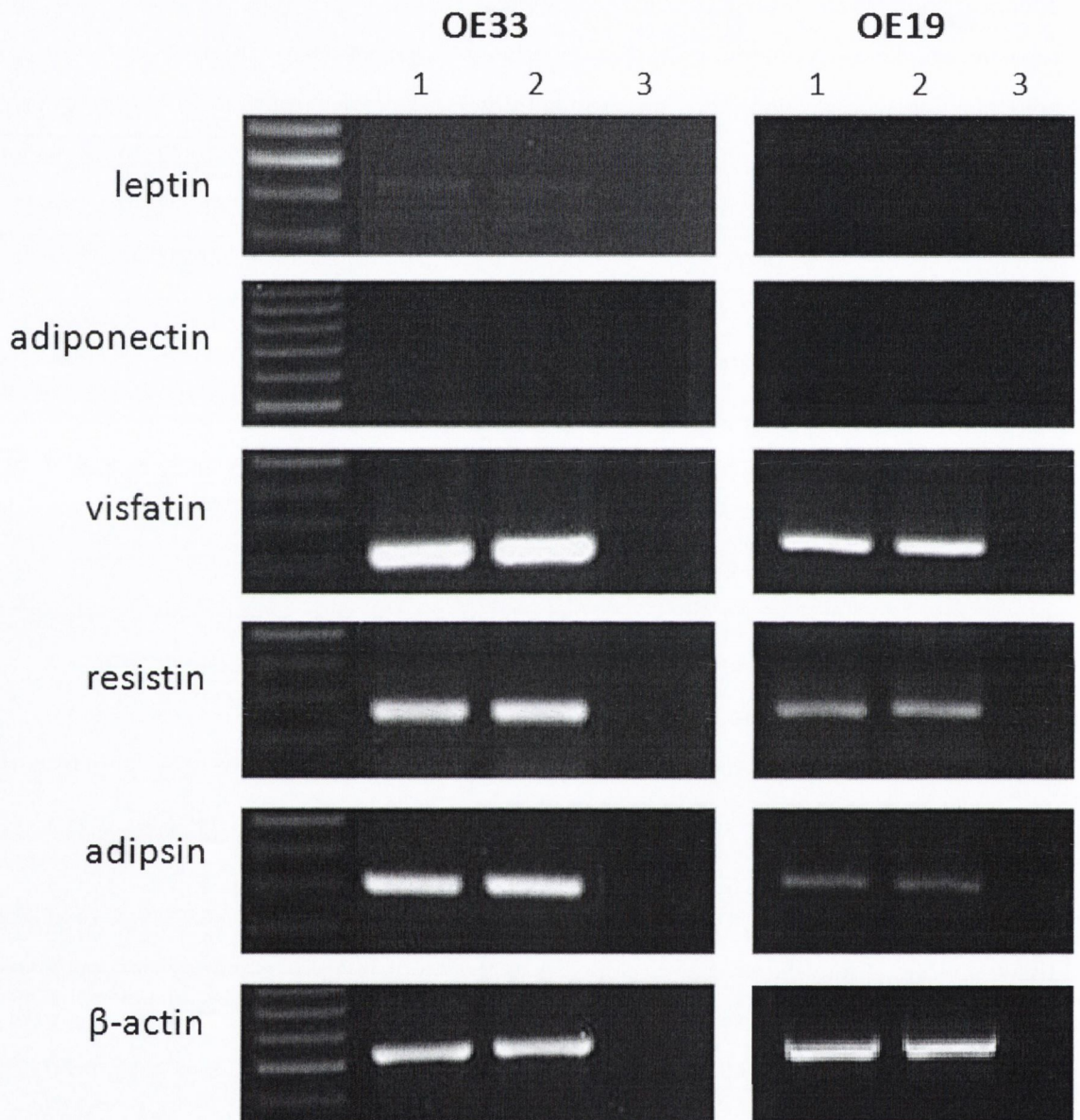
Figure 4.3: Oesophageal adenocarcinoma cell lines OE33 and OE19 were cultured with medium containing 10% FCS (lane 1) and 0.5% FCS (lane 2) for 24 hours before gene expression was examined using RT-PCR. Lane 3 sample contains sterile water instead of cDNA, controlling for contamination in the PCR reaction.
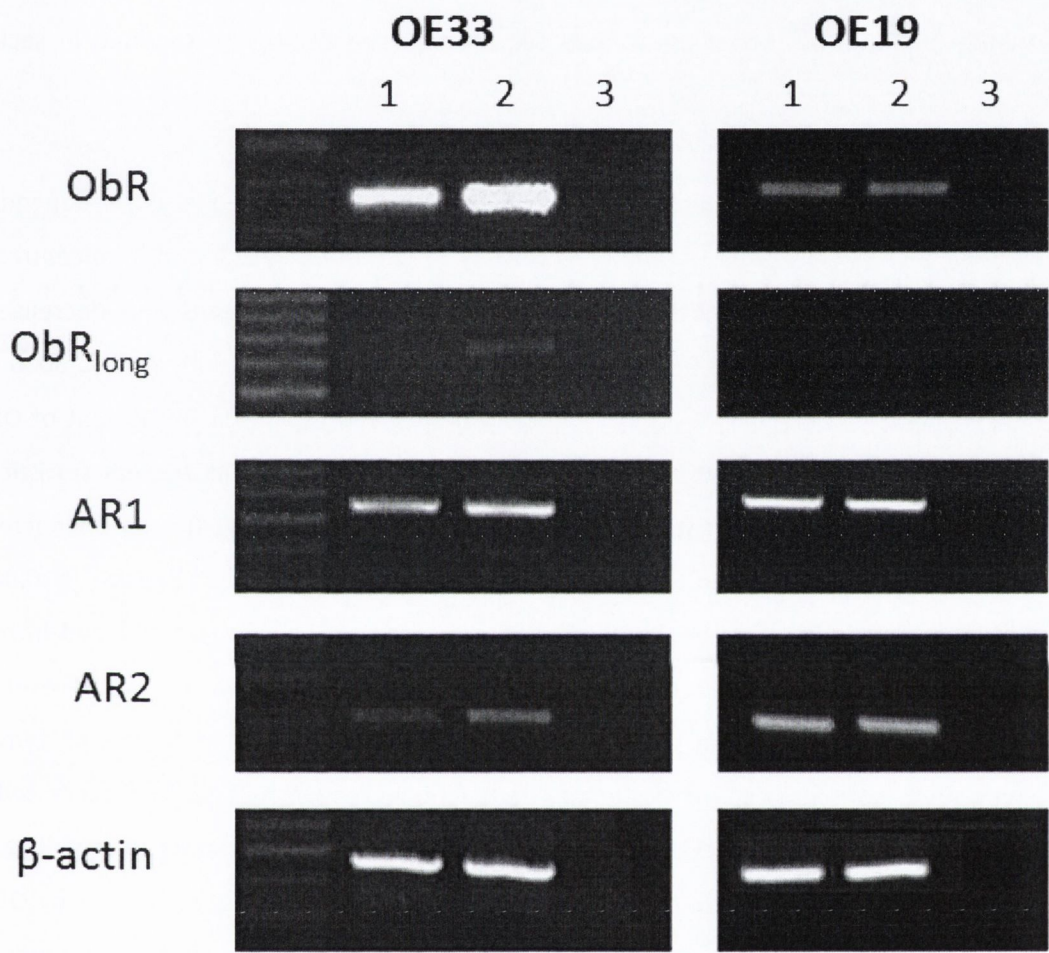
Figure 4.4: Oesophageal adenocarcinoma cell lines OE33 and OE19 were cultured with medium containing 10% FCS (lane 1) and 0.5% FCS (lane 2) for 24 hours before receptor expression was measured using RT-PCR. The sample in lane 3 contains sterile water instead of cDNA to control for contamination of the PCR reaction.

4.3.8 Leptin and adiponectin alter OE33 and OE19 oesophageal adenocarcinoma cell line proliferation in a dose dependent manner.

OE33 and OE19 expressed detectable expression levels of leptin and adiponectin receptors. In addition, expression in OE33 was inducible under serum depleted conditions. These data demonstrate that OAD cell lines are capable of responding to both leptin and adiponectin. The effect of treating OE33 and OE19 with increasing concentrations of human recombinant leptin and adiponectin was examined using BrdU cell proliferation ELISA (as described in section 2.15).

Leptin induced a dose dependent increase and adiponectin induced a dose dependent decrease in OE33 and OE19 proliferation (Figure 4.5). Treatment of OE33 with a concentration of 500 µM leptin and adiponectin induced a significant 20% increase and decrease in proliferation, respectively ($p < 0.05$). Treatment of OE33 with between 1000 µM and 5000 µM adiponectin induced a significant 30% decrease in proliferation ($p < 0.01$). Treatment of OE19 with 500 µM leptin induced a 30% increase in proliferation; however this was not statistically significant. Treatment of OE19 with 5000 µM adiponectin induced a significant 40% decrease in proliferation ($p < 0.05$). Leptin was significantly elevated in serum in obesity ($p < 0.001$). Conversely, adiponectin was significantly lowered in serum in obesity ($p < 0.05$) and in male patients ($p < 0.001$). Raised levels of pro-proliferative leptin together with lowered levels of anti-proliferative adiponectin in obesity could therefore contribute to increased tumour growth in obese patients. As both leptin and its functional receptor ObR$_{long}$ are expressed by OE33, this adipokine could function in both a paracrine and autocrine manner to contribute to tumour growth. Although the functional leptin receptor ObR$_{long}$ was not expressed by OE19, the ubiquitous ObR was expressed and OE19 was shown to be responsive to leptin induced proliferation. This indicates that ObR$_{long}$ may not the only leptin receptor with signalling capacity.

ACM contains not only leptin and adiponectin but a range of pro- and anti-inflammatory adipokines. Many of these were demonstrated to be altered in obesity, male sex and cancer, including IL-6, IL-8, MCP-1, VEGF and IFNγ. To determine the potential physiological effect of altered levels of these soluble mediators in visceral obesity, the functional effect of ACM treatment of OAD cell lines was investigated through measurement of OE33 and OE19 proliferation and apoptosis.
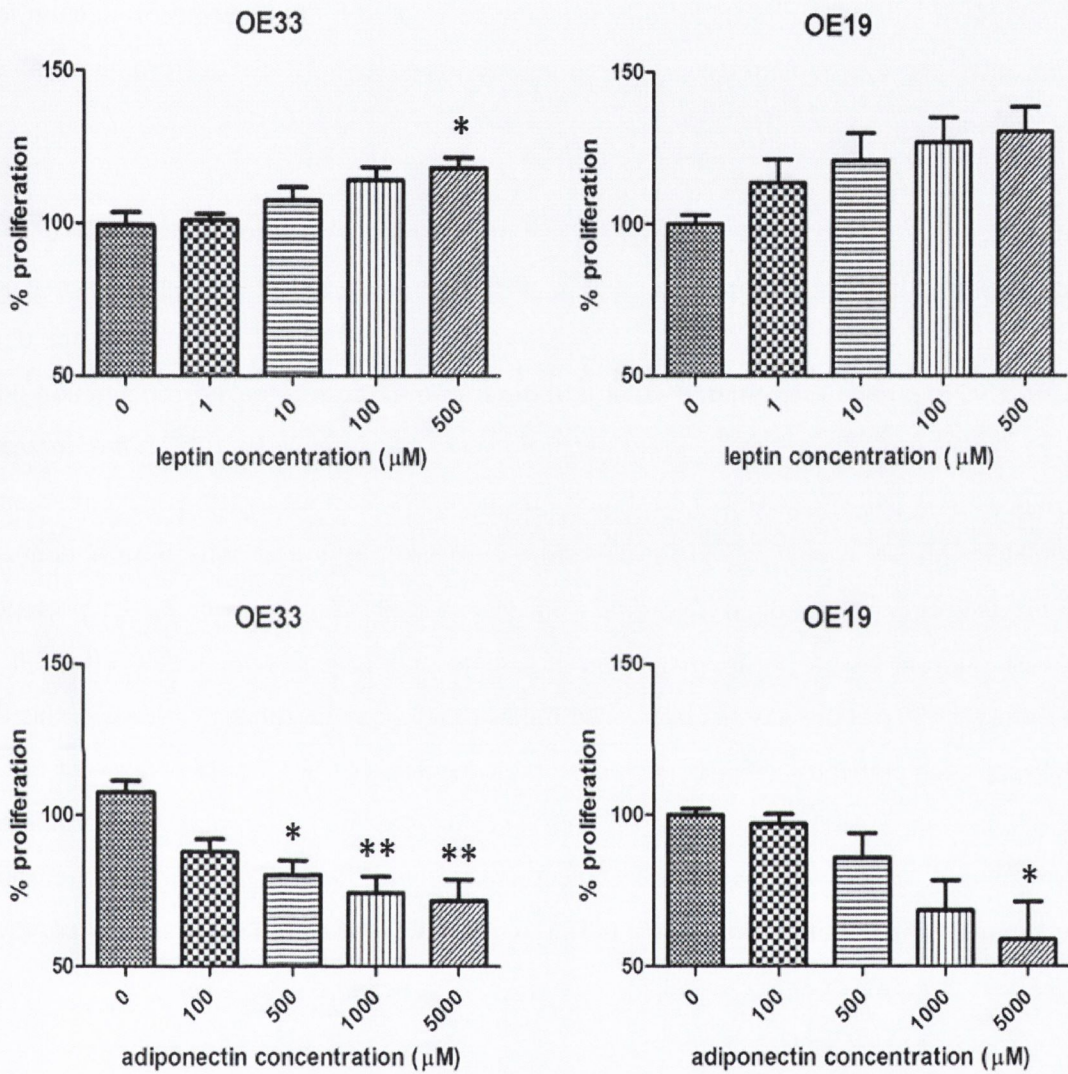
Figure 4.5: Leptin and adiponectin dose dependant responses following 24 hour treatment in OE33 oesophageal adenocarcinoma. OE33 proliferation was assessed by BrdU cell proliferation ELISA. Data are expressed as mean ± SEM and OE33 treated with medium alone was used to normalise results. Data are represented as the mean of three independent experimental replicates. Statistical analysis was performed using ANOVA (one way analysis of variance) with Tukey multiple comparisons post test (*$p < 0.05$, **$p < 0.001$).

4.3.9 ACM induces proliferation in oesophageal adenocarcinoma cell lines OE33 and OE19.

ACM was prepared from omental adipose tissue from viscerally obese (n=20) and non obese (n=20) oesophageal adenocarcinoma patients (as described in section 2.4.2). Oesophageal adenocarcinoma OE33 and OE19 cell lines were treated with ACM or control medium for 24 and 48 hours and percentage proliferation was assessed by BrdU cell proliferation ELISA (described in section 2.15).

ACM significantly increased OE33 and OE19 proliferation by approximately 40% and 50%, respectively, following 24 hour treatment ($p < 0.05$) (Figure 4.6). OE33 are derived from a poorly differentiated pathological stage IIA oesophageal adenocarcinoma while OE19 are derived from a moderately differentiated stage III tumour of the oesophageal gastric junction (Pierini et al., 2008). The more pathologically advanced stage OE19 showed a 10% greater increase in proliferation relative to OE33, indicating it may be more sensitive to the effects of an altered adipokine profile in obesity. While ACM from viscerally obese and non obese patients both induced a significant proliferative effect on oesophageal adenocarcinoma, the presence of excess adipose tissue in viscerally obese patients may give rise to a bulk effect *in vivo*. Although proliferation was also increased following 48 hour treatment with ACM, this effect did not reach statistical significance. These data suggest that an altered balance of pro- and anti-inflammatory adipokines in visceral obesity could give rise to increased OAD proliferation. With leptin already demonstrated to induce OAD proliferation, it remains to be elucidated whether other components of ACM could also contribute to the proliferative effect of ACM.
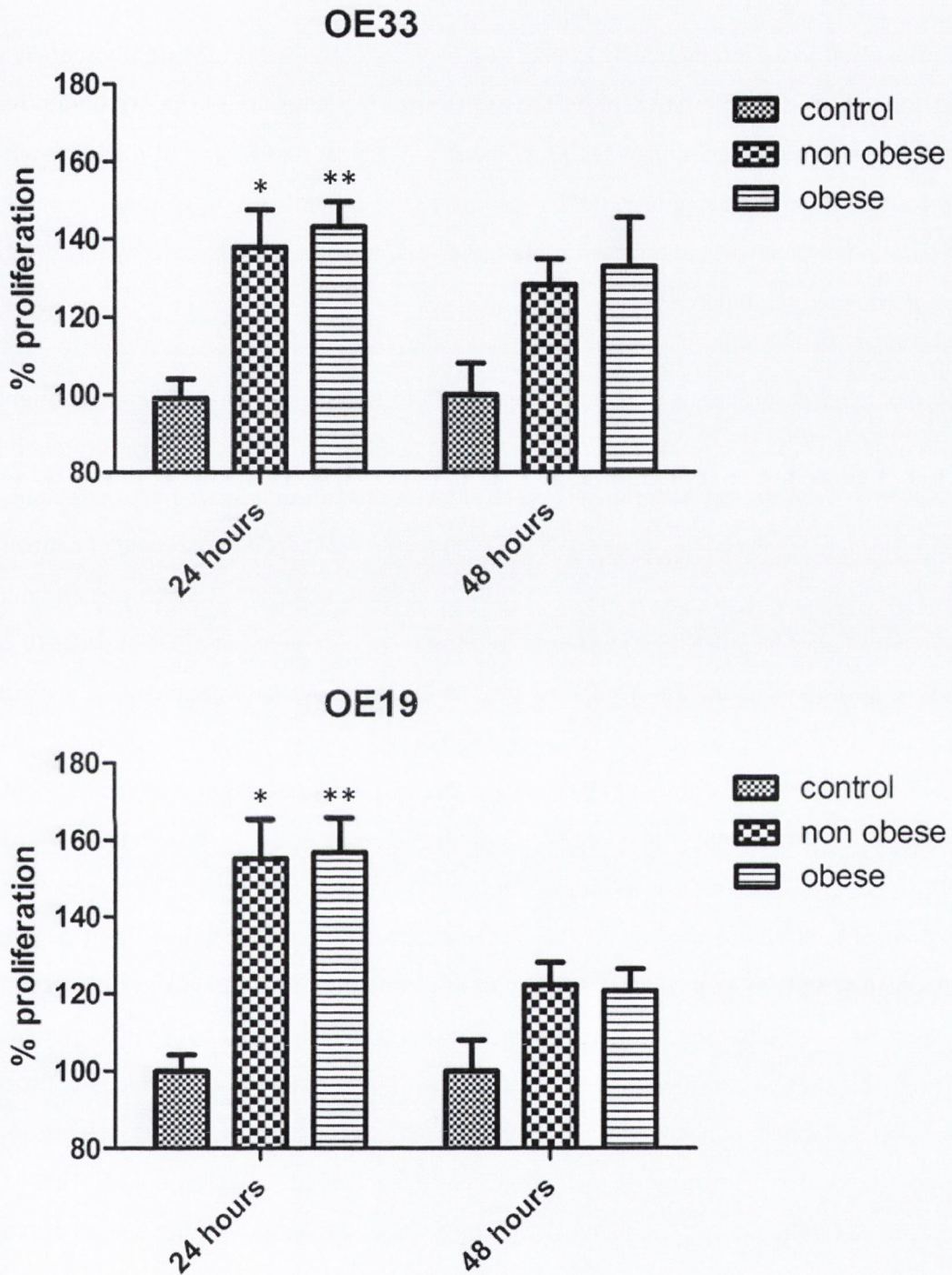
Figure 4.6: Oesophageal adenocarcinoma proliferation in response to treatment with ACM from viscerally obese and non obese OAD patients. Data are expressed as mean ± SEM. Statistical analysis was performed using ANOVA (one way analysis of variance) with Tukey multiple comparisons post test (*p<0.05, **p<0.01).

4.3.10 ACM induces apoptosis in oesophageal adenocarcinoma cell lines OE33 and OE19.

Oesophageal adenocarcinoma OE33 and OE19 were treated with ACM from viscerally obese (n=3) and non obese patients (n=3), or with control medium, for 24 and 48 hours. As ACM contains no serum, the control M199 medium was also serum free, and thus any observed effects were due to factors secreted by adipose tissue and not cell starvation. The percentage of cells undergoing early apoptosis or late apoptosis/necrosis was assessed by flow cytometry (as described in section 2.18).

There was no difference in percentage apoptosis of OE33 or OE19 following treatment with ACM from viscerally obese and non obese patients and so these groups were combined (n=6). Levels of early apoptosis following treatment with serum free control medium were approximately 5% in both cell lines at both 24 and 48 hours, while percentage of control OE33 and OE19 cells undergoing late apoptosis or necrosis was approximately 10% at 24 hours and 15% at 48 hours (Figure 4.7). There was no difference in percentage of OE33 or OE19 cells in early apoptosis following 24 or 48 hour treatment with ACM. Late apoptosis or necrosis was induced 20% in OE19 following both 24 and 48 hours, however this effect was not statistically significant (Figure 4.7). Late apoptosis or necrosis was induced between 6% and 15% in OE33 following 24 and 48 hour ACM treatment, respectively. The induction of late apoptosis/necrosis in OE33 was statistically significant at 48 hours (p<0.05). This result could in part explain why there was lower ACM-induced proliferation at this time point (Figure 4.6). Adipose tissue secretes a wide variety of factors, including the 20 adipokines analysed in this study. These include pro- and anti-inflammatory adipokines in addition to mediators of angiogenesis, which can function in both to induce proliferation and to induce apoptosis. For example, adiponectin has been demonstrated to exert anti-proliferative effects *in vitro*, inhibiting leptin induced growth of OAD cell lines (Ogunwobi and Beales, 2008a). These results indicate that although ACM induced both proliferation and apoptosis, the overall outcome of ACM treatment of OAD was that of increased proliferation (Figure 4.6).
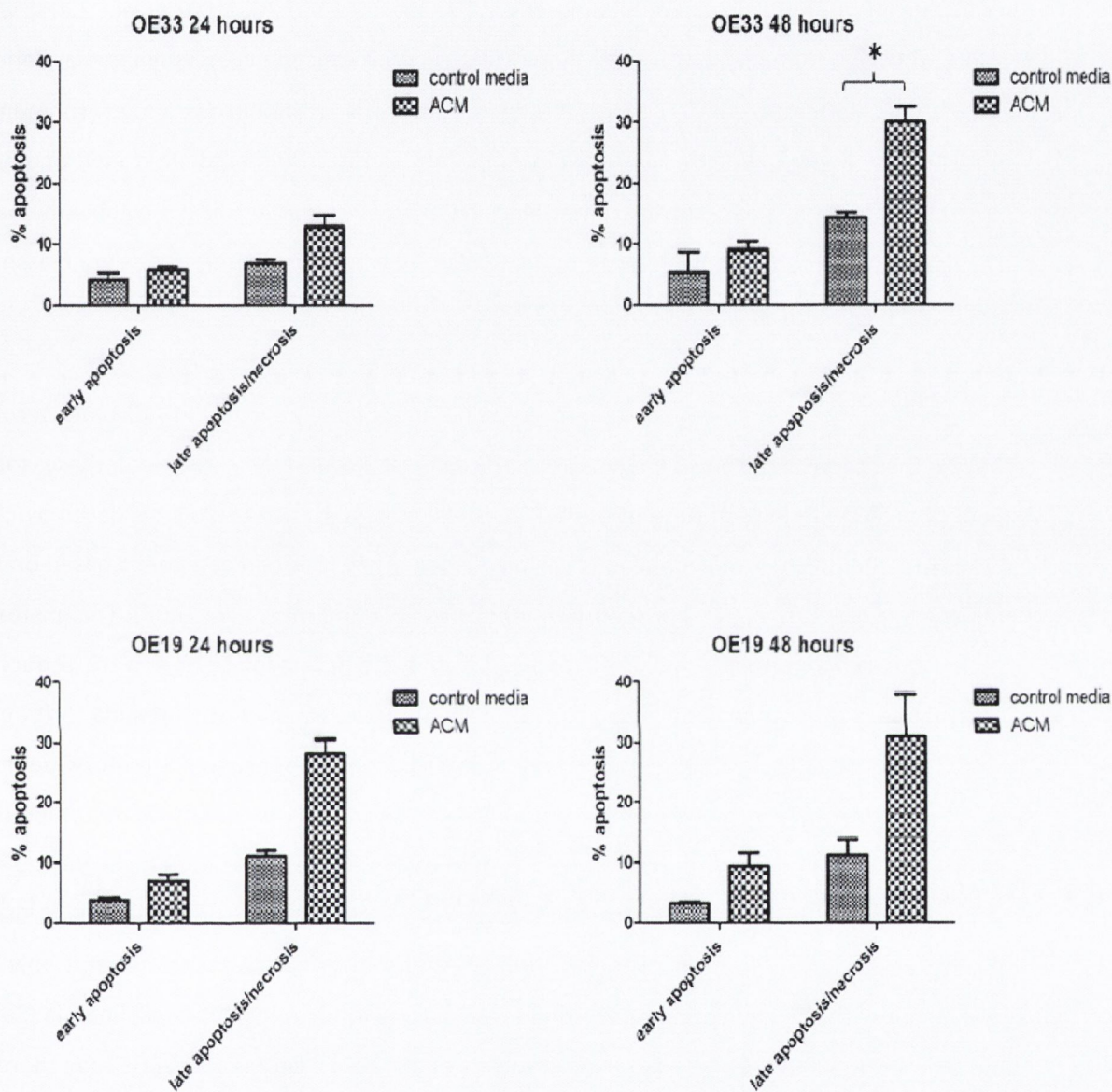
Figure 4.7: Apoptosis in oesophageal cell lines OE33 and OE19 in response to treatment with ACM from viscerally obese (n=3) and non obese (n=3) OAD patients. As there was no difference in percentage apoptosis according to obesity status, patients were pooled. Data are expressed as mean ± SEM. Statistical analysis was performed using a paired student's t-test (*p<0.05).

4.4 Discussion

The recent global obesity pandemic carries with it increased incidence of related disorders including OAD (Calle et al., 2003; Team, 2005). Visceral obesity has recently been characterised as a state of chronic low-grade inflammation (Weisberg et al., 2003; Xu et al., 2003) which could contribute, along with other mechanisms such as prolonged hyperinsulinaemia (Renehan et al., 2006; Roberts et al., 2009), to the generation of a pro-tumourigenic environment. In order to fully understand the basis for development of this pro-inflammatory environment in visceral adiposity, it is necessary to determine the expression pattern of the soluble mediators of inflammation produced by adipose tissue, which may be deregulated in obesity (Fasshauer and Paschke, 2003; Tilg and Moschen, 2006).

This novel study determined cytokine, chemokine and adipokine levels in ACM and serum in the context of visceral obesity and cancer. Preliminary multiplex screens of these soluble mediators of inflammation formed the basis of this work, and results were validated by ELISA. Cytokines, chemokines and adipokines can be divided into two broad categories based on their induction of a T_H1 or T_H2 response in T lymphocytes (Tilg and Moschen, 2006). The expression of the anti-inflammatory adipokine adiponectin and the T_H2 cytokine IL-4 were reduced in visceral obesity, and this finding was consistent with previously published results (Arita et al., 1999; Lord et al., 1998). While there was no difference in levels of pro-inflammatory mediators in ACM, there was increased leptin and VEGF in serum of viscerally obese patients, in accordance with previously published results (Kim et al., 2006). These data highlight the roles of leptin and VEGF as important mediators of chronic low grade inflammation in visceral obesity. An elevation in levels of these cytokines and chemokines is associated not only with obesity but with the development of insulin resistance and resulting hyperinsulinemia (Sartipy and Loskutoff, 2003; Segal et al., 1996; Vozarova et al., 2001). Leptin and VEGF may therefore be useful targets for the prevention and treatment of obesity related pathogenesis.

There was increased production of pro-inflammatory adipokines IL-6, IL-8, MCP-1 and pro-angiogenic adipokine VEGF in the omental relative to the subcutaneous adipose tissue depot, highlighting the importance of visceral adiposity compared with overall obesity. Mirroring these findings, male sex was also associated with increased levels of pro-inflammatory IL-6, IL-8 and MCP-1. While alterations in circulating levels of sex hormones between males and females has been shown to contribute to this observation, differential fat deposition between sexes could also play a role in the establishment of an enhanced pro-inflammatory profile in

males. Adipose tissue is stored preferentially in the visceral depot in males, while in females it is preferentially stored in the subcutaneous depot (Misra and Vikram, 2003). With elevated secretion of pro-inflammatory adipokines from the visceral relative to the subcutaneous depot, increased fat deposition in this compartment could contribute to the male associated pro-inflammatory profile. These results therefore present a molecular mechanism by which male sex is an independent risk factor for OAD (Kubo and Corley, 2002). Together these data indicate that elevated circulating levels of pro-inflammatory mediators in both visceral obesity and male sex are linked to the development of the pro-inflammatory phenotype associated with insulin resistance and hyperinsulinaemia.

Chronic inflammation has recently been established as a hallmark of cancer and is linked to tumour cell survival, proliferation and angiogenesis (Colotta et al., 2009). In this study, elevated levels of pro-inflammatory mediators IL-6, IL-8 were found to be associated with cancer, independent of obesity status, sex and neoadjuvant therapy. Increased levels of serum IL-6 have been previously demonstrated in cancer (Egler et al., 2008) including small cell lung cancer (Wojcik et al., 2010), multiple myeloma (Wierzbowska et al., 1999) and chronic lymphocytic leukaemia (Robak et al., 1999). Elevated levels of IL-8 have also been confirmed in small cell lung cancer (Tas et al., 2006; Wojcik et al., 2010). In addition to its pro-inflammatory role, IL-6 has been shown to induce VEGF transcription in cervical cancer cells (Wei et al., 2003) and therefore could play an important role in tumour angiogenesis and neo-vascularisation (Ara and Declerck, 2010). These results indicate a pro-inflammatory, pro-angiogenic state present in visceral obesity comparable to that of the tumour microenvironment. It therefore follows that the establishment of a state of chronic inflammation in visceral obesity could both predispose to and generate an environment favourable for tumour development.

A number of issues were raised throughout this work regarding the reliability of the initial Milliplex screen. Counter-intuitively, this screen indicated significantly decreased levels of IL-6, IL-8 and MCP-1 in ACM from viscerally obese patients. Elevated circulating levels of these pro-inflammatory mediators have been previously established in visceral obesity (Kim et al., 2006; Tilg and Moschen, 2006), and these preliminary data were therefore in direct conflict with these published findings. However it was subsequently discovered that these preliminary findings failed to be validated by ELISA in an independent cohort of patients, questioning the dependability of the Milliplex technology. In addition, the Milliplex screen found MCP-1, IL-6 and IL-8 to be significantly elevated in the ACM of cancer patients. Although levels of IL-6 and IL-8 were increased, they were not significantly elevated when measured by ELISA in ACM of

an independent cohort. However, serum levels of these pro-inflammatory mediators were significantly higher in cancer patients, indicating that circulating levels may be a more accurate measure of obesity associated inflammation. Contradictory to Milliplex results, there was no difference in levels of MCP-1 in ACM or serum in viscerally obese patients when measured by ELISA in an independent cohort. Although the Milliplex screen provided a preliminary indication of altered levels of pro-inflammatory mediators in obesity and cancer, it also highlighted the importance of validating data from these screens in an independent cohort. As many analytes identified by the Milliplex screen could not be validated in an independent cohort of samples, it was concluded that this technology may be not be suitable for analysis of ACM. It was subsequently decided to carry out an additional preliminary screen taking advantage of this unit's industrial partnership with Randox. While Milliplex offered relevant adipokine and cytokine panels of analytes, unfortunately there existed no equivalent obesity related panel by Randox. The Randox cytokine panel was therefore used to compare analyte levels in omental and subcutaneous ACM and serum of matched patients, and this panel had the advantage of the inclusion of VEGF, absent from the Milliplex panels. The Randox screen therefore provided valuable extra information on levels of pro-inflammatory mediators between adipose tissue depots and on circulating levels of these mediators in serum. Together, these multiplex screens were used to identify adipokines, cytokines and chemokines of potential interest, however only results validated in an independent cohort of patients by ELISA were subsequently reported.

A pro-inflammatory adipokine secretome was found to be associated with visceral obesity, male sex and cancer. Together these data substantiate the identification of visceral obesity and male sex as risk factors for OAD (Beddy et al., 2010; Kubo and Corley, 2002). The mechanisms whereby this chronic pro-inflammatory phenotype could fuel tumour progression remain to be elucidated. The oesophageal adenocarcinoma OE33 and OE19 cell lines were found to express mRNA encoding adipocyte specific adipokines leptin and adipsin together with ubiquitously expressed adipokines resistin and visfatin. In addition, OE33 expressed mRNA encoding leptin receptors, both the ubiquitous form (ObR) and the functional, signalling form (ObR$_{long}$), and adiponectin receptors, both the ubiquitously expressed receptor for globular adiponectin (AR1) and the receptor for metabolically active HMW isoform (AR2) (Kelesidis et al., 2006). OE19 also expressed ObR and AR1, 2 receptors, however lacked OBR$_{long}$. Both the functional ObR$_{long}$ and the HMW binding AR2 were inducible in OE33 upon nutrient depletion of the cells, mimicking the hypoxic tumour microenvironment. Expression of these receptors allowed OE33 and OE19 to respond to leptin and adiponectin in a dose dependent

148

manner, with leptin inducing proliferation and adiponectin reducing proliferation. This result successfully replicates the effect previously demonstrated in both OE33 and OE19 cell lines (Ogunwobi et al., 2006; Ogunwobi and Beales, 2008b). This work demonstrates that tumour cells, particularly in rapidly expanding hypoxic tumours, may be responsive to elevated levels of adipokines through increased receptor expression. Chronic alterations in circulating levels of adipokines in obesity, such as increased pro-proliferative leptin and decreased anti-proliferative adiponectin (Tilg and Moschen, 2006), could therefore result in increased tumour cell proliferation. Indeed ACM treatment resulted in increased proliferation of both OE33 and OE19 cell lines, indicating that the OAD cell lines are responsive to the combination of adipokines secreted by adipose tissue. This suggests a paracrine role for adipose tissue secreted factors in the promotion of tumourigenesis.

The global obesity pandemic shows no sign of abating and with it comes increased incidence of related disorders including cancer (Calle et al., 2003; Team, 2005). It is recently understood that visceral obesity is a chronic low-grade pro-inflammatory condition (Wellen and Hotamisligil, 2005) which could give rise to the establishment of a pro-tumourigenic environment. This study identifies a pro-inflammatory phenotype common to visceral obesity, male sex and cancer mediated through reduction of IL-4 and adiponectin levels and elevation of leptin, IL-6, IL-8, MCP-1, IFNγ and VEGF levels. Altered levels of these mediators were demonstrated to have functional effects on OAD cells with ACM increasing rate of proliferation. The distorted balance of these soluble mediators of inflammation could therefore represent an important therapeutic target in OAD.

5 Co-culture of adipose tissue with oesophageal tumour cells alters expression of genes involved in pro-tumour pathways.

5.1   Introduction

There has been significant interest in the rapidly rising obesity epidemic and its role in cancer development and progression over the past number of years. While the epidemiological link has now been well described for an ever-expanding list of cancers (Calle et al., 1999; Field et al., 2001), the molecular mechanisms linking obesity and cancer remain poorly defined. It is now known that excess visceral adiposity is more strongly associated with metabolic deregulation and disease states than overall obesity (Federation, 2006; Giorgino et al., 2005). The association of visceral obesity is particularly evident in oesophageal adenocarcinoma (OAD) (Beddy et al., 2010), the incidence of which has increased in Ireland by 48% between 1994 and 2007 (National Cancer Registry Ireland, 2000-2005). This alarming rise in OAD mirrors the exponential increase in rates of obesity, and it is imperative for both the prevention and treatment of these diseases that the molecular mechanisms of their association be delineated.

A seminal contribution to the understanding of mechanisms involved in cancer biology came with a published review identifying six hallmarks of cancer, six essential changes to cell physiology both necessary and sufficient to give rise to carcinoma development. These were proposed to be: self sufficiency in growth signals, insensitivity to anti-growth signals, evasion of apoptosis, limitless replicative potential, sustained angiogenesis and tissue invasion and metastasis (Hanahan and Weinberg, 2000). More recently, a state of 'smouldering' chronic sub-clinical inflammation has been identified as a seventh hallmark of cancer (Colotta et al., 2009). The aim of this chapter was to delineate the role of visceral obesity in modulation of these seven hallmarks of cancer.

Proliferation in normal cell types is tightly controlled and deregulation of this process is necessary for tumourigenesis to occur (Perego et al., 2010). This can be accomplished through autocrine or self-stimulated tumour growth, combined with an acquired resistance of tumour cells to anti-growth and apoptotic signals produced by neighbouring cells of the tumour microenvironment (Hanahan and Weinberg, 2000). Levels of growth factors such as insulin and IGF-1 are elevated in visceral obesity, together with growth promoting adipokines such as leptin (Roberts et al., 2009). With high circulating levels of these growth factors in obesity, the tumour can prime itself to respond by expressing high levels of receptors for these molecules, and both obesity and tumour stage have been associated with increased leptin receptor expression in oesophageal adenocarcinoma (Howard et al., 2010).

In order for a tumour to grow beyond a certain size, *de novo* angiogenesis is required (Hanahan and Weinberg, 2000). A budding tumour quickly outgrows its blood supply, thus creating a hypoxic microenvironment. It has been demonstrated that pro-angiogenic factors such as VEGFA, induced by the development of hypoxia in rapidly expanding tissue, can trigger the angiogenic switch, a fundamental mechanism by which a new blood supply is established to the growing tumour (Bergers et al., 2000). This process has been well characterised in tumourigenesis and has recently been proposed to occur during the process of accumulation of excess adipose tissue in visceral obesity (Trayhurn et al., 2008). The development of a systemic hypoxic environment in visceral obesity could therefore contribute to the creation of a milieu favourable for tumourigenesis. Invasion of epithelial cells into the extracellular matrix is necessary for the establishment of a new blood supply and proteolytic cleavage and degradation of ECM is also necessary for invasion and metastasis of tumour cells to occur (Liotta et al., 1991; Ludwig, 2005). Following ECM degradation by tumour cells, metastasis requires movement of tumour cells through the basement membrane and epithelium into the blood stream and lymphatic system (Turpeenniemi-Hujanen, 2005). Oesophageal adenocarcinoma is associated with early lymphatic and haematogenous dissemination (Lagarde et al., 2007) implying that pathways involved in tumour invasion and metastasis are of particular significance.

Tumour recruitment of macrophages, T lymphocytes and natural killer cells can produce a pro-tumour immune phenotype associated with the tumour microenvironment (Ruffell et al., 2010). It is established that chronic inflammation can increase the risk of cancer development, with *H. pylori* infection one of the strongest risk factors for gastric cancer (Herrera and Parsonnet, 2009). Reflux of gastro duodenal contents and consequential inflammatory responses are associated with the development of pre-malignant Barrett's oesophagus and promotion of OAD (Duggan et al., 2010) through molecular changes such as activation of pro-inflammatory transcription factor NFκB (Babar et al., 2010b). An inflammatory phenotype, characterised by primary inflammatory cytokines such as IL-6 and TNF-α, is also often present in the tumour microenvironment of tumours which are not epidemiologically related to inflammation (Colotta et al., 2009). This phenotype of 'smouldering' inflammation is also associated with visceral obesity (Das, 2001; Weisberg et al., 2003) and thus visceral obesity contributes towards the development of a state of low grade systemic inflammation, providing a favourable environment for tumourigenesis.

In order to identify candidate pathways in this complex area, Human Cancer Profiler qPCR arrays were utilised, measuring 84 genes involved in six pathways of carcinogenesis, representing the six hallmarks of cancer (invasion, angiogenesis, apoptosis, cell cycle, signal transduction and adhesion). Although inflammation was not included as a separate category in these arrays, genes involved in inflammation, such as NFκB, were integrated throughout the six hallmarks of cancer (Appendix V). This initial screen was followed by Affymetrix microarrays, measuring gene expression alterations across almost two thirds of the human genome. Microarray technology has been widely and successfully used to date in cancer research, including oesophageal adenocarcinoma, across many areas such as progression from Barrett's oesophagus (Helm et al., 2005; Kimchi et al., 2005), neoadjuvant therapy response (Hartojo et al., 2010; Schauer et al., 2010), prognostic biomarker discovery (Kalinina et al., 2010), epigenetic regulation (Peng et al., 2009; Seder et al., 2009) and microRNA signatures (Mathe et al., 2009; Yang et al., 2009b) but has yet to be applied to the study of interactions between oesophageal adenocarcinoma and obesity. Complex disease processes such as these involve deregulation of multiple gene networks and microarray technology is well suited to this challenge, enabling reproducible and quantitative analysis of thousands of transcripts simultaneously (Lipshutz et al., 1999). Following a preliminary screen of pro-tumour pathways using Human Cancer Profiler Arrays, alterations in pathways of the six hallmarks of cancer were identified as possible candidates. Both to validate these preliminary data, and to further elucidate gene changes within these complex pathways, high throughput microarray technology was subsequently employed. Together these techniques were used to uncover novel molecular mechanisms behind the strong epidemiological association between oesophageal adenocarcinoma and obesity (Reeves et al., 2007; Ryan et al., 2006).

5.2   Aims and objectives

The overall aim of this chapter was to investigate the molecular mechanisms by which visceral adiposity is linked to increased incidence and accelerated progression of oesophageal adenocarcinoma. Gene expression alterations in the OE33 oesophageal adenocarcinoma cell line were investigated following culture with omental adipose tissue from viscerally obese oesophageal adenocarcinoma patients.

Specific objectives:

- Identification of altered pro-tumour pathways in oesophageal adenocarcinoma in response to exposure to omental adipose tissue from viscerally obese patients.
- Dissection of candidate pathways to identify single gene alterations.

- Validation of functional alterations in the tumourigenic phenotype of oesophageal adenocarcinoma in response to treatment with omental adipose tissue and adipose tissue conditioned medium (ACM) from viscerally obese patients.

5.3   Results

5.3.1   Co-culture of SGBS with oesophageal adenocarcinoma alters the expression of genes involved in pro-tumour pathways.

SGBS were demonstrated to be a clinically relevant *in vitro* model, behaving both functionally and biochemically like mature primary human adipocytes once differentiated (Chapter 3) (Fischer-Posovszky et al., 2008). Gene and pathway alterations in the OE33 oesophageal adenocarcinoma cell line were investigated following co-culture with SGBS. OE33 cells were co-cultured in a non-contact system with pre-differentiated SGBS, differentiated SGBS and control medium (as described in section 2.3.5). Following 24 hours, RNA was extracted from OE33 and gene expression changes were investigated using Human Cancer Profiler qPCR arrays (as described in section 2.6.11). Co-culture with both pre-differentiated and differentiated SGBS generated an altered gene expression profile in OE33 with differentiated SGBS adipocytes inducing the most pronounced gene expression changes (Figure 5.1).

The Human Cancer Profiler array was used to measure differential expression of 84 genes in six biological pathways involved in tumourigenesis (Appendix V). Low expression genes amplifying later than 35 cycles were excluded from the analysis and genes altered twofold or more were selected for further investigation. Gene expression changes in OE33 following co-culture with both pre-differentiated and differentiated SGBS were found to be evenly distributed between cell cycle (32.5%), invasion (37.5%) and apoptosis (30.5%) pathways, with no alterations in cell signalling, adhesion or angiogenesis pathways (Figure 5.2). Following co-culture with pre-differentiated SGBS, cell cycle regulator ataxia telangiectasia mutated (ATM) was down regulated twofold in OE33, while p53 target and negative feedback inhibitor MDM2 was down regulated 2.7 fold. Matrix metalloproteinase 2 (MMP2) was up regulated over 4 fold and non-metastatic cells 4 (NME4) was down regulated 3 fold. Tumour necrosis factor receptor super family 1A (TNFRSF1A) was up regulated over 120 fold while TNFRSF25 was down regulated over 4 fold. Following co-culture with differentiated SGBS, gene changes were more pronounced, with MDM2 down regulated by almost 4 fold and MMP2 and TNFRSF1A up regulated by over 10 fold and 200 fold, respectively (Table 5.1).

Based on the results of these arrays, indicating gene expression alterations in oesophageal adenocarcinoma following co-culture with both pre-differentiated and differentiated SGBS adipocytes, gene expression changes in OE33 were examined in response to co-culture with primary human omental adipose tissue and adipocytes.
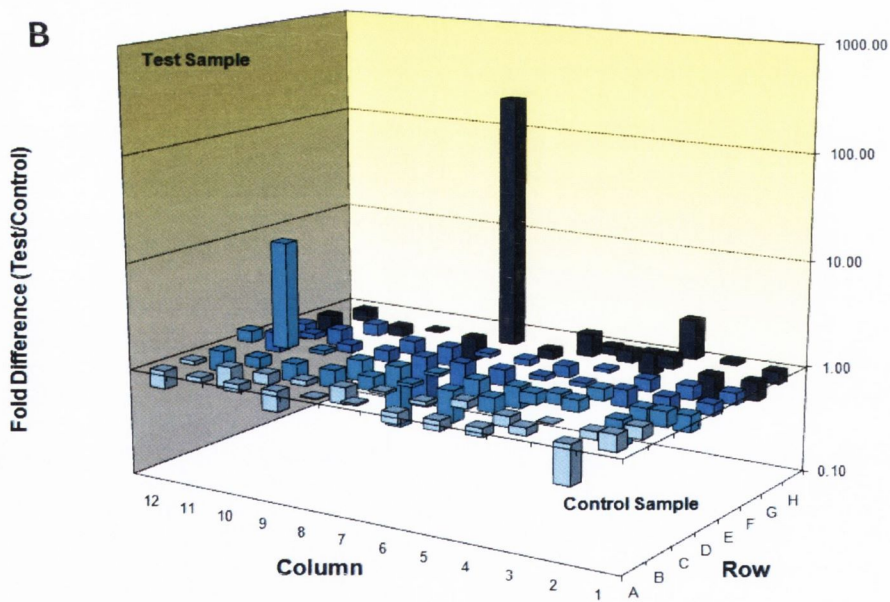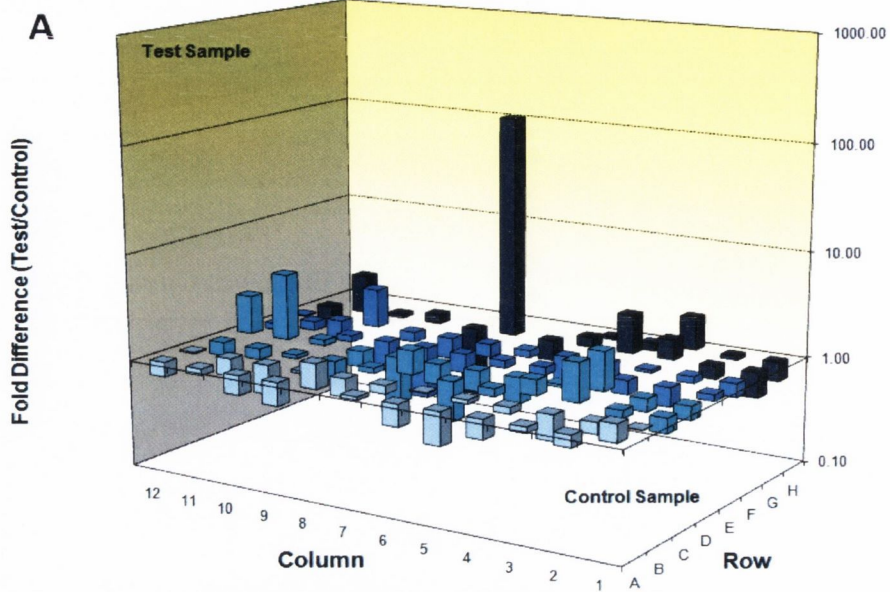
Figure 5.1: Changes in gene expression profiles in OE33 following 24 hour co-culture with pre-differentiated (A) and differentiated SGBS (B) analysed using Human Cancer Pathway Finder arrays. Fold changes in gene expression were calculated using the C_T method.
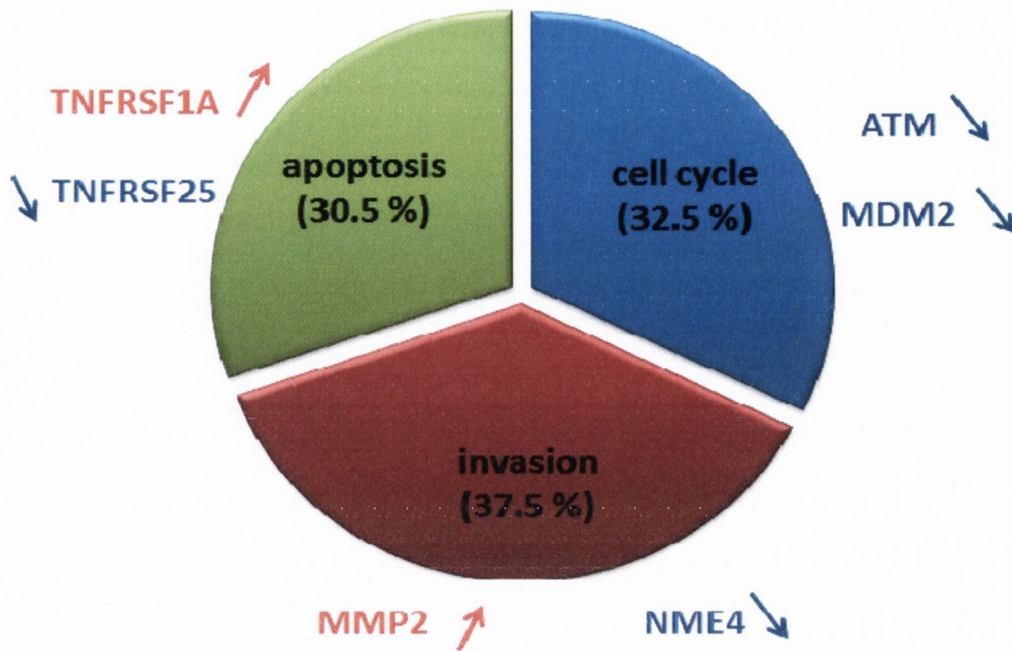
Figure 5.2: Alterations in pro-tumour pathways in the OE33 oesophageal adenocarcinoma cell line following 24 hour co-culture with pre-differentiated and differentiated SGBS. Overall pathway alterations were calculated based on the number of gene changes twofold or greater in each of the six pathways of carcinogenesis, measured by the Human Cancer Profiler array.

Table 5.1: Fold changes in expression of genes altered in OE33 following co-culture with pre-differentiated (A) and differentiated SGBS (B).

Gene	Pathway	Fold change (A)	Fold change (B)
ATM	Cell cycle	-2	-1.2
MDM2	Cell cycle	-2.7	-3.8
MMP2	Invasion	4.2	10.6
NME4	Invasion	-3	-3.1
TNFRSF1A	Apoptosis	123.3	233.4
TNFRSF25	Apoptosis	-4.5	-1.6

Fold changes were calculated relative to OE33 treated with control medium and changes of greater than twofold are in bold. Up regulated genes are highlighted in red while down regulated genes are highlighted in blue.

5.3.2 Omental adipose tissue increases the proliferative, migratory and invasive capacity of oesophageal adenocarcinoma via up regulation of MMP2, MMP9 and PAI-1 and down regulation of tumour suppressors ATM and p53.

With SGBS demonstrated to alter gene expression in OE33, it was investigated whether whole omental adipose tissue and adipocytes could also induce gene and pathway changes in OE33. Omental adipose tissue biopsies was obtained from viscerally obese male OAD patients (n=3) (anthropometric details listed in Table 5.2) and adipocytes were isolated (as described in section 2.3.3). OE33 was co-cultured in a non-contact system with fragments of whole omental adipose tissue, adipocytes and control medium (as described in section 2.3.6). Following 24 hours, RNA was extracted from OE33 and alterations in gene expression were investigated using Human Cancer Profiler qPCR arrays (as described in section 2.6.11).

The highest proportion of genes differentially expressed in oesophageal adenocarcinoma following culture with omental adipose tissue were involved in the invasion and metastasis pathway (34%) and cell cycle pathway (29%)(Figure 5.3). Two specific genes involved in the invasion and metastasis pathway, matrix metalloproteinase 9 (MMP9) and plasminogen activator inhibitor-1 (SERPINE1/PAI-1), were up regulated 42 and 5.5 fold, respectively. The tumour suppressor genes, ATM and p53, part of the cell cycle pathway, were down regulated over twofold (Table 5.3). Following culture of OE33 with ACM, MMP9 and PAI-1 were up regulated by 4 and 4.9 fold, respectively while ATM and p53 were down regulated by 0.4 and 1.5 fold, respectively. Following co-culture of OE33 with adipocytes, MMP9 and PAI-1 were up regulated by 2.6 and 1.7 fold, respectively, while ATM and p53 were unchanged (Table 5.3).

Although co-culture with adipocytes resulted in differential regulation of gene expression in OE33, the greatest change in expression was observed following co-culture of OE33 with fragments of whole omental adipose tissue and ACM. This finding suggests that gene alterations are mediated, at least in part, by secreted factors from the adipose tissue stromal vascular fraction (SVF).

SGBS adipocytes, human primary adipocytes and human primary adipose tissue all altered the expression of invasion, metastasis and cell cycle pathways in OAD. A selection of candidate genes involved in these pathways was chosen for validation in a larger cohort of co-cultured samples.

Table 5.2: Anthropometric information for patients (n=3) analysed using Human Cancer Profiler array.

	Sex	Age	Diagnosis	WC (cm)	BMI	VFA (cm²)	MetS?	Neoadj?
1	M	57	OAD	102	28	121	1	1
2	M	60	OAD	101	25	172	1	0
3	M	59	OAD	130	39	298	0	0

The International Diabetes Federation (IDF) cutoff of WC>94 cm was used to define presence of visceral obesity. (WC=waist circumference, BMI=body mass index, VFA=visceral fat area, MetS=metabolic syndrome, Neoadj=neoadjuvant therapy)
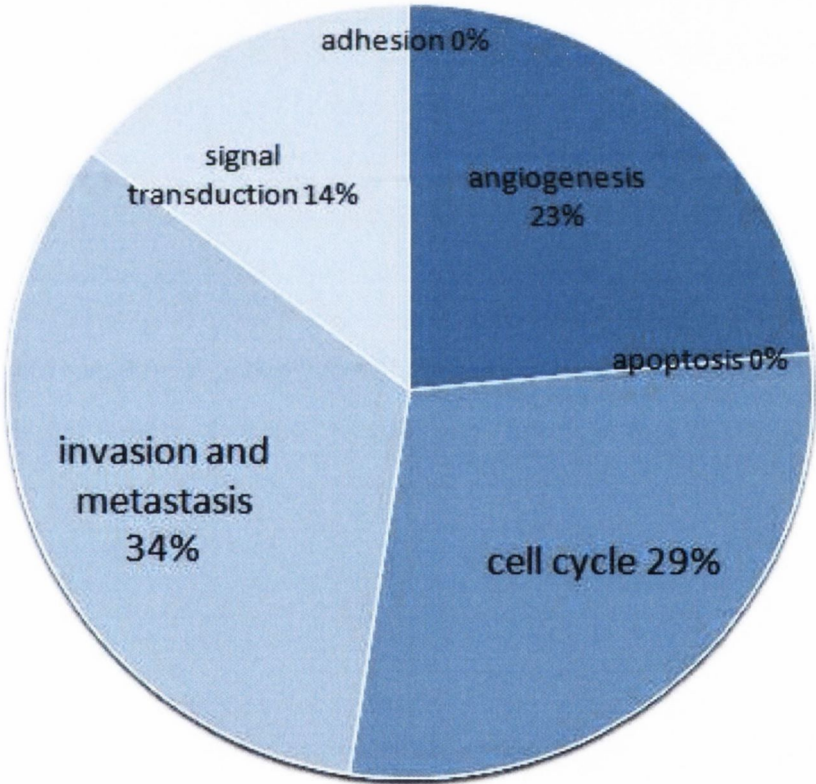
Figure 5.3: Alterations in carcinogenic pathways in OE33 following co-culture with whole adipose tissue fragments, ACM and adipocytes from viscerally obese oesophageal adenocarcinoma patients (n=3). Pathway changes were calculated from the number of gene changes twofold or greater in each of the six pathways of tumourigenesis measured by the Human Cancer Profiler array.

Table 5.3: Fold changes in expression of genes altered in OE33 following co-culture with whole adipose tissue fragments, ACM and adipocytes from viscerally obese OAD patients (n=3).

	fat	ACM	adipocyte	fat	ACM	adipocyte	fat	ACM	adipocyte
MMP9	22.5	1.7	1.6	61.1	7.3	2.5	42.2	2.9	3.7
PAI-1	9.0	4.8	-2.8	3.8	2.9	-1.2	3.7	7.0	-1.1
p53	-2.7	-1.6	1.0	-1.6	-1.3	-1.1	-2.0	-1.7	-1.1
ATM	-3.7	1.1	-1.1	-1.1	1.1	1.0	-1.4	-1.0	1.2

Fold changes were calculated relative to OE33 treated with control medium and changes greater than twofold are in colour. Up regulated genes are highlighted in red while down regulated genes are highlighted in blue.

5.3.2.1 Validations of Human Cancer Profiler arrays

Based on the results of the arrays, a selection of genes involved in the invasion and metastasis pathway (MMP2, MMP9, PAI-1) and cell cycle pathway (p53) were chosen for validation. The OE33 cell line was co-cultured with adipose tissue and adipocytes from OAD patients (n=12) (Table 5.4) (as described in section 2.3.6). After 24 hours, RNA was extracted and gene expression was investigated by quantitative qPCR (as described in section 2.6.9.2). The role of these four genes has been well documented in wide range of cancer types (Curran et al., 2004; Hanahan and Weinberg, 2000; Sakakibara et al., 2005; Whibley et al., 2009) however they are all novel targets in the context of obesity and cancer.

Gene expression of these candidates validated the findings of the array, with significant alterations induced in OE33 following co-culture with adipose tissue (Figure 5.4). Expression of MMP9 was increased over 4000 fold (p<0.01), PAI-1 was increased 10 fold (p<0.0001), while expression of p53 was decreased almost twofold (p<0.05). Expression of MMP2 was induced over 200 fold. Following co-culture of OE33 with adipocytes, an increase in expression of MMP2, MMP9 and PAI-1 and a decrease in expression of p53 was observed, however these expression changes were not statistically significant. This finding further substantiated the hypothesis that gene alterations are predominantly mediated by secreted factors from the adipose tissue SVF.

Upon examination of additional clinical parameters, no difference was observed in candidate gene expression in OE33 with respect to sex, obesity, metabolic syndrome or neoadjuvant therapy status.

Table 5.4: Anthropometric information on oesophageal adenocarcinoma patients (n=12) for validation of the Human Cancer Profiler array.

No. subjects	12
Sex (male), n (%)	10 (83.3)
Age at surgery, mean (range)	60.2 (55-69)
Diagnosis	OAD
Waist circumference (cm), mean (range)	103.8 (81-130)
BMI, mean (range)	30 (22-39)
VFA (cm^2), mean (range)	206 (42.5-383.8)
Metabolic syndrome, n (%)	7 (58.3)
Neoadjuvant therapy, n (%)	6 (50)

(BMI=body mass index, VFA=visceral fat area)
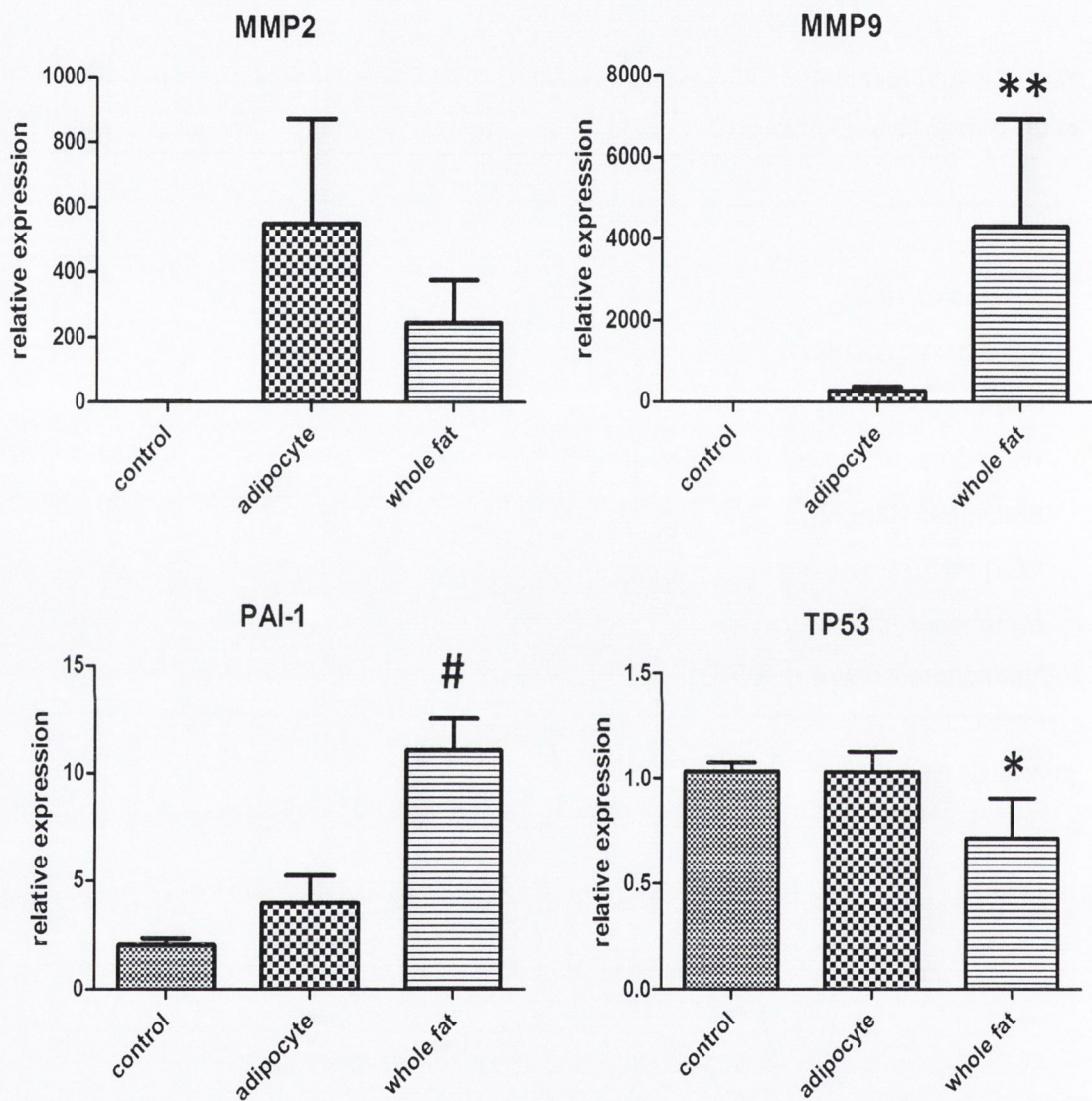
Figure 5.4: Validations of Human Cancer Profiler arrays (n=12) carried out by quantitative qPCR. Data are expressed as mean ± SEM. Statistical analysis was performed using a paired student's t-test (#p<0.001, **p<0.01, *p<0.05 between control and whole fat groups).

5.3.2.2 Co-culture of oesophageal adenocarcinoma with omental adipose tissue up regulates protein expression of MMP2, MMP9 and PAI-1 and down regulates protein expression of p53.

Following validation of the arrays at the mRNA level, protein expression of identified candidate genes was examined in oesophageal adenocarcinoma. OE33 and OE19 were cultured for 24 hours with ACM containing whole adipose tissue fragments from male viscerally obese OAD patients (n=3) (as described in section 2.7.1). Total protein was extracted and investigated by Western analysis (described in section 2.7) and gelatin zymography (described in section 2.7.9). Altered protein expression of MMP2, MMP9, PAI-1 and p53 in OE33 and OE19 in response to co-culture with adipose tissue confirmed the results of the arrays.

Expression of tumour suppressor p53, indicated by a band at 53 kDa, was decreased twofold in OE33 cells in response to co-culture with adipose tissue (Figure 5.5, 5.6). Tumour suppressor p53 was undetectable by Western analysis in OE19 cells (Figure 5.5). PAI-1 was undetectable in OE33 and OE19 controls; however it was strongly induced in both cell lines in response to co-culture with adipose tissue, indicated by a band at 43 kDa (Figure 5.5). MMP9 expression was induced in OE33 and OE19 following co-culture with adipose tissue, indicated by presence of bands at 83 kDa and 92 kDa corresponding to active and pro-MMP9, respectively. Bands at lower molecular weights indicate additional active forms and cleavage products of MMP9 (Shimokawa Ki et al., 2002) (Figure 5.5). The induction of pro-MMP9 reached statistical significance in OE33 following co-culture with adipose tissue fragments ($p < 0.05$) (Figure 5.6).

Using gelatin zymography, MMP gelatinase activity was assessed in OE33 and OE19 following 24 hour culture with control medium and adipose tissue fragments (as described in section 2.7.9). This technique involves electrophoresis of protein samples through a gelatin-containing SDS Page gel. Renaturation of pro and active gelatinases following size separation allows digestion of the gelatin substrate corresponding to the molecular weight of the MMP isoform, thus identifying MMP activity. Following adipose tissue co-culture, bands of enzymatic activity were detected at 92 kDa, corresponding to pro-MMP9, and at 62 kDa, corresponding to active MMP2 (Figure 5.7), while there was an absence of gelatinase activity in both OE33 and OE19 controls.

Together these data demonstrate increased expression of key players in tumour migration and invasion, MMP9 and PAI-1, together with decreased expression of tumour suppressors, notably p53 and ATM.
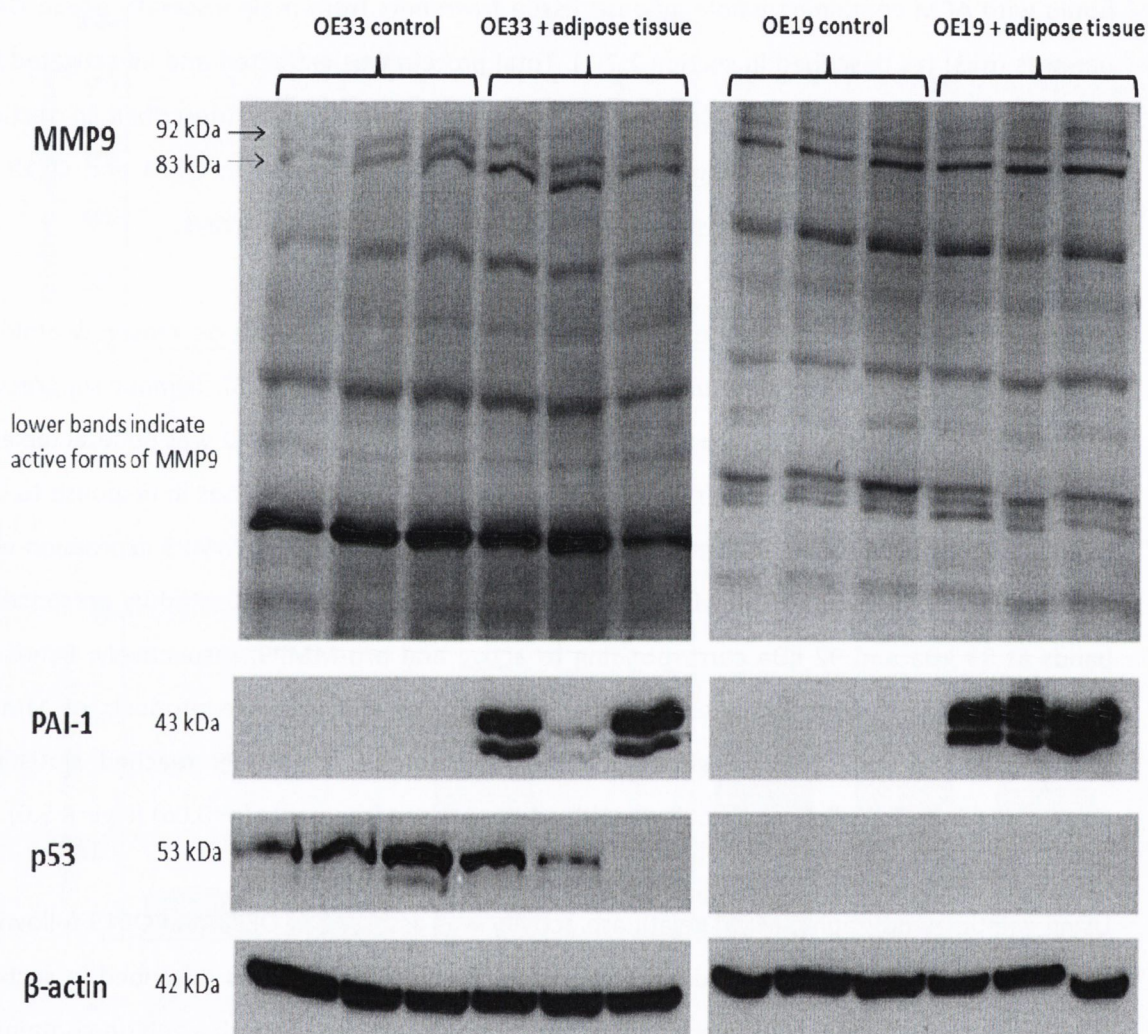
Figure 5.5: MMP9, PAI-1 and p53 expression in protein isolated from OE33 and OE19 following 24 hour co-culture with whole adipose tissue fragments (n=3) and control medium (n=3). All blots were stripped and re-probed for β-actin to normalise for loading differences.
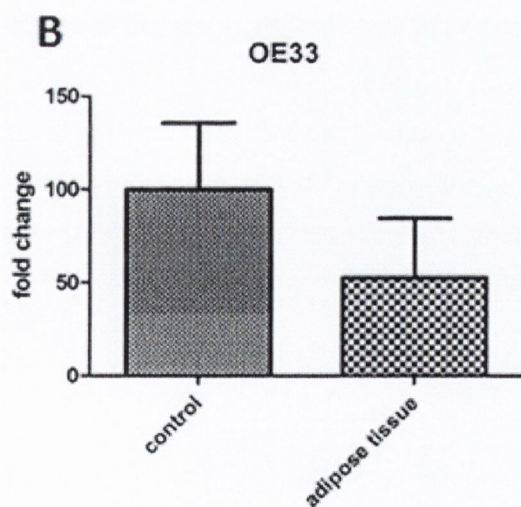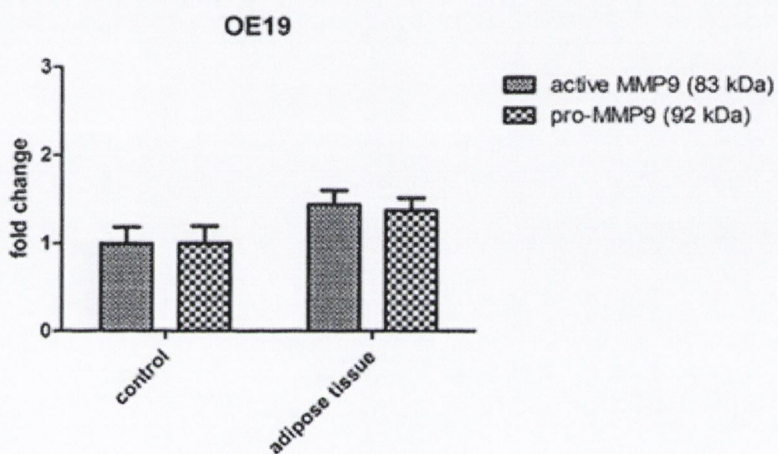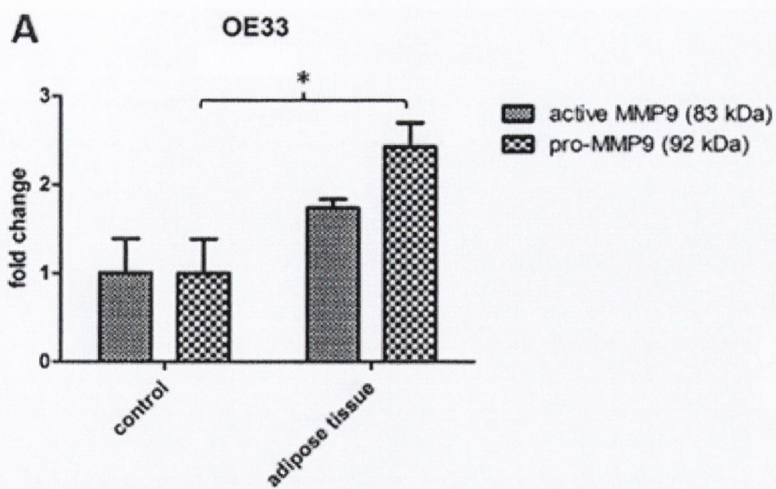
Figure 5.6: Densitometric analysis of MMP9 (A) and p53 (B) expression in protein isolated from OE33 and OE19 oesophageal adenocarcinoma cell lines following 24 hour co-culture with omental adipose tissue (n=3) and control medium (n=3). Data are expressed as mean ± SEM. Statistical analysis was performed using a paired student's t-test (*p<0.05).
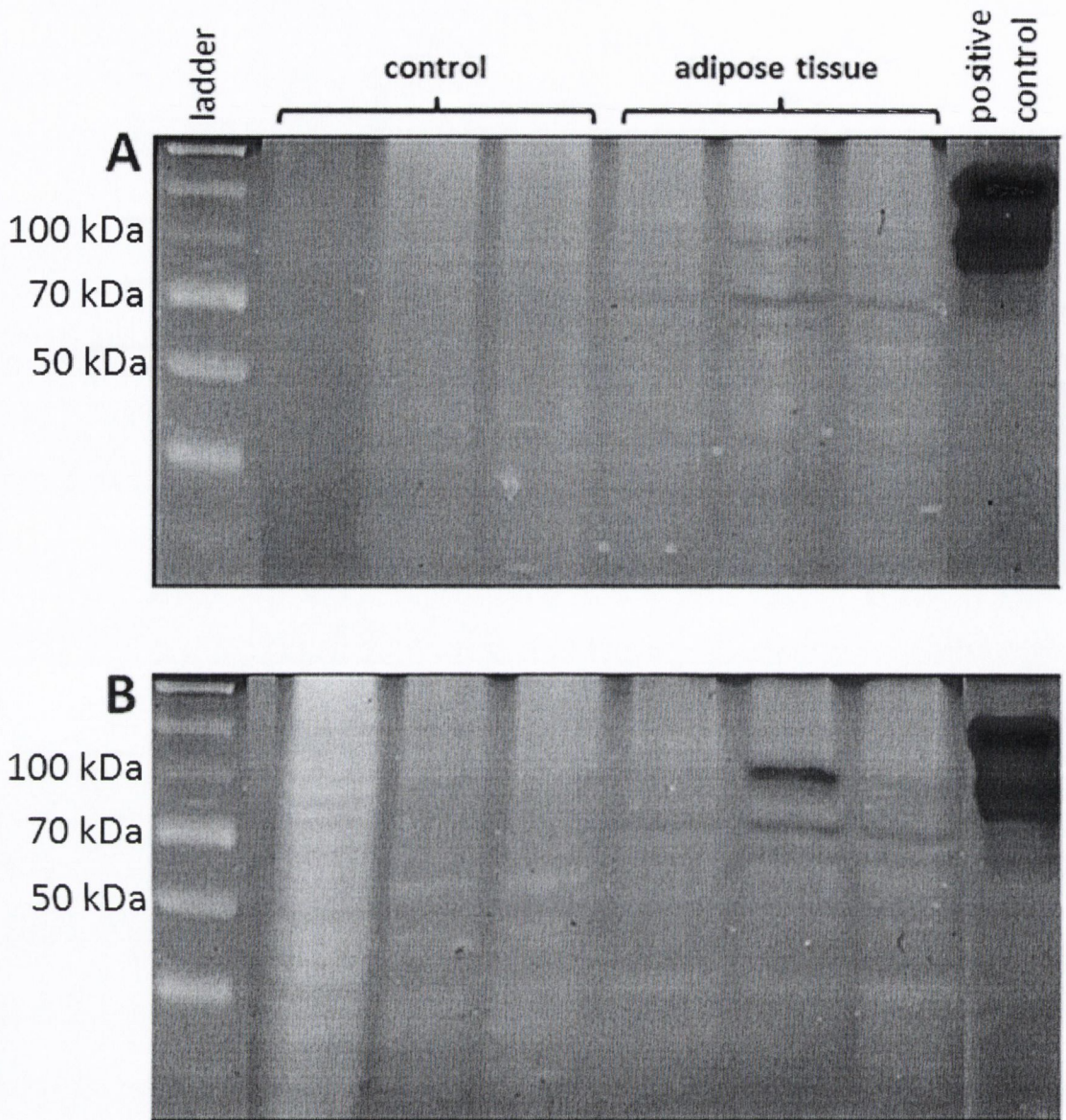
Figure 5.7: Matrix metalloproteinase activity in OE33 (A) and OE19 (B) oesophageal adenocarcinoma following 24 hour co-culture with adipose tissue (n=3) and control medium (n=3). Pre-stained protein ladder was used to determine band size and collagenase F was loaded as a positive zymography control (far right lane). Dark bands, present in the positive control and adipose tissue treated samples, represent areas of gelatinase activity, visualised by Coomassie blue staining.

5.3.2.3   Omental adipose tissue increases the migratory and invasive capacity of oesophageal adenocarcinoma.

Following validation of array results at both the mRNA and protein level, the effect of alterations of identified candidate genes on cell function was examined. Migratory and invasive capacity was examined by measuring the capacity of OE33 to move out of a porous chamber (coated with extracellular matrix (ECM) in the case of the invasion assay) into a reservoir containing ACM from viscerally obese (n=15) and non obese (n=14) OAD patients (as described in section 2.17 and 2.18).

Following 24 hour culture, ACM from viscerally obese and non obese patients increased the migratory capacity of oesophageal adenocarcinoma by 120% and 63%, respectively, while ACM from viscerally obese and non obese patients increased the invasive capacity by 54% and 70%, respectively, relative to control medium (Figure 5.8). Only ACM from viscerally obese OAD patients induced a significant increase ($p<0.0001$) in OE33 migration while ACM from both viscerally obese and non obese OAD patients induced significant increases ($p<0.05$) in OE33 invasion.

These findings demonstrate that visceral adipose tissue, particularly from viscerally obese patients; can increase the migratory capacity of OAD. These data thereby identify a potential biological mechanism responsible for the association of visceral obesity and OAD, contributing to the aggressive nature of this disease (Beddy et al., 2010; Lagarde et al., 2007). The Human Cancer Profiler array, although limited in size to 84 genes, provides a preliminary indication of pro-tumour pathways altered in response to treatment with adipose tissue. In light of these promising initial results, the study was expanded using Affymetrix microarray technology.
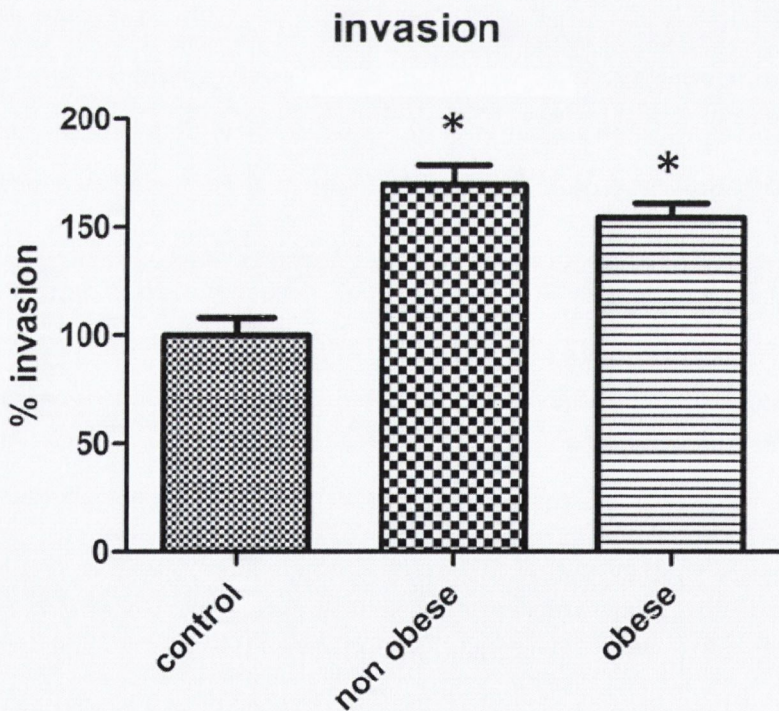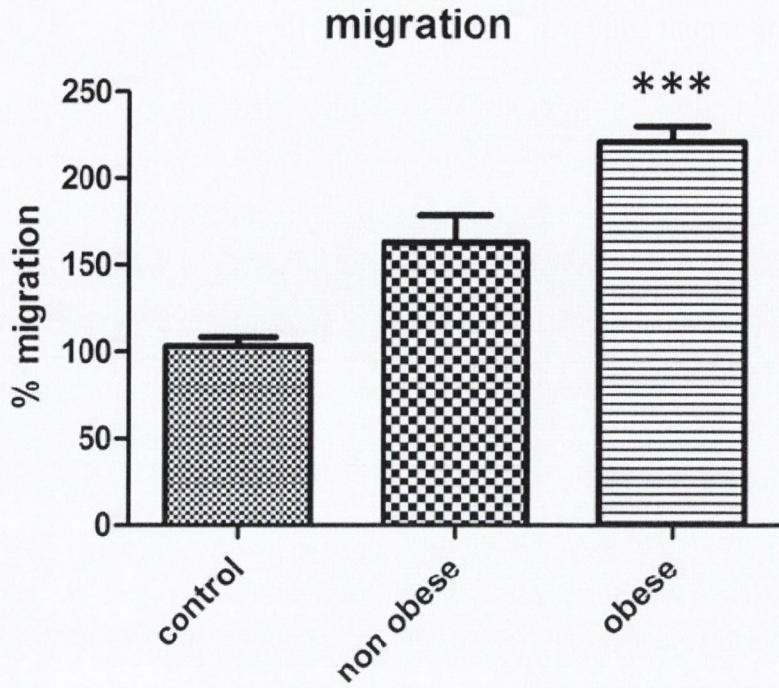
Figure 5.8: Culture with adipose tissue conditioned medium (ACM) resulted in increased migratory and invasive capacity of OE33. OE33 oesophageal adenocarcinoma was treated with ACM from viscerally obese (n=15) and non obese (n=14) OAD patients for 24 hours and the number of cells which migrated/invaded through the membrane was assessed colorimetrically. Data are expressed as mean ± SEM. Statistical analysis was performed using a paired student's t-test (#p<0.0001, *p<0.05).

5.3.3 Omental adipose tissue increases the aggressive phenotype of oesophageal adenocarcinoma via up regulation of glycolysis, focal adhesion and epithelial mesenchymal transition pathways.

Based on the findings of the Human Cancer Profiler arrays, the study was expanded and the effect of co-culture of omental adipose tissue and adipocytes from viscerally obese male OAD patients (n=6) on OE33 was investigated using the Affymetrix Human Genome U133 Plus 2.0 Array. This array is one of the most comprehensive to date, covering approximately two thirds of the human genome (www.affymetrix.com) and the arrays used in this project were custom-designed by the European Nutrigenomics Organisation (NuGO) to include a number of nutrition and obesity related genes. RNA was extracted from OE33 following co-culture with adipose tissue, adipocytes and control medium, assessed for purity and integrity, and run on Affymetrix arrays with Service XS (Leiden, The Netherlands) (as described in sections 2.6.1, 2.6.4, 2.6.5, 2.6.12). Data were analysed in collaboration with bioinformatician Ms. Melissa Morine (Prof. Helen Roche, Nutrigenomics Research Group, Conway Institute, UCD) using predefined scripts and flexible programming with the R software environment for statistical computing (described in section 2.6.12.2).

5.3.3.1 Affymetrix array quality control

It is imperative to the success of a microarray experiment that sufficient quality control checks are carried out after each stage of the sample isolation, sample hybridisation and array analysis process. All RNA samples processed on Affymetrix microarrays had an RNA integrity number (RIN) > 9 and a 260/280 purity ratio > 1.65 (Bioanalyser and Nanodrop results listed in Appendix V). These quality control parameters were investigated on site before sending samples to Service XS (as described in section 2.6.4 and 2.6.5), and again by Service XS upon receipt of the samples. Comprehensive quality control of Affymetrix data were subsequently carried out using the R software environment (as described in section 2.6.12.1) (results listed in Appendix V). All arrays passed these quality control tests and all samples were therefore included in bioinformatic analysis.

5.3.3.2 Analysis of Affymetrix microarray data.

Of the total number of transcripts tested on the array, 50-55% of transcripts were detectable in OE33 following co-culture with adipose tissue and adipocytes. Clustering heat map analysis showed that OE33 co-cultured with whole adipose tissue (1-6_w) clustered together. OE33 co-cultured with adipocytes (1-6_a) and OE33 cultured with control medium (7-10_c) clustered together, suggesting little difference in transcript expression between these two groups

(Figure 5.9). This finding further confirms the hypothesis that secreted factors from adipose tissue SVF play a more important role alteration of gene expression in tumour cells than the adipocytes themselves.

Levels of individual transcripts significantly altered between groups were selected using LIMMA (linear models in microarray) from the R library of functions, with p values adjusted for multiple testing (adj p) (as described in section 2.6.12.2). Gene set enrichment analysis (GSEA) was used to discover altered pathways in response to culture with adipose tissue (Figure 5.10) (as described in section 2.6.12.2). The top five altered pathways, ranked by the number of gene changes (adj p<0.1), were selected for further investigation; these were glycolysis, cytokine signalling, JAK-STAT signalling, focal adhesion and cell junction pathways (Table 5.5). The Kyoto Encyclopaedia of Genes and Genomes (KEGG) database was used to visualise individual transcript alterations within selected biological pathways (Figures 5.11 – 5.13). Ten transcripts were selected from these pathways for subsequent validations at mRNA and protein level. Overall pathway alterations were subsequently examined using functional assays.
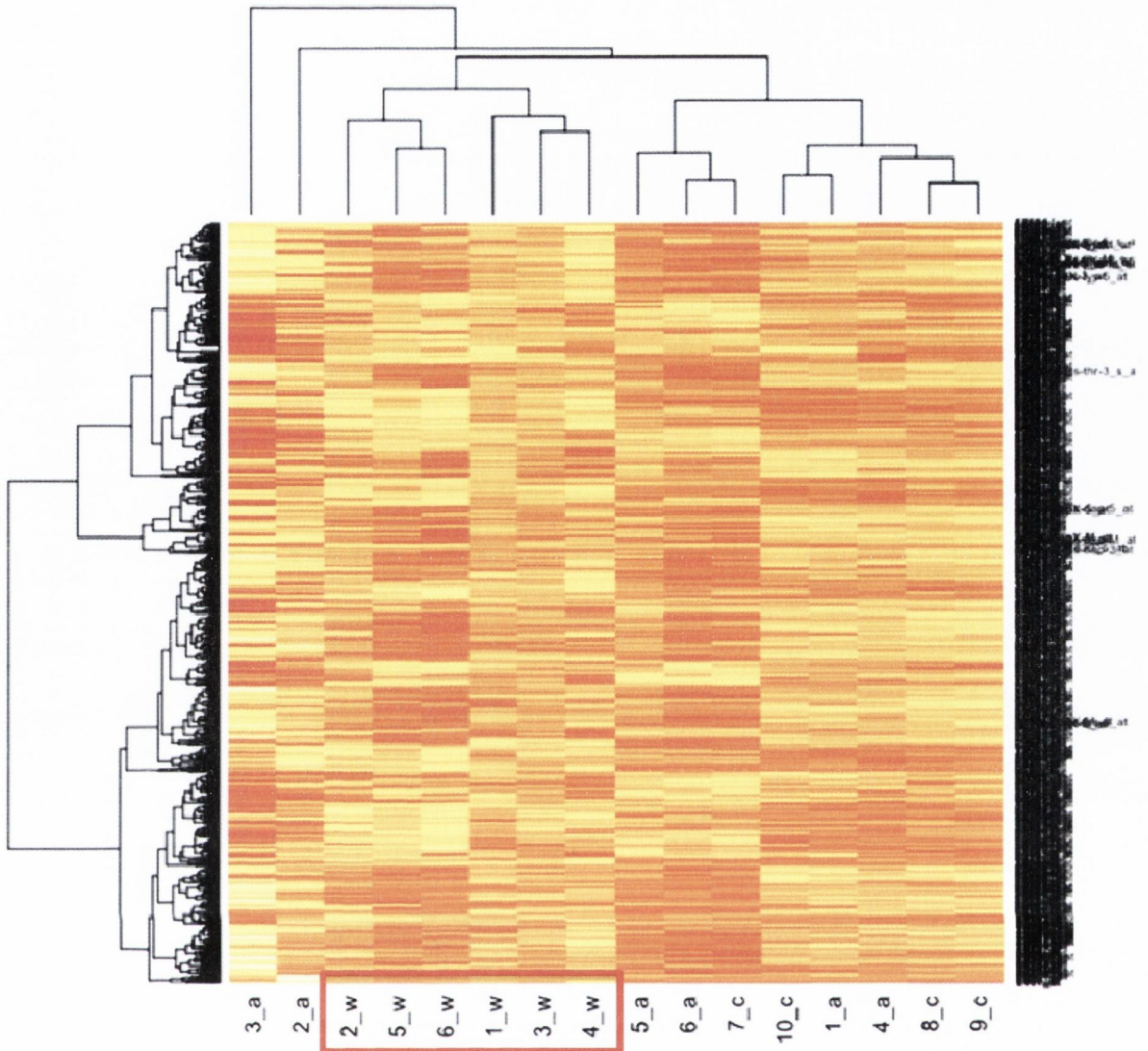
Figure 5.9: Clustering heat map of genes in the highest 5% of variance. Labels show patient numbers and treatment (w=whole adipose tissue, a=adipocytes, c=control medium). OE33 samples following co-culture with whole adipose tissue cluster together while OE33 samples following co-culture with adipocytes and control medium cluster together.
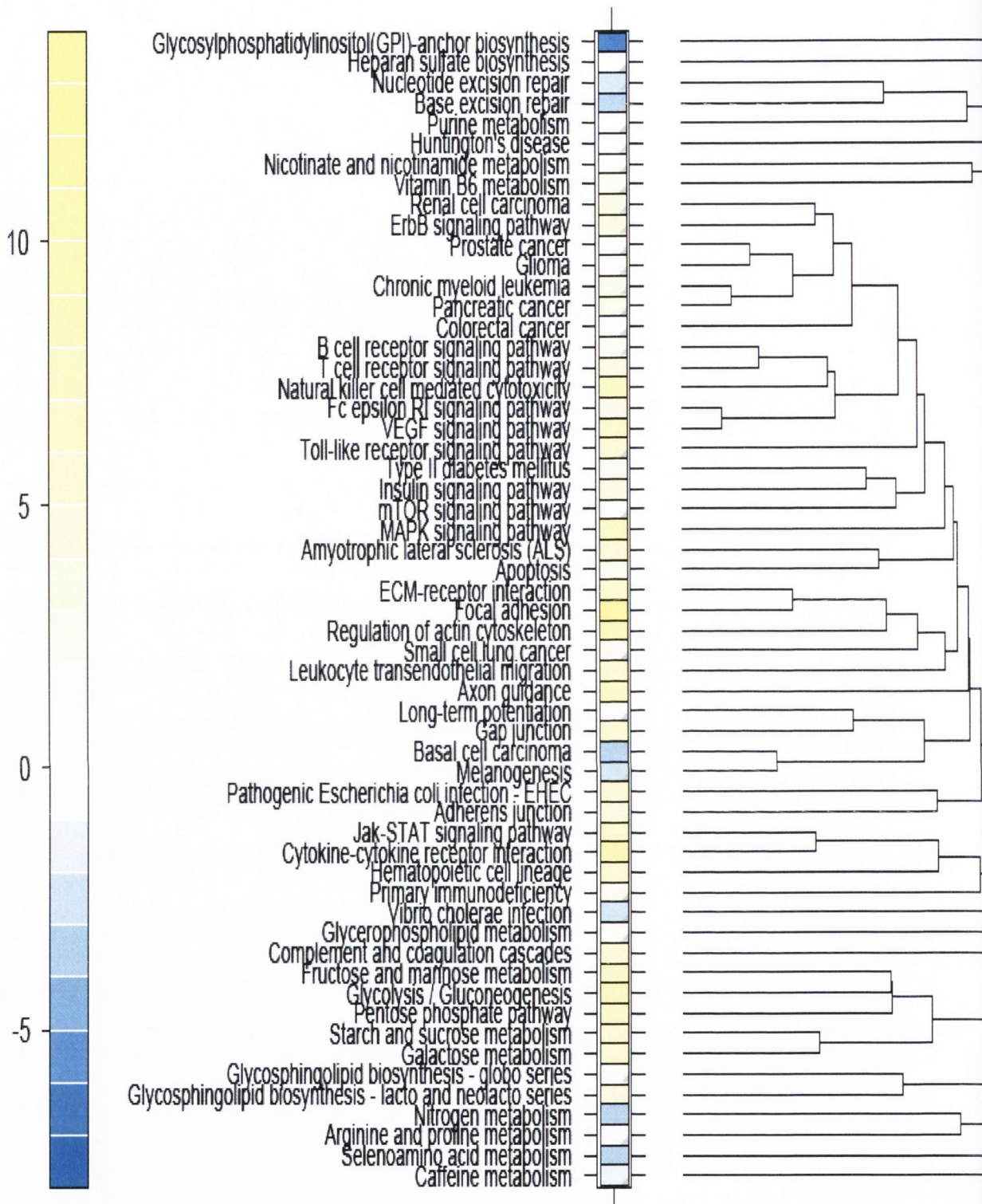
Figure 5.10: Pathway alterations (KEGG) in OE33 following co-culture with adipose tissue fragments. Filled boxes represent unidirectional pathway alterations while partly filled boxes represent bidirectional enrichment. Yellow boxes represent up regulated pathways while blue boxes represent down regulated pathways.

Table 5.5: Pathway alterations in OE33 following co-culture with omental adipose tissue from viscerally obese OAD patients (n=6) identified by GSEA analysis.

Pathway	Raw t value	No. gene changes	No. gene changes (adj.p<0.1)
Glycolysis / Gluconeogenesis	7.9	50	9
Cytokine-cytokine receptor interaction	10.0	196	8
Jak-STAT signaling pathway	6.8	107	6
Focal adhesion	12.3	153	6
Cell junctions	6.8	104	6
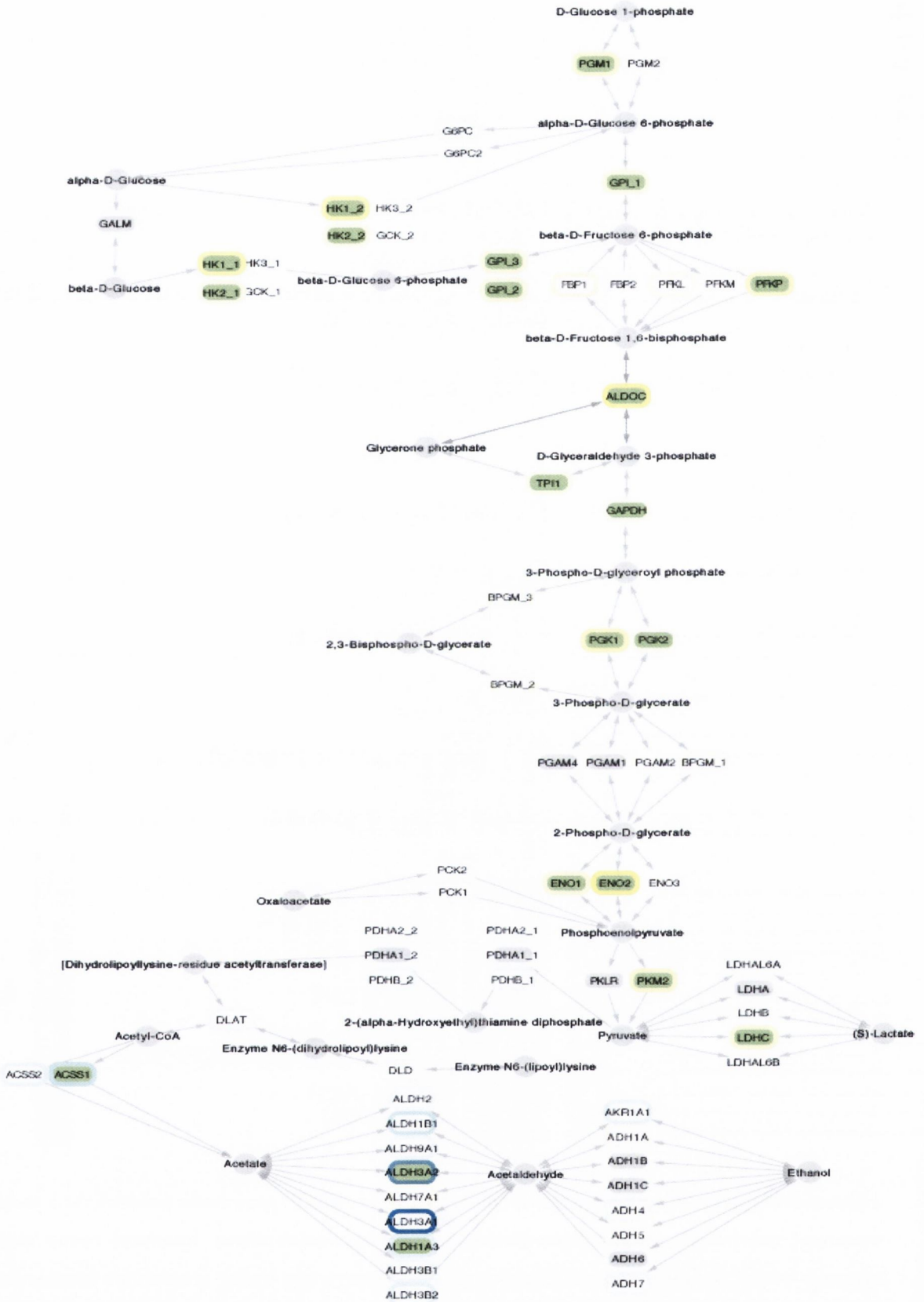
Figure 5.11: Glycolysis pathway adapted from KEGG by Melissa Morine. Blue borders represent down regulated genes, while yellow borders represent up regulated genes. Intensity of blue/yellow shading represents the degree of transcript fold change. Filled nodes represent a significant alteration (p<0.05). Grey nodes represent transcripts either not detected or removed by the variance filter.
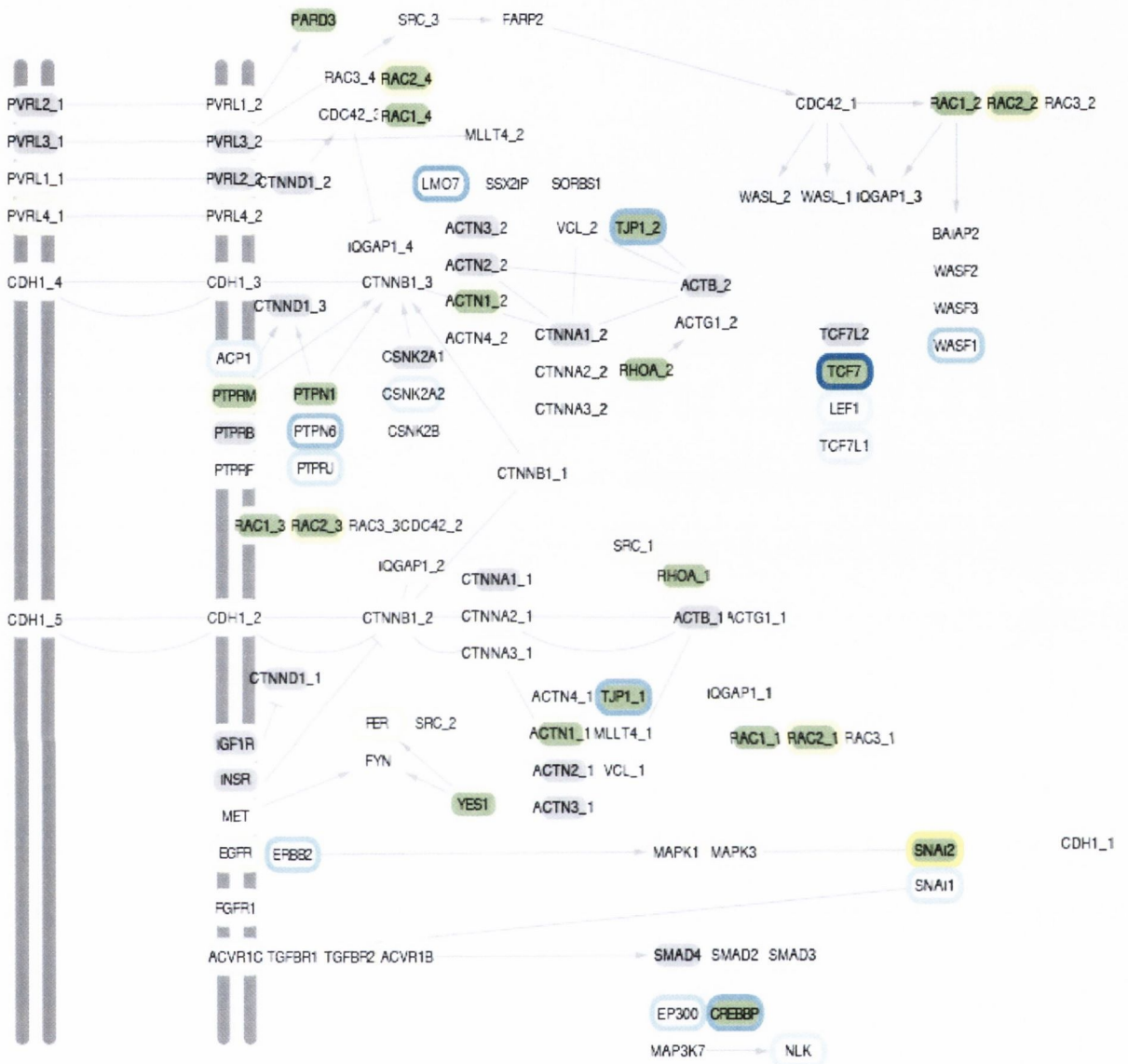
Figure 5.12: Adherens junction pathway adapted from KEGG by Melissa Morine. Blue borders represent down regulated genes, while yellow borders represent up regulated genes. Intensity of blue/yellow shading represents the degree of transcript fold change. Filled nodes represent a significant alteration (p<0.05). Grey nodes represent transcripts either not detected or removed by the variance filter.
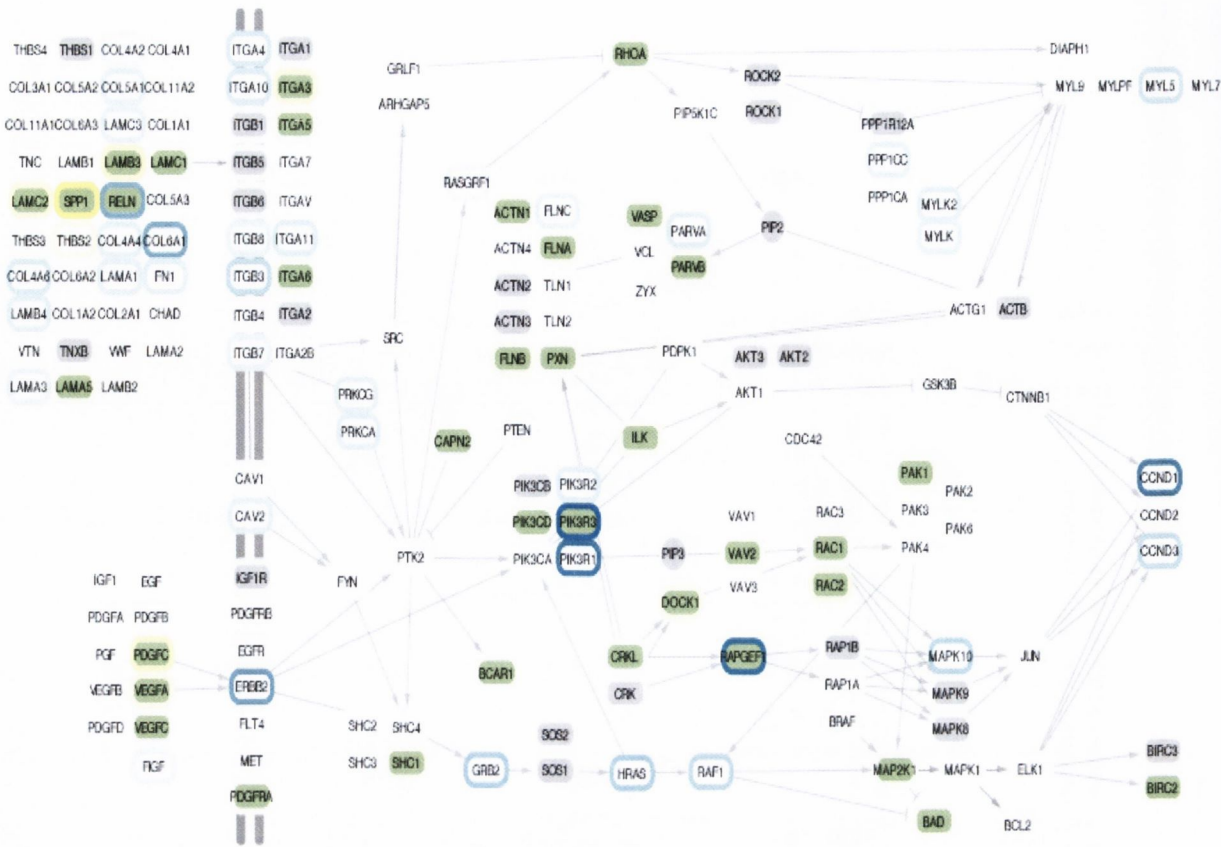
Figure 5.13: Focal adhesion pathway adapted from KEGG by Melissa Morine. Blue borders represent down regulated genes, while yellow borders represent up regulated genes. Intensity of blue/yellow shading represents the degree of transcript fold change. Filled nodes represent a significant alteration (p<0.05). Grey nodes represent transcripts either not detected or removed by the variance filter.

5.3.4   Comparison of Human Cancer Profiler and Affymetrix array results

Although the patients differed, the experimental setup was identical between Human Cancer Profiler and Affymetrix arrays and therefore the genes and pathways identified by these two different array platforms were compared. The Human Cancer Profiler measured 84 genes involved in six pathways of tumourigenesis while the Affymetrix array measured gene alterations across two thirds of the human genome. Therefore the majority of genes tested on the Affymetrix array were not tested on the Human Cancer Profiler array. In addition, as the Affymetrix array investigates expression of thousands of genes and so the statistical adjustments for multiple testing are far more stringent. The Human Cancer Profiler array is therefore more sensitive to subtle yet significant gene alterations. The Human Cancer Profiler qPCR arrays were validated by the Affymetrix microarrays, with down regulation of tumour suppressors p53 and ATM and up regulation of PAI-1 found in both arrays (Table 5.6). Although significant alterations in MMP expression were not observed using Affymetrix microarray, this high throughput technology may not be sensitive enough to pick out subtle changes in gene expression. SerpinE1 (PAI-1), unchanged following culture of OE33 with SGBS, but up regulated in OE33 by omental adipose tissue, was identified by both the Human Cancer Profiler array and the Affymetrix microarray, although this change did not quite reach significance by Affymetrix (adj $p<0.07$). Serine proteases serpinA3, serpinB6, serpinB9, serpinE2 were also up regulated according to the Affymetrix microarray, however these targets were not measured by the Human Cancer Profiler Array (Table 5.6).

Table 5.6: Summary of Human Cancer Profiler qPCR array and Affymetrix microarray results.

Gene	Cancer pathway array SGBS	Cancer pathway array omentum	Affymetrix microarray omentum
ATM	Down regulated	Down regulated	Down regulated
P53	No change	Down regulated	Down regulated
MMP2	Up regulated	Up regulated	No change
MMP9	No change	Up regulated	No change
PAI-1	No change	Up regulated	Up regulated

5.3.4.1 Validation of Affymetrix microarrays

Based on the results of the Human Cancer Profiler arrays and the highest ranked pathways identified by Affymetrix microarrays, ten candidate genes from pathways involved in cytokine signalling and tumour adhesion, invasion, migration and metastasis were selected for validation by qPCR in OE33 following co-culture with adipose tissue and adipocytes from OAD patients (as described in section 2.6.9.2). These gene targets were used to carry out a technical validation of the arrays in the identical cohort of samples (n=6), in addition to a biological validation of the array results in a separate cohort of samples (n=14).

The genes chosen for validation were integrin alpha 3 (ITGA3), laminin gamma 2 (LAMC2), laminin beta 3 (LAMB3), secreted phosphoprotein 1 (SPP1), semaphorin 4B (SEMA4B), S100 calcium binding protein A8 (S100A8), chemokine (CXC motif) ligand 5 (CXCL5), pro-platelet basic protein (CXCL7) (PPBP), snail homologue 2 (SNAI2) and CTD (carboxy-terminal domain, RNA polymerase II, polypeptide A) small phosphatase-like (CTDSPL).

Candidate gene expression measured by qPCR in the same cohort of samples technically validated the microarray. Expression of ITGA3 was up regulated by 2.5 fold (p<0.02), LAMC2 by two fold (p<0.03), LAMB3 by 2.7 fold (p<0.1), SPP1 by 40 fold (p<0.03), SEMA4B by 2.7 fold (p<0.009), S100A8 by 60 fold (p<0.07), CXCL5 by 500 fold (p<0.01), PPBP by 30 fold (p<0.07), SNAI2 by two fold (p<0.04) and CTDSPL down regulated by two fold (p<0.004) in OE33 in response to culture with whole adipose tissue (Figure 5.14). No significant alterations in gene expression were observed following co-culture with adipocytes, as observed following both Human Cancer Profiler and Affymetrix arrays.

The validation in the independent sample cohort (n=14) showed ITGA3 to be up regulated by over three fold (p<0.0004), LAMC2 by over two fold (p<0.04), LAMB3 by over five fold (p<0.002), SPP1 by almost 2000 fold (p<0.004), SEMA4B by 3.7 fold (p<0.005), S100A8 by over 1000 fold (p<0.3), CXCL5 by over 10,000 fold (p<0.09), PPBP by almost 1000 fold (p<0.08), SNAI2 by over seven fold (p<0.004) and CTDSPL down regulated by two fold (p<0.01) in OE33 in response to culture with whole adipose tissue (Figure 5.15). No significant alterations in gene expression were observed following co-culture with adipocytes. Expression of all ten transcripts was found to be altered in the same direction as found in the arrays; however expression changes of CXCL5, PPBP and S100A8 did not reach statistical significance and were therefore dropped from the list of candidates for further investigation.

Gene expression of SNAI2 was significantly up regulated in OE33 following co-culture with adipose tissue (p<0.0004). SNAI2 acts via transcriptional repression of E-cadherin to induce epithelial mesenchymal transition (EMT), playing a key role in tumour migration and invasion (Alves et al., 2009). However, there was no change in E-cadherin expression in OE33 following co-culture with adipose tissue (n=10) (Figure 5.16), and so it is possible that SNAI2 is not functionally active in this experimental model, or that it functions independently of E-cadherin.

As VEGFA levels were found to be elevated in visceral ACM and circulating levels of VEGFA were demonstrated to be raised in visceral obesity, gene expression of this pro-angiogenic cytokine was examined in OE33 following co-culture with adipose tissue. VEGFA was identified by Affymetrix array to be up regulated in OE33 following co-culture with adipose tissue, although this effect was not significant (Figure 5.13). VEGFA gene expression in OE33 increased 25 fold following co-culture with adipose tissue (n=10), however this change did not reach statistical significance (Figure 5.17).

In order to confirm the hypothesis that gene alterations were induced predominantly by factors secreted by adipose tissue SVF, OE33 and OE19 cells were cultured with ACM from viscerally obese oesophageal adenocarcinoma patients (n=10)(as described in section 2.3.7), and gene expression alterations were measured by qPCR (as described in section 2.6.9). Expression of LAMC2 was increased 3 fold in both OE33 (p<0.01) and OE19, expression of SNAI2 was increased 11 fold in OE33 (p<0.01) and 5 fold in OE19 and expression of CTDSPL was decreased twofold in both OE33 and OE19 (p<0.0001) (Figure 5.18). Co-culture with ACM and co-culture with whole adipose tissue therefore induced comparable gene expression changes, confirming that factors secreted by SVF are responsible for gene alterations in OAD. ACM co-culture was subsequently used to carry out functional validations of the Affymetrix microarray results.
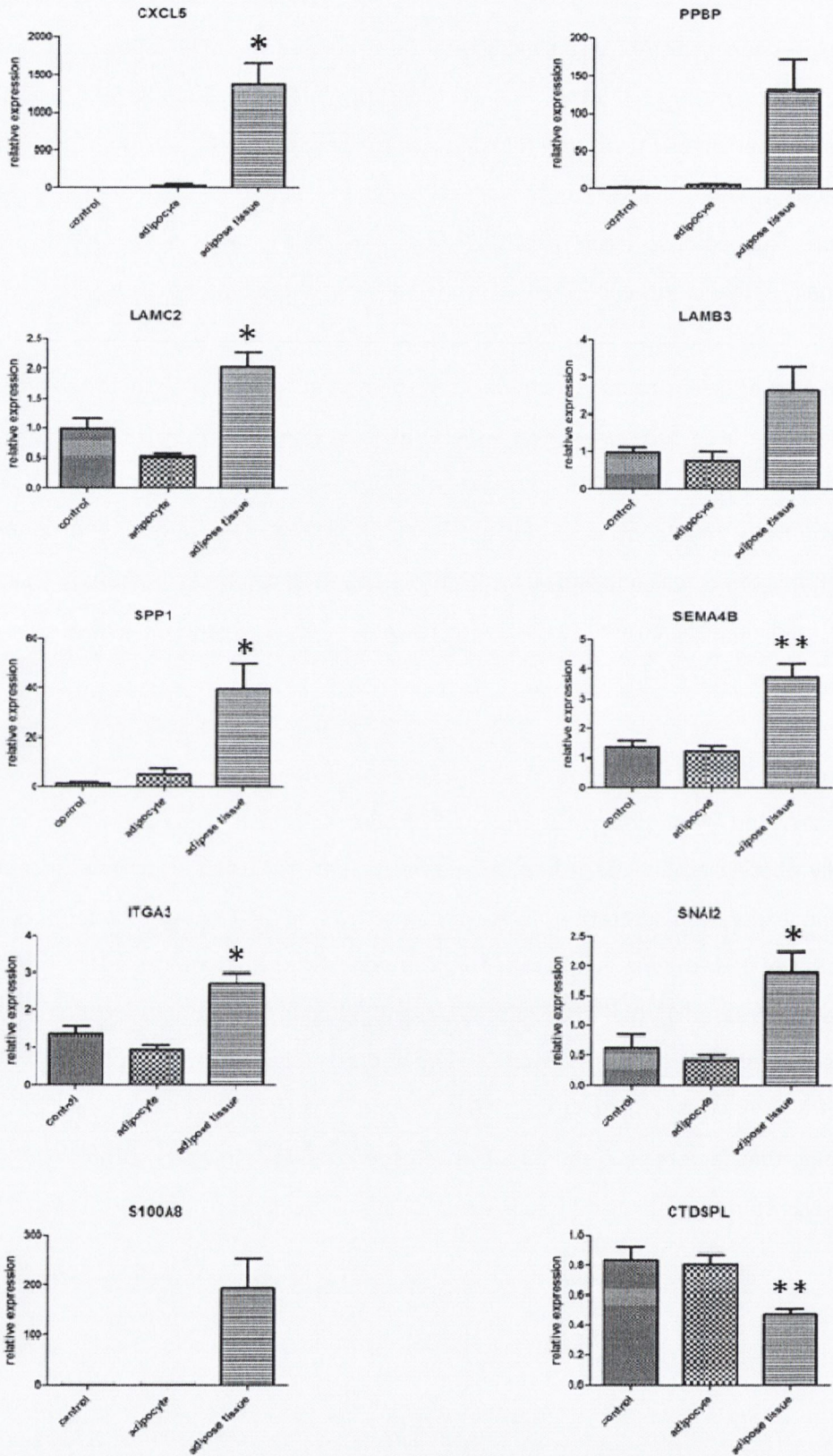
Figure 5.14: Technical validations of Affymetrix microarrays (n=6) carried out by quantitative qPCR. Data are expressed as mean ± SEM. Statistical analysis was performed using a paired student's t-test (#p<0.001, **p<0.01, *p<0.05).

180
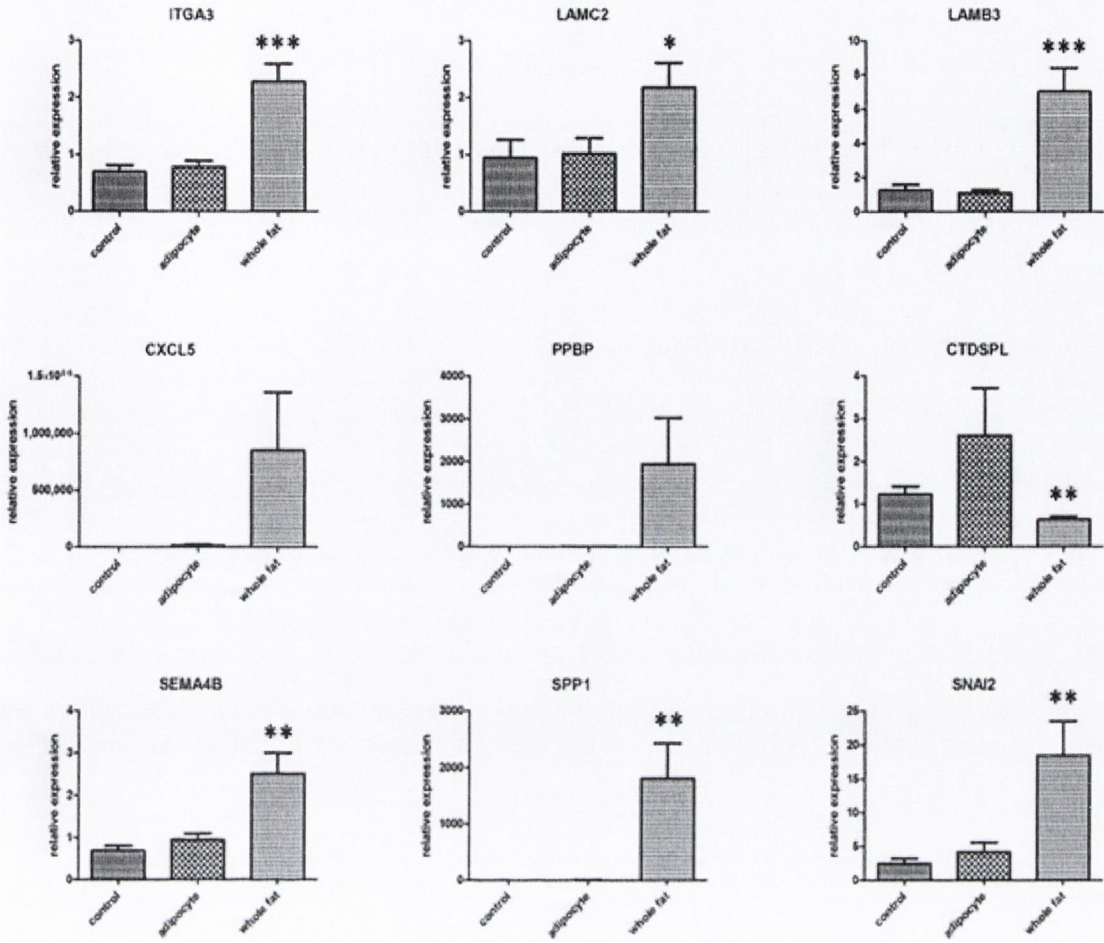
Figure 5.15: Validations of Affymetrix microarrays in a separate cohort (n=14) carried out by quantitative qPCR. Data are expressed as mean ± SEM. Statistical analysis was performed using a paired student's t-test (***p<0.0001, **p<0.001, *p<0.05).
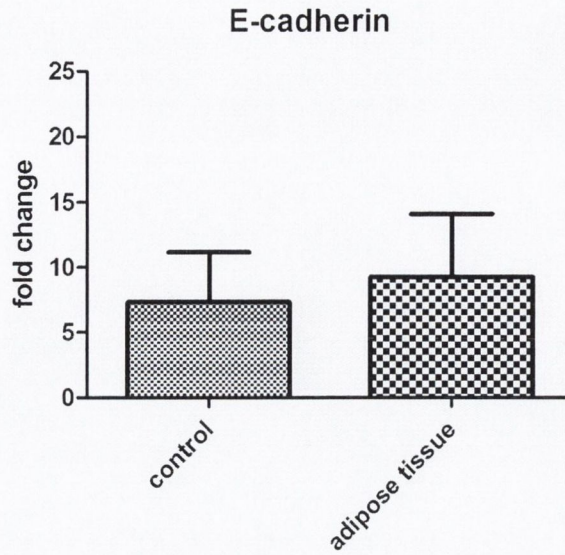
E-cadherin

Figure 5.16: E-cadherin expression in OE33 oesophageal adenocarcinoma following co-culture with adipose tissue fragments (n=10). Data are expressed as mean ± SEM. Statistical analysis was performed using a paired student's t-test.
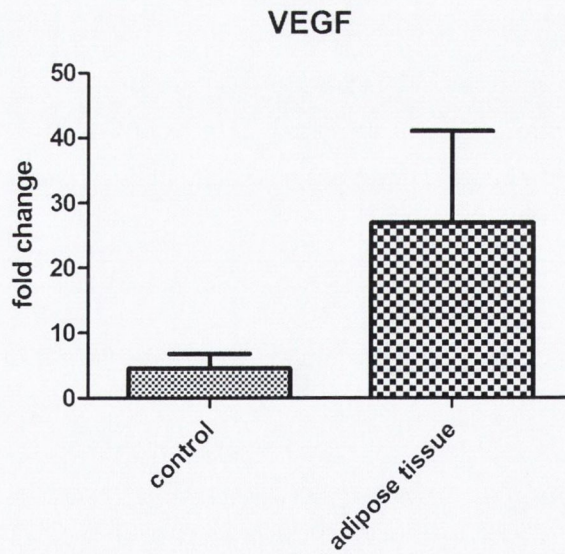
VEGF

Figure 5.17: VEGF expression in OE33 oesophageal adenocarcinoma following co-culture with adipose tissue fragments (n=10). Data are expressed as mean ± SEM. Statistical analysis was performed using a paired student's t-test.
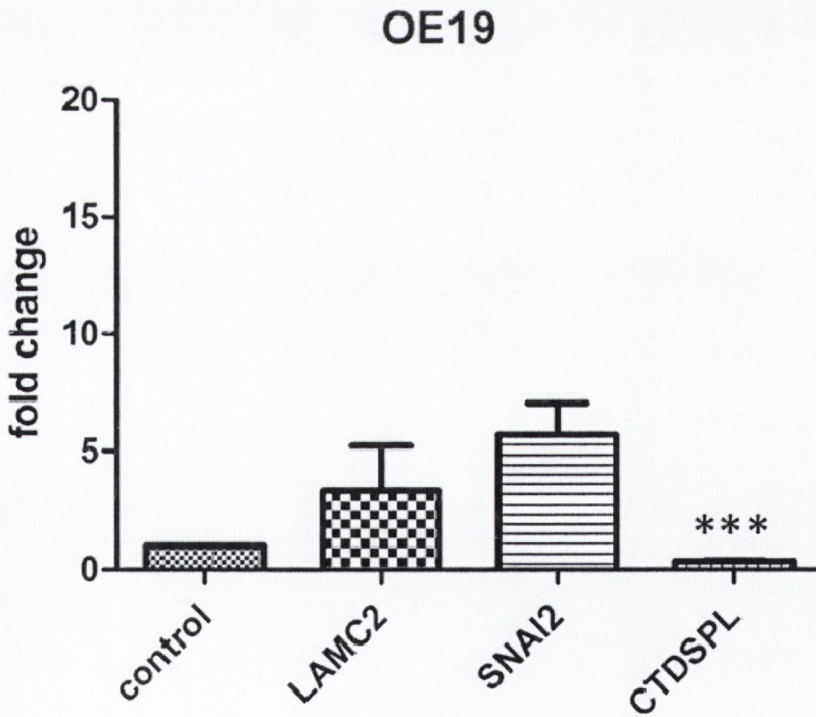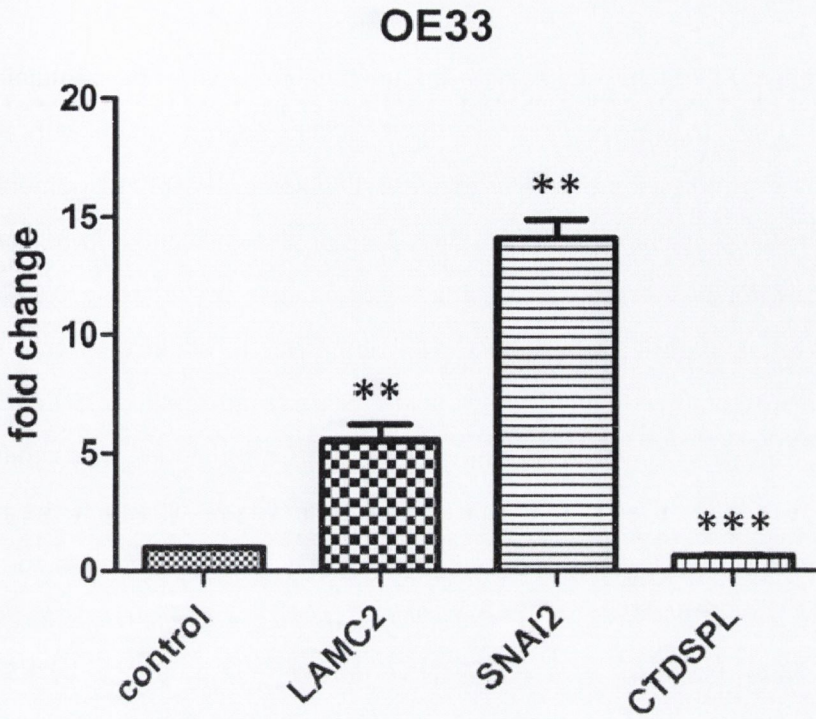
Figure 5.18: Validations of Affymetrix microarrays in OE33 and OE19 oesophageal adenocarcinoma following 24 hour treatment with ACM from viscerally obese patients (n=10) carried out by quantitative qPCR. Data are expressed as mean ± SEM. Statistical analysis was performed using a paired student's t-test (*p<0.0001, **p<0.001, *p<0.05).**

5.3.4.2 Omental adipose tissue increases rate of glycolysis in oesophageal adenocarcinoma.

Glycolysis was identified to be the highest ranked up regulated pathway, containing the greatest number of altered individual transcripts in OE33 following co-culture with adipose tissue. Members of the glycolysis pathway hexokinase 1, glucose phosphate isomerase, 6-phosphofructo-2-kinase and phosphoglycerate kinase 1 were all significantly up regulated in oesophageal adenocarcinoma in response to culture with adipose tissue (adj $p<0.05$), while fructose bisphosphate aldolase C, triosephosphate isomerise 1, enolase 2 and lactate dehydrogenase C were all near significantly up regulated (adj $p<0.1$). SLCA16A3, a monocarboxylic acid transporter involved in exporting lactate from the cell, was significantly up regulated (adj $p<0.05$). To investigate adipose tissue induced alterations in the rate of glycolysis, lactate, the end metabolite of the glycolysis pathway, was quantified in co-culture supernatants (as described in section 2.13). Lactate levels were increased in OE33 in response to co-culture with adipose tissue from viscerally obese and non obese patients by 1.5 and 2 fold, respectively. This effect reached statistical significance in OE33 following co-culture with adipose tissue from viscerally obese oesophageal adenocarcinoma patients ($p<0.0001$) (Figure 5.19). This finding highlights the propensity of tumour cells to preferentially utilise the glycoysis pathway over oxidative phosphorylation. As glycolysis is a relatively inefficient pathway in terms of energy production, tumour cells are forced to compete for limited nutrients by increasing the rate of this pathway (Kelloff et al., 2005). Hyperglycaemia is a common metabolic disorder in visceral obesity (Federation, 2006) and with tumour cells primed to respond to these high circulating levels of glucose, this could be one potential mechanism whereby visceral obesity could contribute to enhanced tumour growth.
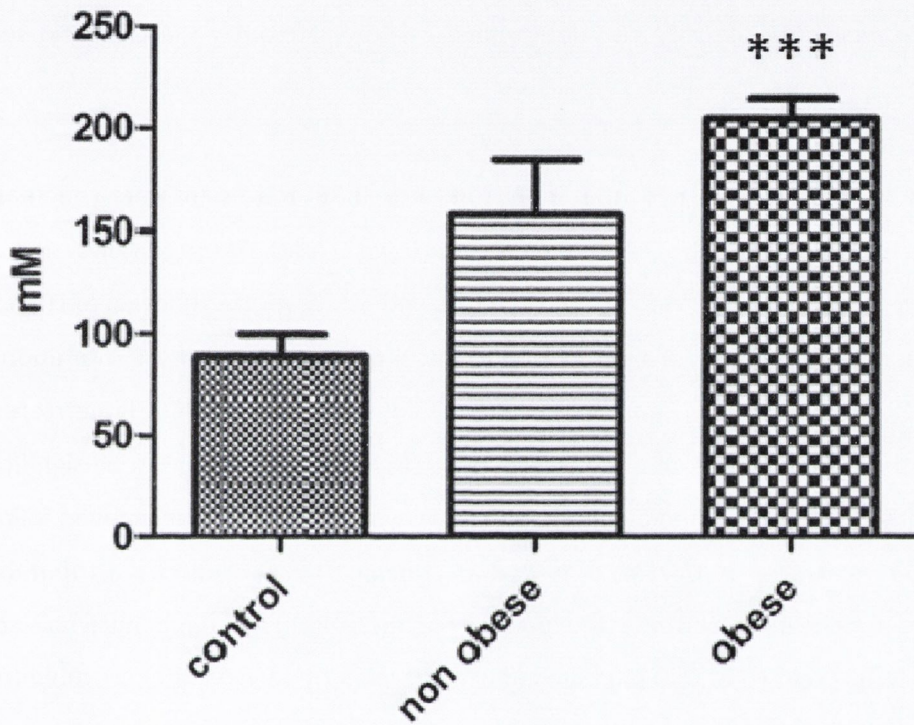
Figure 5.19: Lactate concentration in supernatant of OE33 oesophageal adenocarcinoma following 24 hour co-culture with omental adipose tissue from viscerally obese (n=15) and non obese (n=9) patients, or control medium (n=5). Data are expressed as mean ± SEM. Statistical analysis was performed using one way analysis of variance (ANOVA) with Tukey multiple comparisons post test (***p<0.0001).

5.3.4.3 Integrin mediated cell adhesion is altered in oesophageal adenocarcinoma following co-culture with adipose tissue.

Gene expression of integrin α3, α5 and α6 subunits was found to be increased in OE33 following co-culture with adipose tissue. Protein expression of integrin subunits α3, α5 and α6 (ITGA3, 5, 6) in oesophageal adenocarcinoma was investigated by flow cytometry (described in section 2.11). OE33 and OE19 were cultured for 24 and 48 hours in ACM (prepared as described in section 2.3.2), labelled with fluorescently labelled antibodies against ITGA3, A4 and A5 and fluorescence intensity was determined by flow cytometry (described in section 2.11).

In OE19 expression levels of ITGA3 ($p < 0.01$) and ITGA6 ($p < 0.05$) were significantly increased 3 and 2 fold, respectively, following 48 hour co-culture with ACM. There was no significant change in ITGA5 expression in OE19 following culture with ACM. Although levels of ITGA3 and ITGA5 were increased in OE19 following 24 hour co-culture with ACM, these alterations did not reach statistical significance (Figure 5.20). In OE33, contrary to validated Affymetrix results, protein levels of ITGA3 ($p < 0.01$), A5 ($p < 0.0001$) and A6 ($p < 0.01$) were found to be significantly down regulated following 24 hour co-culture with ACM, while levels were unchanged following 48 hour co-culture (Figure 5.20). This apparently conflicting result could be attributable to several factors. Firstly, increased mRNA expression of these integrin α subunits may not be translated to the protein level in OE33. Secondly, expression of specific integrin subunits has been demonstrated to vary according to tissue origin, tumour histology and stage of progression (Guo and Giancotti, 2004). OE33 are derived from a poorly differentiated pathological stage IIA oesophageal adenocarcinoma while OE19 are derived from a moderately differentiated stage III tumour of the oesophageal gastric junction (Pierini et al., 2008). Decreased integrin expression in OE33 highlights the inherent differences between OE33 and OE19 cell lines, derived from patients with different tumour histology and stage. Thirdly, the acquisition of a migratory phenotype in OE33 following 24 hour culture with ACM together with down regulation of ITGA3, A5 and A6 at this time point could imply an important contribution of other integrins, of which 24 exist in total (Guo and Giancotti, 2004). Together these data indicate altered expression of integrins in oesophageal adenocarcinoma following co-culture with omental adipose tissue. Increased integrin expression in OE19 could indicate a mechanism by which adipose tissue increases the migratory capacity of oesophageal adenocarcinoma.
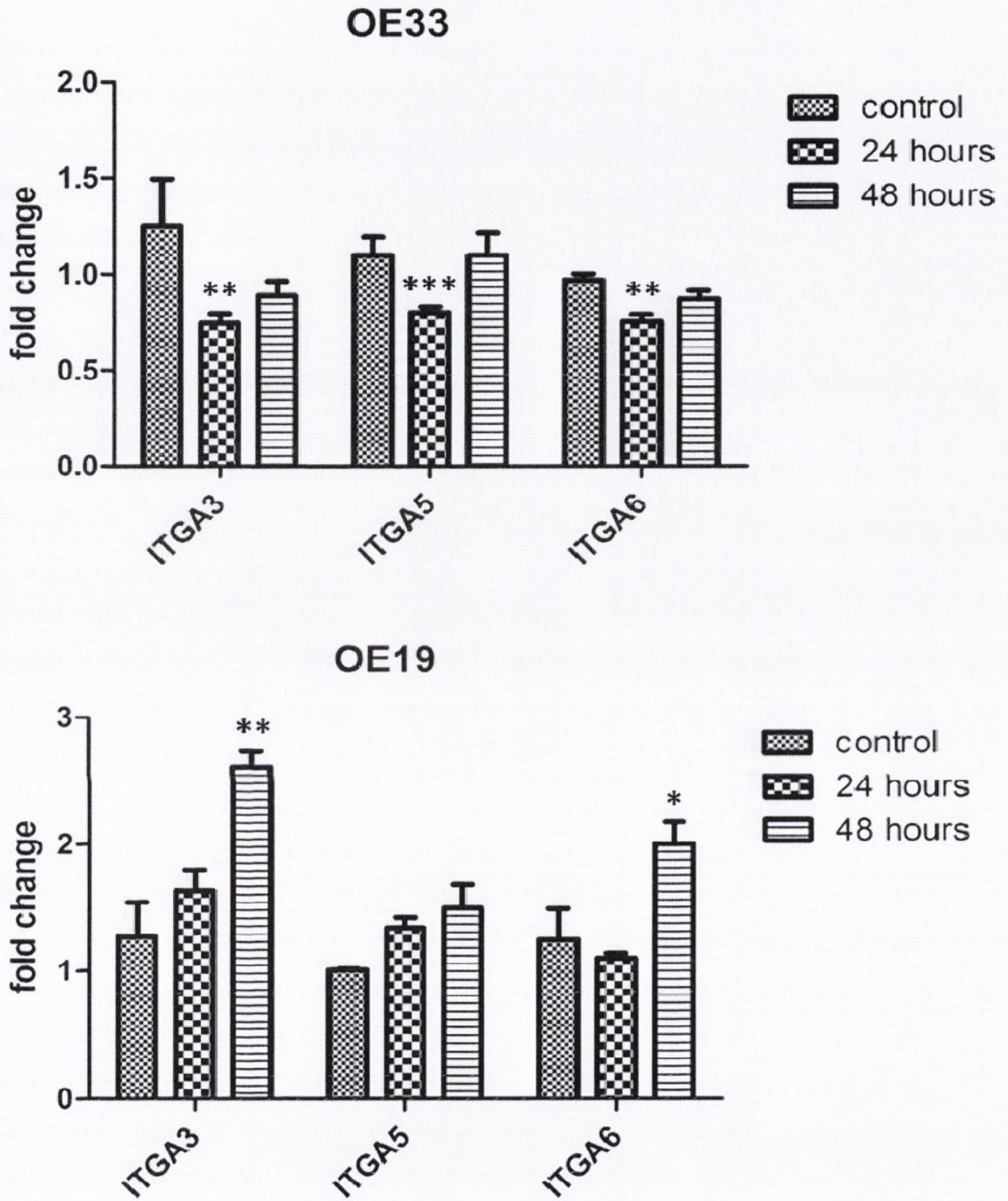
Figure 5.20: Expression of integrin subunits α3, α5 and α6 in OE33 and OE19 oesophageal adenocarcinoma following 24 and 48 hour culture with ACM (n=5). Data are expressed as mean ± SEM. Statistical analysis was performed using a paired student's t-test (***p<0.0001, **p<0.001, *p<0.05).

5.3.5 The focal adhesion pathway is altered in oesophageal adenocarcinoma in response to culture with adipose tissue.

The effect of altered integrin subunit expression on the downstream focal adhesion signalling pathway was examined. OE33 and OE19 were cultured with ACM and whole adipose tissue fragments for 24 hours, total protein was extracted and expression of subunit gamma 2 of laminin 5 (LAMC2), focal adhesion kinase (FAK) and Src were investigated by Western analysis (described in section 2.7). Expression of active phospho-paxillin (Tyr 118) and total FAK was examined by high content screening (HCS) in OE33 (as described in section 2.12).

Expression of LAMC2 was up regulated 3 fold in OE33 and almost 2 fold in OE19 ($p<0.05$) following 24 hour co-culture with adipose tissue (Figure 5.21, 5.22). FAK expression, indicated by a band at 125 kDa, was increased in OE33 ($p<0.05$) and OE19 following co-culture with adipose tissue, and levels of FAK degradation products, indicated by bands at 100 kDa and 85 kDa, were decreased more than three fold in OE33 and 2 fold in OE19 in response to culture with adipose tissue ($p<0.05$) (Figure 5.21, 5.23). Expression of FAK inhibitor FRNK, indicated by bands at 41 kDa and 43 kDa, was down regulated in response to treatment with adipose tissue ($p<0.05$). Levels of FAK binding partner, Src, were almost two fold increased in OE33 and OE19 following co-culture with adipose tissue, however this alteration did not reach statistical significance (Figure 5.21, 5.24). Although protein expression of components of the focal adhesion pathway was found to be increased in OAD following co-culture with adipose tissue, functional activity of these components depends on their localisation to focal adhesion plaques. Localisation was therefore subsequently investigated by HCS.

Examination of phospho-paxillin (Tyr 118) and FAK localisation was optimised by HCS in OE33 following 24 hour co-culture with ACM from viscerally obese OAD patients (n=3) (as described in section 2.12). Initial optimisation showed that phospho-paxillin (Tyr118) localised to points at the edges of the cell, however fluorescence intensity was too low to allow quantification of these focal adhesion plaques using HCS analysis (Figure 5.25). Although initial optimisation of focal adhesion kinase (FAK) staining also showed localisation to spots at the edge of the cytoplasm, there remained significant fluorescence intensity throughout the cytoplasm, preventing discrimination and quantification of focal adhesion plaques by HCS analysis (Figure 5.26). Time constraints prevented complete optimisation of these antibodies; however preliminary results showed localisation of phospho-paxillin and FAK to focal adhesion plaques in OE33 following treatment with ACM. The formation of focal adhesion plaques, connecting the cell cytoskeleton to the ECM, promotes cell migration (Schwock et al., 2010). This pathway

could therefore represent a mechanism by which adipose tissue increases the migratory capacity of oesophageal adenocarcinoma.
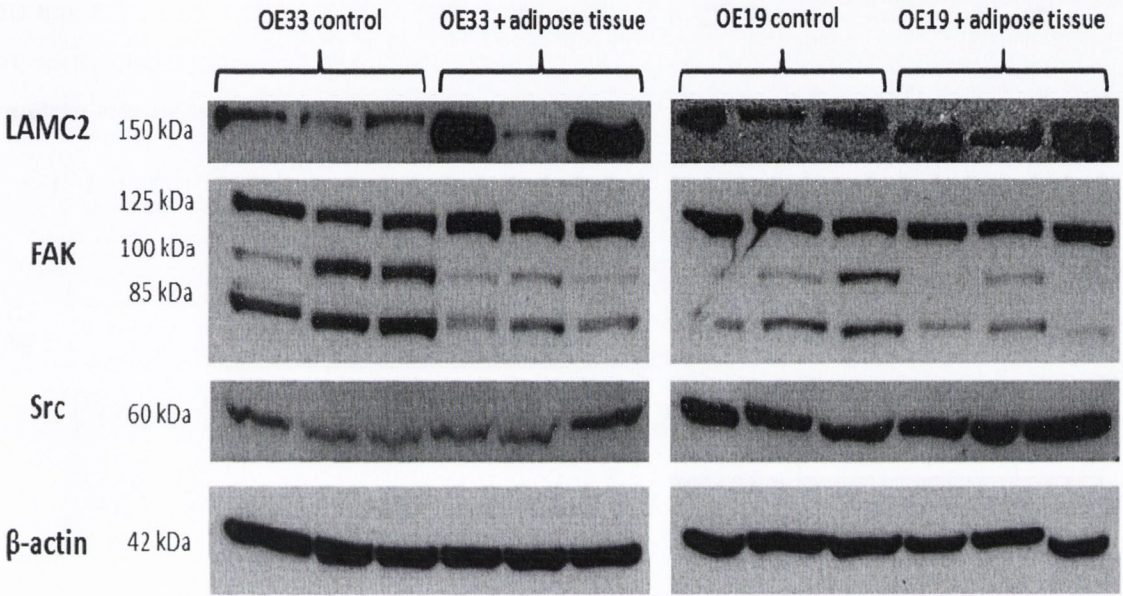
Figure 5.21: Expression of components of the focal adhesion pathway LAMC2, FAK and Src in protein isolated from OE33 and OE19 following 24 hour co-culture with whole adipose tissue fragments (n=3) and control medium (n=3). All blots were stripped and re-probed for β-actin to normalise for loading differences.

189
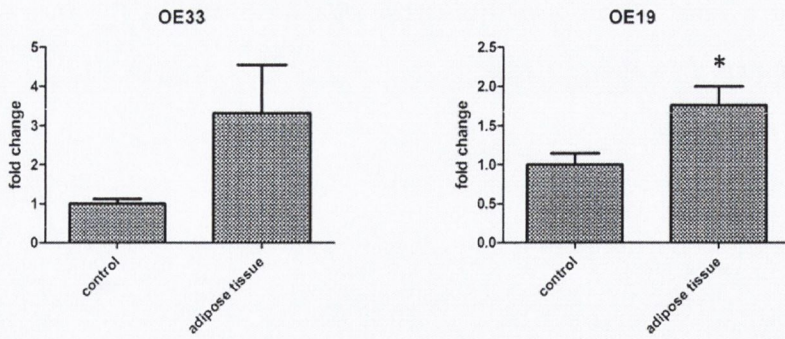
Figure 5.22: Densitometric analysis of LAMC2 expression in protein isolated from OE33 and OE19 oesophageal adenocarcinoma cell lines following 24 hour co-culture with omental adipose tissue (n=3) and control medium (n=3). Data are expressed as mean ± SEM. Statistical analysis was performed using a paired student's t-test (*p<0.05).
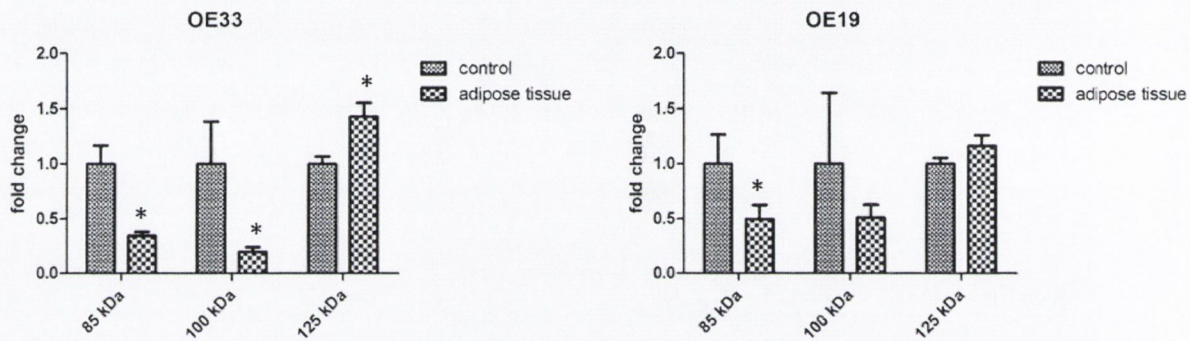
Figure 5.23: Densitometric analysis of expression of FAK (125 kDa) and FAK degradation products (100 kDa, 85 kDa) in protein isolated from OE33 and OE19 oesophageal adenocarcinoma cell lines following 24 hour co-culture with omental adipose tissue (n=3) and control medium (n=3). Data are expressed as mean ± SEM. Statistical analysis was performed using a paired student's t-test (*p<0.05).
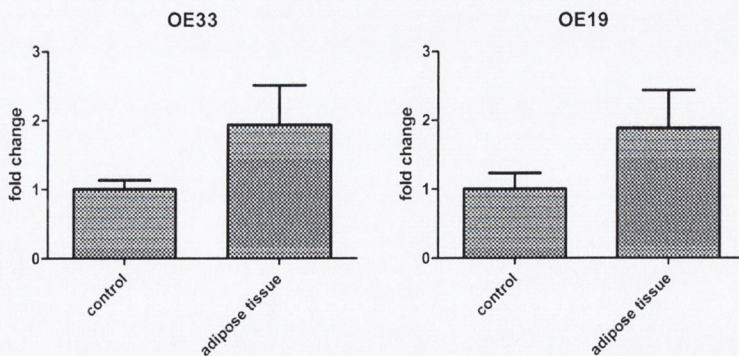
Figure 5.24: Densitometric analysis of Src expression in protein isolated from OE33 and OE19 oesophageal adenocarcinoma cell lines following 24 hour co-culture with omental adipose tissue (n=3) and control medium (n=3). Data are expressed as mean ± SEM. Statistical analysis was performed using a paired student's t-test.

190
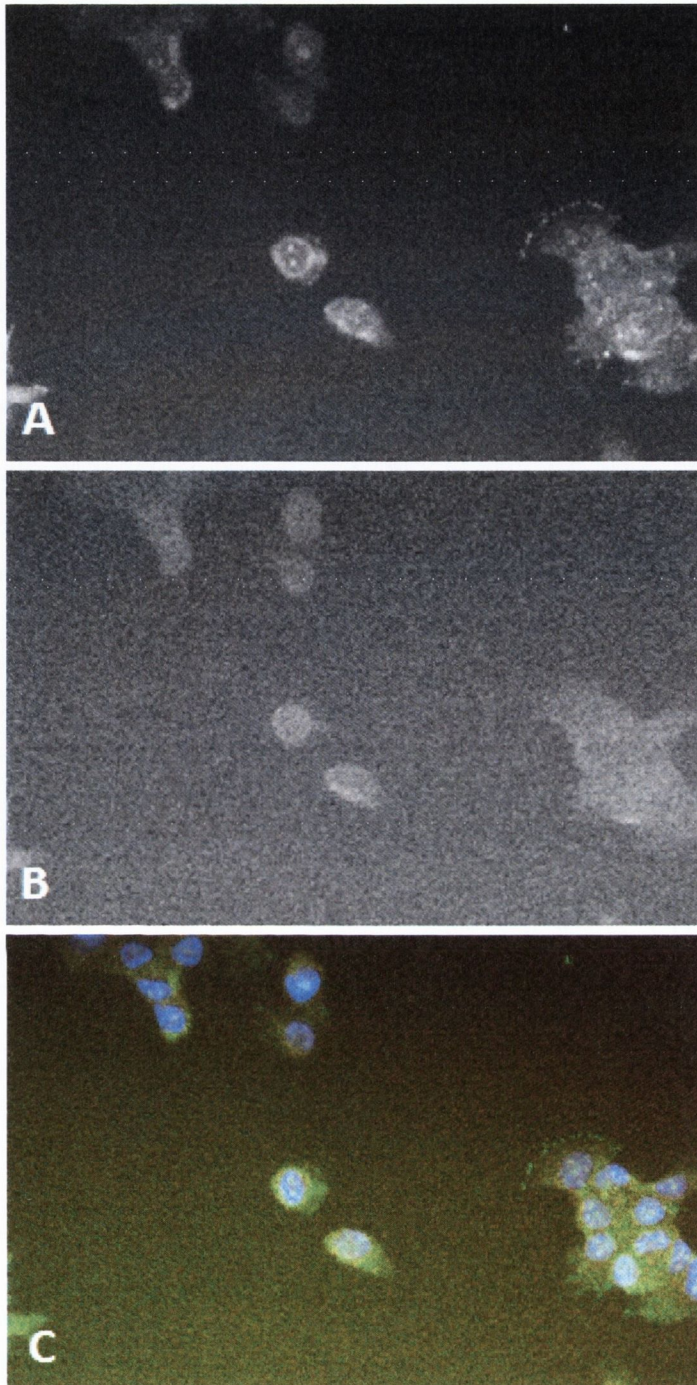
Figure 5.25: Focal adhesion plaques identified using an antibody directed against phosphopaxillin (Tyr118) in a representative image of OE33 oesophageal adenocarcinoma following 24 hour treatment with ACM from viscerally obese oesophageal adenocarcinoma patients (n=3). Nuclei were stained using Hoechst (blue), a fluorescently labelled secondary antibody allowed visualisation of phosphopaxillin localisation (A) (green), the actin cytoskeleton was visualised using phalloidin (B) (red) and the two stains were merged to give a fused image (C). Photographs were taken at 20X magnification.
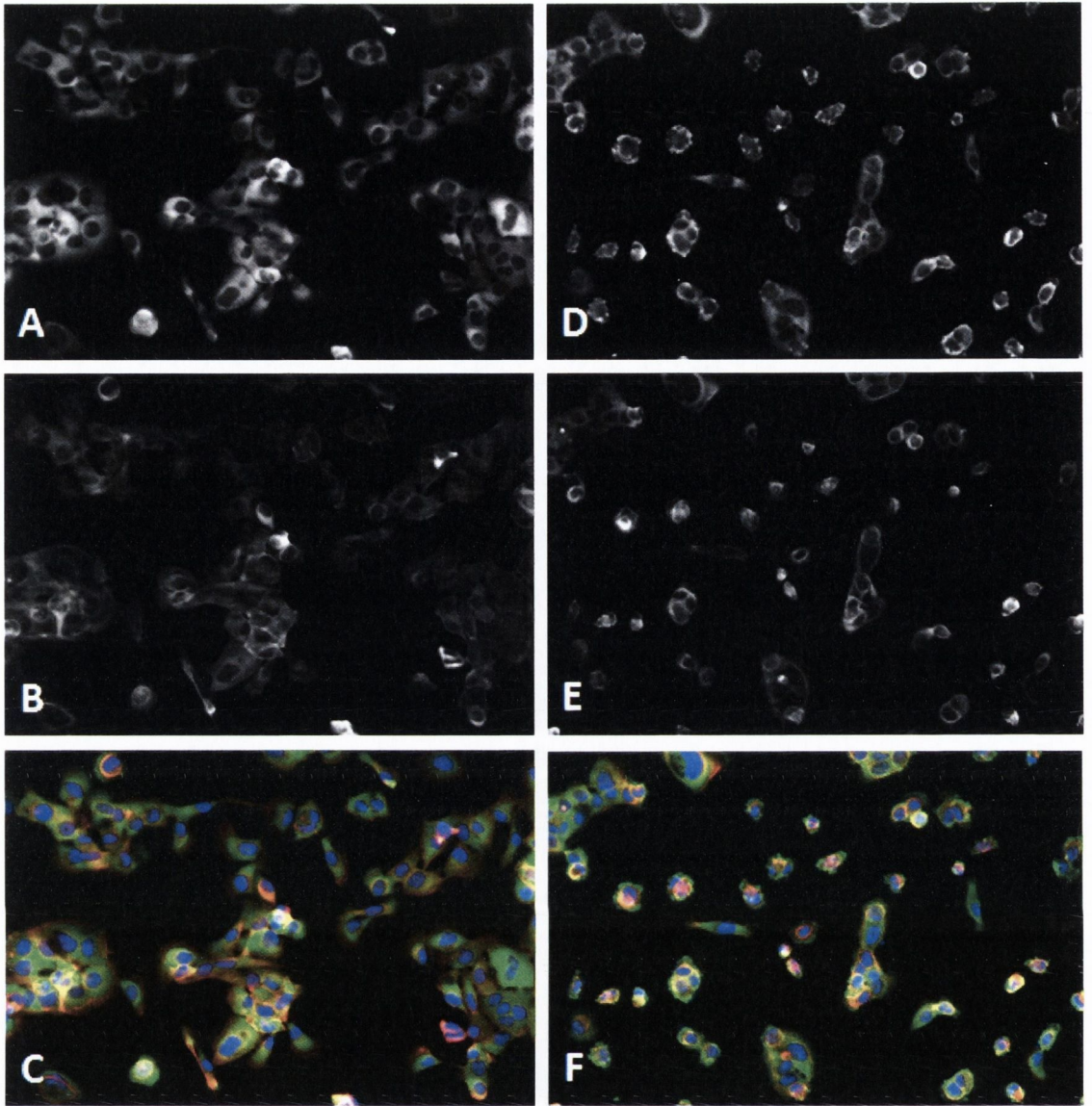
Figure 5.26: Focal adhesion plaques identified using an antibody directed against focal adhesion kinase (FAK) in a representative image of OE33 oesophageal adenocarcinoma following 24 hour treatment with control M199 medium (D-F) and ACM from viscerally obese oesophageal adenocarcinoma patients (n=3) (A-C). Nuclei were stained using Hoechst (blue), a fluorescently labelled secondary antibody allowed visualisation of FAK localisation (A, D) (green), the actin cytoskeleton was visualised using phalloidin (B, E) (red) and the two stains were merged to give a fused image (C, F). Photographs were taken at 10X magnification.

5.4 Discussion

Oesophageal adenocarcinoma (OAD) is an aggressive disease with an extremely poor five year survival rate and early lymphatic and haematogenous spread. This implies that pathways involved in tumour invasion and metastasis, responsible for up to 90% of all cancer mortality (Hanahan and Weinberg, 2000), are of great significance. There is a well established epidemiological link between obesity and OAD (Ryan et al., 2006) and studies aimed at investigating molecular factors responsible for this association are warranted.

Through a series of microarray based experiments examining the effect of omental adipose tissue on OE33 oesophageal adenocarcinoma, a number of altered genes and pathways were identified. Gene expression changes and pathway alterations were validated at the mRNA, protein and functional levels. It was demonstrated that omental adipose tissue promoted an aggressive phenotype in OAD by increasing proliferative, migratory and invasive capacity of tumour cells via up regulation of glycolysis and focal adhesion and epithelial mesenchymal transition (EMT) pathways. These pathway alterations could provide novel evidence for molecular mechanisms by which visceral obesity could give rise to a tumour of increased malignancy.

Proteolytic cleavage and degradation of the extracellular matrix (ECM), necessary for invasion and metastasis to occur, is carried out by enzymes such as the MMPs and serine proteases. Increased mRNA expression, protein levels and enhanced enzymatic activity of MMP2 and MMP9, and induction of mRNA and protein expression of PAI-1, was observed in oesophageal adenocarcinoma in response to culture with adipose tissue. This implies a role for visceral obesity in metastatic gene regulation which has not been demonstrated previously. MMP2 and MMP9 are members of the gelatinase family of matrix metalloproteinases which degrade type IV collagen, the principle component of the basement membrane, leading to increased tumour metastasis (Liotta et al., 1991; Ludwig, 2005; Turpeenniemi-Hujanen, 2005). Plasminogen activator inhibitor 1 (SerpinE1/PAI-1) is a serine protease inhibitor (serpin) which, through inhibition of various plasminogen activator isoforms, prevents plasminogen cleavage to form plasmin. Plasmin is involved in ECM degradation and activation of growth hormones and MMP zymogens including MMP2 and MMP9 (Durand et al., 2004; Festuccia et al., 1998) and thus it is counter-intuitive that elevated PAI-1 is associated with enhanced tumour invasion and metastasis (Duffy and Duggan, 2004; Liotta et al., 1991). However it has been shown that PAI-1 can modulate cell adhesion and migration via direct interactions with integrins and binding to

the ECM protein, vitronectin (Fabre-Guillevin et al., 2008). Elevated expression of MMP2 and 9 is associated with worse prognosis in a variety of cancers including rectal (Curran et al., 2004), oesophageal squamous cell carcinoma (Gu et al., 2005a; Gu et al., 2005b), breast (Jinga et al., 2006; Wu et al., 2008), pancreatic (Mroczko et al., 2009), bladder (Gohji et al., 1998) and non small cell lung carcinoma (Leinonen et al., 2008) but this association has yet to be shown in OAD. MMP2 and MMP9 knockout mice have reduced incidence of metastasis following tumour cell implantation (Itoh et al., 1999; Itoh et al., 1998) demonstrating the important role of these MMPs in metastatic cancer. PAI-1 has also been shown to play a critical role in enhanced tumour invasion and metastasis (Duffy and Duggan, 2004; Liotta et al., 1991) and has been linked to poor prognosis in many cancers including breast (Harbeck et al., 2004; Sternlicht et al., 2006), gastric (Nekarda et al., 1994), rectal (Angenete et al., 2009; Langenskiold et al., 2009) and colorectal carcinoma (Sakakibara et al., 2005), but again, has yet to be associated with OAD prognosis. In a subsequent functional study, ACM from viscerally obese and non obese OAD patients caused increased migration and invasion of OAD. Both the pro-inflammatory environment associated with visceral obesity and the extra volume of adipose tissue present in the viscerally obese patient could therefore increase the proliferative and invasive capacity of OAD *in vivo*, contributing to the early metastasis and poor prognosis associated with this disease (Lagarde et al., 2007).

Vascular endothelial growth factor A (VEGFA), in addition to the MMPs and PAI-1, plays a crucial role in initiation of *de novo* angiogenesis. This process involves epithelial cell invasion into the extracellular matrix to form new blood vessels, necessary for tumours to grow more than a few millimetres in size (Hanahan and Weinberg, 2000; Stetler-Stevenson, 1999). In addition to up regulation of MMP2 and 9, VEGFA was also found to be up regulated over 25 fold in oesophageal adenocarcinoma in response to culture with adipose tissue. PAI-1 has been shown to induce not only cell migration (Chazaud et al., 2002) and tumour invasion but also tumour neovascularisation (Bajou et al., 1998). Both MMP2 and 9 are expressed in tumour associated angiogenic lesions with MMP9 having a role in the release of VEGFA from the extracellular matrix, and VEGFA involved in activation of MMP9, establishing a pro-angiogenesis positive feedback loop (Belotti et al., 2003; Bergers et al., 2000). Elevated expression of MMP9 and VEGFA can result in a shift in the balance of anti- and pro-angiogenic factors present in the tumour microenvironment, triggering the angiogenic switch, the fundamental mechanism by which a new blood supply is established to the growing tumour (Bergers et al., 2000). It is intriguing that the expression of these genes, with key roles not only

in migration and invasion, but also in *de novo* angiogenesis, can be induced in oesophageal adenocarcinoma by adipose tissue.

In addition to deregulation of pathways involved in invasion and metastasis, defects in cell cycle control and apoptosis pathways are necessary events for tumourigenesis to occur (Hanahan and Weinberg, 2000). Expression of tumour suppressors ATM and p53 was decreased in oesophageal adenocarcinoma following culture with both adipocytes and omental adipose tissue. Tumour suppressor ataxia telangiectasia mutated (ATM) detects double stranded DNA breaks and causes cell cycle arrest through stimulation of signal transduction pathways including activation of p53, altered in over 50% of all cancers (Hanahan and Weinberg, 2000; Kastan and Bartek, 2004; Whibley et al., 2009). This sequence of events triggers apoptosis or senescence in tumour cells (Vogelstein et al., 2000; Whibley et al., 2009) and thus down regulation of tumour suppressor genes ATM and p53 can contribute to increased tumour survival and growth. This series of experiments demonstrates for the first time the capacity of omental adipose tissue not only to up regulate migration, invasion and angiogenesis pathways in OAD, but also to down regulate tumour suppressor p53 and ATM expression, potentially contributing to deregulation of cell cycle control to allow unrestricted tumour cell proliferation.

While a small scale qPCR array study provided preliminary insight into gene and pathway changes over the six hallmarks of cancer (Hanahan and Weinberg, 2000), a large scale Affymetrix microarray study offered deeper insight into pathway alterations leading to increased proliferative, invasive and migratory capacity of the tumour, both validating and expanding the initial study. Co-culture with omental adipose tissue strongly up regulated the glycolysis pathway in oesophageal adenocarcinoma, a pathway utilised by tumour cells preferentially over oxidative phosphorylation through a phenomenon known as the Warburg effect. Although in terms of ATP production this is a less efficient pathway than oxidative phosphorylation, tumour cells can effectively compete for limited nutrients through enhancing glycolytic flux (Kelloff et al., 2005), thus choosing increased rate of the pathway over yield. Enhanced production of lactate as the end metabolite of this pathway increases the pH of the tumour microenvironment, eradicating normal cells and expanding margins of the neoplasic area (Kellenberger et al., 2010), promoting increased tumour invasion (Martinez-Zaguilan et al., 1996). Molecular imaging of glucose metabolism by FDG-PET has been shown to be a feasible measure of neoadjuvant response in OAD (Roedl et al., 2009), demonstrating that glycolytic flux is linked to tumour response to therapy. Glycolysis has been found to be up

regulated in Barrett's oesophagus relative to normal squamous oesophagus (van Baal et al., 2006) indicating that this may be an important transformation in the sequence of progression from Barrett's to OAD. Expression of key glycolytic enzymes, including rate limiting hexokinase (HK) and phosphofructokinase (PFK), were significantly up regulated in oesophageal adenocarcinoma in response to culture with adipose tissue. Although adipose tissue from both viscerally obese and normal weight individuals increased production of end metabolite lactate in OE33, this effect was significant only in viscerally obese individuals, implying a novel role for visceral adiposity in induction of the Warburg effect in OAD.

The focal adhesion pathway has been demonstrated to play an important role in tumour initiation, progression and metastasis (Zhao and Guan, 2009). Genes involved in formation of the focal adhesion plaque, linking the cytoskeleton to the ECM, were up regulated in oesophageal adenocarcinoma in response to culture with adipose tissue; these included FAK, Src, α-actinin, paxillin, vinculin, p130Cas and DOCK1. Focal adhesion kinase (FAK), a non receptor tyrosine kinase, is activated upon integrin signalling to form the focal adhesion complex, linking the ECM with the cytoskeleton and playing an important role in cell survival, migration and invasion (Hsia et al., 2003; Schaller, 2001; Schwock et al., 2010). FAK protein expression was significantly increased in oesophageal adenocarcinoma in response to culture with adipose tissue. FAK has been shown to undergo both calpain and caspase dependant cleavage leading to generation of FAK cleavage fragments (Chan et al., 2010; Gervais et al., 1998) which were found to be significantly decreased in oesophageal adenocarcinoma following adipose tissue culture. This finding demonstrates decreased FAK degradation in OE33 in response to culture with adipose tissue. In addition, FAK inhibitor FRNK, a naturally occurring variant of FAK lacking the signalling kinase domain (Gervais et al., 1998), was down regulated in response to treatment with adipose tissue. Gene expression increases in a number of members of the focal adhesion complex, in addition to increases in protein levels of FAK and FAK binding partner, Src, indicates that adipose tissue up regulates the focal adhesion complex in OAD. High content screening (HCS) analysis was used in order to determine the net effect of adipose tissue on this pathway in OAD. Following treatment of OE33 cells with ACM, focal adhesion components FAK and paxillin were found to localise to focal adhesion plaques, thus providing some promising initial results. Signalling molecules acting through the focal adhesion plaque were also up regulated in OAD following culture with adipose tissue with increased expression of integrin alpha subunits and integrin binding molecules SPP1 and laminin-5. These alterations in expression could up regulate activity of the focal adhesion pathway, increasing expression of components of the focal adhesion plaque, reducing

expression of FAK inhibitor, FRNK, and inhibiting FAK cleavage. Increased integrin expression at the mRNA but not the protein level in OE33 in response to culture with adipose tissue indicates the complex regulation of processes of transcription and translation, and highlights the importance of validations at gene, protein and functional levels. As integrin signalling has been shown to be of great importance in cell migration (Guo and Giancotti, 2004), the potential contribution of other integrins to the acquisition of a migratory phenotype in OE33 needs to be investigated.

Signalling through the focal adhesion pathway is necessary for epithelial mesenchymal transition (EMT) to occur (Bianchi et al., 2010). This process, critical for normal wound healing and embryonic development, can be deregulated in cancer resulting in acquisition of a migratory tumour cell phenotype (Alves et al., 2009; Bianchi et al., 2010). SNAI2 (Slug) is a well established transcriptional regulator of EMT associated with poor prognosis in breast (Come et al., 2006; Martin et al., 2005), oesophageal squamous cell (Kumar et al., 2007) and colorectal carcinoma (Shioiri et al., 2006) often, but not always, acting via transcriptional repression of cell adhesion molecule E-cadherin (Alves et al., 2009). There was no change in expression of E-cadherin in oesophageal adenocarcinoma in response to culture with adipose tissue, and there are a variety of possible explanations for this. An increase in mRNA levels of SNAI2 may not always correlate to an increase in functional protein or alternatively, SNAI2 may not always have access to the E-cadherin promoter to exert its repressional activity. Additionally, it is possible that SNAI2 functions independently of E-cadherin in this model (Alves et al., 2009). These data highlight the importance of validations of alterations in mRNA expression at both the protein and functional levels. Together these gene and pathway expression findings indicate that an excess accumulation of omental adipose tissue in visceral obesity could promote adenocarcinoma with increased malignancy.

In order to determine which cell or tissue type had the most pronounced effect on tumour cells, both whole omental adipose tissue and adipocytes were cultured with OE33 oesophageal adenocarcinoma. Differential gene regulation in oesophageal adenocarcinoma was observed following co-culture with whole omental adipose tissue, while no significant effect was observed following co-culture with adipocytes alone. It can therefore be concluded that the stromal vascular fraction (SVF), comprising of fibroblasts, endothelial cells and immune cells (Alvarez-Llamas et al., 2007), is the main effector of these observed gene alterations, with adipocytes playing a much lesser role. This finding is of great interest as the SVF in visceral obesity has been shown to contain greatly increased numbers of immune cells relative to

normal weight individuals (Kintscher et al., 2008; Weisberg et al., 2003; Wu et al., 2007), and these cells could therefore be key players in the association between visceral obesity and cancer.

Interestingly, when oesophageal adenocarcinoma was cultured with SGBS, the invasion and metastasis pathway and cell cycle pathway were the most altered, reflecting the results of the primary human adipocyte co-culture. This provides further evidence for the suitability of SGBS as a clinically relevant adipocyte model. However gene alterations following co-culture with adipocytes (either SGBS or primary human) were not as pronounced as following co-culture with adipose tissue, highlighting a disadvantage of *in vitro* single cell systems where cells are removed from the microenvironment.

This series of experiments demonstrates potential mechanisms by which biological pathways involved in tumourigenesis are altered in visceral obesity. Increased glycolytic flux and up regulation of the focal adhesion pathway, promoting cytoskeletal reorganisation and epithelial mesenchymal transition (EMT), culminates in an increased proliferative, migratory and invasive capacity of oesophageal adenocarcinoma. Identification of these alterations contributes to the delineation of molecular mechanisms by which visceral obesity could give rise not only to increased incidence of oesophageal adenocarcinoma, but also increased tumour aggressiveness resulting in early metastasis and high mortality which is associated with this disease.

6 Expression of markers of invasion and metastasis MMP9, PAI-1, SNAI2 and E-cadherin correlate with visceral obesity and predict aggressive tumour biology and prognosis in oesophageal adenocarcinoma.

6.1   Introduction

Oesophageal adenocarcinoma (OAD) is an aggressive disease due to early tumour dissemination (Lagarde et al., 2007), and five year survival remains low at less than 15% (National Cancer Registry Ireland). Pathways of tumour invasion and metastasis are therefore of great significance. Incidence of OAD is strongly associated with visceral obesity, and visceral obesity is associated with increased cancer mortality (Calle et al., 2003). Upon diagnosis, over half of OAD patients have unresectable tumours due to distant metastases and median survival in this cohort is less than one year (Enzinger and Mayer, 2003). When a complete resection is carried out in patients with resectable tumours, the five year survival rate is increased to merely 50% (Murphy et al., 2008). Multimodal therapy is therefore required to improve the poor prognosis of OAD, and the development of targeted treatments is underway. Previous work investigating the role of candidate genes in OAD has successfully uncovered several targets to date. These include EGFR, involved in tumour cell proliferation, VEGFA, involved in angiogenesis, MMPs, involved in invasion and metastasis, CDK, involved in cell cycle control and COX-2, involved in inflammation (Syrigos et al., 2008). However these pathways have not yet been investigated in the context of visceral obesity, a state of metabolic deregulation of great relevance in OAD. As obesity has been shown to increase cancer incidence and progression, the identification of shared molecular pathways in obesity and cancer could be of great importance for treatment stratification of viscerally obese patients.

In this thesis, microarray technology was utilised to discover pro-tumour pathways altered in OAD following co-culture with adipose tissue. This approach identified up regulation of pathways in invasion and metastasis, focal adhesion and epithelial mesenchymal transition (EMT), with concurrent down regulation of tumour suppressors involved in cell cycle control. Identified targets involved in these pathways were validated at mRNA and protein levels. Furthermore, ACM was demonstrated to increase proliferative, migratory and invasive capacity of OE33. *In vitro* experimental approaches such as these are an essential tool of molecular research enabling the creation of a simplified system through the removal of complex and potentially confounding microenvironmental influences (Fischer-Posovszky et al., 2008). This approach is of particular relevance for the study of molecular interactions between individual cell and tissue types, and was utilised in this thesis to identify altered pathways in OAD cells following exposure to adipose tissue. However, complete reliance on an *in vitro* model system may present fundamental shortcomings for translational research. The tissue microenvironment has been demonstrated to play a primary role in pathological processes

such as obesity and cancer. Inflammation is a recently identified shared hallmark of obesity and cancer, implying vital contribution of infiltrating immune cells to both disease processes (Colotta et al., 2009; Kintscher et al., 2008). In adipose tissue, visceral obesity is associated with increased amounts of infiltrating pro-inflammatory immune cells (Xu et al., 2003), generating a chronic state of inflammation in these individuals. This study demonstrated that whole adipose tissue, but not adipocytes alone, induced significant gene expression alterations in OE33. These findings suggest that the adipose tissue SVF, containing infiltrating immune cells, may play a pivotal role in obesity related pathologies such as cancer. Solid tumours are composed of a mix of neoplastic and stromal cells, the latter comprising fibroblasts, blood and lymphatic vessels and immune cells (Allavena et al., 2008). In addition to these cellular components, the stroma contains a wide variety of biologically active molecules, either in soluble form or associated with ECM proteins. These include angiogenic factors such as VEGF, chemokines such as MCP-1 and proteolytic factors such as PAI-1 and MMPs (Allavena et al., 2008). In summary, this thesis utilised an *in vitro* co-culture system to identify gene and pathway alterations in a controlled environment. The aim of this chapter was to investigate the translational application of these targets in OAD.

6.2   Aims and objectives

The overall aim of this chapter was to investigate if candidate genes identified using microarray technology were associated with a) visceral obesity, b) clinicopathological parameters of tumour biology and c) prognosis in OAD patients. This novel study will identify shared pathways between visceral obesity and OAD which could be targeted for the development of therapies crucial to aid in the treatment of this aggressive disease.

Specific objectives:

- To investigate mRNA expression of MMP9, PAI-1, p53, SNAI2 and E-cadherin in OAD tumour biopsies with respect to visceral obesity status, tumour biology and patient prognosis.
- To examine protein levels of MMP9 in OAD tissue microarrays with respect to visceral obesity status, tumour biology and patient prognosis.

6.3   Results

6.3.1   Expression of markers of metastasis MMP9 and PAI-1 are significantly correlated with visceral obesity in OAD biopsies.

Previously, Human Cancer Profiler Arrays (SABiosciences) identified markers of invasion and metastasis MMP9 and PAI-1 to be up regulated and tumour suppressor p53 to be down regulated in OE33 in response to co-culture with adipose tissue (Chapter 5). These gene alterations were validated at both the gene and protein levels. These alterations translated to a functional effect as ACM increased the proliferative, migratory and invasive capacity of OE33 (Chapter 5). The effect of obesity, measured by BMI, WC and VFA, on expression of these genes was subsequently examined in patient tumour biopsies. Tumour biopsies from OAD and oesophageal squamous cell carcinoma were immediately taken from fresh tumour tissue following surgical resection and processed by a designated biobank technician (Ennis et al., 2010). Anthropometric details are listed in Table 6.1. RNA was extracted (as described in section 2.6.1) and gene expression was investigated using qPCR (as described in section 2.6.9) and statistical analysis carried out using unpaired student t tests (described in section 2.19).

Male sex has previously been reported to be associated with increased risk of OAD (Kubo and Corley, 2004). Although trends did not reach statistical significance, PAI-1 expression was increased 2 fold while p53 expression was decreased 1.5 fold in males relative to females (Tables 6.3, 6.4). There was no difference in MMP9 expression between males and females (Table 6.2). Elevated PAI-1 and lowered p53 in males may offer further explanation for the stronger association of male sex with OAD. Gene expression of MMP9 and PAI-1 were increased 1.5 fold in OAD (n=40) relative to SCC (n=12), however this result did not reach statistical significance (Tables 6.2, 6.3). Expression of p53 was unchanged between histological subtypes (Table 6.4). Increased levels of MMP9 and PAI-1 in OAD relative to SCC indicate the importance of the expression of these genes in pathways of invasion and metastasis in this histological subtype.

While there was no difference in p53, expression of markers of invasion and metastasis MMP9 and PAI-1 were significantly elevated in obese patients when categorised by BMI, WC and VFA. When patients were grouped by visceral obesity, using gold standard measurement VFA, gene expression of MMP9 and PAI-1 was increased 7 fold ($p<0.05$) and 5 fold ($p<0.05$), respectively, in tumours from viscerally obese (n=26) relative to non obese (n=13) OAD patients (Figure 6.1).

This novel result highlights a molecular pathway by which visceral obesity may be associated with early tumour dissemination, a characteristic hallmark of OAD (Lagarde et al., 2007).

Table 6.1: Anthropometric data of patients classified as obese/non obese by visceral fat area.

	non obese	obese
no. subjects	20	27
Sex (male), n (%)	9 (64)	24 (92)
Age at surgery, mean (range)	63 (48-72)	65 (55-81)
OAD, n (%)	14 (70)	26 (96)
Waist circumference (cm), mean (range)	84 (77-101)	107 (80-130) ***
BMI, mean (range)	22 (19-26)	30 (23-39) ***
VFA (cm^2), mean (range)	58 (13-117)	250 (146-384) ***
Metabolic syndrome, n (%)	0 (0)	13 (50)
Neoadjuvant therapy, n (%)	6 (43)	10 (38)

Statistical analysis was carried out using an unpaired student's t-test. (BMI=body mass index, VFA=visceral fat area)
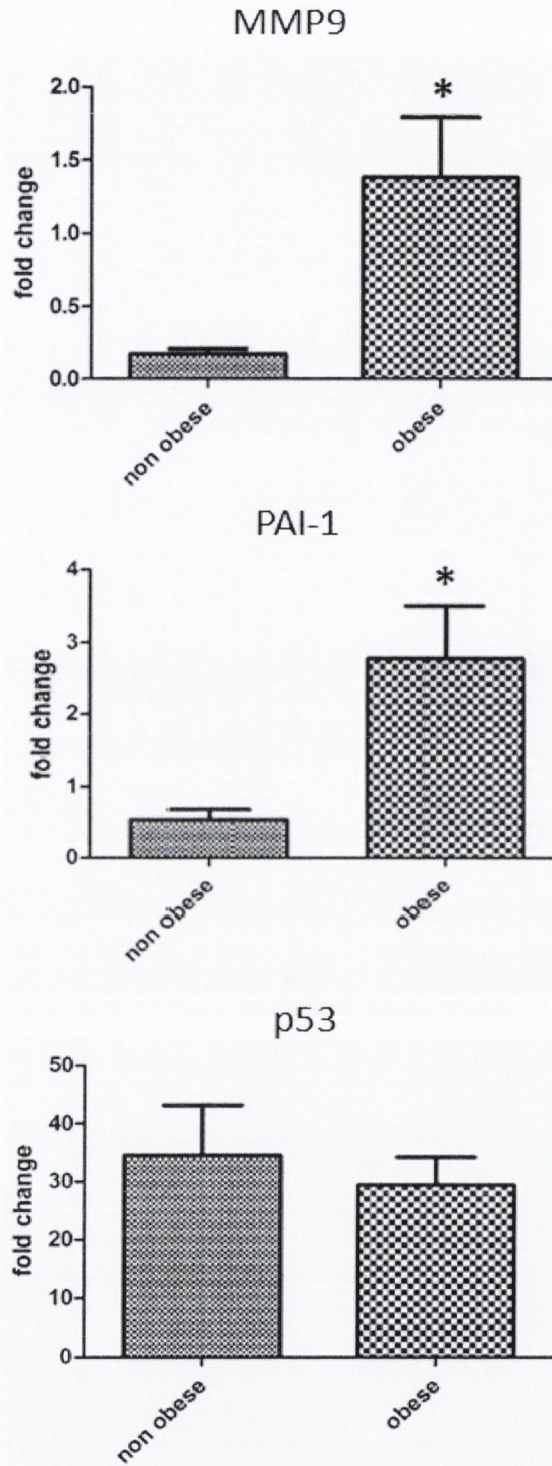
Figure 6.1: Expression of MMP9, PAI-1 and p53 in OAD biopsies of male patients divided into viscerally obese (n=25) and non obese (n=15) categories by visceral fat area (VFA). VFA of 130 cm^2 was used as a cutoff. Data are expressed as mean ± SEM. Statistical analysis was performed using an unpaired student's t-test (*p<0.05).

6.3.2 High MMP9 and PAI-1 and low p53 expression are associated with more aggressive tumour biology.

Intriguingly, markers of invasion and metastasis MMP9 and PAI-1 were found to be up regulated in OAD in viscerally obese patients (section 6.3.1). It was subsequently investigated whether elevated mRNA expression of these regulators of invasion and metastasis was associated with more aggressive tumour biology. Metastasis is responsible for up to 90% of cancer mortality (Hanahan and Weinberg, 2000). The identification of pathways involved in metastasis that may be up regulated by the presence of excess adipose tissue could identify a molecular link between visceral obesity and cancer mortality. Clinicopathological parameters of tumour biology measured were tumour differentiation, lymph involvement, venous involvement, perineural involvement, pathological tumour (T) category and pathological node (N) category. Statistical analysis of tumour biology was performed using unpaired student t tests (as described in section 2.19).

Poor tumour differentiation was associated with a 6 fold increase in MMP9 expression ($p<0.05$), a 1.7 fold increase in PAI-1 expression and a 1.7 fold decrease in p53 expression ($p<0.05$) (Figure 6.2). Poor tumour differentiation is a routinely measured histological marker of increased tumour malignancy (Helm et al., 2005). The statistically significant association of increased MMP9 expression both with visceral obesity and tumour dedifferentiation indicates a mechanism by which excess adipose tissue may predispose to increased malignancy. Lymphatic dissemination was associated with a 4 fold increase in MMP9 expression (Table 6.2) and a twofold increase in PAI-1 expression (Table 6.3). Haematological dissemination was associated with a twofold increase in expression of MMP9 (Table 6.2) and a 1.5 fold increase in PAI-1 expression (Table 6.3). Perineural involvement was associated with a 1.5 fold increase in MMP9 expression (Table 6.2) and a 1.2 fold increase in PAI-1 expression (Table 6.3). There was no association of p53 expression with lymphatic, haematological or perineural dissemination (Table 6.4). As MMP9 and PAI-1 are elevated in visceral obesity, these data indicate a potential molecular mechanism by which visceral obesity may be associated with malignant tumour dissemination. A pathologically advanced T stage was associated with a fivefold increase in MMP9 expression and a twofold increase in PAI-1 expression. A pathologically advanced N stage was associated with a twofold increase in MMP9 expression (Table 6.2). Together, these results highlight the clinical significance of elevated levels of MMP9 and PAI-1 expression in both advanced tumour stage and metastasis. The association of visceral obesity with elevated expression of these markers of invasion and metastasis identifies a novel mechanism by which excess visceral adiposity may contribute to increased OAD malignancy.
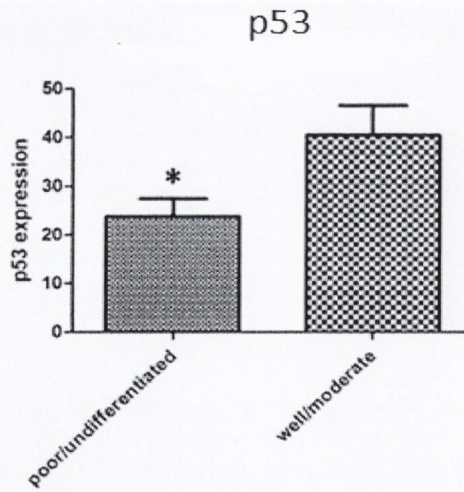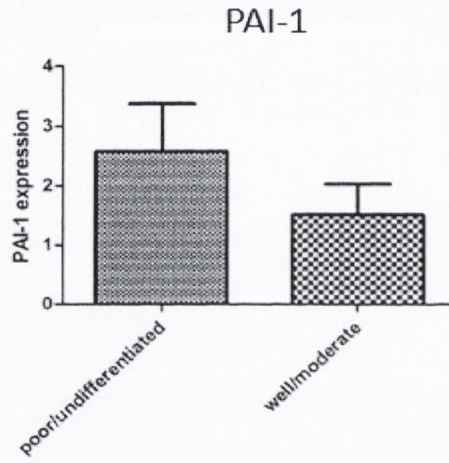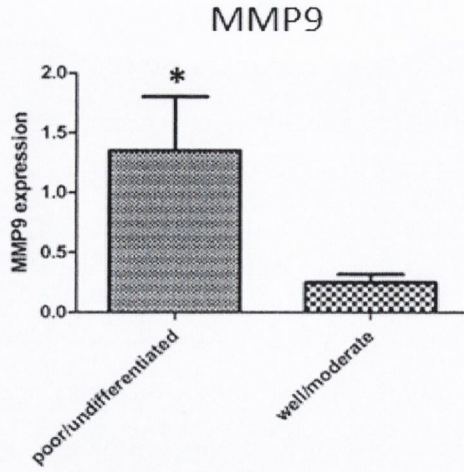
Figure 6.2: Levels of MMP9, PAI-1 and p53 expression with respect to tumour differentiation. Tumours from male OAD patients were categorised into groups of poorly/undifferentiated or well/moderately differentiated by a pathologist. Statistical analysis was carried out by unpaired student's t test. (*p<0.05)

Table 6.2: Tumour MMP9 expression in relation to clinical, anthropometric and pathological data.

	MMP9 expression, mean (SEM)	p
Age at diagnosis (years)		0.6242
< median (62)	0.618 (0.25)	
≥ median (62)	1.135 (0.38)	
Diagnosis		0.9453
OAD	0.939 (0.275)	
SCC	0.584 (0.221)	
Sex		0.6854
Male	0.945 (0.302)	
Female	0.737 (0.342)	
Body mass index (kg/m^2)		0.006
Non obese < 30	0.411 (0.175)	
Obese ≥ 30	1.980 (0.665)	
Waist circumference (cm)		0.031
Non obese < 94 (M), 80 (F)	0.264 (0.072)	
Obese ≥ 94 (M), 80 (F)	1.475 (0.46)	
Visceral fat area (cm^2)		0.0309
Non obese < 130 cm^2	0.168 (0.033)	
Obese ≥ 130 cm^2	1.385 (0.41)	
Tumour differentiation		0.0375
Well/moderate	0.355 (0.090)	
Poor/undifferentiated	1.247 (0.415)	
Pathological tumour category		0.181
T0 – T1	0.198 (0.077)	
T2 – T3	1.073 (0.293)	
Pathological node category		0.3143
N0	0.54 (0.233)	
N1	1.053 (0.355)	
Lymph node involvement		0.2034
Yes	1.043 (0.312)	
No	0.320 (0.123)	
Venous involvement		0.2781
Yes	1.14 (0.344)	
No	0.556 (0.297)	
Perineural involvement		0.3855
Yes	1.26 (0.533)	
No	0.792 (0.269)	

MMP9 expression is described as mean (SEM), statistical analysis was carried out using an unpaired student's t-test. Statistically significant pvalues < 0.05 are highlighted in red.

Table 6.3: Tumour PAI-1 expression in relation to clinical, anthropometric and pathological data.

	PAI-1 expression, mean (SEM)	p
Age at diagnosis (years)		0.4806
< median (62)	1.627 (0.564)	
≥ median (62)	2.234 (0.639)	
Diagnosis		0.9629
OAD	1.929 (0.48)	
SCC	1.985 (0.48)	
Sex		0.3806
Male	2.183 (0.589)	
Female	1.358 (0.313)	
Body mass index (kg/m^2)		0.009
Non obese < 30	1.014 (0.299)	
Obese ≥ 30	3.691 (1.195)	
Waist circumference (cm)		0.0397
Non obese < 94 (M), 80 (F)	0.74 (0.164)	
Obese ≥ 94 (M), 80 (F)	2.833 (0.808)	
Visceral fat area (cm^2)		0.031
Non obese < 130 cm^2	0.529 (0.149)	
Obese ≥ 130 cm^2	2.775 (0.74)	
Tumour differentiation		0.2782
Well/moderate	1.517 (0.492)	
Poor/undifferentiated	2.467 (0.727)	
Pathological tumour category		0.1632
T0 – T1	1.415 (0.477)	
T2 – T3	2.634 (0.748)	
Pathological node category		0.5241
N0	1.569 (0.671)	
N1	2.166 (0.557)	
Lymph node involvement		0.3262
Yes	2.26 (0.582)	
No	1.198 (0.489)	
Venous involvement		0.4164
Yes	2.299 (0.606)	
No	1.504 (0.561)	
Perineural involvement		0.6496
Yes	2.338 (0.985)	
No	1.9 (0.466)	

PAI-1 expression is described as mean (SEM), statistical analysis was carried out using an unpaired student's t-test. Statistically significant pvalues < 0.05 are highlighted in red.

Table 6.4: Tumour p53 expression in relation to clinical, anthropometric and pathological data.

	p53 expression, mean (SEM)	p
Age at diagnosis (years)		*0.2969*
< median (62)	27.924 (4.852)	
≥ median (62)	35.505 (5.322)	
Diagnosis		*0.7576*
OAD	31.154 (4.15)	
SCC	34.254 (5.661)	
Sex		*0.302*
Male	29.219 (4.14)	
Female	37.451 (7.151)	
Body mass index (kg/m²)		*0.5796*
Non obese < 30	32.686 (5.82)	
Obese ≥ 30	27.607 (5.4)	
Waist circumference (cm)		*0.7104*
Non obese < 94 (M), 80 (F)	32.941 (7.242)	
Obese ≥ 94 (M), 80 (F)	29.668 (5.283)	
Visceral fat area (cm²)		*0.5875*
Non obese < 130 cm²	34.463 (8.697)	
Obese ≥ 130 cm²	29.485 (4.765)	
Tumour differentiation		*0.0253*
Well/moderate	39.448 (6.024)	
Poor/undifferentiated	23.185 (3.335)	
Pathological tumour category		*0.6404*
T0 – T1	30.091 (4.916)	
T2 – T3	33.663 (5.866)	
Pathological node category		*0.3358*
N0	26.693 (6.967)	
N1	34.352 (4.395)	
Lymph node involvement		*0.4478*
Yes	31.374 (4.446)	
No	25.045 (5.457)	
Venous involvement		*0.2517*
Yes	35.238 (5.393)	
No	25.735 (4.453)	
Perineural involvement		*0.84*
Yes	33.059 (6.36)	
No	31.371 (4.984)	

p53 expression is described as mean (SEM), statistical analysis was carried out using an unpaired student's t-test. Statistically significant pvalues < 0.05 are highlighted in red.

6.3.3 PAI-1 is associated with prognosis in OAD.

OAD is an aggressive disease associated with high patient mortality due to early malignant tumour dissemination (Lagarde et al., 2007). In addition, there is evidence to suggest that obesity is linked to increased cancer mortality (Calle et al., 2003). It is therefore of great significance that markers of invasion and metastasis MMP9 and PAI-1 were found to be up regulated in OAD in viscerally obese patients, and that these markers were associated with increased tumour aggressiveness. It was subsequently investigated whether markers of invasion and metastasis MMP9 and PAI-1 and tumour suppressor p53 were correlated with patient survival. Gene expression of MMP9, PAI-1 and p53 above or equal to the median was designated 'high' while gene expression below the median was designated 'low'. Statistical analysis of patient survival was carried out using the Kaplan-Meier estimator and the Gehan-Breslow-Wilcoxon statistical test in GraphPad Prism (as described in section 2.19). Forward likelyhood multivariate Cox regression analysis was carried out in SPSS.

High PAI-1 expression was negatively associated with patient survival, and this finding reached statistical significance ($p<0.05$), identifying PAI-1 as a prognostic factor in OAD. Although increased MMP9 and decreased p53 expression was associated with aggressive tumour biology and in particular with poor tumour differentiation, neither high MMP9 expression nor low p53 expression had a negative impact on patient survival (Figure 6.3). As visceral obesity was significantly associated with elevated MMP9 expression, a combined survival analysis was subsequently carried out. High MMP9 expression in viscerally obese patients (n=14) and low MMP9 expression in non obese patients (n=10) were compared (data not shown). Although this reduced the p value from $p<0.9$ to $p<0.3$, the result did not reach statistical significance. Combined analysis of MMP9 with visceral obesity decreased patient numbers from 40 to 24 and thus the reduction in sample size may account for lack of statistical significance. MMP9 has previously been associated with nodal metastasis and poor tumour differentiation in cervical (Yu et al., 2009) and oesophageal squamous cell carcinoma (Gu et al., 2005b) but not yet in OAD. While PAI-1 has been linked with poor prognosis in breast (Harbeck et al., 2004; Sternlicht et al., 2006), gastric (Nekarda et al., 1994) and colorectal carcinoma (Angenete et al., 2009; Langenskiold et al., 2009), this is the first study to demonstrate an association with OAD prognosis. Elevated levels of prognostic factor PAI-1 in visceral obesity could therefore highlight an important molecular pathway by which visceral obesity could negatively impact on OAD prognosis.

Figure 6.3: Kaplan Meiers analysis showing effect of MMP9, PAI-1 and p53 expression on survival in OAD. Gene expression was separated into above and below the median expression value. Statistical analysis was performed using the Gehan-Breslow-Wilcoxon test (*p<0.05).

6.3.4 Down regulation of epithelial marker E-cadherin is significantly correlated with visceral obesity in OAD biopsies.

Previously, Affymetrix microarrays identified markers of epithelial mesenchymal transition (EMT) to be altered in OE33 in response to co-culture with adipose tissue (Chapter 5). SNAI2 is a key transcription factor in this process commonly, but not exclusively, acting via transcriptional repression of epithelial cell marker E-cadherin (Alves et al., 2009). SNAI2 gene expression was significantly up regulated in OE33 following culture with adipose tissue (p<0.04) (Chapter 5). The effect of obesity on the expression of SNAI2 and E-cadherin was examined in patient tumour biopsies from OAD patients. Clinical significance of altered gene expression was subsequently investigated, in relation to measures of tumour differentiation, lymph involvement, venous involvement, perineural involvement, pathological tumour (T) category and pathological node (N) category. Statistical analysis of tumour biology was performed using unpaired student t tests (as described in section 2.19).

Gene expression of EMT transcription factor SNAI2 was increased twofold in tumour biopsies from obese relative to non obese OAD patients. This trend approached statistical significance when patients were grouped by BMI (p<0.07), however not when patients were grouped by measures of visceral obesity, WC (p<0.4) and VFA (p<0.3) (Table 6.5). This finding indicates that elevated SNAI2 expression may be associated with overall obesity rather than with visceral adiposity. Gene expression of SNAI2 target, E-cadherin was decreased almost twofold in tumour biopsies from obese relative to non obese OAD patients. This association reached statistical significance when patients were grouped by waist circumference (p<0.05) and approached significance when patients were grouped by visceral fat area (p<0.07) (Table 6.6). There was no association when patients were grouped by BMI (p<0.3). These data indicate that, in contrast to SNAI2, E-cadherin expression is associated with visceral obesity rather than overall adiposity. Male sex was significantly associated with a twofold decrease in E-cadherin expression (p<0.007) (Table 6.6). However, there was no association between elevated SNAI2 expression or reduced E-cadherin expression on pathological tumour or node stage, tumour differentiation or measures of tumour dissemination (Tables 6.5, 6.6). Together these novel results highlight a potential molecular mechanism whereby male sex and visceral obesity, two known risk factors of OAD, could promote the acquisition of a migratory mesenchymal phenotype by malignant tumour cells.

Table 6.5: Tumour SNAI2 expression in relation to clinical, anthropometric and pathological data.

	SNAI2 expression, mean (SEM)	p
Age at diagnosis (years)		0.2458
< median (62)	44.143 (14.189)	
≥ median (62)	76.251 (24.861)	
Diagnosis		0.0001
OAD	38.464 (9.288)	
SCC	188.078 (64.0)	
Sex		0.1323
Male	46.0 (14.119)	
Female	92.534 (32.282)	
Body mass index (kg/m²)		0.0693
Non obese < 30	25.623 (3.549)	
Obese ≥ 30	61.411 (24.515)	
Waist circumference (cm)		0.3097
Non obese < 94 (M), 80 (F)	26.659 (4.976)	
Obese ≥ 94 (M), 80 (F)	46.731 (2.533)	
Visceral fat area (cm²)		0.2437
Non obese < 130 cm²	23.839 (4.134)	
Obese ≥ 130 cm²	46.655 (14.145)	
Tumour differentiation		0.2809
Well/moderate	73.584 (26.049)	
Poor/undifferentiated	43.901 (9.297)	
Pathological tumour category		0.1796
T0 – T1	95.248 (49.316)	
T2 – T3	48.598 (12.171)	
Pathological node category		0.7256
N0	64.717 (28.545)	
N1	54.382 (15.01)	
Lymph node involvement		0.5117
Yes	55.127 (15.53)	
No	77.695 (37.67)	
Venous involvement		0.4169
Yes	48.616 (15.974)	
No	72.395 (26.047)	
Perineural involvement		0.4895
Yes	44.257 (13.09)	
No	66.371 (20.284)	

SNAI2 expression is described as mean (SEM), statistical analysis was carried out using an unpaired student's t-test. Statistically significant pvalues < 0.05 are highlighted in red.

Table 6.6: Tumour E-cadherin expression in relation to clinical, anthropometric and pathological data.

	E-cadherin expression, mean (SEM)	p
Age at diagnosis (years)		0.7611
< median (62)	3.96 (0.584)	
≥ median (62)	4.294 (0.981)	
Diagnosis		0.591
OAD	3.99 (0.598)	
SCC	4.856 (1.11)	
Sex		0.0069
Male	3.255 (0.406)	
Female	6.457 (1.526)	
Body mass index (kg/m^2)		0.2218
Non obese < 30	4.546 (0.847)	
Obese ≥ 30	3.01 (0.656)	
Waist circumference (cm)		0.0447
Non obese < 94 (M), 80 (F)	5.423 (1.232)	
Obese ≥ 94 (M), 80 (F)	2.999 (0.468)	
Visceral fat area (cm^2)		0.0602
Non obese < 130 cm^2	5.49 (1.415)	
Obese ≥ 130 cm^2	3.155 (0.442)	
Tumour differentiation		0.5852
Well/moderate	4.413 (0.639)	
Poor/undifferentiated	3.817 (0.865)	
Pathological tumour category		0.4062
T0 – T1	3.158 (0.803)	
T2 – T3	4.301 (0.656)	
Pathological node category		0.2184
N0	3.168 (0.551)	
N1	4.581 (0.792)	
Lymph node involvement		0.6864
Yes	3.90 (0.581)	
No	4.45 (1.566)	
Venous involvement		0.8639
Yes	3.963 (0.569)	
No	4.161 (1.103)	
Perineural involvement		0.3857
Yes	4.195 (0.949)	
No	3.403 (0.433)	

SNAI2 expression is described as mean (SEM), statistical analysis was carried out using an unpaired student's t-test. Statistically significant pvalues < 0.05 are highlighted in red.

6.3.5   SNAI2 is an independent prognostic factor in OAD.

Visceral obesity was associated with twofold increased expression of SNAI2 and significantly decreased expression levels of E-cadherin (p<0.05). Down regulation of E-cadherin is associated with loss of the epithelial phenotype and transition to the more motile mesenchymal phenotype, necessary for tumour cell invasion and metastasis to occur (Alves et al., 2009). It was subsequently investigated whether markers of EMT, SNAI2 and E-cadherin, were correlated with patient survival. Gene expression of SNAI2 and E-cadherin above or equal to the median was designated 'high' while gene expression below the median was designated 'low'. Statistical analysis of patient survival was carried out using the Kaplan-Meier estimator and the Gehan-Breslow-Wilcoxon statistical test in GraphPad Prism (described in section 2.19). Forward likelyhood multivariate Cox regression analysis was carried out in SPSS.

High SNAI2 expression was negatively associated with patient survival, and this finding reached statistical significance (p<0.05), identifying an association of SNAI2 with OAD prognosis (Figure 6.4). Subsequent Cox regression multivariate analysis identified SNAI2 to be an independent prognostic factor in OAD. In contrast, low expression of SNAI2 target, E-cadherin, was not associated with patient survival (Figure 6.4). As SNAI2 is an important transcriptional repressor of E-cadherin, a combined survival analysis was subsequently conducted. High SNAI2 with low E-cadherin expression (n=10) and low SNAI2 with high E-cadherin expression (n=11) were compared. High SNAI2 combined with low E-cadherin expression was not associated with poor prognosis (p<0.2) (Figure 6.4). Combined analysis decreased patient numbers from n=40 to n=21 and thus the reduction in sample size may account for lack of statistical significance. However, there was some separation between survival curves following one year and it would therefore be worthwhile to reanalyse this data after a longer follow-up period. Alternatively, the mechanism of action of SNAI2 in OAD may be independent of E-cadherin repression, as published in oesophageal squamous cell and breast carcinoma (Come et al., 2006; Uchikado et al., 2005). Linear regression analysis was employed to investigate the relationship between transcriptional repressor, SNAI2, and its target cell adhesion molecule and key marker of epithelial phenotype, E-cadherin. There was no significant correlation between SNAI2 and E-cadherin (r^2=0.024, p<0.37) (Figure 6.5). With high SNAI2 expression, but not low E-cadherin expression, an independent prognostic factor in OAD, this finding indicates that E-cadherin independent pathways may be of importance in SNAI2 mediated pathogenesis in OAD.

The association of PAI-1 and SNAI2 with both obesity and prognosis in OAD highlights potential mechanisms by which obesity may promote malignant tumour dissemination, contributing to the poor prognosis associated with this aggressive cancer.
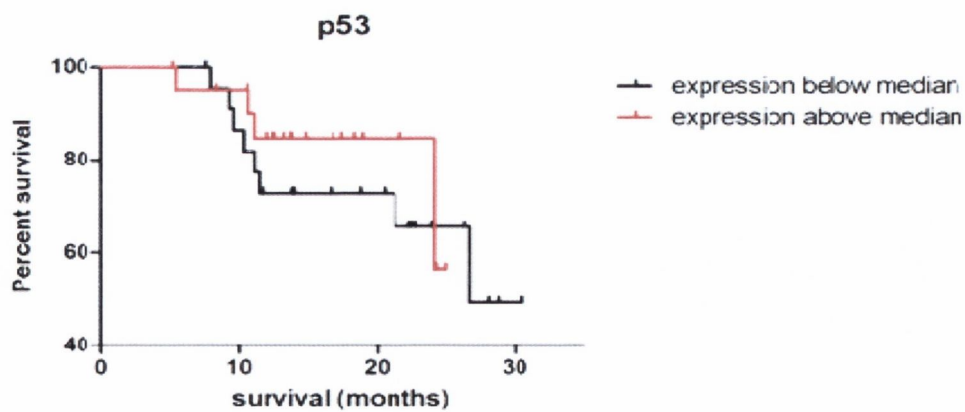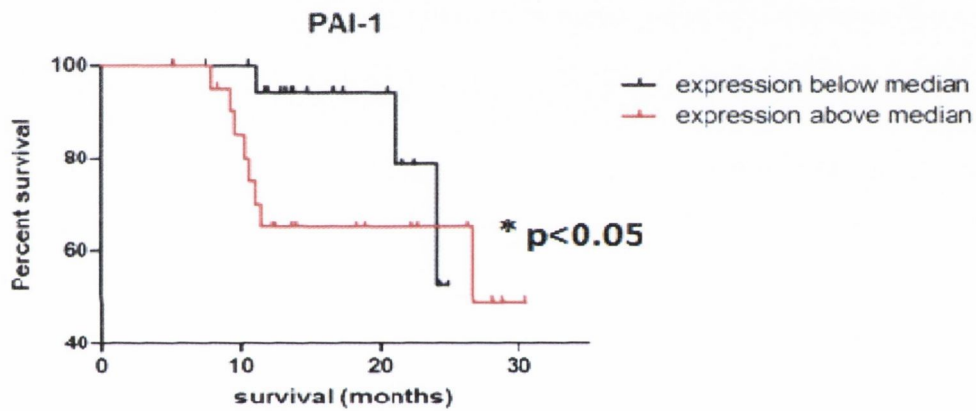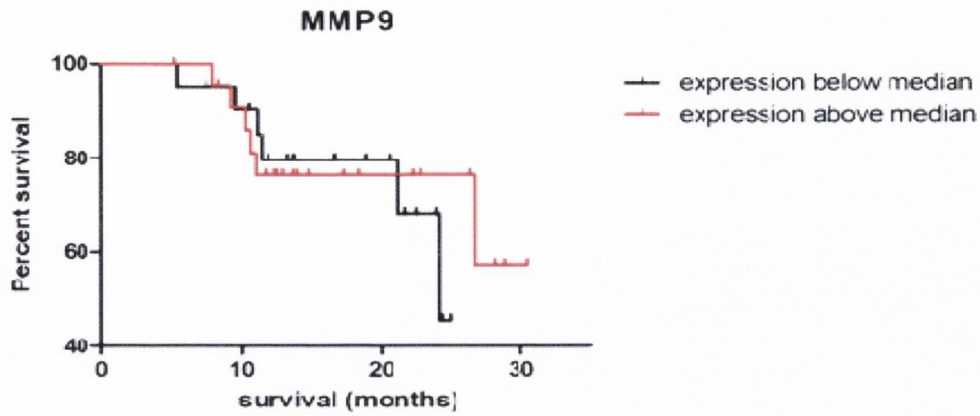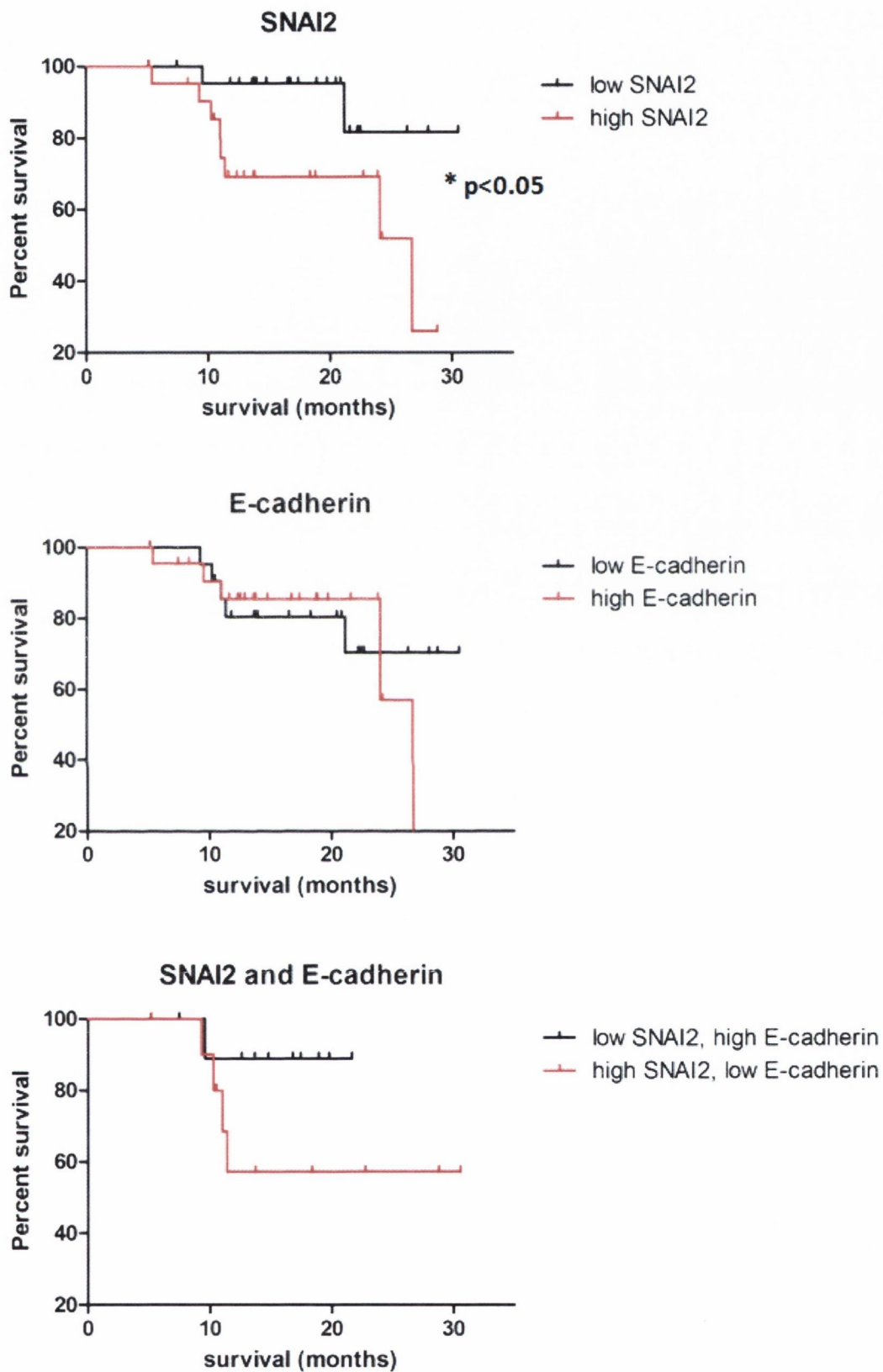
Figure 6.4: Kaplan Meiers analysis showing effect of SNAI2 and E-cadherin expression on survival in OAD. Gene expression was separated into above and below the median expression value. Statistical analysis was performed using the Gehan-Breslow-Wilcoxon test (*p<0.05).
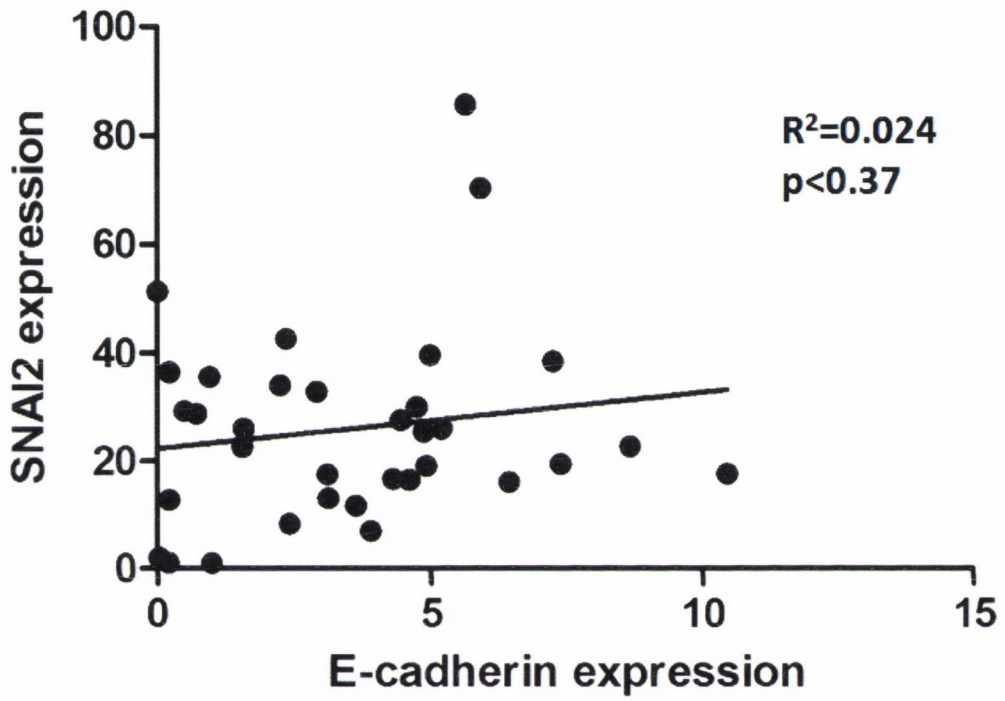
Figure 6.5: Correlation of SNAI2 and E-cadherin expression in male OAD patients. Statistical analysis was performed using linear regression analysis.

6.3.6 Immunohistochemical analysis

MMP inhibitor Prinomastat is currently being investigated in clinical trials for use in conjunction with neo-adjuvant therapy in oesophageal cancer treatment (Heath et al., 2006; Syrigos et al., 2008). This is the first study to demonstrate that high mRNA levels of MMP9 correlate with visceral obesity in OAD patients (section 6.3.1), and this finding could be of interest for treatment stratification of patients according to their obesity status. MMP9 was therefore selected for further investigation, and levels of protein expression were measured in OAD tumour biopsies by immunohistochemical (IHC) analysis of tissue microarrays (TMAs) (as described in section 2.14.2).

Although both PAI-1 and SNAI2 have been demonstrated to be independent prognostic indicators in both OAD (section 6.3.3, 6.3.5) and breast cancer (Harbeck et al., 2008), there are currently no ongoing clinical trials for these important markers of tumour invasion and metastasis. This study was the first, not only to identify PAI-1 and SNAI2 as independent prognostic factors in OAD, but also to demonstrate that high levels of these genes were associated with visceral obesity. However, the lack of appropriate commercially available antibodies against SNAI2 and PAI-1 prevented investigation of protein expression of these markers. A full face IHC study of SNAI2 and PAI-1 expression in OAD patients (n=20) using a range of antibody concentrations (1/50, 1/100, 1/500) failed to detect any tumour expression of these proteins (data not shown). When more appropriate antibodies against these proteins become available it would be of great interest to investigate levels of protein expression of SNAI2 and PAI-1 in OAD.

6.3.7 Antibody optimisation

MMP9 was optimised in full face OAD tissue sections (as described in section 2.14.1) to enable specific detection of tumour cells relative to normal oesophagus, and to allow discernment of expression variability across tumours from different patients. Antibody dilutions of 1/100 and 1/500 resulted in strong staining of both tumour and surrounding stroma (Figure 6.6). An antibody dilution of 1/1000 resulted in specific staining of tumour cells while allowing discernment of variability in MMP9 expression within different areas of tumour (Figure 6.6). TMA staining was carried out in collaboration with Dr Robert Cummins at Beaumont Hospital, Dublin 9, Ireland using a Bond III automated immunostainer (Leica Microsystems, Wetzlar, Germany) (as described in section 2.14.2). Antibody concentrations were re-optimised using this automated platform and an antibody dilution of 1/2000 was found to allow optimal

219

detection of variability of MMP9 expression across tumours from different patients (Figure 6.7).

6.3.8 Tissue microarray construction

Tissue microarrays (TMAs) were constructed from resected tumours of patients undergoing surgery for OAD or SCC between 1998 and 2010. Limited BMI information exists for patients who underwent surgery prior to July 2007, while BMI, WC and VFA information exists for all patients who underwent surgery after July 2007, the date of commencement of the adipose tissue biobank and associated obesity research projects (Table 6.7). Tumour biopsies were immediately taken from fresh tumour tissue, processed in formalin and embedded in paraffin wax by a designated biobank technician (Ennis et al., 2010) (as described in section 2.14). Areas of viable tumour in the tissue blocks were identified by an experienced pathologist and cores of these areas were taken in triplicate for each patient. TMAs were constructed from triplicate cores of 14 oesophageal carcinoma patients. Two prostate cores were added to the top right of each TMA for orientation purposes (Figure 6.7).

Table 6.7: Anthropometric details for complete cohort of TMAs

No. subjects	198
Sex (male), n (%)	136 (68.7)
OAD, n (%)	158 (79.8)
Age at surgery, mean (range)	64.2 (26-84)
BMI (kg/m^2), mean (range)	25.8 (16.7-48.3)[†]
WC (cm), mean (range)	92.7 (67-121)[‡]
VFA (cm^2), mean (range)	148.4 (21.4-322.6)[~]
Neoadjuvant therapy, n (%)	102 (51.5)

[†]only available for 160 patients, [‡]only available for 46 patients, [~]only available for 41 patients
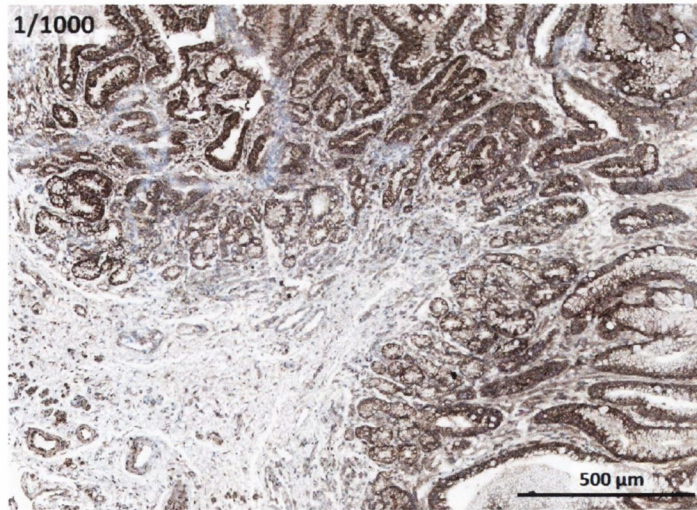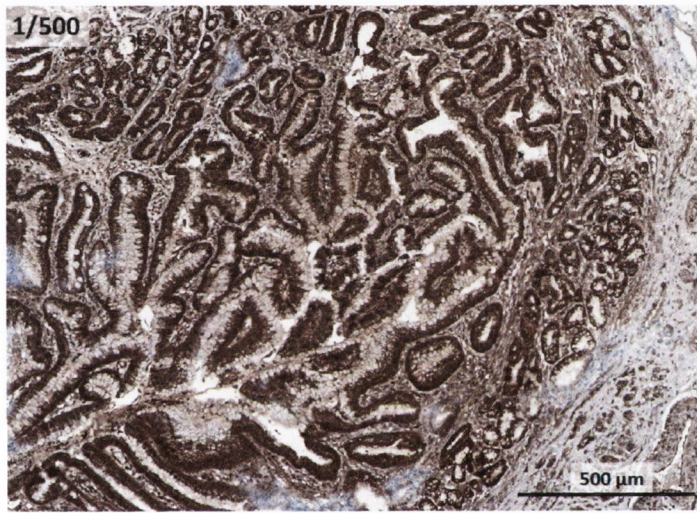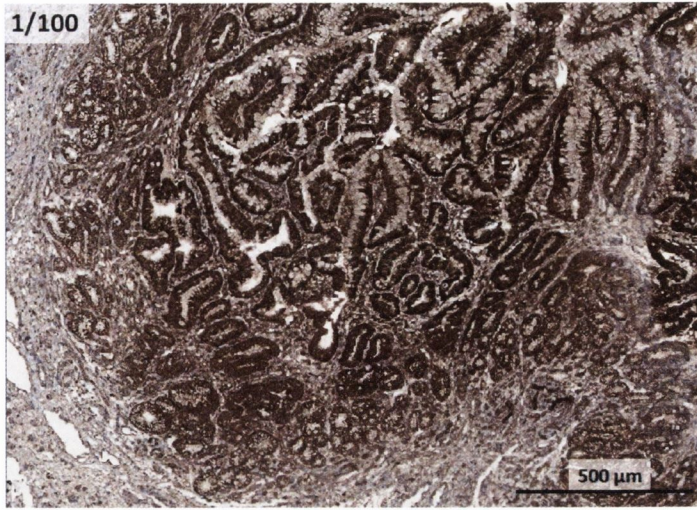
Figure 6.6: Optimisation of MMP9 in full face sections using antibody dilution of 1/100, 1/500 and 1/1000. Slides were scanned using Image Pro-Plus 4.1 software and images were saved at a magnification of 10 X.
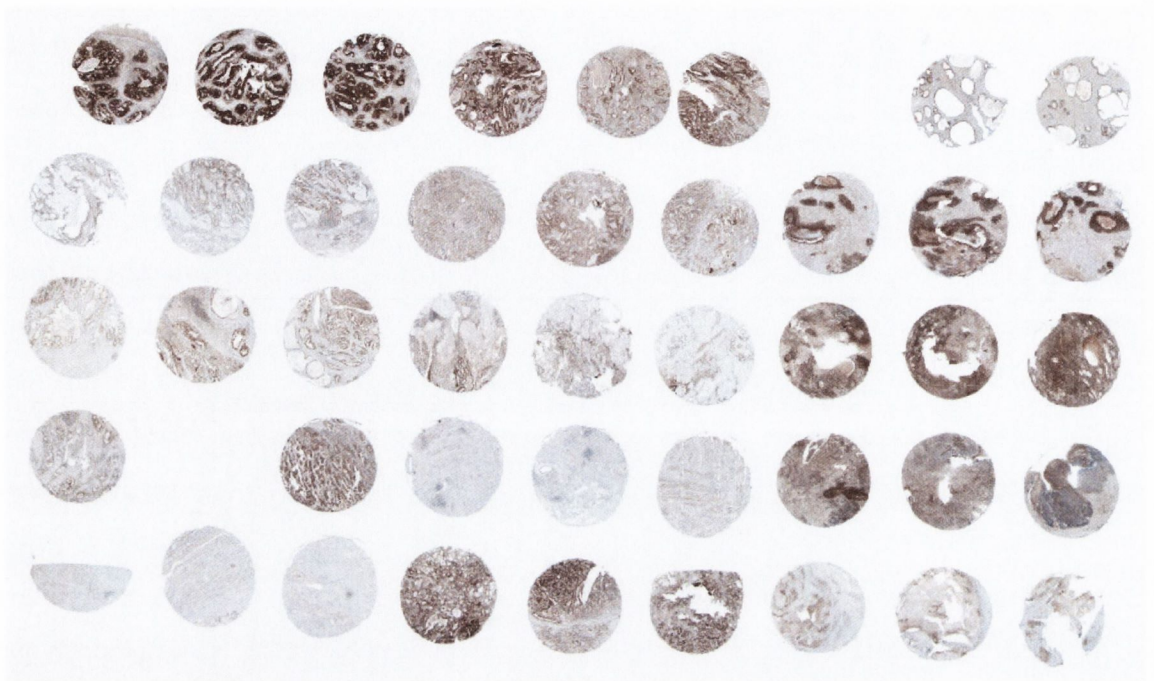
Figure 6.7: Representative MMP9 oesophageal carcinoma tissue microarray. Areas of tumour are identified in tissue blocks by a pathologist. Tumour cores 2 mm in width from each patient block are taken in triplicate and paraffin embedded to create a tissue microarray comprising 14 patients in total. Two prostate cores are included in the upper right corner of the TMA for orientation purposes.

6.3.9 Protein levels of MMP9 are elevated in visceral obesity.

Gene expression of MMP9 was significantly associated both with visceral obesity and with poor tumour differentiation (sections 6.3.1 and 6.3.2), and protein levels of this important marker of tumour invasion and metastasis were subsequently investigated in TMAs. TMAs were independently graded by three individuals, and the average score for each patient was determined (as described in section 2.14.3). Cores were analysed with respect to intensity and extent of staining with intensity graded 0 – 3 and extent in quartile percentages. Tissue cores representative of intensity scores of 0, 1, 2, and 3 are shown in Figure 6.8.
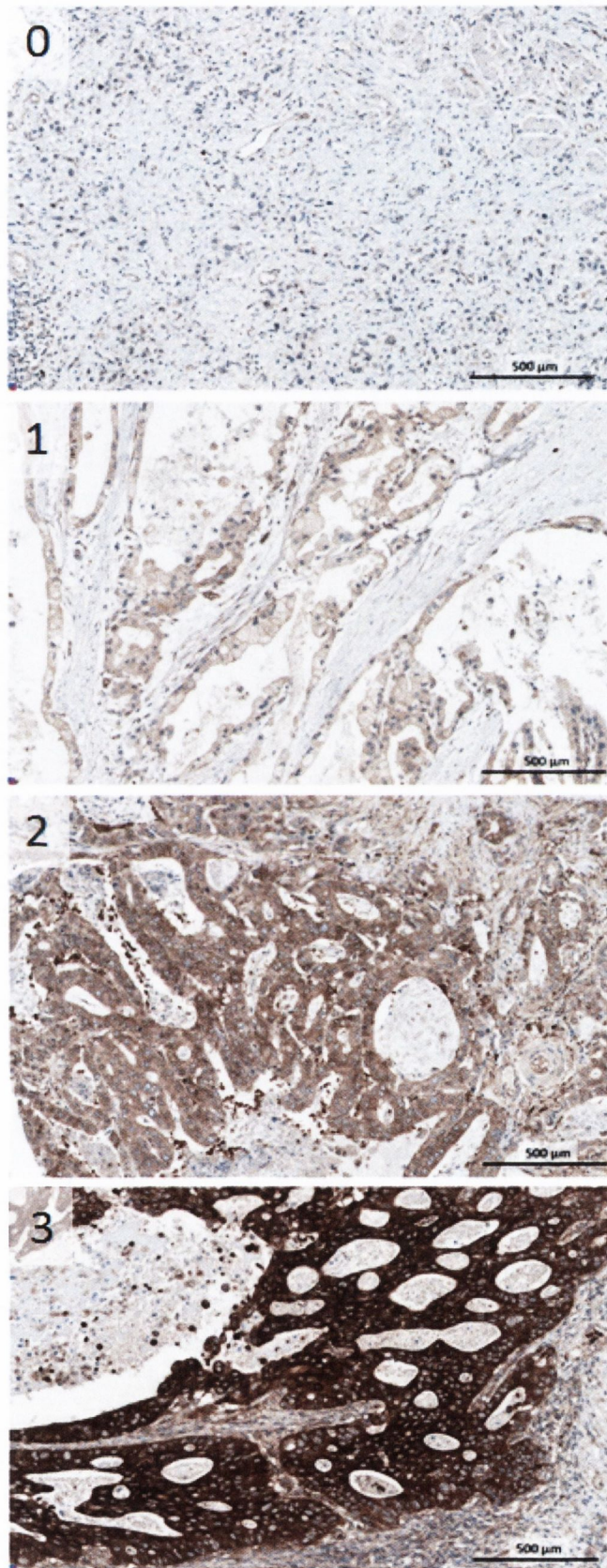
Figure 6.8: MMP9 TMA grading. TMAs were grading by three independent observers on a scale from 0, no expression, 1, low expression, 2, medium expression and 3, high expression. Slides were scanned using Image Pro-Plus 4.1 software and images were saved at a magnification of 10 X.

While there was no difference in tumour MMP9 expression between male and female patients or between OAD and SCC patients, expression of MMP9 in stroma was significantly elevated both in female patients ($p<0.01$) and in SCC patients ($p<0.05$) (Figure 6.9). Therefore, in order to avoid these potentially confounding factors, it was decided to proceed with analysis in a cohort of male OAD patients (Table 6.8).
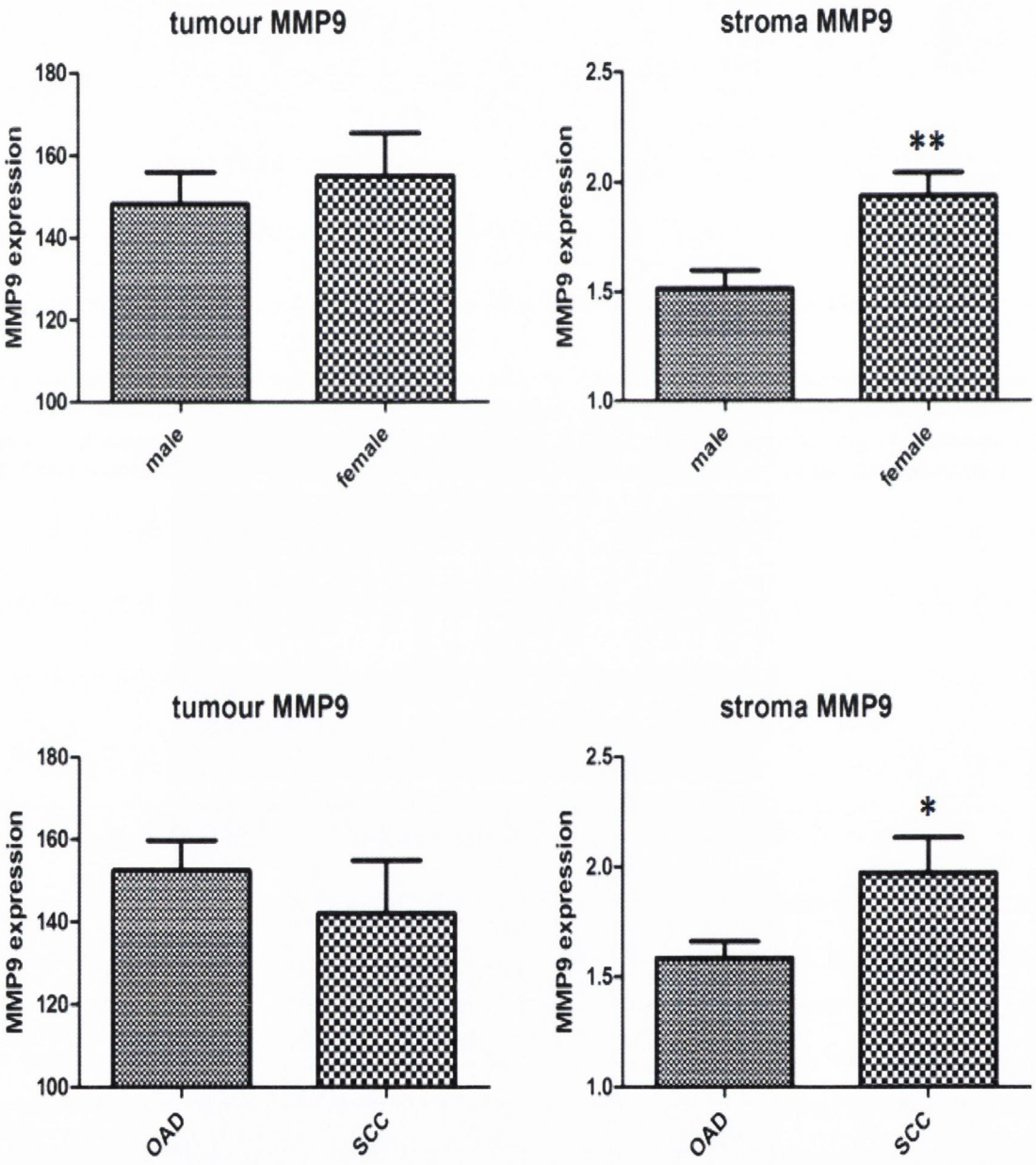
Figure 6.9: Levels of MMP9 expression in tumour and stroma of TMAs. Patients were grouped by male (n=136) and female sex (n=62) and by OAD (n=158) and SCC (n=40) tumour type. Statistical analysis was carried out by unpaired student's t test. (*p<0.05)

Table 6.8: Anthropometric details for male OAD patients included in TMA analysis.

no. subjects	114
sex (male), n (%)	114 (100)
diagnosis	OAD
age at surgery, mean (range)	64.5 (30-84)
BMI (kg/m^2), mean (range)	26.45 (17.43-43.26) [†]
WC (cm), mean (range)	97.96 (79-121) [‡]
VFA (cm^2), mean (range)	183.84 (27.1-322.6) [~]
neoadjuvant therapy, n (%)	43 (37.7)

†only available for 84 patients, ‡only available for 31 patients, ~only available for 27 patients

Obesity status, available in a subset of male OAD patients, was determined by BMI (n=84), WC (n=31) and VFA (n=27) and was investigated with respect to protein expression of MMP9. Clinicopathological parameters of tumour biology in male OAD patients (n=114) were analysed with respect to protein expression of MMP9; these were tumour differentiation, lymph involvement, venous involvement, perineural involvement, pathological tumour (T) category and pathological node (N) category. Statistical analysis of MMP9 expression and tumour biology was performed using unpaired student t tests (as described in section 2.19). Although no association was found between high MMP9 gene expression and survival (section 6.3.3), it was subsequently investigated whether protein expression of MMP9 was correlated with patient survival in male OAD patients. Patients who had died of other causes, or post-operative deaths were excluded from analysis, giving a final cohort size of n=94. Protein expression of MMP9 above or equal to the median was designated 'high' while expression below the median was designated 'low'. Statistical analysis of patient survival was carried out using the Kaplan-Meier estimator and the Gehan-Breslow-Wilcoxon statistical test in GraphPad Prism (as described in section 2.19).

As MMP9 is a marker of tumour invasion and metastasis, it was expected that high expression would be associated with more aggressive tumour biology and poorer patient prognosis. High gene expression of MMP9 was indeed found to significantly correlate with poor tumour

differentiation (section 6.3.2). However, in direct contrast with these results, high protein expression of MMP9 in tumour was inversely associated with tumour differentiation (p<0.02) (Table 6.9). Additionally, while high MMP9 gene expression was shown to have no effect on patient survival (section 6.3.3), high protein expression of MMP9 was near significantly associated with improved patient prognosis (p<0.07) (Figure 6.13). These findings at the protein level were counterintuitive and in direct conflict with results demonstrated at the gene level. Indeed, linear regression analysis of MMP9 expression in a subgroup of matched patients (n=15) revealed that gene and protein expression did not correlate (r^2=0.022, p<0.6141) (Figure 6.11). There are several explanations for these apparently conflicting results between gene and protein expression. MMP9 is an enzyme secreted by the tumour cell into the microenvironment where it functions to degrade the ECM to allow tumour invasion and metastasis (Belotti et al., 2003). Therefore, MMP9 staining was re-graded based solely on the stromal compartment of the tumour. A staining intensity score on a scale of 0 to 3 was allocated to the stromal compartment within each tumour core, with 0 representing negative expression and 3 representing strong expression (Figure 6.10). Tumour expression of MMP9 correlated significantly with stromal expression of MMP9 (Figure 6.12). This result suggests, intuitively, that high protein levels of tumour MMP9 lead to high levels of secreted MMP9 in the surrounding tumour microenvironment. While tumour MMP9 did not correlate with visceral obesity status, stromal MMP9 expression was 1.4 fold higher in viscerally obese patients, measured by visceral fat area (Table 6.9). However, this result did not reach statistical significance (p<0.2), perhaps due to much reduced sample size of the cohort on which VFA information exists (n=27). There was no difference in stromal MMP9 expression with respect to clinicopathological markers of tumour biology (Table 6.9) and altered stromal MMP9 expression had no effect on patient prognosis (Figure 6.13). However, the measurement of stromal expression of MMP9, involved in the pathological alteration of the tumour microenvironment, could be of great clinical relevance. MMP expression in the ECM surrounding the leading edge of the tumour could be of particular significance, as this is the area of tumour which is actively growing and potentially invading into the basement membrane. Although these TMAs do not include matched leading edge tumour samples, this may be an extremely relevant area for future studies. In addition, it would be of great interest to examine localisation of MMP9 activity in tissue using *in situ* zymography. As these proteolytic enzymes exist in a latent form prior to activation, it is possible that active rather than total MMP9 may be an important marker of aggressive tumour biology and patient prognosis.

Together these findings suggest that stromal expression of MMP9 may be the superior marker of tumour malignancy. MMP9 expression at both gene and protein levels is elevated in viscerally obese patients. Although high MMP9 gene expression is linked to poor tumour differentiation, protein MMP9 levels are not associated with markers of aggressive tumour biology. MMP9 expression alone is not associated with patient prognosis, however there may be potential for the use of MMP9 in combination with other biomarkers. These results suggest for the first time that MMP9 expression could be of use in treatment stratification of OAD patients according to their visceral obesity status.
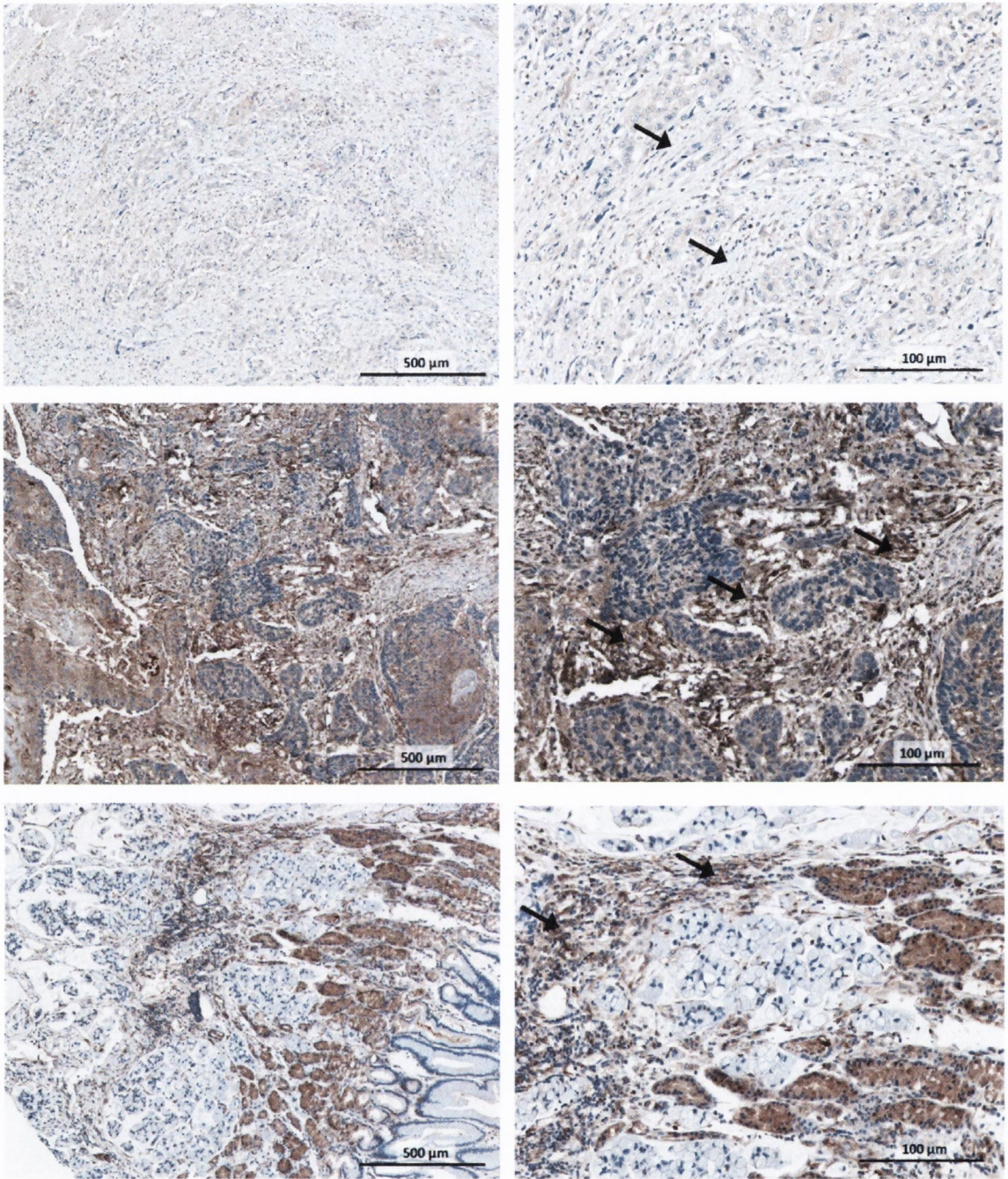
Figure 6.10: Representative images of MMP9 stromal staining. Slides were scanned using Image Pro-Plus 4.1 software and images were saved at a magnification of both 5 X and 20 X. The upper panel shows weak or absent stromal staining. The middle panel shows strong stromal staining. The lower panel shows MMP9 expression in the stroma surrounding the tumour leading edge.

Table 6.9: MMP9 protein expression in tumour and stroma.

	Tumour MMP9, mean (SEM)	p	Stroma MMP9, mean (SEM)	p
Age at diagnosis (years)		0.3280		0.9934
< median (65)	140.645 (12.44)		1.57 (0.1342)	
≥ median (65)	158.838 (13.558)		1.569 (0.1117)	
Body mass index (kg/m^2)		0.1890		0.4941
Non obese < 30	149.072 (10.859)		1.547 (0.097)	
Obese ≥ 30	183.803 (22.03)		1.376 (0.201)	
Waist circumference (cm)		0.2579		0.3502
Non obese < 94 (M), 80 (F)	201.486 (30.154)		1.375 (0.267)	
Obese ≥ 94 (M), 80 (F)	162.54 (18.705)		1.696 (0.198)	
Visceral fat area (cm^2)		0.9782		0.1931
Non obese < 130 cm^2	186.415 (36.89)		1.375 (0.249)	
Obese ≥ 130 cm^2	187.408 (17.308)		1.863 (0.184)	
Tumour differentiation		*0.0165*		0.8173
Well/moderate	167.45 (11.35)		1.554 (0.107)	
Poor/undifferentiated	122.22 (14.78)		1.595 (1.146)	
Pathological tumour category		0.3243		0.8743
T0 – T1	171.146 (25.153)		1.548 (0.187)	
T2 – T3	146.138 (9.915)		1.587 (0.098)	
Pathological node category		0.1290		0.7992
N0	167.841 (16.237)		1.542 (0.143)	
N1	138.826 (11.05)		1.587 (0.109)	
Lymph node involvement		0.4979		0.7905
Yes	146.525 (11.058)		1.557 (0.097)	
No	160.668 (18.206)		1.607 (0.179)	
Venous involvement		0.4232		0.4524
Yes	141.404 (14.605)		1.635 (0.115)	
No	156.541 (12.084)		1.503 (0.133)	
Perineural involvement		0.1942		0.9326
Yes	135.832 (12.952)		1.561 (0.134)	
No	160.266 (12.769)		1.567 (0.114)	

MMP9 expression is described as mean (SEM), statistical analysis was carried out using an unpaired student's t-test. Statistically significant pvalues < 0.05 are highlighted in red.
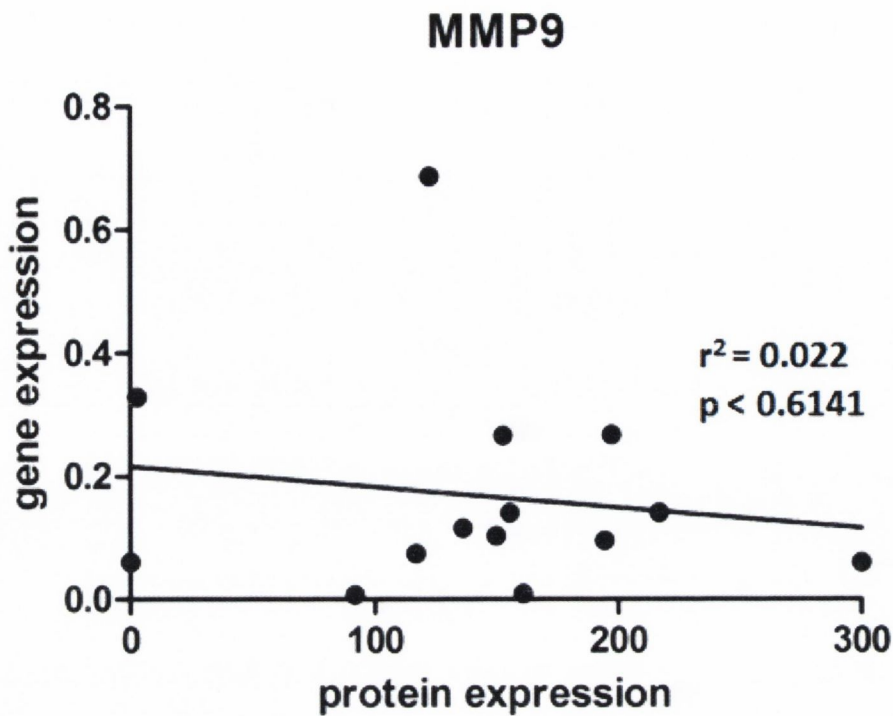
Figure 6.11: Correlation of gene and protein expression of MMP9 in a cohort of matched patients (n=15). Statistical analysis was performed using linear regression analysis.
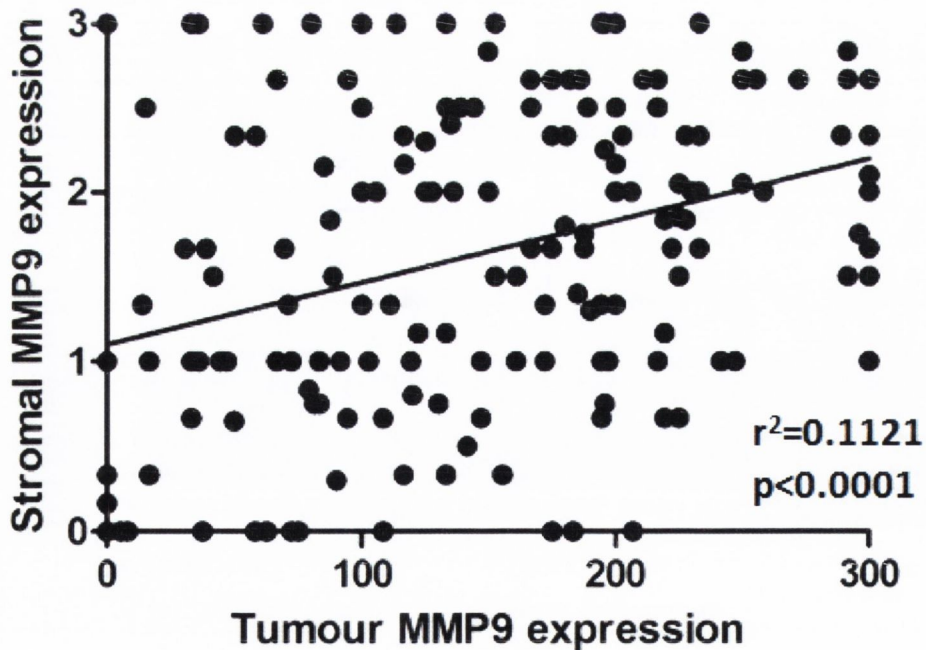
Figure 6.12: Correlation of tumour and stromal MMP9 protein expression (n=114). Statistical analysis was performed using linear regression analysis.
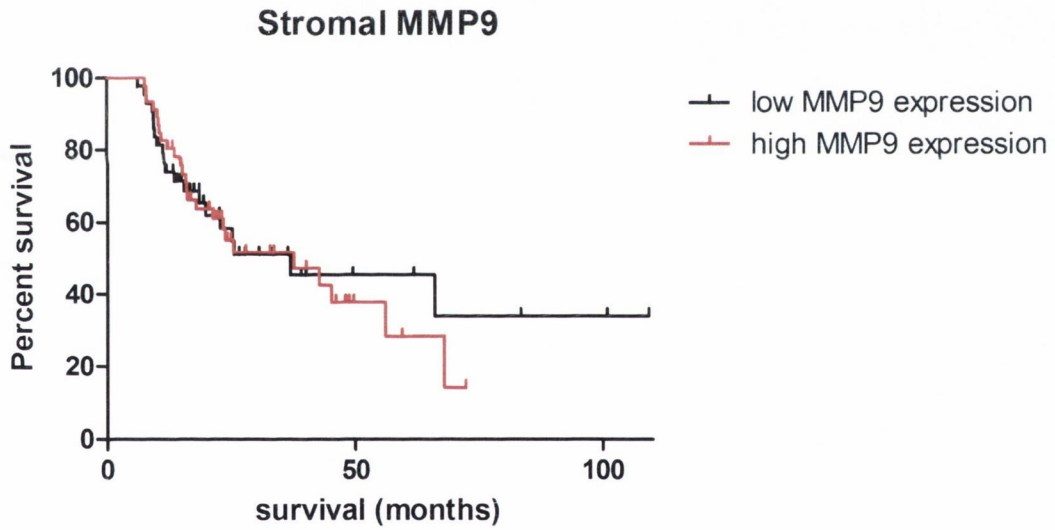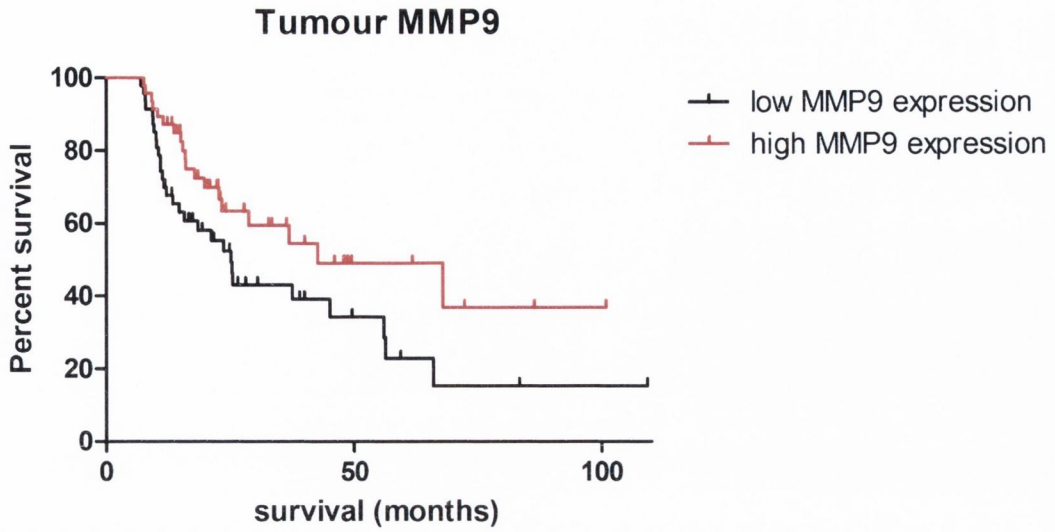
Figure 6.13: Kaplan Meiers analysis showing effect of stromal and tumour MMP9 protein expression on survival in OAD. Gene expression was separated into above and below the median expression value. Statistical analysis was performed using the Gehan-Breslow-Wilcoxon test.

6.4   Discussion

An *in vitro* experimental model was utilised to discover altered pro-tumour pathways induced in OAD by co-culture with adipose tissue. Affymetrix microarray technology identified genes involved in pathways of invasion and metastasis (MMP9, PAI-1), cell cycle control (p53) and EMT (SNAI2, E-cadherin). To investigate the role of these markers in patients, mRNA and protein levels were measured in OAD tumour biopsies. This research will contribute to the improved understanding of altered hallmark pathways of OAD in visceral obesity and could eventually lead to stratification of patient treatment based on the individual's obesity status.

Gene expression of markers of invasion and metastasis MMP9 and PAI-1 were found to be significantly elevated in the tumours of viscerally obese OAD patients, suggesting a novel role for these genes in obesity fuelled cancer. In addition, poor tumour differentiation was significantly associated with elevated MMP9 and reduced p53 gene expression. It is widely accepted that carcinogenesis can occur via regression of tumour cells to a dedifferentiated state, and p53 has been implicated as a master regulator of this process (Molchadsky et al., 2010). This process of dedifferentiation has also been demonstrated to be an important molecular alteration in the sequence of malignant transformation of the normal oesophagus to Barrett's oesophagus to adenocarcinoma (Helm et al., 2005). Therefore this novel association of marker of tumour dedifferentiation, MMP9, with visceral obesity may have important implications for the understanding of obesity fuelled neoplastic progression. Although not statistically significant, high MMP9 and PAI-1 gene expression were associated with more advanced pathological tumour and nodal stage and with lymphatic, haematogenous and perineural dissemination of malignant tumour cells. MMP9 has previously been associated with nodal metastasis and poor tumour differentiation in cervical (Yu et al., 2009) and oesophageal squamous cell carcinoma (Gu et al., 2005b). While PAI-1 has been linked with poor prognosis in many cancers including breast (Harbeck et al., 2004; Sternlicht et al., 2006), gastric (Nekarda et al., 1994), rectal (Angenete et al., 2009; Langenskiold et al., 2009) and colorectal carcinoma (Sakakibara et al., 2005), this study is the first to demonstrate an association with OAD prognosis. Intriguingly, PAI-1 was also associated with visceral obesity in OAD, highlighting a molecular mechanism by which visceral obesity could give rise to increased cancer mortality. The novel association of MMP9 and PAI-1 with visceral obesity highlights a role for visceral obesity in the aggressive tumour biology and poor prognosis associated with OAD.

In addition to MMP9 and PAI-1, epithelial mesenchymal transition (EMT) regulator SNAI2 has also been implicated in pathways of tumour invasion and metastasis. SNAI2 was originally identified to be important in chick embryonic development where it is expressed in cells undergoing EMT (Nieto et al., 1994). It is now known that the process of EMT is necessary not only for development but is also of great importance in tumour invasion and metastasis (Alves et al., 2009). The process of EMT occurs via down regulation of epithelial markers and up regulation of mesenchymal markers culminating in the disappearance of cell junctions and reorganisation of the cytoskeleton enabling increased cell motility (Alves et al., 2009). SNAI2 is a well established transcriptional regulator of EMT demonstrated to play a fundamental role in the down regulation of key epithelial cell markers such as E-cadherin, resulting in increased epithelial tumour cell migration and invasion. SNAI2 over expression is associated with poor prognosis in breast (Come et al., 2006; Martin et al., 2005), oesophageal squamous cell (Kumar et al., 2007) and colorectal carcinoma (Shioiri et al., 2006) and this is the first study to demonstrate an independent association with OAD prognosis. In addition, this novel study demonstrated that gene expression of SNAI2 was increased twofold, while gene expression of its target, E-cadherin, was decreased twofold in tumours from viscerally obese OAD patients. This highlights a molecular mechanism by which visceral obesity may contribute to the poor prognosis of OAD by increasing the tumour cell motility via down regulation of cell adhesion molecules. This finding is particularly relevant in the context of increased migratory and invasive capacity of oesophageal adenocarcinoma cell lines following treatment with ACM. In OAD, nuclear localisation together with increased expression of transcription factor SNAI2 has been demonstrated in the progression from Barrett's oesophagus to OAD. In addition, transfection of SNAI2 into OAD cell line OE33 caused E-cadherin repression and induction of mesechymal markers vimentin and fibronectin (Jethwa et al., 2008). In another study, SNAI2 transfection of OAD cell line TE7 increased invasiveness while SNAI2 knockdown in the OE33 cell line decreased invasiveness and increased apoptosis. Mice injected with SNAI2 silenced OE33 has significantly less seeded tumour and more tumour apoptosis. On the other hand, mice injected with SNAI2 over expressing TE7 had significantly more seeded tumour (Zhang et al., 2010). Together these studies in OAD indicate the importance of SNAI2 and EMT in the malignant progression from Barrett's to adenocarcinoma, and in OAD tumour invasiveness. Interestingly, SNAI2 over expression is not always associated with E-cadherin repression (Alves et al., 2009). In this study, gene expression levels of SNAI2 and E-cadherin did not correlate with each other, and E-cadherin was not associated with OAD prognosis. These findings suggest an E-cadherin independent role for SNAI2, which has been demonstrated in several cancers. In breast cancer SNAI2 correlates with E-cadherin expression in cell lines (Come et al.,

2006; Hajra et al., 2002) but not in primary tumours (Come et al., 2006; Martin et al., 2005). In oesophageal squamous cell carcinoma, high protein levels of SNAI2 were significantly associated with prognosis in tumours with intact E-cadherin expression, indicating that SNAI2 is important in promoting tumour invasion independent of E-cadherin repression (Uchikado et al., 2005). Future work needs to be conducted to investigate poorly understood E-cadherin independent mechanisms by which SNAI2 is associated with tumour invasion and metastasis.

Although PAI-1 and SNAI2 were promising candidates to follow through to the protein level, difficulties with antibody optimisation prevented TMA staining with these antibodies. Despite mixed success, clinical trials are already underway for inhibitors of MMPs, demonstrating the potential translational relevance of MMPs in treatment of oesophageal (Heath et al., 2006; Syrigos et al., 2008), breast (Sparano et al., 2004) and lung cancers (Shepherd et al., 2002). While MMP inhibitors have not been widely studied in OAD, the existence of therapies at clinical trial stage provides the potential to carry this work through the clinic. Tumour biopsies, used to examine gene expression, commonly contain a heterogenous mix of stromal tissue and tumour tissue which is representative of the tumour *in vivo*. Therefore gene expression of both tumour and microenvironment is assessed simultaneously in extracted RNA. On the other hand, TMAs enable localisation of protein expression as they contain viable areas of tumour in addition to areas of stroma. Surprisingly, and in direct contrast to gene expression results, high protein levels of MMP9 were found to be associated with well differentiated tumours, with less advanced pathological tumour and nodal stage and with improved patient prognosis. In addition, comparison of gene and protein levels in 15 matched patients demonstrated that protein expression did not correlate with gene expression. While contradiction of gene and protein expression levels of MMP9 was unexpected, it was hypothesised that secretion of MMP9 into the stromal compartment may be responsible for this confounding result. MMP9 is an extracellular protease which specifically degrades the major structural component of the basement membrane, collagen IV, to facilitate tumour invasion. This suggests significant involvement of the stromal compartment and, for this reason, analysis of peritumoural stroma expression of MMPs has been previously examined in colorectal carcinoma (Jensen et al., 2010), salivary gland adenoma (Zhang et al., 2009) and squamous cell carcinoma of the skin (Vosseler et al., 2009). In this study, elevated stromal expression of MMP9 was found to be associated with visceral obesity, however, no association of stromal MMP9 expression was found with markers of tumour biology or patient prognosis. For future work, it may be important to investigate stromal expression of MMP9 surrounding the leading invasive edge of the tumour. However, the association of MMP9 gene expression with poor tumour

differentiation identifies the potential usefulness of this gene as a biomarker and therapeutic target in OAD. There is also the possibility that MMP9 could be more informative when used in combination with other biomarkers, and this could be investigated in future studies. However, the identification of an association of MMP9 expression with visceral obesity in OAD could lead to improved treatment stratification of patients according to obesity status.

While initially promising, clinical trials investigating the use of inhibitors of MMPs to date have been met with mixed results (Coussens et al., 2002), due in part to poor specificity resulting in high toxicity (Radisky and Radisky, 2010). While more work needs to be carried out in the clinical trial setting, this work has identified PAI-1 and SNAI2 as additional targets for therapeutic strategies targeting pathways of tumour dissemination. In conclusion, this work demonstrates a novel prognostic role of PAI-1 and SNAI2 in OAD. In addition, a novel association of markers of tumour metastasis with visceral obesity has been identified, highlighting the potential for future application of MMP9, PAI-1, SNAI2 and E-cadherin in the treatment stratification of viscerally obese OAD patients.

7 General discussion

Oesophageal adenocarcinoma (OAD) is a highly aggressive disease with poor five year survival, due in part to early haematogenous and lymphatic dissemination (Lagarde et al., 2007). Strong epidemiological evidence links OAD incidence to visceral obesity however the molecular mechanisms linking these remain poorly understood. The overall aim of this thesis was to dissect the molecular pathways linking obesity with OAD and to determine if obesity is associated with increased aggressiveness of this disease. Uncovering the mechanisms of interaction of visceral obesity and cancer could identify shared pathways as potential preventative and therapeutic targets. This strategy may be particularly relevant in the development of stratified therapies to target viscerally obese OAD patients.

The excess accumulation of visceral adipose tissue, rather than overall adiposity, has recently been identified to be largely responsible for obesity related pathologies (Federation, 2006), including OAD (Beddy et al., 2010). Indeed, it was demonstrated in this thesis that the omental adipose tissue depot secreted higher levels of both the pro-inflammatory adipokine, IL-6, and the pro-angiogenic adipokine, VEGF, compared to matched subcutaneous depots. IL-6, in addition to its pro-inflammatory effects, has been demonstrated to induce VEGF transcription (Wei et al., 2003), implying an important role for this adipokine in angiogenesis. It was also demonstrated that visceral obesity was associated with increased circulating levels of leptin, IL-6, MCP-1 and VEGF, and decreased circulating levels of the anti-inflammatory adipokine adiponectin, relative to normal weight. MCP-1 is known to be important in the establishment of a chronic pro-inflammatory environment through its role in macrophage recruitment into expanding adipose tissue (Duffield, 2003), particularly in the visceral depot (Kintscher et al., 2008). Together, these findings identify pro-inflammatory, pro-angiogenic and pro-proliferative mediators which may contribute to visceral obesity associated pathogenesis. Interestingly, circulating levels of IL-6 and IL-8 were also significantly elevated in cancer patients, independent of obesity status, sex and neoadjuvant therapy. Chronic inflammation is a hallmark of cancer, linked to tumour survival, proliferation and angiogenesis (Colotta et al., 2009), and levels of IL-6 and IL-8 have previously been demonstrated to be raised in non small cell lung cancer (Wojcik et al., 2010). These data therefore highlight shared pro-inflammatory and pro-angiogenic pathways in both visceral obesity and cancer. Altered levels of these adipokines, cytokines and chemokines in visceral obesity could contribute to the generation of an environment favourable for tumourigenesis. There is increasing evidence that leptin, in addition to its role in the development of insulin resistance, can exert a proliferative effect on tumour cells (Ogunwobi and Beales, 2008, Hu et al., 2002). It was demonstrated in this thesis that treatment of OAD cell lines with leptin increased their proliferative capacity, while

adiponectin decreased their proliferation, respectively. While both OE33 and OE19 expressed basal levels of receptors for these adipokines, serum depletion was found to induce receptor expression in OE33. This finding suggests increased responsiveness of a rapidly growing, hypoxic tumour to the altered circulating adipokine profile characteristic of visceral obesity. ACM, comprising many soluble factors including both pro- and anti-growth adipokines, was found to induce proliferation in OAD cell lines. Although there was no additional proliferative effect observed in ACM from viscerally obese patients, the increased bulk of adipose tissue in viscerally obese patients could potentially contribute to an increased effect *in vivo*. The altered balance of soluble mediators of inflammation, angiogenesis and proliferation suggests molecular mechanisms whereby paracrine effects exerted by the presence of excess visceral adipose tissue could fuel tumourigenic pathways. Elevated levels of IL-6 and IL-8 in visceral obesity and cancer could represent potential therapeutic targets in OAD, and these may be particularly relevant in viscerally obese individuals.

Using high throughput microarray technology, pathways involved in inflammation and angiogenesis were demonstrated to be up regulated in the omentum of viscerally obese patients. Notably, sphingolipid metabolism was one of the most up regulated pathways, via significant induction of regulatory enzymes ASAH1, PAP and DEGS1. This pathway has previously been demonstrated to be up regulated in skeletal muscle of obese insulin resistant individuals relative to lean, insulin sensitive individuals (Adams et al., 2004). Circulating factors associated with obesity such as saturated fatty acids and pro-inflammatory cytokines, IL-1 and TNFα, have been shown to induce enzymes that promote sphingolipid metabolism (Holland and Summers, 2008). Inhibition of ceramide synthesis in high fat diet mouse models prevented the development of insulin resistance, indicating an important role for sphingolipid metabolism in obesity related pathologies (Holland et al., 2007). Pharmacological reduction of glycosphingolipids in mice has been demonstrated to improve insulin sensitivity and decrease adipose tissue inflammation (van Eijk et al., 2009), in part via reduction of PAI-1 and MCP-1 levels (Yang et al., 2009). Management of glycosphingolipid levels may therefore be an interesting approach for therapeutic intervention in obesity related human disease. In addition, recent developments in treatment of gastrointestinal cancers have focussed on targeting of epidermal growth factor receptors EGFR and ErbB2 using inhibitors such as cetuximab, trastuzumab and gefitinib, with some success (Ferry et al., 2007; Safran et al., 2008). MAPK, PI3K and STAT are the major signalling pathways targeted by these receptors and play important roles in cellular processes of survival, proliferation and inflammation. Individual components belonging to these pathways, MEK1, PI3K regulatory subunit 3, protein

tyrosine phosphatase non-receptor 11 and STAT5B, were all significantly up regulated in the omentum of viscerally obese OAD patients. These pathways may therefore offer potential downstream targets of EGFR for the development of new obesity related targeted therapies in gastrointestinal cancer.

BMI is a measure of overall adiposity and therefore does not take into consideration either composition of body mass or distribution of adipose tissue (Hu, 2007). Meanwhile, visceral adiposity has been shown to be a stronger predictor of related morbidity and mortality than overall obesity (Gesta et al., 2006; Giorgino et al., 2005). While BMI is traditionally used to measure obesity, visceral fat area was demonstrated in this study to be the strongest predictor of obesity induced gene alterations in the omentum. This finding provides support for the use of VFA, or its surrogate measure WC, to determine an individual's risk of obesity related morbidity and mortality. It is important to note that the presence of visceral obesity measured by a WC of greater than 80 cm for women or 94 cm for men is the underlying requirement for classification of patients using the International Diabetes Federation definition of the Metabolic Syndrome. While less than 25% of adults in Ireland are classified as obese by BMI, over 60% of adults are classified as obese by WC, a surrogate measure of visceral obesity (Survey of Lifestyle, Attitudes and Nutrition (SLAN), 2007). Indeed, the recent IDF definition increases the population prevalence of Metabolic Syndrome by approximately 20% (Donohoe et al., 2010). The data in this thesis underline the significant role of visceral adipose tissue in the development of a circulating state of chronic low grade inflammation characteristic not only of visceral obesity (Xu et al., 2003), but also of tumourigenesis (Colotta et al., 2009). Deregulation of the balance of circulating inflammatory mediators therefore indicates a potential mechanism by which visceral adiposity may fuel the tumourigenic process.

The study of molecular interactions between cell types in obesity and cancer relies upon *in vitro* models for preliminary identification of pathways in the context of a simplified and controlled system. This approach is ideally followed by validation of identified pathways in context of the tissue microenvironment *in vivo*. The use of model systems in obesity research has traditionally relied upon the well characterised murine 3T3 adipocyte cell lines. However, in studies of human disease, greater clinical relevance would be derived from working with both human cell lines and human tissue. This thesis has demonstrated the recently available SGBS human adipocyte cell strain to be similar to primary human adipocytes in terms of morphology, adipocyte specific gene expression and function. SGBS expressed comparable levels of leptin, LPL, AP2 and PPARγ, necessary for adipocyte function, to human primary

239

adipocytes. Furthermore, co-culture of the OE33 cell line with SGBS or with primary human adipocytes induced similar gene alterations in OE33, specifically down regulation of tumour suppressor ATM and up regulation of MMP2, involved in tumour invasion and metastasis. These data highlight the translational relevance of the SGBS cell line in the study of molecular interactions in obesity and cancer. However, the study of adipocytes alone fails to acknowledge the important contribution of the adipose tissue SVF, containing fibroblasts, immune cells, endothelial cells and pre-adipocytes. Indeed, while co-culture with both SGBS and primary human adipocytes induced gene changes in pro-tumour pathways in OE33, co-culture with whole adipose tissue induced the most pronounced gene alterations. This finding underlines the fundamental role of the tissue microenvironment in adipose tissue, and highlights the advantages of the use of adipose tissue explants, as employed in this thesis. Similarly, in solid tumours, immune cells and endothelial cells play pivotal roles in the establishment of the pro-inflammatory and pro-angiogenic state which is of great significance in the tumour microenvironment. Despite these possible shortcomings, the use of this model co-culture system demonstrated potential mechanisms by which biological pathways involved in tumourigenesis are altered in visceral obesity.

In the study of poorly understood complex pathophysiological disease processes such as obesity and cancer, it is important to begin by examining global pathway alterations before proceeding to single gene analysis, as these disease processes most certainly involve deregulation of multiple gene networks. Genes and pathways altered in the model co-culture system were discovered using microarray technology, ideally suited for delineation of complex networks at play in both obesity and cancer. Alternative techniques employed to study gene expression, such as PCR and Northern blotting, measure single gene alterations and therefore can run the risk of literature bias, created by selecting known function, previously published genes. At the same time, these more sensitive techniques are indispensible for technical and biological validation of the microarray and subsequent studies in pathway dissection and single gene and biomarker analysis. The strength of microarray technology is largely dependent on the quality of RNA samples analysed, in addition to the quality of the analysis conducted. The stringent quality control measures applied at all stages of the process, from sample extraction, sample hybridisation and array analysis, was therefore a great strength of this study. Validations at the mRNA level were carried out in an independent cohort using the robust, reliable and sensitive qPCR technique. Subsequent validations at the protein level were carried out using a variety of techniques including Western blotting, FACS and High Content Screening analysis. Finally, functional assays were conducted to examine *in vitro* effects of gene

alterations in OAD cell lines. A two stage approach was adopted in this thesis; the Human Cancer Profiler qPCR array was used to initially identify gene and pathway alterations in a small set of 84 genes, representative of the six hallmarks of cancer. These findings were subsequently validated and expanded using Affymetrix microarrays. The use of the comprehensive Affymetrix Human Genome U133 Plus 2.0 Array, custom designed by The European Nutrigenomics Organisation (NuGO) to contain a selection of nutrition and obesity related genes, was a positive aspect of this study. Furthermore, collaboration with a highly experienced bioinformatician was indispensible to the success of this study. This powerful approach enabled the delineation of poorly understood molecular mechanisms responsible for the strong epidemiological association of visceral obesity and OAD.

The qPCR array was used to investigate gene alterations in OE33 following co-culture with SGBS adipocytes, primary human adipocytes and whole adipose tissue fragments. Co-culture of OE33 both with SGBS and with primary human adipocytes induced expression of MMP2, involved in invasion and metastasis, and reduced expression of cell cycle regulator ATM. The identification of these gene alterations following co-culture with both SGBS and primary human adipocytes highlights the functional relevance of the SGBS model for studies of obesity and cancer. However, whole adipose tissue induced the most pronounced gene alterations, indicating the important contribution of the stromal vascular fraction containing endothelial and immune cells. qPCR array analysis of OE33 following co-culture with whole adipose tissue also identified invasion, migration and cell cycle pathways to be altered, via up regulation of MMP2 and down regulation of ATM, as identified from the adipocyte co-cultures. While ATM was twofold down regulated following co-culture with both adipocytes and adipose tissue, MMP2 was altered to a greater extent in OE33 following co-culture with adipose tissue. This regulator of invasion and metastasis was up regulated 10 fold following co-culture with SGBS adipocytes and by 500 fold following co-culture with primary human adipocytes. While co-culture with adipocytes had no effect, co-culture with adipose tissue up regulated MMP9 and PAI-1 by 4,000 and 10 fold, respectively, and tumour suppressor p53 was down regulated twofold. Affymetrix microarray analysis of the *in vitro* co-culture model demonstrated increased glycolytic flux and up regulation of the focal adhesion pathway, promoting cytoskeletal reorganisation and epithelial mesenchymal transition (EMT). Rate limiting glycolysis enzymes hexokinase (HK) and phosphofructokinase (PFK), focal adhesion plaque components laminin-5, integrin α3, focal adhesion kinase and Src, and EMT regulator SNAI2 were all demonstrated to be significantly up regulated in OE33 following co-culture with adipose tissue by Affymetrix array technology. In addition, individual gene changes initially

identified by the Human Cancer Profiler qPCR arrays were subsequently validated by the Affymetrix microarrays. Down regulation of tumour suppressors p53 and ATM and up regulation of PAI-1 was identified in both arrays. However, significant alterations in MMP expression demonstrated by the qPCR array were not observed using Affymetrix microarray technology. Bioinformatic analysis of Affymetrix microarrays was far more stringent due to the increased risk of false positive results associated with multiple testing of over 15,000 genes included on the array. As a result, this high throughput technology is less sensitive and may not pick out subtle changes in gene expression. Therefore, all validations were subsequently carried out using qPCR technology, a robust and highly sensitive technique, followed by analysis of protein levels by Western blotting, flow cytometry and High Content Screening. Using gelatin containing SDS gels, zymography demonstrated increased MMP2 and MMP9 gelatinase activity in OE33 and OE19 cells following treatment with whole adipose tissue. This data indicated induction of functional MMP activity in OAD cell lines by adipose tissue. Subsequent functional assays identified an increase in migratory and invasive capacity of OAD cell lines following treatment with ACM, potentiated by the identified gene alterations in pathways of invasion and metastasis. Indeed, ACM from viscerally obese patients had the most pronounced effect of the migratory capacity of OE33, underlining the pathological importance of this depot. OAD is a disease associated with early lymphatic and haematogenous dissemination, implying these pathways of invasion and metastasis are of great significance. The induction of these pathways by adipose tissue could therefore suggest a molecular mechanism by which visceral obesity could give rise not only to increased incidence of oesophageal adenocarcinoma, but also increased tumour aggressiveness resulting in the early metastasis and high mortality associated with this disease.

Genes identified by qPCR and Affymetrix arrays were subsequently investigated in OAD tumour biopsies from this unit's tumour biorepository. A novel association was demonstrated between visceral obesity, elevated levels of MMP9, PAI-1 and SNAI2 and reduced levels of E-cadherin. Markers of tumour invasion and metastasis MMP9 and PAI-1 were elevated 7 fold and 5 fold, respectively, in tumours of viscerally obese OAD patients. EMT regulator, SNAI2, was up regulated twofold, while expression of cell adhesion molecule, E-cadherin, was decreased twofold in viscerally obese OAD patients. In addition, elevated expression of MMP9 and PAI-1 correlated with increased haematological and lymphatic dissemination. Poor tumour differentiation, a routinely measured histological marker of tumour malignancy, was associated with a six fold increase in MMP9 expression. While p53 was not associated with obesity, twofold decreased expression was significantly associated with poor tumour

differentiation. These findings imply an association of visceral obesity with aggressive tumour biology via up regulation of MMP9 and PAI-1 and down regulation of p53. While SNAI2 over expression has been associated with poor prognosis in breast (Come et al., 2006; Martin et al., 2005), oesophageal squamous cell (Kumar et al., 2007) and colorectal carcinoma (Shioiri et al., 2006), this was the first study to demonstrate an independent association with OAD prognosis. In addition, while PAI-1 has been linked with poor prognosis in many cancers including breast (Harbeck et al., 2004; Sternlicht et al., 2006), gastric (Nekarda et al., 1994), rectal (Angenete et al., 2009; Langenskiold et al., 2009) and colorectal carcinoma (Sakakibara et al., 2005), this study was the first to demonstrate an independent association with OAD prognosis. These data highlight molecular mechanisms by which visceral obesity may contribute to the poor prognosis of OAD by increasing tumour cell motility via up regulation of MMP9, PAI-1 and SNAI2 and down regulation of cell adhesion molecule E-cadherin. These findings are particularly relevant in the context of increased activity of MMP gelatinases and increased migratory and invasive capacity of OAD cell lines following treatment with ACM. These data may be particularly relevant in OAD, a disease associated with early lymphatic and haematogenous dissemination. These intriguing findings highlight a new importance for these established markers of tumour metastasis in viscerally obese patients, thus contributing to the understanding of mechanisms by which visceral obesity could be linked to increased malignant tumour dissemination and high mortality.

Following degradation of the basement membrane by proteolytic enzymes, metastasis requires movement of tumour cells through the basement membrane and epithelium into the blood stream and lymphatic system, before re-establishment of the tumour cells at a distant site. The synthesis of stromal remodelling factors, such as MMP9 and PAI-1, has been demonstrated to be highly induced during the process of EMT (Samarakoon et al., 2009). The findings of this thesis suggested therefore that the presence of visceral obesity, resulting in increased tumour expression of SNAI2, MMP9 and PAI-1, could promote the process of EMT in tumours of these patients. Targeting MMP9 and PAI-1 function using established small molecule inhibitors may therefore impact on tumour metastasis, particularly in the context of visceral obesity. While initially promising, clinical trials investigating the use of inhibitors of MMPs to date have met with mixed results (Coussens et al., 2002), due in part to poor specificity resulting in high toxicity (Radisky and Radisky, 2010). In OAD, a phase II trial of Prinomastat encountered unexpected life-threatening thrombo-embolic events and was closed before clinical benefit could be assessed (Heath et al., 2006). While there remains hope for successful development of MMP inhibitors, PAI-1 may represent an additional target.

Although not yet in clinical trials, small molecule PAI-1 inhibitors are being developed as anti-thrombotic agents and are currently under investigation in animal models of pulmonary fibrosis (Brown, 2010). The findings of this thesis suggest that it would be of great interest to examine the effect of PAI-1 inhibitors in tumour animal models, particularly in animal models of obesity. Epidermal growth factor receptor tyrosine kinases EGFR and ErbB2 (HER2/neu) are over expressed in many cancers including OAD, with EGFR associated with advanced tumour stage, lymph node metastasis and poorer patient survival (Wang et al., 2007). EGF has recently been shown to stimulate EMT in many cancer types including oesophageal squamous cell carcinoma (Cai et al., 2010) and breast cancer (Hardy et al., 2010). Therefore, combinatorial targeting of PAI-1 and EGFR (e.g. with Phase II inhibitors cetuximab or gefitinib) may further impact on inhibition of tumour EMT and invasion. The findings of this thesis offer a new perspective on these well characterised genes, suggesting their use as potential targets in the stratified treatment of viscerally obese OAD patients.

Attempts to validate gene expression findings of MMP9 at the protein level were met with mixed success. Elevated tumour protein levels of MMP9 did not correlate with visceral obesity and were found to be inversely associated with aggressive tumour biology and poor prognosis. MMP9 is an extracellular protease, secreted mainly by tumour associated stromal cells, which specifically degrades the major structural component of the basement membrane, collagen IV, to facilitate tumour invasion. It was therefore anticipated that measurement of peritumoural stromal expression of MMP9 may be more informative than measurement of tumour expression. While elevated stromal protein levels of MMP9 correlated with visceral obesity, no effect was observed on tumour biology or prognosis. There are a number of factors to consider. Although MMPs are located throughout the peritumoural stroma, leading edge areas of active tumour invasion would be expected to be associated with higher levels of these proteolytic enzymes. It would therefore be of future interest to examine stromal MMP expression associated with leading edge tumour; however this option is not currently available in this research unit. While MMPs are present both as latent zymogens and as active proteolytic enzymes in the peritumoural stroma, total levels were measured in this study by IHC. It may be of future interest to examine activity of MMPs using *in situ* zymography. However this technique requires frozen rather than paraffinised tissue in order to maintain enzymatic activity and this is a resource not currently available at this research unit. Although it would be interesting to pursue these lines of investigation, the association of elevated gene expression of MMP9 with visceral obesity and tumour dedifferentiation remains of great clinical significance in OAD.

In conclusion, this thesis identified a pro-inflammatory circulatory profile characteristic of both visceral obesity and cancer. OAD cell lines were responsive to leptin and ACM induced proliferation, suggesting that this altered adipokine profile present in visceral obesity may promote tumourigenesis via paracrine mechanisms. The SGBS adipocyte cell strain was demonstrated to be a relevant model for *in vitro* obesity and cancer research, although a human tissue explant model may be the ideal model system, and was therefore utilised in this work. Visceral obesity measured by visceral fat area was demonstrated to be the strongest predictor of pathway alterations associated with adipose tissue inflammation and angiogenesis. There are multiple molecular mechanisms by which visceral obesity may affect cancer initiation and progression. Using microarray technology, this hypothesis based approach has identified pathways of tumour invasion and metastasis to be of key importance in the interaction between visceral obesity and OAD. Omental adipose tissue up regulated the focal adhesion pathway promoting cytoskeletal reorganisation and EMT, culminating in increased proliferative, migratory and invasive capacity of OAD cell lines. In addition to these *in vitro* data, this thesis highlighted a novel *in vivo* association of markers of invasion and metastasis MMP9 and PAI-1, and markers of EMT SNAI2 and E-cadherin, with visceral obesity. Gene expression of MMP9 and PAI-1 correlated with markers of aggressive tumour biology and PAI-1 and SNAI2 were identified to be independent prognostic indicators in OAD. Together these data indicate a potential role for MMP9, PAI-1 and SNAI2 as promising targets in the development of targeted therapies for stratified treatment of viscerally obese OAD patients.

Future direction

While the majority of studies of obesity related pathogenesis to date rely on BMI as the traditional measure of obesity, this thesis identified visceral fat area (VFA) to be the strongest predictor of gene alterations in omentum. Correlation analysis was utilised as there is currently no universally accepted VFA cut-off value to predict obesity related disease. This is an area of work ongoing in this unit as it is vital to define cut-offs that can be brought into widespread use, standardising the VFA measurement and allowing accurate comparison between studies. In addition to the adipokines, cytokines and chemokines identified by Milliplex and Randox and subsequently quantified by ELISA, it may be of future interest to quantify less well characterised soluble mediators. NGF, resistin and IL-2 were near significantly altered in visceral obesity and it may be worthwhile to validate levels these adipokines in ACM in addition to quantification of serum levels in viscerally obese individuals. Additionally, in future

it would be of great interest to conduct further functional validations into pathways of focal adhesion and EMT, identified by the Affymetrix microarray. High Content Screening technology may present a promising technique by which to study these pathways, and preliminary optimisation has been completed as part of this thesis. Finally, it would be of immense interest to examine protein expression of PAI-1 and SNAI2 expression using tissue microarrays, as these genes were identified to be independent indicators of prognosis at the mRNA level. This work will be carried out in this unit in the short term future. While MMP9 gene expression was found to be associated with poor tumour differentiation, this association was not observed at the protein level. To address this issue, it would be of great interest to examine MMP9 expression in tumour leading edge, an area of active tumour growth and metastasis. TMAs containing tumour leading edge are currently under construction in this laboratory, and will be completed in the near future. This future work has the potential to answer several of the questions raised throughout the course of this thesis and could further contribute towards an increased understanding of the molecular mechanisms involved in the epidemiological association of obesity and cancer.

References

Abdel-Latif, M.M., O'Riordan, J., Windle, H.J., Carton, E., Ravi, N., Kelleher, D., and Reynolds, J.V. (2004). NF-kappaB activation in esophageal adenocarcinoma: relationship to Barrett's metaplasia, survival, and response to neoadjuvant chemoradiotherapy. *Ann Surg.* **239**, 491-500.

Adams, J.M., 2nd, Pratipanawatr, T., Berria, R., Wang, E., DeFronzo, R.A., Sullards, M.C., and Mandarino, L.J. (2004). Ceramide content is increased in skeletal muscle from obese insulin-resistant humans. *Diabetes.* **53**, 25-31.

Aerts, J.M., Ottenhoff, R., Powlson, A.S., Grefhorst, A., van Eijk, M., Dubbelhuis, P.F., Aten, J., Kuipers, F., Serlie, M.J., Wennekes, T., *et al.* (2007). Pharmacological inhibition of glucosylceramide synthase enhances insulin sensitivity. *Diabetes.* **56**, 1341-1349.

Alberti, K.G., Zimmet, P., and Shaw, J. (2005). The metabolic syndrome--a new worldwide definition. *Lancet.* **366**, 1059-1062.

Alexander, M., Curtis, G., Avruch, J., and Goodman, H.M. (1985). Insulin regulation of protein biosynthesis in differentiated 3T3 adipocytes. Regulation of glyceraldehyde-3-phosphate dehydrogenase. *J Biol Chem.* **260**, 11978-11985.

Allavena, P., Sica, A., Solinas, G., Porta, C., and Mantovani, A. (2008). The inflammatory micro-environment in tumor progression: the role of tumor-associated macrophages. *Crit Rev Oncol Hematol.* **66**, 1-9.

Allender, S., and Rayner, M. (2007). The burden of overweight and obesity-related ill health in the UK. *Obes Rev.* **8**, 467-473.

Alvarez-Llamas, G., Szalowska, E., de Vries, M.P., Weening, D., Landman, K., Hoek, A., Wolffenbuttel, B.H., Roelofsen, H., and Vonk, R.J. (2007). Characterization of the human visceral adipose tissue secretome. *Mol Cell Proteomics.* **6**, 589-600.

Alves, C.C., Carneiro, F., Hoefler, H., and Becker, K.F. (2009). Role of the epithelial-mesenchymal transition regulator Slug in primary human cancers. *Front Biosci.* **14**, 3035-3050.
Anderson, E.K., Gutierrez, D.A., and Hasty, A.H. (2010). Adipose tissue recruitment of leukocytes. *Curr Opin Lipidol.* **21**, 172-177.

Anderson, L.A., Murphy, S.J., Johnston, B.T., Watson, R.G., Ferguson, H.R., Bamford, K.B., Ghazy, A., McCarron, P., McGuigan, J., Reynolds, J.V., *et al.* (2008). Relationship between Helicobacter pylori infection and gastric atrophy and the stages of the oesophageal inflammation, metaplasia, adenocarcinoma sequence: results from the FINBAR case-control study. *Gut.* **57**, 734-739.

Anderson, L.A., Watson, R.G., Murphy, S.J., Johnston, B.T., Comber, H., Mc Guigan, J., Reynolds, J.V., and Murray, L.J. (2007). Risk factors for Barrett's oesophagus and oesophageal adenocarcinoma: results from the FINBAR study. *World J Gastroenterol.* **13**, 1585-1594.

Angenete, E., Langenskiold, M., Palmgren, I., Falk, P., Oresland, T., and Ivarsson, M.L. (2009). uPA and PAI-1 in rectal cancer--relationship to radiotherapy and clinical outcome. *J Surg Res.* **153**, 46-53.

Ara, T., and Declerck, Y.A. (2010). Interleukin-6 in bone metastasis and cancer progression. *Eur J Cancer.* **46**, 1223-1231.

Argiles, J.M., and Lopez-Soriano, F.J. (2001). Insulin and cancer (Review). *Int J Oncol.* **18**, 683-687.

Arita, Y., Kihara, S., Ouchi, N., Takahashi, M., Maeda, K., Miyagawa, J., Hotta, K., Shimomura, I., Nakamura, T., Miyaoka, K., *et al.* (1999). Paradoxical decrease of an adipose-specific protein, adiponectin, in obesity. *Biochem Biophys Res Commun.* **257**, 79-83.

Awan, A.K., Iftikhar, S.Y., Morris, T.M., Clarke, P.A., Grabowska, A.M., Waraich, N., and Watson, S.A. (2007). Androgen receptors may act in a paracrine manner to regulate oesophageal adenocarcinoma growth. *Eur J Surg Oncol.* **33**, 561-568.

Babar, M., Abdel-Latif, M.M., Ravi, N., Murphy, A., Byrne, P.J., Kelleher, D., and Reynolds, J.V. (2010a). Pilot translational study of dietary vitamin C supplementation in Barrett's esophagus. *Dis Esophagus.* **23**, 271-276.

Babar, M., Ennis, D., Abdel-Latif, M., Byrne, P.J., Ravi, N., and Reynolds, J.V. (2010b). Differential molecular changes in patients with asymptomatic long-segment Barrett's esophagus treated by antireflux surgery or medical therapy. *Am J Surg.* **199**, 137-143.

Bajou, K., Noel, A., Gerard, R.D., Masson, V., Brunner, N., Holst-Hansen, C., Skobe, M., Fusenig, N.E., Carmeliet, P., Collen, D., *et al.* (1998). Absence of host plasminogen activator inhibitor 1 prevents cancer invasion and vascularization. *Nat Med.* **4**, 923-928.

Balkwill, F., and Mantovani, A. (2001). Inflammation and cancer: back to Virchow? *Lancet.* **357**, 539-545.

Banegas, J.R., Lopez-Garcia, E., Gutierrez-Fisac, J.L., Guallar-Castillon, P., and Rodriguez-Artalejo, F. (2003). A simple estimate of mortality attributable to excess weight in the European Union. *Eur J Clin Nutr.* **57**, 201-208.

Bani-Hani, K., Martin, I.G., Hardie, L.J., Mapstone, N., Briggs, J.A., Forman, D., and Wild, C.P. (2000). Prospective study of cyclin D1 overexpression in Barrett's esophagus: association with increased risk of adenocarcinoma. *J Natl Cancer Inst.* **92**, 1316-1321.

Beales, I.L., and Ogunwobi, O.O. (2007). Leptin synergistically enhances the anti-apoptotic and growth-promoting effects of acid in OE33 oesophageal adenocarcinoma cells in culture. *Mol Cell Endocrinol.* **274**, 60-68.

Beddy, P., Howard, J., McMahon, C., Knox, M., de Blacam, C., Ravi, N., Reynolds, J.V., and Keogan, M.T. (2010). Association of visceral adiposity with oesophageal and junctional adenocarcinomas. *Br J Surg.* **97**, 1028-1034.

Belotti, D., Paganoni, P., Manenti, L., Garofalo, A., Marchini, S., Taraboletti, G., and Giavazzi, R. (2003). Matrix metalloproteinases (MMP9 and MMP2) induce the release of vascular endothelial growth factor (VEGF) by ovarian carcinoma cells: implications for ascites formation. *Cancer Res.* **63**, 5224-5229.

Bergers, G., Brekken, R., McMahon, G., Vu, T.H., Itoh, T., Tamaki, K., Tanzawa, K., Thorpe, P., Itohara, S., Werb, Z., *et al.* (2000). Matrix metalloproteinase-9 triggers the angiogenic switch during carcinogenesis. *Nat Cell Biol.* **2**, 737-744.

Bianchi, A., Gervasi, M.E., and Bakin, A.V. (2010). Role of beta5-integrin in epithelial-mesenchymal transition in response to TGFbeta. *Cell Cycle.* **9**.

Blum, W.F., Englaro, P., Hanitsch, S., Juul, A., Hertel, N.T., Muller, J., Skakkebaek, N.E., Heiman, M.L., Birkett, M., Attanasio, A.M., *et al.* (1997). Plasma leptin levels in healthy children and adolescents: dependence on body mass index, body fat mass, gender, pubertal stage, and testosterone. *J Clin Endocrinol Metab.* **82**, 2904-2910.

Bodles, A.M., Banga, A., Rasouli, N., Ono, F., Kern, P.A., and Owens, R.J. (2006). Pioglitazone increases secretion of high-molecular-weight adiponectin from adipocytes. *Am J Physiol Endocrinol Metab.* **291**, E1100-1105.

Boivin, A., Brochu, G., Marceau, S., Marceau, P., Hould, F.S., and Tchernof, A. (2007). Regional differences in adipose tissue metabolism in obese men. *Metabolism.* **56**, 533-540.

Bollschweiler, E., Wolfgarten, E., Nowroth, T., Rosendahl, U., Monig, S.P., and Holscher, A.H. (2002). Vitamin intake and risk of subtypes of esophageal cancer in Germany. *J Cancer Res Clin Oncol.* **128**, 575-580.

Bour, S., Daviaud, D., Gres, S., Lefort, C., Prevot, D., Zorzano, A., Wabitsch, M., Saulnier-Blache, J.S., Valet, P., and Carpene, C. (2007). Adipogenesis-related increase of semicarbazide-sensitive amine oxidase and monoamine oxidase in human adipocytes. *Biochimie.* **89**, 916-925.

Brakenhielm, E., Veitonmaki, N., Cao, R., Kihara, S., Matsuzawa, Y., Zhivotovsky, B., Funahashi, T., and Cao, Y. (2004). Adiponectin-induced antiangiogenesis and antitumor activity involve caspase-mediated endothelial cell apoptosis. *Proc Natl Acad Sci U S A.* **101**, 2476-2481.

Bramhall, S.R., Hallissey, M.T., Whiting, J., Scholefield, J., Tierney, G., Stuart, R.C., Hawkins, R.E., McCulloch, P., Maughan, T., Brown, P.D., *et al.* (2002). Marimastat as maintenance therapy for patients with advanced gastric cancer: a randomised trial. *Br J Cancer.* **86**, 1864-1870.

Brooks, T.D., Slomp, J., Quax, P.H., De Bart, A.C., Spencer, M.T., Verheijen, J.H., and Charlton, P.A. (2000). Antibodies to PAI-1 alter the invasive and migratory properties of human tumour cells in vitro. *Clin Exp Metastasis.* **18**, 445-453.

Brown, N.J. (2010). Therapeutic potential of plasminogen activator inhibitor-1 inhibitors. *Ther Adv Cardiovasc Dis.* **4**, 315-24

Bujalska, I.J., Walker, E.A., Hewison, M., and Stewart, P.M. (2002). A switch in dehydrogenase to reductase activity of 11 beta-hydroxysteroid dehydrogenase type 1 upon differentiation of human omental adipose stromal cells. *J Clin Endocrinol Metab.* **87**, 1205-1210.

Cadena, D.L., Kurten, R.C., and Gill, G.N. (1997). The product of the MLD gene is a member of the membrane fatty acid desaturase family: overexpression of MLD inhibits EGF receptor biosynthesis. *Biochemistry.* **36**, 6960-6967.

Cai, Z., Wang, Q., Zhou, Y., Zheng, L., Chiu, J.F., and He, Q.Y. (2010). Epidermal growth factor-induced epithelial-mesenchymal transition in human esophageal carcinoma cells--a model for the study of metastasis. *Cancer Lett*. **296**, 88-95.

Calle, E.E., and Kaaks, R. (2004). Overweight, obesity and cancer: epidemiological evidence and proposed mechanisms. *Nat Rev Cancer*. **4**, 579-591.

Calle, E.E., Rodriguez, C., Walker-Thurmond, K., and Thun, M.J. (2003). Overweight, obesity, and mortality from cancer in a prospectively studied cohort of U.S. adults. *N Engl J Med*. **348**, 1625-1638.

Calle, E.E., Thun, M.J., Petrelli, J.M., Rodriguez, C., and Heath, C.W., Jr. (1999). Body-mass index and mortality in a prospective cohort of U.S. adults. *N Engl J Med*. **341**, 1097-1105.

Cancello, R., Tordjman, J., Poitou, C., Guilhem, G., Bouillot, J.L., Hugol, D., Coussieu, C., Basdevant, A., Bar Hen, A., Bedossa, P., *et al.* (2006). Increased infiltration of macrophages in omental adipose tissue is associated with marked hepatic lesions in morbid human obesity. *Diabetes*. **55**, 1554-1561.

Carmichael, A.R. (2006). Obesity and prognosis of breast cancer. *Obes Rev*. **7**, 333-340.

Carmichael, A.R., and Bates, T. (2004). Obesity and breast cancer: a review of the literature. *Breast*. **13**, 85-92.

Caspar-Bauguil, S., Cousin, B., Galinier, A., Segafredo, C., Nibbelink, M., Andre, M., Casteilla, L., and Penicaud, L. (2005). Adipose tissues as an ancestral immune organ: site-specific change in obesity. *FEBS Lett*. **579**, 3487-3492.

Castracane, V.D., Kraemer, R.R., Franken, M.A., Kraemer, G.R., and Gimpel, T. (1998). Serum leptin concentration in women: effect of age, obesity, and estrogen administration. *Fertil Steril*. **70**, 472-477.

Catalan, V., Gomez-Ambrosi, J., Rodriguez, A., Ramirez, B., Silva, C., Rotellar, F., Gil, M.J., Cienfuegos, J.A., Salvador, J., and Fruhbeck, G. (2009). Increased adipose tissue expression of lipocalin-2 in obesity is related to inflammation and matrix metalloproteinase-2 and metalloproteinase-9 activities in humans. *J Mol Med*. **87**, 803-813.

Cazzaniga, M., Bonanni, B., Guerrieri-Gonzaga, A., and Decensi, A. (2009). Is it time to test metformin in breast cancer clinical trials? *Cancer Epidemiol Biomarkers Prev*. **18**, 701-705.

Chan, K.T., Bennin, D.A., and Huttenlocher, A. (2010). Regulation of adhesion dynamics by calpain-mediated proteolysis of focal adhesion kinase (FAK). *J Biol Chem*. **285**, 11418-11426.

Chazaud, B., Ricoux, R., Christov, C., Plonquet, A., Gherardi, R.K., and Barlovatz-Meimon, G. (2002). Promigratory effect of plasminogen activator inhibitor-1 on invasive breast cancer cell populations. *Am J Pathol*. **160**, 237-246.

Christiaens, V., and Lijnen, H.R. (2010). Angiogenesis and development of adipose tissue. *Mol Cell Endocrinol*. **318**, 2-9.

Chua, S.C., Jr., Chung, W.K., Wu-Peng, X.S., Zhang, Y., Liu, S.M., Tartaglia, L., and Leibel, R.L. (1996). Phenotypes of mouse diabetes and rat fatty due to mutations in the OB (leptin) receptor. *Science*. **271**, 994-996.

Cinti, S., Mitchell, G., Barbatelli, G., Murano, I., Ceresi, E., Faloia, E., Wang, S., Fortier, M., Greenberg, A.S., and Obin, M.S. (2005). Adipocyte death defines macrophage localization and function in adipose tissue of obese mice and humans. *J Lipid Res*. **46**, 2347-2355.

Cnop, M., Havel, P.J., Utzschneider, K.M., Carr, D.B., Sinha, M.K., Boyko, E.J., Retzlaff, B.M., Knopp, R.H., Brunzell, J.D., and Kahn, S.E. (2003). Relationship of adiponectin to body fat distribution, insulin sensitivity and plasma lipoproteins: evidence for independent roles of age and sex. *Diabetologia*. **46**, 459-469.

Cohen, P. (1992). Signal integration at the level of protein kinases, protein phosphatases and their substrates. *Trends Biochem Sci*. **17**, 408-413.

Colotta, F., Allavena, P., Sica, A., Garlanda, C., and Mantovani, A. (2009). Cancer-related inflammation, the seventh hallmark of cancer: links to genetic instability. *Carcinogenesis*. **30**, 1073-1081.

Come, C., Magnino, F., Bibeau, F., De Santa Barbara, P., Becker, K.F., Theillet, C., and Savagner, P. (2006). Snail and slug play distinct roles during breast carcinoma progression. *Clin Cancer Res*. **12**, 5395-5402.

Corley, D.A., Kerlikowske, K., Verma, R., and Buffler, P. (2003). Protective association of aspirin/NSAIDs and esophageal cancer: a systematic review and meta-analysis. *Gastroenterology*. **124**, 47-56.

Corley, D.A., Kubo, A., and Zhao, W. (2007). Abdominal obesity, ethnicity and gastro-oesophageal reflux symptoms. *Gut*. **56**, 756-762.

Corley, D.A., Kubo, A., and Zhao, W. (2008). Abdominal obesity and the risk of esophageal and gastric cardia carcinomas. *Cancer Epidemiol Biomarkers Prev*. **17**, 352-358.

Coussens, L.M., Fingleton, B., and Matrisian, L.M. (2002). Matrix metalloproteinase inhibitors and cancer: trials and tribulations. *Science*. **295**, 2387-2392.

Cunningham, D., Humblet, Y., Siena, S., Khayat, D., Bleiberg, H., Santoro, A., Bets, D., Mueser, M., Harstrick, A., Verslype, C., *et al.* (2004). Cetuximab monotherapy and cetuximab plus irinotecan in irinotecan-refractory metastatic colorectal cancer. *N Engl J Med*. **351**, 337-345.

Curran, S., Dundas, S.R., Buxton, J., Leeman, M.F., Ramsay, R., and Murray, G.I. (2004). Matrix metalloproteinase/tissue inhibitors of matrix metalloproteinase phenotype identifies poor prognosis colorectal cancers. *Clin Cancer Res*. **10**, 8229-8234.

Dal Maso, L., Zucchetto, A., Talamini, R., Serraino, D., Stocco, C.F., Vercelli, M., Falcini, F., and Franceschi, S. (2008). Effect of obesity and other lifestyle factors on mortality in women with breast cancer. *Int J Cancer*. **123**, 2188-2194.

Daly, J.M., Fry, W.A., Little, A.G., Winchester, D.P., McKee, R.F., Stewart, A.K., and Fremgen, A.M. (2000). Esophageal cancer: results of an American College of Surgeons Patient Care Evaluation Study. *J Am Coll Surg*. **190**, 562-572; discussion 572-563.

Das, U.N. (2001). Is obesity an inflammatory condition? *Nutrition*. **17**, 953-966.

Despres, J.P. (2001). Health consequences of visceral obesity. *Ann Med*. **33**, 534-541.

Despres, J.P., and Lamarche, B. (1993). Effects of diet and physical activity on adiposity and body fat distribution: implications for the prevention of cardiovascular disease. *Nutr Res Rev*. **6**, 137-159.

Dignam, J.J., Polite, B.N., Yothers, G., Raich, P., Colangelo, L., O'Connell, M.J., and Wolmark, N. (2006). Body mass index and outcomes in patients who receive adjuvant chemotherapy for colon cancer. *J Natl Cancer Inst*. **98**, 1647-1654.

Donohoe, C.L., Pidgeon, G.P., Lysaght, J., and Reynolds, J.V. (2010). Obesity and gastrointestinal cancer. *Br J Surg*. **97**, 628-642.

Duffield, J.S. (2003). The inflammatory macrophage: a story of Jekyll and Hyde. *Clin Sci (Lond)*. **104**, 27-38.

Duffy, M.J., and Duggan, C. (2004). The urokinase plasminogen activator system: a rich source of tumour markers for the individualised management of patients with cancer. *Clin Biochem*. **37**, 541-548.

Duggan, S.P., Behan, F.M., Kirca, M., Smith, S., Reynolds, J.V., Long, A., and Kelleher, D. (2010). An integrative genomic approach in oesophageal cells identifies TRB3 as a bile acid responsive gene, downregulated in Barrett's oesophagus, which regulates NF-kappaB activation and cytokine levels. *Carcinogenesis*. **31**, 936-945.

Durand, M.K., Bodker, J.S., Christensen, A., Dupont, D.M., Hansen, M., Jensen, J.K., Kjelgaard, S., Mathiasen, L., Pedersen, K.E., Skeldal, S., *et al*. (2004). Plasminogen activator inhibitor-I and tumour growth, invasion, and metastasis. *Thromb Haemost*. **91**, 438-449.

Dvorakova, K., Payne, C.M., Ramsey, L., Holubec, H., Sampliner, R., Dominguez, J., Dvorak, B., Bernstein, H., Bernstein, C., Prasad, A., *et al*. (2004). Increased expression and secretion of interleukin-6 in patients with Barrett's esophagus. *Clin Cancer Res*. **10**, 2020-2028.

Dwyer, J., Li, H., Xu, D., and Liu, J.P. (2007). Transcriptional regulation of telomerase activity: roles of the the Ets transcription factor family. *Ann N Y Acad Sci*. **1114**, 36-47.

Edelstein, Z.R., Farrow, D.C., Bronner, M.P., Rosen, S.N., and Vaughan, T.L. (2007). Central adiposity and risk of Barrett's esophagus. *Gastroenterology*. **133**, 403-411.

Egler, R.A., Burlingame, S.M., Nuchtern, J.G., and Russell, H.V. (2008). Interleukin-6 and soluble interleukin-6 receptor levels as markers of disease extent and prognosis in neuroblastoma. *Clin Cancer Res*. **14**, 7028-7034.

el-Serag, H.B., and Sonnenberg, A. (1998). Opposing time trends of peptic ulcer and reflux disease. *Gut*. **43**, 327-333.

El-Tamer, M.B., Ward, B.M., Schifftner, T., Neumayer, L., Khuri, S., and Henderson, W. (2007). Morbidity and mortality following breast cancer surgery in women: national benchmarks for standards of care. *Ann Surg*. **245**, 665-671.

Engel, L.S., Chow, W.H., Vaughan, T.L., Gammon, M.D., Risch, H.A., Stanford, J.L., Schoenberg, J.B., Mayne, S.T., Dubrow, R., Rotterdam, H., *et al.* (2003). Population attributable risks of esophageal and gastric cancers. *J Natl Cancer Inst.* **95**, 1404-1413.

Ennis, D.P., Pidgeon, G.P., Millar, N., Ravi, N., and Reynolds, J.V. (2010). Building a bioresource for esophageal research: lessons from the early experience of an academic medical center. *Dis Esophagus.* **23**, 1-7.

Enzinger, P.C., and Mayer, R.J. (2003). Esophageal cancer. *N Engl J Med.* **349**, 2241-2252.

Evans, J.M., Donnelly, L.A., Emslie-Smith, A.M., Alessi, D.R., and Morris, A.D. (2005). Metformin and reduced risk of cancer in diabetic patients. *BMJ.* **330**, 1304-1305.

Fabre-Guillevin, E., Malo, M., Cartier-Michaud, A., Peinado, H., Moreno-Bueno, G., Vallee, B., Lawrence, D.A., Palacios, J., Cano, A., Barlovatz-Meimon, G., *et al.* (2008). PAI-1 and functional blockade of SNAI1 in breast cancer cell migration. *Breast Cancer Res.* **10**, R100.

Fantuzzi, G. (2005). Adipose tissue, adipokines, and inflammation. *J Allergy Clin Immunol.* **115**, 911-919; quiz 920.

Farrow, D.C., Vaughan, T.L., Hansten, P.D., Stanford, J.L., Risch, H.A., Gammon, M.D., Chow, W.H., Dubrow, R., Ahsan, H., Mayne, S.T., *et al.* (1998). Use of aspirin and other nonsteroidal anti-inflammatory drugs and risk of esophageal and gastric cancer. *Cancer Epidemiol Biomarkers Prev.* **7**, 97-102.

Farrow, D.C., Vaughan, T.L., Sweeney, C., Gammon, M.D., Chow, W.H., Risch, H.A., Stanford, J.L., Hansten, P.D., Mayne, S.T., Schoenberg, J.B., *et al.* (2000). Gastroesophageal reflux disease, use of H2 receptor antagonists, and risk of esophageal and gastric cancer. *Cancer Causes Control.* **11**, 231-238.

Fasshauer, M., and Paschke, R. (2003). Regulation of adipocytokines and insulin resistance. *Diabetologia.* **46**, 1594-1603.

Ferlay, J., Shin, H.R., Bray, F., Forman, D., Mathers, C., and Parkin, D.M. (2010). Estimates of worldwide burden of cancer in 2008: GLOBOCAN 2008. *Int J Cancer.* (in press)

Fernandes, M.L., Seow, A., Chan, Y.H., and Ho, K.Y. (2006). Opposing trends in incidence of esophageal squamous cell carcinoma and adenocarcinoma in a multi-ethnic Asian country. *Am J Gastroenterol.* **101**, 1430-1436.

Ferry, D.R., Anderson, M., Beddard, K., Tomlinson, S., Atherfold, P., Obszynska, J., Harrison, R., and Jankowski, J. (2007). A phase II study of gefitinib monotherapy in advanced esophageal adenocarcinoma: evidence of gene expression, cellular, and clinical response. *Clin Cancer Res.* **13**, 5869-5875.

Festuccia, C., Dolo, V., Guerra, F., Violini, S., Muzi, P., Pavan, A., and Bologna, M. (1998). Plasminogen activator system modulates invasive capacity and proliferation in prostatic tumor cells. *Clin Exp Metastasis.* **16**, 513-528.

Field, A.E., Coakley, E.H., Must, A., Spadano, J.L., Laird, N., Dietz, W.H., Rimm, E., and Colditz, G.A. (2001). Impact of overweight on the risk of developing common chronic diseases during a 10-year period. *Arch Intern Med.* **161**, 1581-1586.

Fiorica, F., Di Bona, D., Schepis, F., Licata, A., Shahied, L., Venturi, A., Falchi, A.M., Craxi, A., and Camma, C. (2004). Preoperative chemoradiotherapy for oesophageal cancer: a systematic review and meta-analysis. *Gut.* **53**, 925-930.

Fiorio, E., Mercanti, A., Terrasi, M., Micciolo, R., Remo, A., Auriemma, A., Molino, A., Parolin, V., Di Stefano, B., Bonetti, F., *et al.* (2008). Leptin/HER2 crosstalk in breast cancer: in vitro study and preliminary in vivo analysis. *BMC Cancer.* **8**, 305.

Fischer-Posovszky, P., Newell, F.S., Wabitsch, M., and Tornqvist, H.E. (2008). Human SGBS cells - a unique tool for studies of human fat cell biology. *Obes Facts.* **1**, 184-189.

Flegal, K.M., Graubard, B.I., Williamson, D.F., and Gail, M.H. (2005). Excess deaths associated with underweight, overweight, and obesity. *JAMA.* **293**, 1861-1867.

Flejou, J.F. (2005). Barrett's oesophagus: from metaplasia to dysplasia and cancer. *Gut.* **54 Suppl 1**, i6-12.

Ford, E.S., Abbasi, F., and Reaven, G.M. (2005). Prevalence of insulin resistance and the metabolic syndrome with alternative definitions of impaired fasting glucose. *Atherosclerosis.* **181**, 143-148.

Frank, S., Stallmeyer, B., Kampfer, H., Kolb, N., and Pfeilschifter, J. (2000). Leptin enhances wound re-epithelialization and constitutes a direct function of leptin in skin repair. *J Clin Invest.* **106**, 501-509.

Friedman, J.M., and Halaas, J.L. (1998). Leptin and the regulation of body weight in mammals. *Nature.* **395**, 763-770.

Fruhbeck, G. (2006). Intracellular signalling pathways activated by leptin. *Biochem J.* **393**, 7-20.

Fukuhara, A., Matsuda, M., Nishizawa, M., Segawa, K., Tanaka, M., Kishimoto, K., Matsuki, Y., Murakami, M., Ichisaka, T., Murakami, H., *et al.* (2005). Visfatin: a protein secreted by visceral fat that mimics the effects of insulin. *Science.* **307**, 426-430.

Galic, S., Oakhill, J.S., and Steinberg, G.R. (2010). Adipose tissue as an endocrine organ. *Mol Cell Endocrinol.* **316**, 129-139.

Gami, A.S., Witt, B.J., Howard, D.E., Erwin, P.J., Gami, L.A., Somers, V.K., and Montori, V.M. (2007). Metabolic syndrome and risk of incident cardiovascular events and death: a systematic review and meta-analysis of longitudinal studies. *J Am Coll Cardiol.* **49**, 403-414.

Gannon, P.O., Godin-Ethier, J., Hassler, M., Delvoye, N., Aversa, M., Poisson, A.O., Peant, B., Alam Fahmy, M., Saad, F., Lapointe, R., *et al.* (2010). Androgen-regulated expression of arginase 1, arginase 2 and interleukin-8 in human prostate cancer. *PLoS One.* **5**, e12107.

Gao, Q., Mezei, G., Nie, Y., Rao, Y., Choi, C.S., Bechmann, I., Leranth, C., Toran-Allerand, D., Priest, C.A., Roberts, J.L., *et al.* (2007). Anorectic estrogen mimics leptin's effect on the rewiring of melanocortin cells and Stat3 signaling in obese animals. *Nat Med.* **13**, 89-94.

Gertler, R., Doll, D., Maak, M., Feith, M., and Rosenberg, R. (2008). Telomere length and telomerase subunits as diagnostic and prognostic biomarkers in Barrett carcinoma. *Cancer.* **112**, 2173-2180.

Gervais, F.G., Thornberry, N.A., Ruffolo, S.C., Nicholson, D.W., and Roy, S. (1998). Caspases cleave focal adhesion kinase during apoptosis to generate a FRNK-like polypeptide. *J Biol Chem.* **273**, 17102-17108.

Gesta, S., Bluher, M., Yamamoto, Y., Norris, A.W., Berndt, J., Kralisch, S., Boucher, J., Lewis, C., and Kahn, C.R. (2006). Evidence for a role of developmental genes in the origin of obesity and body fat distribution. *Proc Natl Acad Sci U S A.* **103**, 6676-6681.

Giorgino, F., Laviola, L., and Eriksson, J.W. (2005). Regional differences of insulin action in adipose tissue: insights from in vivo and in vitro studies. *Acta Physiol Scand.* **183**, 13-30.

Gohji, K., Fujimoto, N., Ohkawa, J., Fujii, A., and Nakajima, M. (1998). Imbalance between serum matrix metalloproteinase-2 and its inhibitor as a predictor of recurrence of urothelial cancer. *Br J Cancer.* **77**, 650-655.

Goktas, S., Yilmaz, M.I., Caglar, K., Sonmez, A., Kilic, S., and Bedir, S. (2005). Prostate cancer and adiponectin. *Urology.* **65**, 1168-1172.

Goldstein, B.J., and Scalia, R. (2004). Adiponectin: A novel adipokine linking adipocytes and vascular function. *J Clin Endocrinol Metab.* **89**, 2563-2568.

Gomez-Ambrosi, J., Catalan, V., Diez-Caballero, A., Martinez-Cruz, L.A., Gil, M.J., Garcia-Foncillas, J., Cienfuegos, J.A., Salvador, J., Mato, J.M., and Fruhbeck, G. (2004). Gene expression profile of omental adipose tissue in human obesity. *FASEB J.* **18**, 215-217.

Gong, Z., Agalliu, I., Lin, D.W., Stanford, J.L., and Kristal, A.R. (2007). Obesity is associated with increased risks of prostate cancer metastasis and death after initial cancer diagnosis in middle-aged men. *Cancer.* **109**, 1192-1202.

Gonzalez-Angulo, A.M., and Meric-Bernstam, F. (2010). Metformin: a therapeutic opportunity in breast cancer. *Clin Cancer Res.* **16**, 1695-1700.

Gonzalez, C.A., Pera, G., Agudo, A., Bueno-de-Mesquita, H.B., Ceroti, M., Boeing, H., Schulz, M., Del Giudice, G., Plebani, M., Carneiro, F., *et al.* (2006). Fruit and vegetable intake and the risk of stomach and oesophagus adenocarcinoma in the European Prospective Investigation into Cancer and Nutrition (EPIC-EURGAST). *Int J Cancer.* **118**, 2559-2566.

Gordon, S. (2003). Alternative activation of macrophages. *Nat Rev Immunol.* **3**, 23-35.

Greene, F.L. (2002). The American Joint Committee on Cancer: updating the strategies in cancer staging. *Bull Am Coll Surg.* **87**, 13-15.

Griffiths, E.A., Pritchard, S.A., McGrath, S.M., Valentine, H.R., Price, P.M., Welch, I.M., and West, C.M. (2007). Increasing expression of hypoxia-inducible proteins in the Barrett's metaplasia-dysplasia-adenocarcinoma sequence. *Br J Cancer.* **96**, 1377-1383.

Griggs, J.J., Sorbero, M.E., and Lyman, G.H. (2005). Undertreatment of obese women receiving breast cancer chemotherapy. *Arch Intern Med*. **165**, 1267-1273.

Gu, Z.D., Chen, K.N., Li, M., Gu, J., and Li, J.Y. (2005a). Clinical significance of matrix metalloproteinase-9 expression in esophageal squamous cell carcinoma. *World J Gastroenterol*. **11**, 871-874.

Gu, Z.D., Li, J.Y., Li, M., Gu, J., Shi, X.T., Ke, Y., and Chen, K.N. (2005b). Matrix metalloproteinases expression correlates with survival in patients with esophageal squamous cell carcinoma. *Am J Gastroenterol*. **100**, 1835-1843.

Guh, D.P., Zhang, W., Bansback, N., Amarsi, Z., Birmingham, C.L., and Anis, A.H. (2009). The incidence of co-morbidities related to obesity and overweight: a systematic review and meta-analysis. *BMC Public Health*. **9**, 88.

Guo, W., and Giancotti, F.G. (2004). Integrin signalling during tumour progression. *Nat Rev Mol Cell Biol*. **5**, 816-826.

Hajra, K.M., Chen, D.Y., and Fearon, E.R. (2002). The SLUG zinc-finger protein represses E-cadherin in breast cancer. *Cancer Res*. **62**, 1613-1618.

Halberg, N., Khan, T., Trujillo, M.E., Wernstedt-Asterholm, I., Attie, A.D., Sherwani, S., Wang, Z.V., Landskroner-Eiger, S., Dineen, S., Magalang, U.J., *et al*. (2009). Hypoxia-inducible factor 1alpha induces fibrosis and insulin resistance in white adipose tissue. *Mol Cell Biol*. **29**, 4467-4483.

Hanahan, D., and Weinberg, R.A. (2000). The hallmarks of cancer. *Cell*. **100**, 57-70.

Harbeck, N., Kates, R.E., Schmitt, M., Gauger, K., Kiechle, M., Janicke, F., Thomassen, C., Look, M.P., and Foekens, J.A. (2004). Urokinase-type plasminogen activator and its inhibitor type 1 predict disease outcome and therapy response in primary breast cancer. *Clin Breast Cancer*. **5**, 348-352.

Harbeck, N., Schmitt, M., Vetter, M., Krol, J., Paepke, D., Uhlig, M., Paepke, S., Janicke, F., Geurts-Moespot, A., von Minckwitz, G., *et al*. (2008). Prospective Biomarker Trials Chemo N0 and NNBC-3 Europe Validate the Clinical Utility of Invasion Markers uPA and PAI-1 in Node-Negative Breast Cancer. *Breast Care (Basel)*. **3**, 11-15.

Hardy, K.M., Booth, B.W., Hendrix, M.J., Salomon, D.S., and Strizzi, L. (2010). ErbB/EGF signaling and EMT in mammary development and breast cancer. *J Mammary Gland Biol Neoplasia*. **15**, 191-199.

Harris, S.L., and Levine, A.J. (2005). The p53 pathway: positive and negative feedback loops. *Oncogene*. **24**, 2899-2908.

Hartojo, W., Silvers, A.L., Thomas, D.G., Seder, C.W., Lin, L., Rao, H., Wang, Z., Greenson, J.K., Giordano, T.J., Orringer, M.B., *et al*. (2010). Curcumin promotes apoptosis, increases chemosensitivity, and inhibits nuclear factor kappaB in esophageal adenocarcinoma. *Transl Oncol*. **3**, 99-108.

Haydon, A.M., Macinnis, R.J., English, D.R., and Giles, G.G. (2006). Effect of physical activity and body size on survival after diagnosis with colorectal cancer. *Gut*. **55**, 62-67.

Headrick, J.R., Nichols, F.C., 3rd, Miller, D.L., Allen, M.S., Trastek, V.F., Deschamps, C., Schleck, C.D., Thompson, A.M., and Pairolero, P.C. (2002). High-grade esophageal dysplasia: long-term survival and quality of life after esophagectomy. *Ann Thorac Surg*. **73**, 1697-1702; discussion 1702-1693.

Heath, E.I., Burtness, B.A., Kleinberg, L., Salem, R.R., Yang, S.C., Heitmiller, R.F., Canto, M.I., Knisely, J.P., Topazian, M., Montgomery, E., *et al.* (2006). Phase II, parallel-design study of preoperative combined modality therapy and the matrix metalloprotease (mmp) inhibitor prinomastat in patients with esophageal adenocarcinoma. *Invest New Drugs*. **24**, 135-140.

Heitmiller, R.F., and Sharma, R.R. (1996). Comparison of prevalence and resection rates in patients with esophageal squamous cell carcinoma and adenocarcinoma. *J Thorac Cardiovasc Surg*. **112**, 130-136.

Helm, J., Enkemann, S.A., Coppola, D., Barthel, J.S., Kelley, S.T., and Yeatman, T.J. (2005). Dedifferentiation precedes invasion in the progression from Barrett's metaplasia to esophageal adenocarcinoma. *Clin Cancer Res*. **11**, 2478-2485.

Henegar, C., Tordjman, J., Achard, V., Lacasa, D., Cremer, I., Guerre-Millo, M., Poitou, C., Basdevant, A., Stich, V., Viguerie, N., *et al.* (2008). Adipose tissue transcriptomic signature highlights the pathological relevance of extracellular matrix in human obesity. *Genome Biol*. **9**, R14.

Herrera, V., and Parsonnet, J. (2009). Helicobacter pylori and gastric adenocarcinoma. *Clin Microbiol Infect*. **15**, 971-976.

Hileman, S.M., Pierroz, D.D., Masuzaki, H., Bjorbaek, C., El-Haschimi, K., Banks, W.A., and Flier, J.S. (2002). Characterizaton of short isoforms of the leptin receptor in rat cerebral microvessels and of brain uptake of leptin in mouse models of obesity. *Endocrinology*. **143**, 775-783.

Hochreiter, A.E., Xiao, H., Goldblatt, E.M., Gryaznov, S.M., Miller, K.D., Badve, S., Sledge, G.W., and Herbert, B.S. (2006). Telomerase template antagonist GRN163L disrupts telomere maintenance, tumor growth, and metastasis of breast cancer. *Clin Cancer Res*. **12**, 3184-3192.

Holcomb, I.N., Kabakoff, R.C., Chan, B., Baker, T.W., Gurney, A., Henzel, W., Nelson, C., Lowman, H.B., Wright, B.D., Skelton, N.J., *et al.* (2000). FIZZ1, a novel cysteine-rich secreted protein associated with pulmonary inflammation, defines a new gene family. *EMBO J*. **19**, 4046-4055.

Holland, W.L., and Summers, S.A. (2008). Sphingolipids, insulin resistance, and metabolic disease: new insights from in vivo manipulation of sphingolipid metabolism. *Endocr Rev*. **29**, 381-402.

Holness, M.J., Munns, M.J., and Sugden, M.C. (1999). Current concepts concerning the role of leptin in reproductive function. *Mol Cell Endocrinol*. **157**, 11-20.

Howard, J.M., Beddy, P., Ennis, D., Keogan, M., Pidgeon, G.P., and Reynolds, J.V. (2010). Associations between leptin and adiponectin receptor upregulation, visceral obesity and tumour stage in oesophageal and junctional adenocarcinoma. *Br J Surg*. **97**, 1020-1027.

Hsia, D.A., Mitra, S.K., Hauck, C.R., Streblow, D.N., Nelson, J.A., Ilic, D., Huang, S., Li, E., Nemerow, G.R., Leng, J., *et al.* (2003). Differential regulation of cell motility and invasion by FAK. *J Cell Biol*. **160**, 753-767.

Hu, E., Liang, P., and Spiegelman, B.M. (1996). AdipoQ is a novel adipose-specific gene dysregulated in obesity. *J Biol Chem*. **271**, 10697-10703.

Hu, F.B. (2007). Obesity and mortality: watch your waist, not just your weight. *Arch Intern Med*. **167**, 875-876.

Hu, X., Juneja, S.C., Maihle, N.J., and Cleary, M.P. (2002). Leptin--a growth factor in normal and malignant breast cells and for normal mammary gland development. *J Natl Cancer Inst*. **94**, 1704-1711.

Huber, J., Loffler, M., Bilban, M., Reimers, M., Kadl, A., Todoric, J., Zeyda, M., Geyeregger, R., Schreiner, M., Weichhart, T., *et al.* (2007). Prevention of high-fat diet-induced adipose tissue remodeling in obese diabetic mice by n-3 polyunsaturated fatty acids. *Int J Obes (Lond)*. **31**, 1004-1013.

Hunter, G.R., Snyder, S.W., Kekes-Szabo, T., Nicholson, C., and Berland, L. (1994). Intra-abdominal adipose tissue values associated with risk of possessing elevated blood lipids and blood pressure. *Obes Res*. **2**, 563-568.

Hurtado del Pozo, C., Calvo, R.M., Vesperinas-Garcia, G., Gomez-Ambrosi, J., Fruhbeck, G., Corripio-Sanchez, R., Rubio, M.A., and Obregon, M.J. (2010). IPO8 and FBXL10: new reference genes for gene expression studies in human adipose tissue. *Obesity (Silver Spring)*. **18**, 897-903.

Hurwitz, H., Fehrenbacher, L., Novotny, W., Cartwright, T., Hainsworth, J., Heim, W., Berlin, J., Baron, A., Griffing, S., Holmgren, E., *et al.* (2004). Bevacizumab plus irinotecan, fluorouracil, and leucovorin for metastatic colorectal cancer. *N Engl J Med*. **350**, 2335-2342.

Ingalls, A.M., Dickie, M.M., and Snell, G.D. (1950). Obese, a new mutation in the house mouse. *J Hered*. **41**, 317-318.

Ishida, T., Iwai, A., Hijikata, M., and Shimotohno, K. (2007). The expression of phosphatidic acid phosphatase 2a, which hydrolyzes lipids to generate diacylglycerol, is regulated by p73, a member of the p53 family. *Biochem Biophys Res Commun*. **353**, 74-79.

Ishikawa, M., Kitayama, J., Kazama, S., Hiramatsu, T., Hatano, K., and Nagawa, H. (2005). Plasma adiponectin and gastric cancer. *Clin Cancer Res*. **11**, 466-472.

Itoh, T., Tanioka, M., Matsuda, H., Nishimoto, H., Yoshioka, T., Suzuki, R., and Uehira, M. (1999). Experimental metastasis is suppressed in MMP-9-deficient mice. *Clin Exp Metastasis*. **17**, 177-181.

Itoh, T., Tanioka, M., Yoshida, H., Yoshioka, T., Nishimoto, H., and Itohara, S. (1998). Reduced angiogenesis and tumor progression in gelatinase A-deficient mice. *Cancer Res*. **58**, 1048-1051.

Jensen, S.A., Vainer, B., Bartels, A., Brunner, N., and Sorensen, J.B. (2010). Expression of matrix metalloproteinase 9 (MMP-9) and tissue inhibitor of metalloproteinases 1 (TIMP-1) by

colorectal cancer cells and adjacent stroma cells - Associations with histopathology and patients outcome. *Eur J Cancer*. (in press)

Jethwa, P., Naqvi, M., Hardy, R.G., Hotchin, N.A., Roberts, S., Spychal, R., and Tselepis, C. (2008). Overexpression of Slug is associated with malignant progression of esophageal adenocarcinoma. *World J Gastroenterol*. **14**, 1044-1052.

Jinga, D.C., Blidaru, A., Condrea, I., Ardeleanu, C., Dragomir, C., Szegli, G., Stefanescu, M., and Matache, C. (2006). MMP-9 and MMP-2 gelatinases and TIMP-1 and TIMP-2 inhibitors in breast cancer: correlations with prognostic factors. *J Cell Mol Med*. **10**, 499-510.

Kadowaki, T., and Yamauchi, T. (2005). Adiponectin and adiponectin receptors. *Endocr Rev*. **26**, 439-451.

Kahn, B.B., and Flier, J.S. (2000). Obesity and insulin resistance. *J Clin Invest*. **106**, 473-481.

Kalinina, T., Bockhorn, M., Kaifi, J.T., Thieltges, S., Gungor, C., Effenberger, K.E., Strelow, A., Reichelt, U., Sauter, G., Pantel, K., *et al.* (2010). Insulin-like growth factor-1 receptor as a novel prognostic marker and its implication as a cotarget in the treatment of human adenocarcinoma of the esophagus. *Int J Cancer*. (in press)

Kamei, N., Tobe, K., Suzuki, R., Ohsugi, M., Watanabe, T., Kubota, N., Ohtsuka-Kowatari, N., Kumagai, K., Sakamoto, K., Kobayashi, M., *et al.* (2006). Overexpression of monocyte chemoattractant protein-1 in adipose tissues causes macrophage recruitment and insulin resistance. *J Biol Chem*. **281**, 26602-26614.

Karamouzis, M.V., Grandis, J.R., and Argiris, A. (2007). Therapies directed against epidermal growth factor receptor in aerodigestive carcinomas. *JAMA*. **298**, 70-82.

Kastan, M.B., and Bartek, J. (2004). Cell-cycle checkpoints and cancer. *Nature*. **432**, 316-323.

Katoh, M. (2007). Notch signaling in gastrointestinal tract (review). *Int J Oncol*. **30**, 247-251.

Katsuki, A., Sumida, Y., Murashima, S., Murata, K., Takarada, Y., Ito, K., Fujii, M., Tsuchihashi, K., Goto, H., Nakatani, K., *et al.* (1998). Serum levels of tumor necrosis factor-alpha are increased in obese patients with noninsulin-dependent diabetes mellitus. *J Clin Endocrinol Metab*. **83**, 859-862.

Kelesidis, I., Kelesidis, T., and Mantzoros, C.S. (2006). Adiponectin and cancer: a systematic review. *Br J Cancer*. **94**, 1221-1225.

Kellenberger, L.D., Bruin, J.E., Greenaway, J., Campbell, N.E., Moorehead, R.A., Holloway, A.C., and Petrik, J. (2010). The role of dysregulated glucose metabolism in epithelial ovarian cancer. *J Oncol*. **2010**, 514310.

Kelloff, G.J., Hoffman, J.M., Johnson, B., Scher, H.I., Siegel, B.A., Cheng, E.Y., Cheson, B.D., O'Shaughnessy, J., Guyton, K.Z., Mankoff, D.A., *et al.* (2005). Progress and promise of FDG-PET imaging for cancer patient management and oncologic drug development. *Clin Cancer Res*. **11**, 2785-2808.

Kern, P.A., Saghizadeh, M., Ong, J.M., Bosch, R.J., Deem, R., and Simsolo, R.B. (1995). The expression of tumor necrosis factor in human adipose tissue. Regulation by obesity, weight loss, and relationship to lipoprotein lipase. *J Clin Invest*. **95**, 2111-2119.

Kersten, S., Mandard, S., Tan, N.S., Escher, P., Metzger, D., Chambon, P., Gonzalez, F.J., Desvergne, B., and Wahli, W. (2000). Characterization of the fasting-induced adipose factor FIAF, a novel peroxisome proliferator-activated receptor target gene. *J Biol Chem*. **275**, 28488-28493.

Kim, C.S., Park, H.S., Kawada, T., Kim, J.H., Lim, D., Hubbard, N.E., Kwon, B.S., Erickson, K.L., and Yu, R. (2006). Circulating levels of MCP-1 and IL-8 are elevated in human obese subjects and associated with obesity-related parameters. *Int J Obes (Lond)*. **30**, 1347-1355.

Kim, K.H., Lee, K., Moon, Y.S., and Sul, H.S. (2001). A cysteine-rich adipose tissue-specific secretory factor inhibits adipocyte differentiation. *J Biol Chem*. **276**, 11252-11256.

Kimchi, E.T., Posner, M.C., Park, J.O., Darga, T.E., Kocherginsky, M., Karrison, T., Hart, J., Smith, K.D., Mezhir, J.J., Weichselbaum, R.R., *et al.* (2005). Progression of Barrett's metaplasia to adenocarcinoma is associated with the suppression of the transcriptional programs of epidermal differentiation. *Cancer Res*. **65**, 3146-3154.

King, C.R., Spiotto, M.T., and Kapp, D.S. (2009). Obesity and risk of biochemical failure for patients receiving salvage radiotherapy after prostatectomy. *Int J Radiat Oncol Biol Phys*. **73**, 1017-1022.

Kintscher, U., Hartge, M., Hess, K., Foryst-Ludwig, A., Clemenz, M., Wabitsch, M., Fischer-Posovszky, P., Barth, T.F., Dragun, D., Skurk, T., *et al.* (2008). T-lymphocyte infiltration in visceral adipose tissue: a primary event in adipose tissue inflammation and the development of obesity-mediated insulin resistance. *Arterioscler Thromb Vasc Biol*. **28**, 1304-1310.

Kitani, T., Okuno, S., and Fujisawa, H. (2003). Growth phase-dependent changes in the subcellular localization of pre-B-cell colony-enhancing factor. *FEBS Lett*. **544**, 74-78.

Kjaerbye-Thygesen, A., Frederiksen, K., Hogdall, E.V., Hogdall, C.K., Blaakaer, J., and Kjaer, S.K. (2006). Do risk factors for epithelial ovarian cancer have an impact on prognosis? Focus on previous pelvic surgery and reproductive variables. *Eur J Gynaecol Oncol*. **27**, 467-472.

Kleespies, A., Guba, M., Jauch, K.W., and Bruns, C.J. (2004). Vascular endothelial growth factor in esophageal cancer. *J Surg Oncol*. **87**, 95-104.

Klein, S., Allison, D.B., Heymsfield, S.B., Kelley, D.E., Leibel, R.L., Nonas, C., and Kahn, R. (2007). Waist Circumference and Cardiometabolic Risk: a Consensus Statement from Shaping America's Health: Association for Weight Management and Obesity Prevention; NAASO, the Obesity Society; the American Society for Nutrition; and the American Diabetes Association. *Obesity (Silver Spring)*. **15**, 1061-1067.

Kobayashi, H., Ouchi, N., Kihara, S., Walsh, K., Kumada, M., Abe, Y., Funahashi, T., and Matsuzawa, Y. (2004). Selective suppression of endothelial cell apoptosis by the high molecular weight form of adiponectin. *Circ Res*. **94**, e27-31.

Konnikova, L., Simeone, M.C., Kruger, M.M., Kotecki, M., and Cochran, B.H. (2005). Signal transducer and activator of transcription 3 (STAT3) regulates human telomerase reverse

transcriptase (hTERT) expression in human cancer and primary cells. *Cancer Res.* **65**, 6516-6520.

Korpal, M., and Kang, Y. (2010). Targeting the transforming growth factor-beta signalling pathway in metastatic cancer. *Eur J Cancer.* **46**, 1232-1240.

Kroenke, C.H., Chen, W.Y., Rosner, B., and Holmes, M.D. (2005). Weight, weight gain, and survival after breast cancer diagnosis. *J Clin Oncol.* **23**, 1370-1378.

Kubo, A., and Corley, D.A. (2002). Marked regional variation in adenocarcinomas of the esophagus and the gastric cardia in the United States. *Cancer.* **95**, 2096-2102.

Kubo, A., and Corley, D.A. (2004). Marked multi-ethnic variation of esophageal and gastric cardia carcinomas within the United States. *Am J Gastroenterol.* **99**, 582-588.

Kumar, A., Chatopadhyay, T., Raziuddin, M., and Ralhan, R. (2007). Discovery of deregulation of zinc homeostasis and its associated genes in esophageal squamous cell carcinoma using cDNA microarray. *Int J Cancer.* **120**, 230-242.

Kyo, S., Takakura, M., Kanaya, T., Zhuo, W., Fujimoto, K., Nishio, Y., Orimo, A., and Inoue, M. (1999). Estrogen activates telomerase. *Cancer Res.* **59**, 5917-5921.

Kyrgidis, A., Kountouras, J., Zavos, C., and Chatzopoulos, D. (2005). New molecular concepts of Barrett's esophagus: clinical implications and biomarkers. *J Surg Res.* **125**, 189-212.

Lagarde, S.M., ten Kate, F.J., Richel, D.J., Offerhaus, G.J., and van Lanschot, J.J. (2007). Molecular prognostic factors in adenocarcinoma of the esophagus and gastroesophageal junction. *Ann Surg Oncol.* **14**, 977-991.

Lagergren, J. (2005). Adenocarcinoma of oesophagus: what exactly is the size of the problem and who is at risk? *Gut.* **54 Suppl 1**, i1-5.

Lagergren, J., Bergstrom, R., Lindgren, A., and Nyren, O. (1999a). Symptomatic gastroesophageal reflux as a risk factor for esophageal adenocarcinoma. *N Engl J Med.* **340**, 825-831.

Lagergren, J., Bergstrom, R., and Nyren, O. (1999b). Association between body mass and adenocarcinoma of the esophagus and gastric cardia. *Ann Intern Med.* **130**, 883-890.

Lambert, J.D., Hong, J., Yang, G.Y., Liao, J., and Yang, C.S. (2005). Inhibition of carcinogenesis by polyphenols: evidence from laboratory investigations. *Am J Clin Nutr.* **81**, 284S-291S.

Lammert, A., Kiess, W., Bottner, A., Glasow, A., and Kratzsch, J. (2001). Soluble leptin receptor represents the main leptin binding activity in human blood. *Biochem Biophys Res Commun.* **283**, 982-988.

Langenskiold, M., Holmdahl, L., Angenete, E., Falk, P., Nordgren, S., and Ivarsson, M.L. (2009). Differential prognostic impact of uPA and PAI-1 in colon and rectal cancer. *Tumour Biol.* **30**, 210-220.

Langman, M.J., Cheng, K.K., Gilman, E.A., and Lancashire, R.J. (2000). Effect of anti-inflammatory drugs on overall risk of common cancer: case-control study in general practice research database. *BMJ*. **320**, 1642-1646.

Lazar, M.A. (2005). How obesity causes diabetes: not a tall tale. *Science*. **307**, 373-375.

Leinonen, T., Pirinen, R., Bohm, J., Johansson, R., and Kosma, V.M. (2008). Increased expression of matrix metalloproteinase-2 (MMP-2) predicts tumour recurrence and unfavourable outcome in non-small cell lung cancer. *Histol Histopathol*. **23**, 693-700.

Lijnen, H.R. (2008). Angiogenesis and obesity. *Cardiovasc Res*. **78**, 286-293.

Lincoln, D.W., 2nd, and Bove, K. (2005). The transcription factor Ets-1 in breast cancer. *Front Biosci*. **10**, 506-511.

Linder, K., Arner, P., Flores-Morales, A., Tollet-Egnell, P., and Norstedt, G. (2004). Differentially expressed genes in visceral or subcutaneous adipose tissue of obese men and women. *J Lipid Res*. **45**, 148-154.

Liotta, L.A., Steeg, P.S., and Stetler-Stevenson, W.G. (1991). Cancer metastasis and angiogenesis: an imbalance of positive and negative regulation. *Cell*. **64**, 327-336.

Lipshutz, R.J., Fodor, S.P., Gingeras, T.R., and Lockhart, D.J. (1999). High density synthetic oligonucleotide arrays. *Nat Genet*. **21**, 20-24.

Litton, J.K., Gonzalez-Angulo, A.M., Warneke, C.L., Buzdar, A.U., Kau, S.W., Bondy, M., Mahabir, S., Hortobagyi, G.N., and Brewster, A.M. (2008). Relationship between obesity and pathologic response to neoadjuvant chemotherapy among women with operable breast cancer. *J Clin Oncol*. **26**, 4072-4077.

Liu, H., Zhang, W., Kennard, S., Caldwell, R.B., and Lilly, B. (2010). Notch3 Is Critical for Proper Angiogenesis and Mural Cell Investment. *Circ Res*.(in press)

Liu, J., Divoux, A., Sun, J., Zhang, J., Clement, K., Glickman, J.N., Sukhova, G.K., Wolters, P.J., Du, J., Gorgun, C.Z., *et al.* (2009). Genetic deficiency and pharmacological stabilization of mast cells reduce diet-induced obesity and diabetes in mice. *Nat Med*. **15**, 940-945.

Lord, G.M., Matarese, G., Howard, J.K., Baker, R.J., Bloom, S.R., and Lechler, R.I. (1998). Leptin modulates the T-cell immune response and reverses starvation-induced immunosuppression. *Nature*. **394**, 897-901.

Ludwig, T. (2005). Local proteolytic activity in tumor cell invasion and metastasis. *Bioessays*. **27**, 1181-1191.

Lumeng, C.N., Bodzin, J.L., and Saltiel, A.R. (2007). Obesity induces a phenotypic switch in adipose tissue macrophage polarization. *J Clin Invest*. **117**, 175-184.

Ma, L.J., Mao, S.L., Taylor, K.L., Kanjanabuch, T., Guan, Y., Zhang, Y., Brown, N.J., Swift, L.L., McGuinness, O.P., Wasserman, D.H., *et al.* (2004). Prevention of obesity and insulin resistance in mice lacking plasminogen activator inhibitor 1. *Diabetes*. **53**, 336-346.

MacDougald, O.A., Hwang, C.S., Fan, H., and Lane, M.D. (1995). Regulated expression of the obese gene product (leptin) in white adipose tissue and 3T3-L1 adipocytes. *Proc Natl Acad Sci U S A*. **92**, 9034-9037.

MacDougald, O.A., and Lane, M.D. (1995). Transcriptional regulation of gene expression during adipocyte differentiation. *Annu Rev Biochem*. **64**, 345-373.

MacLaren, R., Cui, W., Simard, S., and Cianflone, K. (2008). Influence of obesity and insulin sensitivity on insulin signaling genes in human omental and subcutaneous adipose tissue. *J Lipid Res*. **49**, 308-323.

Madani, K., Zhao, R., Lim, H.J., and Casson, A.G. (2010). Prognostic value of p53 mutations in oesophageal adenocarcinoma: final results of a 15-year prospective study. *Eur J Cardiothorac Surg*. **37**, 1427-1432.

Madsen, E.L., Bruun, J.M., Skogstrand, K., Hougaard, D.M., Christiansen, T., and Richelsen, B. (2009). Long-term weight loss decreases the nontraditional cardiovascular risk factors interleukin-18 and matrix metalloproteinase-9 in obese subjects. *Metabolism*. **58**, 946-953.

Mandard, S., Zandbergen, F., Tan, N.S., Escher, P., Patsouris, D., Koenig, W., Kleemann, R., Bakker, A., Veenman, F., Wahli, W., *et al*. (2004). The direct peroxisome proliferator-activated receptor target fasting-induced adipose factor (FIAF/PGAR/ANGPTL4) is present in blood plasma as a truncated protein that is increased by fenofibrate treatment. *J Biol Chem*. **279**, 34411-34420.

Mantovani, A., Allavena, P., Sica, A., and Balkwill, F. (2008). Cancer-related inflammation. *Nature*. **454**, 436-444.

Martin, T.A., Goyal, A., Watkins, G., and Jiang, W.G. (2005). Expression of the transcription factors snail, slug, and twist and their clinical significance in human breast cancer. *Ann Surg Oncol*. **12**, 488-496.

Martinez-Zaguilan, R., Seftor, E.A., Seftor, R.E., Chu, Y.W., Gillies, R.J., and Hendrix, M.J. (1996). Acidic pH enhances the invasive behavior of human melanoma cells. *Clin Exp Metastasis*. **14**, 176-186.

Maruthur, N.M., Bolen, S., Brancati, F.L., and Clark, J.M. (2009a). Obesity and mammography: a systematic review and meta-analysis. *J Gen Intern Med*. **24**, 665-677.

Maruthur, N.M., Bolen, S.D., Brancati, F.L., and Clark, J.M. (2009b). The association of obesity and cervical cancer screening: a systematic review and meta-analysis. *Obesity (Silver Spring)*. **17**, 375-381.

Mathe, E.A., Nguyen, G.H., Bowman, E.D., Zhao, Y., Budhu, A., Schetter, A.J., Braun, R., Reimers, M., Kumamoto, K., Hughes, D., *et al*. (2009). MicroRNA expression in squamous cell carcinoma and adenocarcinoma of the esophagus: associations with survival. *Clin Cancer Res*. **15**, 6192-6200.

Mathieu, P., Lemieux, I., and Despres, J.P. (2010). Obesity, inflammation, and cardiovascular risk. *Clin Pharmacol Ther*. **87**, 407-416.

Matoba, S., Kang, J.G., Patino, W.D., Wragg, A., Boehm, M., Gavrilova, O., Hurley, P.J., Bunz, F., and Hwang, P.M. (2006). p53 regulates mitochondrial respiration. *Science*. **312**, 1650-1653.

Meyerhardt, J.A., Catalano, P.J., Haller, D.G., Mayer, R.J., Benson, A.B., 3rd, Macdonald, J.S., and Fuchs, C.S. (2003). Influence of body mass index on outcomes and treatment-related toxicity in patients with colon carcinoma. *Cancer*. **98**, 484-495.

Miele, L., Golde, T., and Osborne, B. (2006). Notch signaling in cancer. *Curr Mol Med*. **6**, 905-918.

Miller, C.T., Moy, J.R., Lin, L., Schipper, M., Normolle, D., Brenner, D.E., Iannettoni, M.D., Orringer, M.B., and Beer, D.G. (2003). Gene amplification in esophageal adenocarcinomas and Barrett's with high-grade dysplasia. *Clin Cancer Res*. **9**, 4819-4825.

Misra, A., and Vikram, N.K. (2003). Clinical and pathophysiological consequences of abdominal adiposity and abdominal adipose tissue depots. *Nutrition*. **19**, 457-466.

Miyoshi, Y., Funahashi, T., Kihara, S., Taguchi, T., Tamaki, Y., Matsuzawa, Y., and Noguchi, S. (2003). Association of serum adiponectin levels with breast cancer risk. *Clin Cancer Res*. **9**, 5699-5704.

Mohamed-Ali, V., Goodrick, S., Rawesh, A., Katz, D.R., Miles, J.M., Yudkin, J.S., Klein, S., and Coppack, S.W. (1997). Subcutaneous adipose tissue releases interleukin-6, but not tumor necrosis factor-alpha, in vivo. *J Clin Endocrinol Metab*. **82**, 4196-4200.

Molchadsky, A., Rivlin, N., Brosh, R., Rotter, V., and Sarig, R. (2010). p53 is balancing development, differentiation and de-differentiation to assure cancer prevention. *Carcinogenesis*. **31**, 1501-1508.

Moloney, F., Toomey, S., Noone, E., Nugent, A., Allan, B., Loscher, C.E., and Roche, H.M. (2007). Antidiabetic effects of cis-9, trans-11-conjugated linoleic acid may be mediated via anti-inflammatory effects in white adipose tissue. *Diabetes*. **56**, 574-582.

Mootha, V.K., Lindgren, C.M., Eriksson, K.F., Subramanian, A., Sihag, S., Lehar, J., Puigserver, P., Carlsson, E., Ridderstrale, M., Laurila, E., *et al.* (2003). PGC-1alpha-responsive genes involved in oxidative phosphorylation are coordinately downregulated in human diabetes. *Nat Genet*. **34**, 267-273.

Morine, M.J., O'Brien, C., and Roche, H.M. (2008). Session 2: Personalised nutrition. Transcriptomic signatures that have identified key features of metabolic syndrome. *Proc Nutr Soc*. **67**, 395-403.

Mroczko, B., Lukaszewicz-Zajac, M., Wereszczynska-Siemiatkowska, U., Groblewska, M., Gryko, M., Kedra, B., Jurkowska, G., and Szmitkowski, M. (2009). Clinical significance of the measurements of serum matrix metalloproteinase-9 and its inhibitor (tissue inhibitor of metalloproteinase-1) in patients with pancreatic cancer: metalloproteinase-9 as an independent prognostic factor. *Pancreas*. **38**, 613-618.

Murphy, T.J., Ravi, N., and Reynolds, J.V. (2008). Treatment options for esophageal cancer. *Expert Opin Pharmacother*. **9**, 3197-3210.

Must, A., Spadano, J., Coakley, E.H., Field, A.E., Colditz, G., and Dietz, W.H. (1999). The disease burden associated with overweight and obesity. *JAMA*. **282**, 1523-1529.

Mutoh, M., Niho, N., Komiya, M., Takahashi, M., Ohtsubo, R., Nakatogawa, K., Ueda, K., Sugimura, T., and Wakabayashi, K. (2008). Plasminogen activator inhibitor-1 (Pai-1) blockers suppress intestinal polyp formation in Min mice. *Carcinogenesis*. **29**, 824-829.

National Cancer Registry Ireland. Incidence, mortality, treatment and survival. 1994-2007 (downloaded from www.ncri.ie)

Neale, R.E., Doecke, J.D., Pandeya, N., Sadeghi, S., Green, A.C., Webb, P.M., and Whiteman, D.C. (2009). Does type 2 diabetes influence the risk of oesophageal adenocarcinoma? *Br J Cancer*. **100**, 795-798.

Neels, J.G., and Olefsky, J.M. (2006). Inflamed fat: what starts the fire? *J Clin Invest*. **116**, 33-35. Nekarda, H., Schmitt, M., Ulm, K., Wenninger, A., Vogelsang, H., Becker, K., Roder, J.D., Fink, U., and Siewert, J.R. (1994). Prognostic impact of urokinase-type plasminogen activator and its inhibitor PAI-1 in completely resected gastric cancer. *Cancer Res*. **54**, 2900-2907.

Newell, F.S., Su, H., Tornqvist, H., Whitehead, J.P., Prins, J.B., and Hutley, L.J. (2006). Characterization of the transcriptional and functional effects of fibroblast growth factor-1 on human preadipocyte differentiation. *FASEB J*. **20**, 2615-2617.

Nieto, M.A., Sargent, M.G., Wilkinson, D.G., and Cooke, J. (1994). Control of cell behavior during vertebrate development by Slug, a zinc finger gene. *Science*. **264**, 835-839.

Nishizawa, H., Shimomura, I., Kishida, K., Maeda, N., Kuriyama, H., Nagaretani, H., Matsuda, M., Kondo, H., Furuyama, N., Kihara, S., *et al.* (2002). Androgens decrease plasma adiponectin, an insulin-sensitizing adipocyte-derived protein. *Diabetes*. **51**, 2734-2741.

O'Riordan, J.M., Abdel-latif, M.M., Ravi, N., McNamara, D., Byrne, P.J., McDonald, G.S., Keeling, P.W., Kelleher, D., and Reynolds, J.V. (2005). Proinflammatory cytokine and nuclear factor kappa-B expression along the inflammation-metaplasia-dysplasia-adenocarcinoma sequence in the esophagus. *Am J Gastroenterol*. **100**, 1257-1264.

Ogden, C.L., Carroll, M.D., Curtin, L.R., McDowell, M.A., Tabak, C.J., and Flegal, K.M. (2006). Prevalence of overweight and obesity in the United States, 1999-2004. *JAMA*. **295**, 1549-1555.

Ogunwobi, O., Mutungi, G., and Beales, I.L. (2006). Leptin stimulates proliferation and inhibits apoptosis in Barrett's esophageal adenocarcinoma cells by cyclooxygenase-2-dependent, prostaglandin-E2-mediated transactivation of the epidermal growth factor receptor and c-Jun NH2-terminal kinase activation. *Endocrinology*. **147**, 4505-4516.

Ogunwobi, O.O., and Beales, I.L. (2007). The anti-apoptotic and growth stimulatory actions of leptin in human colon cancer cells involves activation of JNK mitogen activated protein kinase, JAK2 and PI3 kinase/Akt. *Int J Colorectal Dis*. **22**, 401-409.

Ogunwobi, O.O., and Beales, I.L. (2008a). Globular adiponectin, acting via adiponectin receptor-1, inhibits leptin-stimulated oesophageal adenocarcinoma cell proliferation. *Mol Cell Endocrinol*. **285**, 43-50.

Ogunwobi, O.O., and Beales, I.L. (2008b). Leptin stimulates the proliferation of human oesophageal adenocarcinoma cells via HB-EGF and Tgfalpha mediated transactivation of the epidermal growth factor receptor. *Br J Biomed Sci.* **65**, 121-127.

Ohmura, K., Ishimori, N., Ohmura, Y., Tokuhara, S., Nozawa, A., Horii, S., Andoh, Y., Fujii, S., Iwabuchi, K., Onoe, K., *et al.* (2010). Natural killer T cells are involved in adipose tissues inflammation and glucose intolerance in diet-induced obese mice. *Arterioscler Thromb Vasc Biol.* **30**, 193-199.

Onat, A., Avci, G.S., Barlan, M.M., Uyarel, H., Uzunlar, B., and Sansoy, V. (2004). Measures of abdominal obesity assessed for visceral adiposity and relation to coronary risk. *Int J Obes Relat Metab Disord.* **28**, 1018-1025.

Onwuegbusi, B.A., Aitchison, A., Chin, S.F., Kranjac, T., Mills, I., Huang, Y., Lao-Sirieix, P., Caldas, C., and Fitzgerald, R.C. (2006). Impaired transforming growth factor beta signalling in Barrett's carcinogenesis due to frequent SMAD4 inactivation. *Gut.* **55**, 764-774.

Otani, K., Kitayama, J., Kamei, T., Soma, D., Miyato, H., Yamauchi, T., Kadowaki, T., and Nagawa, H. (2010). Adiponectin receptors are downregulated in human gastric cancer. *J Gastroenterol.* (in press)

Otero, M., Lago, R., Lago, F., Casanueva, F.F., Dieguez, C., Gomez-Reino, J.J., and Gualillo, O. (2005). Leptin, from fat to inflammation: old questions and new insights. *FEBS Lett.* **579**, 295-301.

Pajvani, U.B., Hawkins, M., Combs, T.P., Rajala, M.W., Doebber, T., Berger, J.P., Wagner, J.A., Wu, M., Knopps, A., Xiang, A.H., *et al.* (2004). Complex distribution, not absolute amount of adiponectin, correlates with thiazolidinedione-mediated improvement in insulin sensitivity. *J Biol Chem.* **279**, 12152-12162.

Park, H.J., Della-Fera, M.A., Hausman, D.B., Rayalam, S., Ambati, S., and Baile, C.A. (2009). Genistein inhibits differentiation of primary human adipocytes. *J Nutr Biochem.* **20**, 140-148.

Patel, L., Buckels, A.C., Kinghorn, I.J., Murdock, P.R., Holbrook, J.D., Plumpton, C., Macphee, C.H., and Smith, S.A. (2003). Resistin is expressed in human macrophages and directly regulated by PPAR gamma activators. *Biochem Biophys Res Commun.* **300**, 472-476.

Peng, D.F., Razvi, M., Chen, H., Washington, K., Roessner, A., Schneider-Stock, R., and El-Rifai, W. (2009). DNA hypermethylation regulates the expression of members of the Mu-class glutathione S-transferases and glutathione peroxidases in Barrett's adenocarcinoma. *Gut.* **58**, 5-15.

Pera, M., Trastek, V.F., Carpenter, H.A., Allen, M.S., Deschamps, C., and Pairolero, P.C. (1992). Barrett's esophagus with high-grade dysplasia: an indication for esophagectomy? *Ann Thorac Surg.* **54**, 199-204.

Perego, P., Cossa, G., Zuco, V., and Zunino, F. (2010). Modulation of cell sensitivity to antitumor agents by targeting survival pathways. *Biochem Pharmacol.* (in press).

Perez-Mancera, P.A., Bermejo-Rodriguez, C., Gonzalez-Herrero, I., Herranz, M., Flores, T., Jimenez, R., and Sanchez-Garcia, I. (2007). Adipose tissue mass is modulated by SLUG (SNAI2). *Hum Mol Genet.* **16**, 2972-2986.

Perrini, S., Laviola, L., Cignarelli, A., Melchiorre, M., De Stefano, F., Caccioppoli, C., Natalicchio, A., Orlando, M.R., Garruti, G., De Fazio, M., *et al.* (2008). Fat depot-related differences in gene expression, adiponectin secretion, and insulin action and signalling in human adipocytes differentiated in vitro from precursor stromal cells. *Diabetologia.* **51**, 155-164.

Peters, C.J., and Fitzgerald, R.C. (2007). Systematic review: the application of molecular pathogenesis to prevention and treatment of oesophageal adenocarcinoma. *Aliment Pharmacol Ther.* **25**, 1253-1269.

Petridou, E., Mantzoros, C., Dessypris, N., Koukoulomatis, P., Addy, C., Voulgaris, Z., Chrousos, G., and Trichopoulos, D. (2003). Plasma adiponectin concentrations in relation to endometrial cancer: a case-control study in Greece. *J Clin Endocrinol Metab.* **88**, 993-997.

Pierini, R., Kroon, P.A., Guyot, S., Ivory, K., Johnson, I.T., and Belshaw, N.J. (2008). Procyanidin effects on oesophageal adenocarcinoma cells strongly depend on flavan-3-ol degree of polymerization. *Mol Nutr Food Res.* **52**, 1399-1407.

Portale, G., Hagen, J.A., Peters, J.H., Chan, L.S., DeMeester, S.R., Gandamihardja, T.A., and DeMeester, T.R. (2006). Modern 5-year survival of resectable esophageal adenocarcinoma: single institution experience with 263 patients. *J Am Coll Surg.* **202**, 588-596; discussion 596-588.

Pouliot, M.C., Despres, J.P., Lemieux, S., Moorjani, S., Bouchard, C., Tremblay, A., Nadeau, A., and Lupien, P.J. (1994). Waist circumference and abdominal sagittal diameter: best simple anthropometric indexes of abdominal visceral adipose tissue accumulation and related cardiovascular risk in men and women. *Am J Cardiol.* **73**, 460-468.

Prenzel, N., Zwick, E., Daub, H., Leserer, M., Abraham, R., Wallasch, C., and Ullrich, A. (1999). EGF receptor transactivation by G-protein-coupled receptors requires metalloproteinase cleavage of proHB-EGF. *Nature.* **402**, 884-888.

Radisky, E.S., and Radisky, D.C. (2010). Matrix metalloproteinase-induced epithelial-mesenchymal transition in breast cancer. *J Mammary Gland Biol Neoplasia.* **15**, 201-212.

Rasouli, N., and Kern, P.A. (2008). Adipocytokines and the metabolic complications of obesity. *J Clin Endocrinol Metab.* **93**, S64-73.

Reed, C.E. (1999). Surgical management of esophageal carcinoma. *Oncologist.* **4**, 95-105.

Reeves, G.K., Pirie, K., Beral, V., Green, J., Spencer, E., and Bull, D. (2007). Cancer incidence and mortality in relation to body mass index in the Million Women Study: cohort study. *BMJ.* **335**, 1134.

Reid, B.J., Li, X., Galipeau, P.C., and Vaughan, T.L. (2010). Barrett's oesophagus and oesophageal adenocarcinoma: time for a new synthesis. *Nat Rev Cancer.* **10**, 87-101.

Ren, H., Zhao, T., Wang, X., Gao, C., Wang, J., Yu, M., and Hao, J. (2010). Leptin upregulates telomerase activity and transcription of human telomerase reverse transcriptase in MCF-7 breast cancer cells. *Biochem Biophys Res Commun.* **394**, 59-63.

Renehan, A.G., Frystyk, J., and Flyvbjerg, A. (2006). Obesity and cancer risk: the role of the insulin-IGF axis. *Trends Endocrinol Metab*. **17**, 328-336.

Renehan, A.G., Tyson, M., Egger, M., Heller, R.F., and Zwahlen, M. (2008). Body-mass index and incidence of cancer: a systematic review and meta-analysis of prospective observational studies. *Lancet*. **371**, 569-578.

Renehan, A.G., Zwahlen, M., Minder, C., O'Dwyer, S.T., Shalet, S.M., and Egger, M. (2004). Insulin-like growth factor (IGF)-I, IGF binding protein-3, and cancer risk: systematic review and meta-regression analysis. *Lancet*. **363**, 1346-1353.

Robak, T., Wierzbowska, A., Blasinska-Morawiec, M., Korycka, A., and Blonski, J.Z. (1999). Serum levels of IL-6 type cytokines and soluble IL-6 receptors in active B-cell chronic lymphocytic leukemia and in cladribine induced remission. *Mediators Inflamm*. **8**, 277-286.

Roberts, D.L., Dive, C., and Renehan, A.G. (2009). Biological Mechanisms Linking Obesity and Cancer Risk: New Perspectives. *Annu Rev Med*. **61**, 301-16.

Roberts, R.Z., and Morris, A.J. (2000). Role of phosphatidic acid phosphatase 2a in uptake of extracellular lipid phosphate mediators. *Biochim Biophys Acta*. **1487**, 33-49.

Rocha, V.Z., Folco, E.J., Sukhova, G., Shimizu, K., Gotsman, I., Vernon, A.H., and Libby, P. (2008). Interferon-gamma, a Th1 cytokine, regulates fat inflammation: a role for adaptive immunity in obesity. *Circ Res*. **103**, 467-476.

Rodvold, K.A., Rushing, D.A., and Tewksbury, D.A. (1988). Doxorubicin clearance in the obese. *J Clin Oncol*. **6**, 1321-1327.

Roedl, J.B., Blake, M.A., Holalkere, N.S., Mueller, P.R., Colen, R.R., and Harisinghani, M.G. (2009). Lymph node staging in esophageal adenocarcinoma with PET-CT based on a visual analysis and based on metabolic parameters. *Abdom Imaging*. **34**, 610-617.

Rosen, E.D., and MacDougald, O.A. (2006). Adipocyte differentiation from the inside out. *Nat Rev Mol Cell Biol*. **7**, 885-896.

Rosenow, A., Arrey, T., Bouwman, F.G., Noben, J.P., Wabitsch, M., Mariman, E.C., Karas, M., and Renes, J. (2010). Identification of novel human adipocyte secreted proteins by using SGBS cells. *J Proteome Res*. **9**, 5389-401

Ruckhaberle, E., Holtrich, U., Engels, K., Hanker, L., Gatje, R., Metzler, D., Karn, T., Kaufmann, M., and Rody, A. (2009). Acid ceramidase 1 expression correlates with a better prognosis in ER-positive breast cancer. *Climacteric*. **12**, 502-513.

Ruffell, B., DeNardo, D.G., Affara, N.I., and Coussens, L.M. (2010). Lymphocytes in cancer development: polarization towards pro-tumor immunity. *Cytokine Growth Factor Rev*. **21**, 3-10.

Ryan, A.M., Healy, L.A., Power, D.G., Byrne, M., Murphy, S., Byrne, P.J., Kelleher, D., and Reynolds, J.V. (2008). Barrett esophagus: prevalence of central adiposity, metabolic syndrome, and a proinflammatory state. *Ann Surg*. **247**, 909-915.

Ryan, A.M., Rowley, S.P., Fitzgerald, A.P., Ravi, N., and Reynolds, J.V. (2006). Adenocarcinoma of the oesophagus and gastric cardia: male preponderance in association with obesity. *Eur J Cancer*. **42**, 1151-1158.

Safran, H., Dipetrillo, T., Akerman, P., Ng, T., Evans, D., Steinhoff, M., Benton, D., Purviance, J., Goldstein, L., Tantravahi, U., *et al.* (2007). Phase I/II study of trastuzumab, paclitaxel, cisplatin and radiation for locally advanced, HER2 overexpressing, esophageal adenocarcinoma. *Int J Radiat Oncol Biol Phys*. **67**, 405-409.

Safran, H., Suntharalingam, M., Dipetrillo, T., Ng, T., Doyle, L.A., Krasna, M., Plette, A., Evans, D., Wanebo, H., Akerman, P., *et al.* (2008). Cetuximab with concurrent chemoradiation for esophagogastric cancer: assessment of toxicity. *Int J Radiat Oncol Biol Phys*. **70**, 391-395.

Sakakibara, T., Hibi, K., Koike, M., Fujiwara, M., Kodera, Y., Ito, K., and Nakao, A. (2005). Plasminogen activator inhibitor-1 as a potential marker for the malignancy of colorectal cancer. *Br J Cancer*. **93**, 799-803.

Sakamoto, K., Hikiba, Y., Nakagawa, H., Hayakawa, Y., Yanai, A., Akanuma, M., Ogura, K., Hirata, Y., Kaestner, K.H., Omata, M., *et al.* (2010). Inhibitor of kappaB kinase beta regulates gastric carcinogenesis via interleukin-1alpha expression. *Gastroenterology*. **139**, 226-238 e226.

Samad, F., Pandey, M., and Loskutoff, D.J. (1998). Tissue factor gene expression in the adipose tissues of obese mice. *Proc Natl Acad Sci U S A*. **95**, 7591-7596.

Samad, F., Yamamoto, K., Pandey, M., and Loskutoff, D.J. (1997). Elevated expression of transforming growth factor-beta in adipose tissue from obese mice. *Mol Med*. **3**, 37-48.

Samarakoon, R., Higgins, C.E., Higgins, S.P., and Higgins, P.J. (2009). TGF-beta1-Induced Expression of the Poor Prognosis SERPINE1/PAI-1 Gene Requires EGFR Signaling: A New Target for Anti-EGFR Therapy. *J Oncol*. **2009**, 342391.

Sandler, A., Gray, R., Perry, M.C., Brahmer, J., Schiller, J.H., Dowlati, A., Lilenbaum, R., and Johnson, D.H. (2006). Paclitaxel-carboplatin alone or with bevacizumab for non-small-cell lung cancer. *N Engl J Med*. **355**, 2542-2550.

Sartipy, P., and Loskutoff, D.J. (2003). Monocyte chemoattractant protein 1 in obesity and insulin resistance. *Proc Natl Acad Sci U S A*. **100**, 7265-7270.

Saxena, N.K., Taliaferro-Smith, L., Knight, B.B., Merlin, D., Anania, F.A., O'Regan, R.M., and Sharma, D. (2008). Bidirectional crosstalk between leptin and insulin-like growth factor-I signaling promotes invasion and migration of breast cancer cells via transactivation of epidermal growth factor receptor. *Cancer Res*. **68**, 9712-9722.

Schaffler, A., Scholmerich, J., and Buechler, C. (2007). Mechanisms of disease: adipokines and breast cancer - endocrine and paracrine mechanisms that connect adiposity and breast cancer. *Nat Clin Pract Endocrinol Metab*. **3**, 345-354.

Schaller, M.D. (2001). Biochemical signals and biological responses elicited by the focal adhesion kinase. *Biochim Biophys Acta*. **1540**, 1-21.

Schauer, M., Janssen, K.P., Rimkus, C., Raggi, M., Feith, M., Friess, H., and Theisen, J. (2010). Microarray-based response prediction in esophageal adenocarcinoma. *Clin Cancer Res*. **16**, 330-337.

Schelbert, K.B. (2009). Comorbidities of obesity. *Prim Care*. **36**, 271-285.

Schneider, P.M., Stoeltzing, O., Roth, J.A., Hoelscher, A.H., Wegerer, S., Mizumoto, S., Becker, K., Dittler, H.J., Fink, U., and Siewert, J.R. (2000). P53 mutational status improves estimation of prognosis in patients with curatively resected adenocarcinoma in Barrett's esophagus. *Clin Cancer Res*. **6**, 3153-3158.

Schram, K., De Girolamo, S., Madani, S., Munoz, D., Thong, F., and Sweeney, G. (2010). Leptin regulates MMP-2, TIMP-1 and collagen synthesis via p38 MAPK in HL-1 murine cardiomyocytes. *Cell Mol Biol Lett*. **15**, 551-63.

Schwock, J., Dhani, N., and Hedley, D.W. (2010). Targeting focal adhesion kinase signaling in tumor growth and metastasis. *Expert Opin Ther Targets*. **14**, 77-94.

Seder, C.W., Hartojo, W., Lin, L., Silvers, A.L., Wang, Z., Thomas, D.G., Giordano, T.J., Chen, G., Chang, A.C., Orringer, M.B., *et al.* (2009). INHBA overexpression promotes cell proliferation and may be epigenetically regulated in esophageal adenocarcinoma. *J Thorac Oncol*. **4**, 455-462.

Segal, K.R., Landt, M., and Klein, S. (1996). Relationship between insulin sensitivity and plasma leptin concentration in lean and obese men. *Diabetes*. **45**, 988-991.

Sentinelli, F., Romeo, S., Arca, M., Filippi, E., Leonetti, F., Banchieri, M., Di Mario, U., and Baroni, M.G. (2002). Human resistin gene, obesity, and type 2 diabetes: mutation analysis and population study. *Diabetes*. **51**, 860-862.

Sewter, C.P., Blows, F., Vidal-Puig, A., and O'Rahilly, S. (2002). Regional differences in the response of human pre-adipocytes to PPARgamma and RXRalpha agonists. *Diabetes*. **51**, 718-723.

Seyrantepe, V., Poupetova, H., Froissart, R., Zabot, M.T., Maire, I., and Pshezhetsky, A.V. (2003). Molecular pathology of NEU1 gene in sialidosis. *Hum Mutat*. **22**, 343-352.

Shah, C., Yang, G., Lee, I., Bielawski, J., Hannun, Y.A., and Samad, F. (2008). Protection from high fat diet-induced increase in ceramide in mice lacking plasminogen activator inhibitor 1. *J Biol Chem*. **283**, 13538-13548.

Shammas, M.A., Qazi, A., Batchu, R.B., Bertheau, R.C., Wong, J.Y., Rao, M.Y., Prasad, M., Chanda, D., Ponnazhagan, S., Anderson, K.C., *et al.* (2008). Telomere maintenance in laser capture microdissection-purified Barrett's adenocarcinoma cells and effect of telomerase inhibition in vivo. *Clin Cancer Res*. **14**, 4971-4980.

Shay, J.W., and Bacchetti, S. (1997). A survey of telomerase activity in human cancer. *Eur J Cancer*. **33**, 787-791.

Shepherd, F.A., Giaccone, G., Seymour, L., Debruyne, C., Bezjak, A., Hirsh, V., Smylie, M., Rubin, S., Martins, H., Lamont, A., *et al.* (2002). Prospective, randomized, double-blind, placebo-controlled trial of marimastat after response to first-line chemotherapy in patients with small-

cell lung cancer: a trial of the National Cancer Institute of Canada-Clinical Trials Group and the European Organization for Research and Treatment of Cancer. *J Clin Oncol*. **20**, 4434-4439.

Shibata, A., Matsuda, T., Ajiki, W., and Sobue, T. (2008). Trend in incidence of adenocarcinoma of the esophagus in Japan, 1993-2001. *Jpn J Clin Oncol*. **38**, 464-468.

Shimokawa Ki, K., Katayama, M., Matsuda, Y., Takahashi, H., Hara, I., Sato, H., and Kaneko, S. (2002). Matrix metalloproteinase (MMP)-2 and MMP-9 activities in human seminal plasma. *Mol Hum Reprod*. **8**, 32-36.

Shioiri, M., Shida, T., Koda, K., Oda, K., Seike, K., Nishimura, M., Takano, S., and Miyazaki, M. (2006). Slug expression is an independent prognostic parameter for poor survival in colorectal carcinoma patients. *Br J Cancer*. **94**, 1816-1822.

Shishodia, S., Koul, D., and Aggarwal, B.B. (2004). Cyclooxygenase (COX)-2 inhibitor celecoxib abrogates TNF-induced NF-kappa B activation through inhibition of activation of I kappa B alpha kinase and Akt in human non-small cell lung carcinoma: correlation with suppression of COX-2 synthesis. *J Immunol*. **173**, 2011-2022.

Sierra-Honigmann, M.R., Nath, A.K., Murakami, C., Garcia-Cardena, G., Papapetropoulos, A., Sessa, W.C., Madge, L.A., Schechner, J.S., Schwabb, M.B., Polverini, P.J., *et al*. (1998). Biological action of leptin as an angiogenic factor. *Science*. **281**, 1683-1686.

Siewert, J.R., Stein, H.J., Feith, M., Bruecher, B.L., Bartels, H., and Fink, U. (2001). Histologic tumor type is an independent prognostic parameter in esophageal cancer: lessons from more than 1,000 consecutive resections at a single center in the Western world. *Ann Surg*. **234**, 360-367; discussion 368-369.

Silha, J.V., Krsek, M., Sucharda, P., and Murphy, L.J. (2005). Angiogenic factors are elevated in overweight and obese individuals. *Int J Obes (Lond)*. **29**, 1308-1314.

Smith, E.R., Merrill, A.H., Obeid, L.M., and Hannun, Y.A. (2000). Effects of sphingosine and other sphingolipids on protein kinase C. *Methods Enzymol*. **312**, 361-373.

Somasundar, P., Riggs, D., Jackson, B., Vona-Davis, L., and McFadden, D.W. (2003). Leptin stimulates esophageal adenocarcinoma growth by nonapoptotic mechanisms. *Am J Surg*. **186**, 575-578.

Spano, J.P., Fagard, R., Soria, J.C., Rixe, O., Khayat, D., and Milano, G. (2005). Epidermal growth factor receptor signaling in colorectal cancer: preclinical data and therapeutic perspectives. *Ann Oncol*. **16**, 189-194.

Sparano, J.A., Bernardo, P., Stephenson, P., Gradishar, W.J., Ingle, J.N., Zucker, S., and Davidson, N.E. (2004). Randomized phase III trial of marimastat versus placebo in patients with metastatic breast cancer who have responding or stable disease after first-line chemotherapy: Eastern Cooperative Oncology Group trial E2196. *J Clin Oncol*. **22**, 4683-4690.

Spiegelman, B.M., and Farmer, S.R. (1982). Decreases in tubulin and actin gene expression prior to morphological differentiation of 3T3 adipocytes. *Cell*. **29**, 53-60.

Steppan, C.M., Bailey, S.T., Bhat, S., Brown, E.J., Banerjee, R.R., Wright, C.M., Patel, H.R., Ahima, R.S., and Lazar, M.A. (2001). The hormone resistin links obesity to diabetes. *Nature.* **409**, 307-312.

Sternlicht, M.D., Dunning, A.M., Moore, D.H., Pharoah, P.D., Ginzinger, D.G., Chin, K., Gray, J.W., Waldman, F.M., Ponder, B.A., and Werb, Z. (2006). Prognostic value of PAI1 in invasive breast cancer: evidence that tumor-specific factors are more important than genetic variation in regulating PAI1 expression. *Cancer Epidemiol Biomarkers Prev.* **15**, 2107-2114.

Stetler-Stevenson, W.G. (1999). Matrix metalloproteinases in angiogenesis: a moving target for therapeutic intervention. *J Clin Invest.* **103**, 1237-1241.

Strissel, K.J., Stancheva, Z., Miyoshi, H., Perfield, J.W., 2nd, DeFuria, J., Jick, Z., Greenberg, A.S., and Obin, M.S. (2007). Adipocyte death, adipose tissue remodeling, and obesity complications. *Diabetes.* **56**, 2910-2918.

Suganami, E., Takagi, H., Ohashi, H., Suzuma, K., Suzuma, I., Oh, H., Watanabe, D., Ojima, T., Suganami, T., Fujio, Y., *et al.* (2004). Leptin stimulates ischemia-induced retinal neovascularization: possible role of vascular endothelial growth factor expressed in retinal endothelial cells. *Diabetes.* **53**, 2443-2448.

Sun, J., Sukhova, G.K., Wolters, P.J., Yang, M., Kitamoto, S., Libby, P., MacFarlane, L.A., Mallen-St Clair, J., and Shi, G.P. (2007). Mast cells promote atherosclerosis by releasing proinflammatory cytokines. *Nat Med.* **13**, 719-724.

Survey of Lifestyle, Attitudes and Nutrition (SLAN) 2007 Main Report (2008). (downloaded from http://www.slan06.ie).

Syrigos, K.N., Zalonis, A., Kotteas, E., and Saif, M.W. (2008). Targeted therapy for oesophageal cancer: an overview. *Cancer Metastasis Rev.* **27**, 273-288.

Szlosarek, P.W., Grimshaw, M.J., Kulbe, H., Wilson, J.L., Wilbanks, G.D., Burke, F., and Balkwill, F.R. (2006). Expression and regulation of tumor necrosis factor alpha in normal and malignant ovarian epithelium. *Mol Cancer Ther.* **5**, 382-390.

Takahata, C., Miyoshi, Y., Irahara, N., Taguchi, T., Tamaki, Y., and Noguchi, S. (2007). Demonstration of adiponectin receptors 1 and 2 mRNA expression in human breast cancer cells. *Cancer Lett.* **250**, 229-236.

Tas, F., Duranyildiz, D., Oguz, H., Camlica, H., Yasasever, V., and Topuz, E. (2006). Serum vascular endothelial growth factor (VEGF) and interleukin-8 (IL-8) levels in small cell lung cancer. *Cancer Invest.* **24**, 492-496.

Tchkonia, T., Giorgadze, N., Pirtskhalava, T., Tchoukalova, Y., Karagiannides, I., Forse, R.A., DePonte, M., Stevenson, M., Guo, W., Han, J., *et al.* (2002). Fat depot origin affects adipogenesis in primary cultured and cloned human preadipocytes. *Am J Physiol Regul Integr Comp Physiol.* **282**, R1286-1296.

Tchkonia, T., Giorgadze, N., Pirtskhalava, T., Thomou, T., DePonte, M., Koo, A., Forse, R.A., Chinnappan, D., Martin-Ruiz, C., von Zglinicki, T., *et al.* (2006). Fat depot-specific characteristics are retained in strains derived from single human preadipocytes. *Diabetes.* **55**, 2571-2578.

Tchkonia, T., Lenburg, M., Thomou, T., Giorgadze, N., Frampton, G., Pirtskhalava, T., Cartwright, A., Cartwright, M., Flanagan, J., Karagiannides, I., *et al.* (2007). Identification of depot-specific human fat cell progenitors through distinct expression profiles and developmental gene patterns. *Am J Physiol Endocrinol Metab.* **292**, E298-307.

The International Diabetes Federation (2006). The IDF Consensus: Worldwide Definition of the Metabolic Syndrome. (downloaded from http:/www.idf.org/webdata/docs/MetS_def_update2006.pdf)

The National Cholesterol Education Program (NCEP). (2001). Executive Summary of the Third Report of the NCEP Expert Panel on detection, evaluation and treatment of High Blood Cholesterol in Adults (Adult Treatment Panel III). *JAMA.* **285**, 2486-97.

Tilg, H., and Moschen, A.R. (2006). Adipocytokines: mediators linking adipose tissue, inflammation and immunity. *Nat Rev Immunol.* **6**, 772-783.

Trayhurn, P., Wang, B., and Wood, I.S. (2008). Hypoxia in adipose tissue: a basis for the dysregulation of tissue function in obesity? *Br J Nutr.* **100**, 227-235.

Trayhurn, P., and Wood, I.S. (2004). Adipokines: inflammation and the pleiotropic role of white adipose tissue. *Br J Nutr.* **92**, 347-355.

Trevisan, M., Liu, J., Muti, P., Misciagna, G., Menotti, A., and Fucci, F. (2001). Markers of insulin resistance and colorectal cancer mortality. *Cancer Epidemiol Biomarkers Prev.* **10**, 937-941.

Turpeenniemi-Hujanen, T. (2005). Gelatinases (MMP-2 and -9) and their natural inhibitors as prognostic indicators in solid cancers. *Biochimie.* **87**, 287-297.

Uchikado, Y., Natsugoe, S., Okumura, H., Setoyama, T., Matsumoto, M., Ishigami, S., and Aikou, T. (2005). Slug Expression in the E-cadherin preserved tumors is related to prognosis in patients with esophageal squamous cell carcinoma. *Clin Cancer Res.* **11**, 1174-1180.

Unal, R., Yao-Borengasser, A., Varma, V., Rasouli, N., Labbate, C., Kern, P.A., and Ranganathan, G. (2010). Matrix metalloproteinase-9 is increased in obese subjects and decreases in response to pioglitazone. *J Clin Endocrinol Metab.* **95**, 2993-3001.

Urschel, J.D., and Vasan, H. (2003). A meta-analysis of randomized controlled trials that compared neoadjuvant chemoradiation and surgery to surgery alone for resectable esophageal cancer. *Am J Surg.* **185**, 538-543.

Valsamakis, G., Chetty, R., Anwar, A., Banerjee, A.K., Barnett, A., and Kumar, S. (2004). Association of simple anthropometric measures of obesity with visceral fat and the metabolic syndrome in male Caucasian and Indo-Asian subjects. *Diabet Med.* **21**, 1339-1345.

van Baal, J.W., Diks, S.H., Wanders, R.J., Rygiel, A.M., Milano, F., Joore, J., Bergman, J.J., Peppelenbosch, M.P., and Krishnadath, K.K. (2006). Comparison of kinome profiles of Barrett's esophagus with normal squamous esophagus and normal gastric cardia. *Cancer Res.* **66**, 11605-11612.

van der Sijs, H., and Guchelaar, H.J. (2002). Formulas for calculating body surface area. *Ann Pharmacother.* **36**, 345-346.

van Eijk, M., Aten, J., Bijl, N., Ottenhoff, R., van Roomen, C.P., Dubbelhuis, P.F., Seeman, I., Ghauharali-van der Vlugt, K., Overkleeft, H.S., Arbeeny, C., *et al.* (2009). Reducing glycosphingolipid content in adipose tissue of obese mice restores insulin sensitivity, adipogenesis and reduces inflammation. *PLoS One*. **4**, e4723.

Veilleux, A., Blouin, K., Rheaume, C., Daris, M., Marette, A., and Tchernof, A. (2009). Glucose transporter 4 and insulin receptor substrate-1 messenger RNA expression in omental and subcutaneous adipose tissue in women. *Metabolism*. **58**, 624-631.

Vogelstein, B., Lane, D., and Levine, A.J. (2000). Surfing the p53 network. *Nature*. **408**, 307-310.

von Gruenigen, V.E., Tian, C., Frasure, H., Waggoner, S., Keys, H., and Barakat, R.R. (2006). Treatment effects, disease recurrence, and survival in obese women with early endometrial carcinoma : a Gynecologic Oncology Group study. *Cancer*. **107**, 2786-2791.

Vosseler, S., Lederle, W., Airola, K., Obermueller, E., Fusenig, N.E., and Mueller, M.M. (2009). Distinct progression-associated expression of tumor and stromal MMPs in HaCaT skin SCCs correlates with onset of invasion. *Int J Cancer*. **125**, 2296-2306.

Vousden, K.H., and Lane, D.P. (2007). p53 in health and disease. *Nat Rev Mol Cell Biol*. **8**, 275-283.

Vozarova, B., Weyer, C., Hanson, K., Tataranni, P.A., Bogardus, C., and Pratley, R.E. (2001). Circulating interleukin-6 in relation to adiposity, insulin action, and insulin secretion. *Obes Res*. **9**, 414-417.

Wabitsch, M., Brenner, R.E., Melzner, I., Braun, M., Moller, P., Heinze, E., Debatin, K.M., and Hauner, H. (2001). Characterization of a human preadipocyte cell strain with high capacity for adipose differentiation. *Int J Obes Relat Metab Disord*. **25**, 8-15.

Wabitsch, M., Jensen, P.B., Blum, W.F., Christoffersen, C.T., Englaro, P., Heinze, E., Rascher, W., Teller, W., Tornqvist, H., and Hauner, H. (1996). Insulin and cortisol promote leptin production in cultured human fat cells. *Diabetes*. **45**, 1435-1438.

Wajchenberg, B.L. (2000). Subcutaneous and visceral adipose tissue: their relation to the metabolic syndrome. *Endocr Rev*. **21**, 697-738.

Walewski, J.L., Ge, F., Gagner, M., Inabnet, W.B., Pomp, A., Branch, A.D., and Berk, P.D. Adipocyte accumulation of long-chain fatty acids in obesity is multifactorial, resulting from increased fatty acid uptake and decreased activity of genes involved in fat utilization. *Obes Surg*. **20**, 93-107.

Walker, G.E., Marzullo, P., Verti, B., Guzzaloni, G., Maestrini, S., Zurleni, F., Liuzzi, A., and Di Blasio, A.M. (2008). Subcutaneous Abdominal Adipose Tissue Subcompartments: Potential Role in Rosiglitazone Effects. *Obesity (Silver Spring)*. (Epub ahead of print).

Walsh, T.N., Noonan, N., Hollywood, D., Kelly, A., Keeling, N., and Hennessy, T.P. (1996). A comparison of multimodal therapy and surgery for esophageal adenocarcinoma. *N Engl J Med*. **335**, 462-467.

Wang, K.L., Wu, T.T., Choi, I.S., Wang, H., Resetkova, E., Correa, A.M., Hofstetter, W.L., Swisher, S.G., Ajani, J.A., Rashid, A., *et al.* (2007). Expression of epidermal growth factor

receptor in esophageal and esophagogastric junction adenocarcinomas: association with poor outcome. *Cancer*. **109**, 658-667.

Wang, M.Y., Zhou, Y.T., Newgard, C.B., and Unger, R.H. (1996). A novel leptin receptor isoform in rat. *FEBS Lett*. **392**, 87-90.

Wang, Y., Beydoun, M.A., Liang, L., Caballero, B., and Kumanyika, S.K. (2008). Will all Americans become overweight or obese? estimating the progression and cost of the US obesity epidemic. *Obesity (Silver Spring)*. **16**, 2323-2330.

Watanabe, S., Hojo, M., and Nagahara, A. (2007). Metabolic syndrome and gastrointestinal diseases. *J Gastroenterol*. **42**, 267-274.

Wei, L.H., Kuo, M.L., Chen, C.A., Chou, C.H., Lai, K.B., Lee, C.N., and Hsieh, C.Y. (2003). Interleukin-6 promotes cervical tumor growth by VEGF-dependent angiogenesis via a STAT3 pathway. *Oncogene*. **22**, 1517-1527.

Weisberg, S.P., Hunter, D., Huber, R., Lemieux, J., Slaymaker, S., Vaddi, K., Charo, I., Leibel, R.L., and Ferrante, A.W., Jr. (2006). CCR2 modulates inflammatory and metabolic effects of high-fat feeding. *J Clin Invest*. **116**, 115-124.

Weisberg, S.P., McCann, D., Desai, M., Rosenbaum, M., Leibel, R.L., and Ferrante, A.W., Jr. (2003). Obesity is associated with macrophage accumulation in adipose tissue. *J Clin Invest*. **112**, 1796-1808.

Wellen, K.E., and Hotamisligil, G.S. (2003). Obesity-induced inflammatory changes in adipose tissue. *J Clin Invest*. **112**, 1785-1788.

Wellen, K.E., and Hotamisligil, G.S. (2005). Inflammation, stress, and diabetes. *J Clin Invest*. **115**, 1111-1119.

Wetterau, L.A., Francis, M.J., Ma, L., and Cohen, P. (2003). Insulin-like growth factor I stimulates telomerase activity in prostate cancer cells. *J Clin Endocrinol Metab*. **88**, 3354-3359. Whibley, C., Pharoah, P.D., and Hollstein, M. (2009). p53 polymorphisms: cancer implications. *Nat Rev Cancer*. **9**, 95-107.

White, R.T., Damm, D., Hancock, N., Rosen, B.S., Lowell, B.B., Usher, P., Flier, J.S., and Spiegelman, B.M. (1992). Human adipsin is identical to complement factor D and is expressed at high levels in adipose tissue. *J Biol Chem*. **267**, 9210-9213.

WHO Global Infobase Team, (2005). The SuRF Report 2. Suveillance of chronic disease risk factors: country-level data and comparable estimates. (Geneva: WHO). (downloaded from https://apps.who.int/infobase/).

Wierzbowska, A., Urbanska-Rys, H., and Robak, T. (1999). Circulating IL-6-type cytokines and sIL-6R in patients with multiple myeloma. *Br J Haematol*. **105**, 412-419.

Wojcik, E., Jakubowicz, J., Skotnicki, P., Sas-Korczynska, B., and Kulpa, J.K. (2010). IL-6 and VEGF in small cell lung cancer patients. *Anticancer Res*. **30**, 1773-1778.

Wood, I.S., Hunter, L., and Trayhurn, P. (2003). Expression of Class III facilitative glucose transporter genes (GLUT-10 and GLUT-12) in mouse and human adipose tissues. *Biochem Biophys Res Commun*. **308**, 43-49.

Wu, H., Ghosh, S., Perrard, X.D., Feng, L., Garcia, G.E., Perrard, J.L., Sweeney, J.F., Peterson, L.E., Chan, L., Smith, C.W., *et al.* (2007). T-cell accumulation and regulated on activation, normal T cell expressed and secreted upregulation in adipose tissue in obesity. *Circulation*. **115**, 1029-1038.

Wu, Z.S., Wu, Q., Yang, J.H., Wang, H.Q., Ding, X.D., Yang, F., and Xu, X.C. (2008). Prognostic significance of MMP-9 and TIMP-1 serum and tissue expression in breast cancer. *Int J Cancer*. **122**, 2050-2056.

Xu, H., Barnes, G.T., Yang, Q., Tan, G., Yang, D., Chou, C.J., Sole, J., Nichols, A., Ross, J.S., Tartaglia, L.A., *et al.* (2003). Chronic inflammation in fat plays a crucial role in the development of obesity-related insulin resistance. *J Clin Invest*. **112**, 1821-1830.

Yamauchi, T., Kamon, J., Ito, Y., Tsuchida, A., Yokomizo, T., Kita, S., Sugiyama, T., Miyagishi, M., Hara, K., Tsunoda, M., *et al.* (2003). Cloning of adiponectin receptors that mediate antidiabetic metabolic effects. *Nature*. **423**, 762-769.

Yamauchi, T., Kamon, J., Waki, H., Terauchi, Y., Kubota, N., Hara, K., Mori, Y., Ide, T., Murakami, K., Tsuboyama-Kasaoka, N., *et al.* (2001). The fat-derived hormone adiponectin reverses insulin resistance associated with both lipoatrophy and obesity. *Nat Med*. **7**, 941-946.

Yang, G., Badeanlou, L., Bielawski, J., Roberts, A.J., Hannun, Y.A., and Samad, F. (2009a). Central role of ceramide biosynthesis in body weight regulation, energy metabolism, and the metabolic syndrome. *Am J Physiol Endocrinol Metab*. **297**, E211-224.

Yang, H., Gu, J., Wang, K.K., Zhang, W., Xing, J., Chen, Z., Ajani, J.A., and Wu, X. (2009b). MicroRNA expression signatures in Barrett's esophagus and esophageal adenocarcinoma. *Clin Cancer Res*. **15**, 5744-5752.

Yang, Q., Graham, T.E., Mody, N., Preitner, F., Peroni, O.D., Zabolotny, J.M., Kotani, K., Quadro, L., and Kahn, B.B. (2005). Serum retinol binding protein 4 contributes to insulin resistance in obesity and type 2 diabetes. *Nature*. **436**, 356-362.

Yin, L., Velazquez, O.C., and Liu, Z.J. (2010). Notch signaling: emerging molecular targets for cancer therapy. *Biochem Pharmacol*. **80**, 690-701.

Yoneda, K., Tomimoto, A., Endo, H., Iida, H., Sugiyama, M., Takahashi, H., Mawatari, H., Nozaki, Y., Fujita, K., Yoneda, M., *et al.* (2008). Expression of adiponectin receptors, AdipoR1 and AdipoR2, in normal colon epithelium and colon cancer tissue. *Oncol Rep*. **20**, 479-483.

Yu, W., Liu, J., Xiong, X., Ai, Y., and Wang, H. (2009). Expression of MMP9 and CD147 in invasive squamous cell carcinoma of the uterine cervix and their implication. *Pathol Res Pract*. **205**, 709-715.

Zabuawala, T., Taffany, D.A., Sharma, S.M., Merchant, A., Adair, B., Srinivasan, R., Rosol, T.J., Fernandez, S., Huang, K., Leone, G., *et al.* (2010). An ets2-driven transcriptional program in tumor-associated macrophages promotes tumor metastasis. *Cancer Res*. **70**, 1323-1333.

Zechner, R., Strauss, J., Frank, S., Wagner, E., Hofmann, W., Kratky, D., Hiden, M., and Levak-Frank, S. (2000). The role of lipoprotein lipase in adipose tissue development and metabolism. *Int J Obes Relat Metab Disord*. **24 Suppl 4**, S53-56.

Zhang, F., Basinski, M.B., Beals, J.M., Briggs, S.L., Churgay, L.M., Clawson, D.K., DiMarchi, R.D., Furman, T.C., Hale, J.E., Hsiung, H.M., *et al.* (1997). Crystal structure of the obese protein leptin-E100. *Nature*. **387**, 206-209.

Zhang, H.H., Kumar, S., Barnett, A.H., and Eggo, M.C. (2000). Ceiling culture of mature human adipocytes: use in studies of adipocyte functions. *J Endocrinol*. **164**, 119-128.

Zhang, K., Zhang, S., Jiao, X., Wang, H., Zhang, D., Niu, Z., Shen, Y., Lv, L., and Zhou, Y. (2010). Slug regulates proliferation and invasiveness of esophageal adenocarcinoma cells in vitro and in vivo. *Med Oncol*. (in press)

Zhang, X., Wang, Y., Yamamoto, G., and Tachikawa, T. (2009). Expression of matrix metalloproteinases MMP-2, MMP-9 and their tissue inhibitors TIMP-1 and TIMP-2 in the epithelium and stroma of salivary gland pleomorphic adenomas. *Histopathology*. **55**, 250-260.

Zhang, Y., Proenca, R., Maffei, M., Barone, M., Leopold, L., and Friedman, J.M. (1994). Positional cloning of the mouse obese gene and its human homologue. *Nature*. **372**, 425-432.

Zhao, J., and Guan, J.L. (2009). Signal transduction by focal adhesion kinase in cancer. *Cancer Metastasis Rev*. **28**, 35-49.

Zhou, Q.L., Jiang, Z.Y., Mabardy, A.S., Del Campo, C.M., Lambright, D.G., Holik, J., Fogarty, K.E., Straubhaar, J., Nicoloro, S., Chawla, A., *et al.* (2010). A novel Pleckstrin Homology domain containing protein enhances insulin-stimulated Akt phosphorylation and GLUT4 translocation in adipocytes. *J Biol Chem*. (in press).

Appendix I: Mycoplasma testing
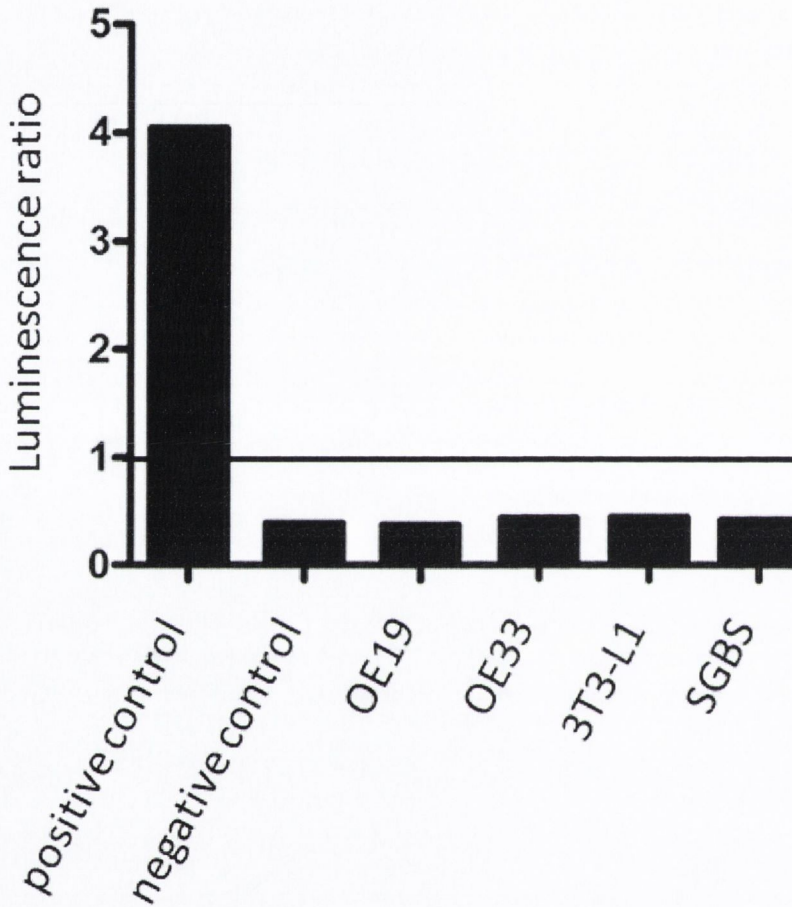
Mycoplasma testing of cell lines. Cell culture supernatants were collected from OE19, OE33, 3T3-L1 and SGBS cells lines on a regular basis, and tested for mycoplasma contamination. The presence of mycoplasma in the cells is determined by a luminescence ratio > 1. All cell lines were negative for the presence of mycoplasma throughout the course of this work.

Appendix II: Standard curves
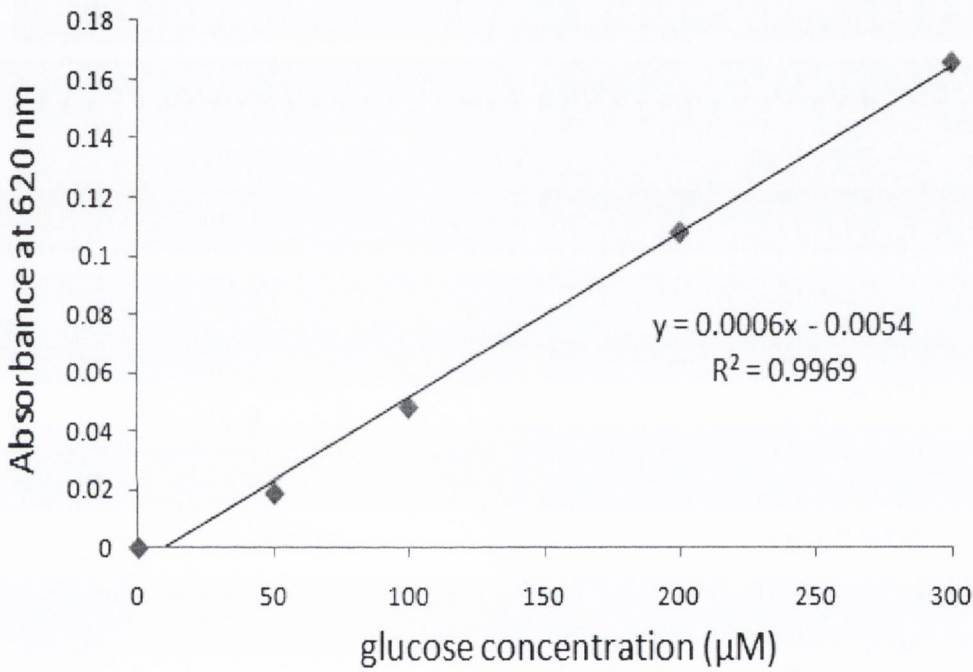
Representative standard curve from glucose assay. The glucose assay was used to measure glucose concentration in the supernatant of adipocytes as a functional assessment of differentiation. (R^2=regression coefficient)

List of analytes tested in adipose tissue conditioned medium (ACM) by Luminex ×Map technology (Millipore).

Human Cytokine panel	Human Adipokine panel
GM-CSF	Adiponectin
IFN-γ	Leptin
IL-10	HGF
IL-12 (p70)	PAI-1 (total)
IL-13	Resistin
IL-1β	IL-1β
IL-2	IL-6
IL-4	IL-8
IL-5	MCP-1
IL-6	TNFα
IL-7	NGF
IL-8	
MCP-1	
TNFα	

List of analytes tested in adipose tissue conditioned medium (ACM) and serum by Randox Evidence Investigator.

Analyte	Range (pg/ml)
IL-1α	0 – 500
IL-1β	0 – 250
IL-2	0 – 3000
IL-4	0 – 900
IL-6	0 – 900
IL-8	0 – 3000
IL-10	0 – 1000
IFNγ	0 – 1500
EGF	0 – 900
MCP-1	0 – 900
TNFα	0 – 1500
VEGF	0 – 3000
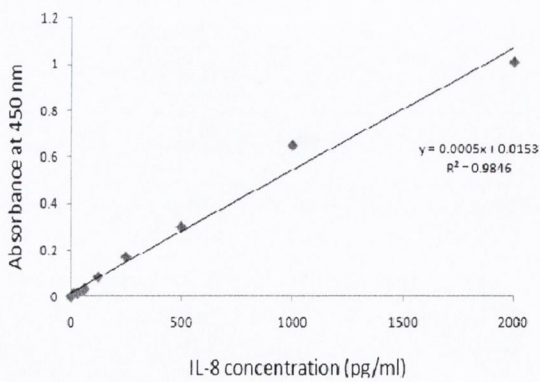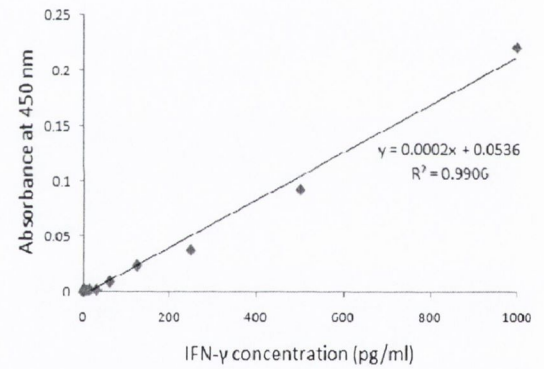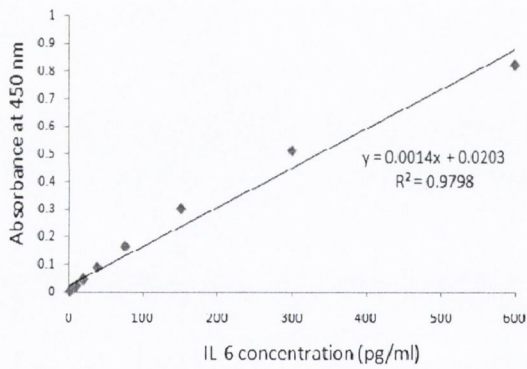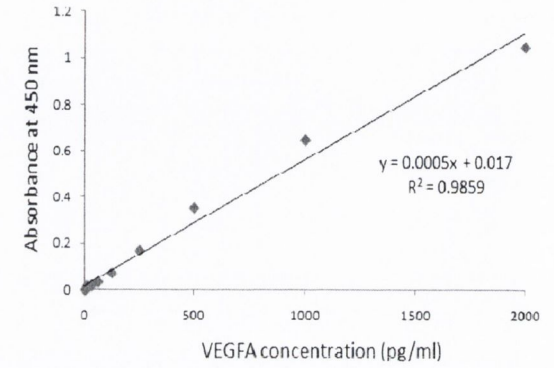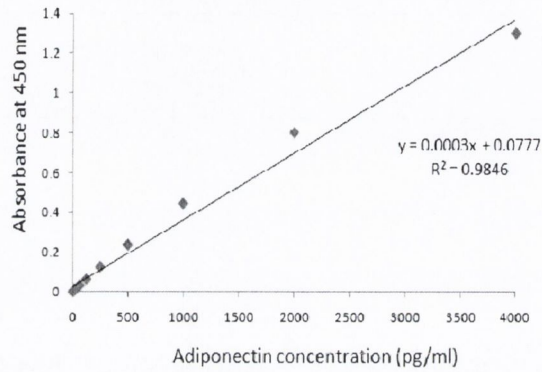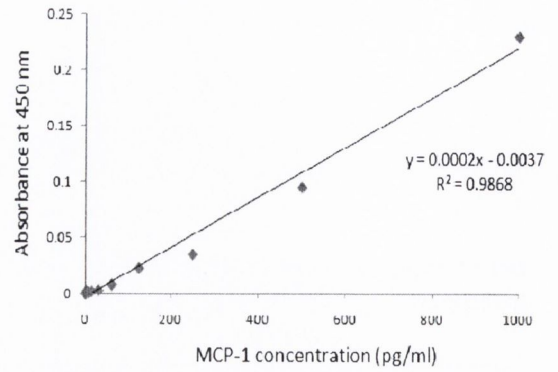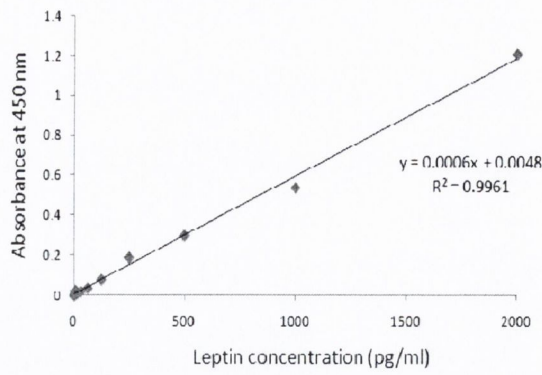
Representative standard curves for leptin, adiponectin, IL-6, IL-8, MCP-1, VEGFA and IFN-γ ELISAs. ELISAs were used to quantify cytokine, chemokine and adipokine levels present in adipose tissue conditioned medium (ACM) and serum. (R^2=regression coefficient)
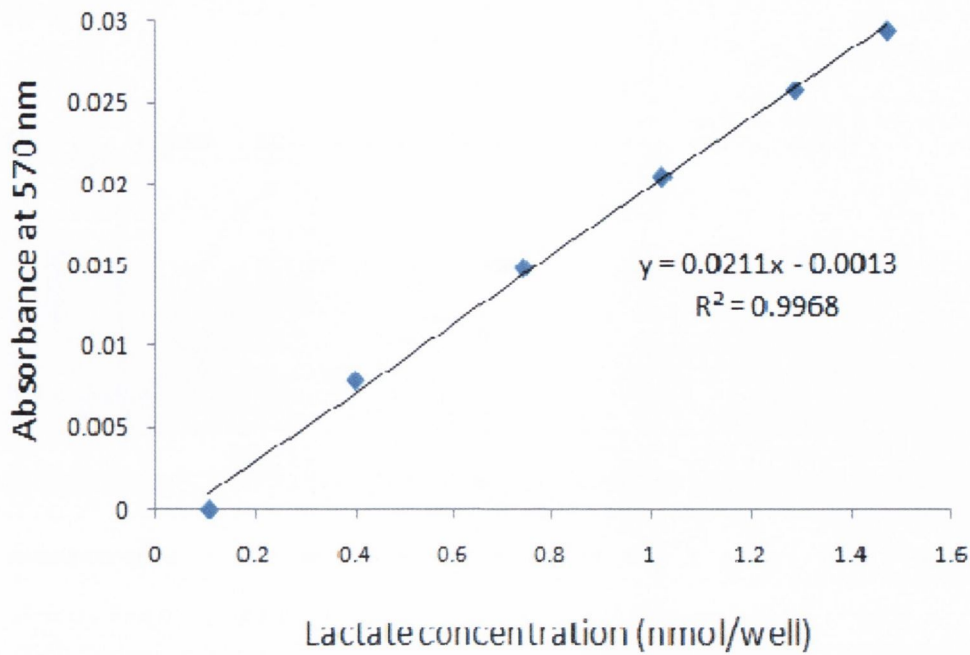
Representative standard curve for lactate assay. This assay was used to quantify levels of lactate, the end metabolite of glycolysis, in supernatant of OE33 tumour cells following co-culture with adipose tissue from viscerally obese and non obese patients. (R^2=regression coefficient)
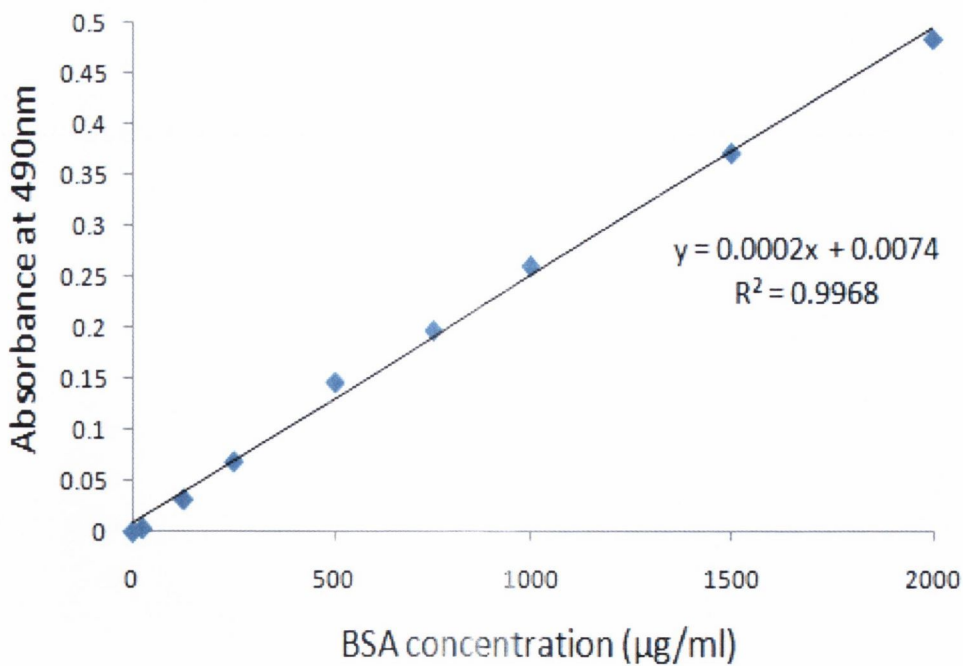
Representative standard curve of bovine serum albumin (BSA) from a BCA assay. The BCA assay was used to quantify protein levels in total cell protein lysates. (R^2=regression coefficient)

Appendix III: Densitometry

Protein densitometric analysis of OE33 and OE19 oesophageal adenocarcinoma (OAD) cell lines treated with adipose tissue from viscerally obese OAD patients (n=3) or control medium (n=3).
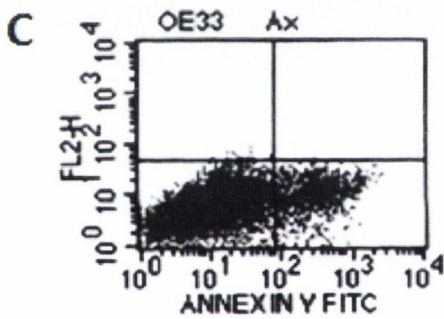
Protein	MW	OE33 control	OE33 adipose tissue	OE19 control	OE19 adipose tissue
MMP9	83 kDa	0.219 ± 0.202	0.381 ± 0.051	0.294 ± 0.131	0.423 ± 0.112
	92 kDa	0.127 ± 0.117	0.307 ± 0.082 *	0.206 ± 0.097	0.283 ± 0.071
p53	53 kDa	0.533 ± 0.190	0.280 ± 0.170	-	-
FAK	125 kDa	0.533 ± 0.034	0.762 ± 0.066 *	0.859 ± 0.044	1.000 ± 0.082
	100 kDa	0.408 ± 0.158	0.079 ± 0.018 *	0.145 ± 0.094	0.074 ± 0.017
	85 kDa	0.640 ± 0.107	0.223 ± 0.024 *	0.224 ± 0.060	0.111 ± 0.029 *
Src	60 kDa	0.069 ± 0.009	0.134 ± 0.040	0.488 ± 0.270	0.918 ± 0.114
LAMC2	150 kDa	0.500 ± 0.096	0.845 ± 0.151	0.074 ± 0.036	0.864 ± 0.096 *

Target protein mRNA expression was normalised to β-actin control, and expressed as a ratio of target protein expression: β-actin expression. Statistical analysis was carried out by a paired 2 tailed student t test. Data are expressed as mean ± SEM and is representative of three independent replicates. (*$p<0.05$ adipose tissue *vs.* control; up regulated, down regulated)
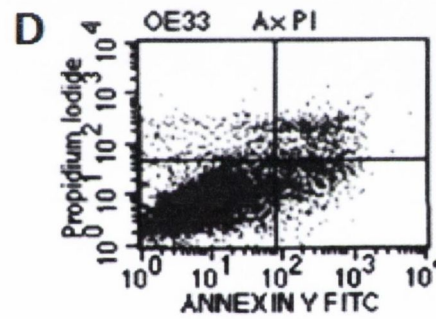
Appendix IV: Flow cytometry dot plots and histograms

A OE33 NS

SSC-H, FSC-H

B OE33 PI

FL2-H, FL1-H
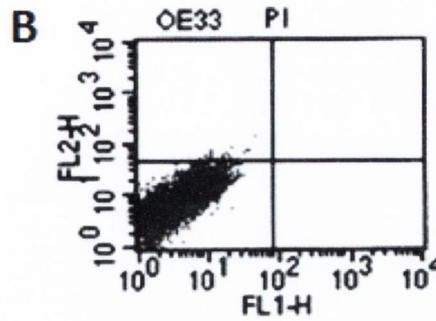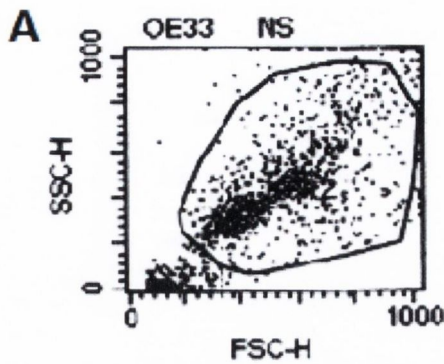
Quad	% Gated	% Total
UL	0.23	0.16
UR	0.00	0.00
LL	99.77	67.16
LR	0.00	0.00

C OE33 Ax

FL2-H, ANNEXIN V FITC

D OE33 Ax PI

Propidium Iodide, ANNEXIN V FITC

Quad	% Gated	% Total
UL	0.17	0.11
UR	0.01	0.01
LL	88.59	58.22
LR	11.23	7.38

Quad	% Gated	% Total
UL	3.95	2.53
UR	4.31	2.76
LL	85.96	55.08
LR	5.79	3.71

E OE33 M199

Propidium Iodide, ANNEXIN V FITC

F OE33 ACM

Propidium Iodide, ANNEXIN V FITC
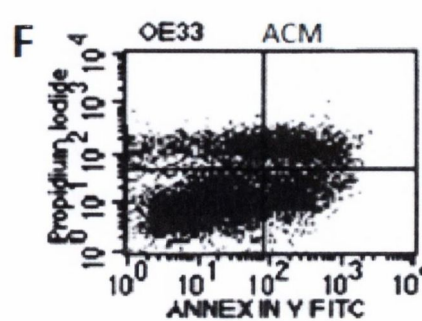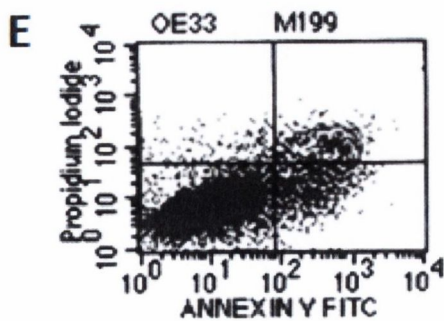
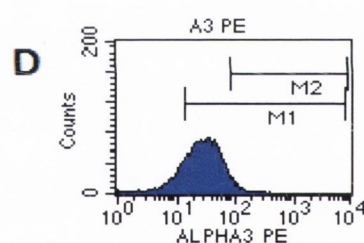Representative dot plots from flow cytometry apoptosis assay. A scatterplot shows the cells taken for analysis (A), propidium iodide (PI) positive control cells (B), annexin V (Ax) positive control cells (C), PI and Ax double positive control cells (D), control M199 medium treated cells (E), adipose tissue conditioned medium (ACM) treated cells (F).

Representative histogram from flow cytometry data measuring integrin alpha subunit expression in OE33. A scatterplot shows the cells taken for analysis (A), staining for isotype controls adjusts for background staining (B: IgG1, C: IgG2a), staining for ITGA3 (isotype IgG1) (D), staining for ITGA5 (isotype IgG1) (E), staining for ITGA6 (isotype IgG2a) (F).

Appendix V: qPCR and Affymetrix array information

Taqman endogenous control qPCR array

Gene symbol	Gene name	Assay ID
18S	Eukaryotic 18S rRNA	Hs99999901_s1
GAPDH	glyceraldehyde-3-phosphate dehydrogenase	Hs99999905_m1
HPRT1	hypoxanthine phosphoribosyltransferase 1 (Lesch-Nyhan syndrome)	Hs99999909_m1
GUSB	glucuronidase, beta	Hs99999908_m1
ACTB	actin, beta	Hs99999903_m1
B2M	beta-2-microglobulin	Hs99999907_m1
HMBS	hydroxymethylbilane synthase	Hs00609297_m1
IPO8	importin 8	Hs00183533_m1
PGK1	phosphoglycerate kinase 1	Hs99999906_m1
RPLP0	ribosomal protein, large, P0	Hs99999902_m1
TBP	TATA box binding protein	Hs99999910_m1
TFRC	transferrin receptor (p90, CD71)	Hs99999911_m1
UBC	ubiquitin C	Hs00824723_m1
YWHAZ	tyrosine 3-monooxygenase/tryptophan 5-monooxygenase activation protein, zeta polypeptide	Hs00237047_m1
PPIA	peptidylprolyl isomerase A (cyclophilin A)	Hs99999904_m1
POLR2A	polymerase (RNA) II (DNA directed) polypeptide A, 220kDa	Hs00172187_m1
CASC3	cancer susceptibility candidate 3	Hs00201226_m1
CDKN1A	cyclin-dependent kinase inhibitor 1A (p21, Cip1)	Hs00355782_m1
CDKN1B	cyclin-dependent kinase inhibitor 1B (p27, Kip1)	Hs00153277_m1
GADD45A	growth arrest and DNA-damage-inducible, alpha	Hs00169255_m1
PUM1	pumilio homolog 1 (Drosophila)	Hs00206469_m1
PSMC4	proteasome (prosome, macropain) 26S subunit, ATPase, 4	Hs00197826_m1
EIF2B1	eukaryotic translation initiation factor 2B, subunit 1 alpha, 26kDa	Hs00426752_m1
PES1	pescadillo homolog 1, containing BRCT domain (zebrafish)	Hs00362795_g1
ABL1	v-abl Abelson murine leukemia viral oncogene homolog 1	Hs00245445_m1
ELF1	E74-like factor 1 (ets domain transcription factor)	Hs00152844_m1
MT-ATP6	mitchondrially encoded ATP synthase 6	Hs02596862_g1
MRPL19	mitochondrial ribosomal protein L19	Hs00608519_m1
POP4	processing of precursor 4, ribonuclease P/MRP subunit (S. cerevisiae)	Hs00198357_m1
RPL37A	ribosomal protein L37a	Hs01102345_m1
RPL30	ribosomal protein L30	Hs00265497_m1
RPS17	ribosomal protein S17	Hs00734303_g1

Gene list on Human Cancer Profiler qPCR Array plates (SABiosciences)

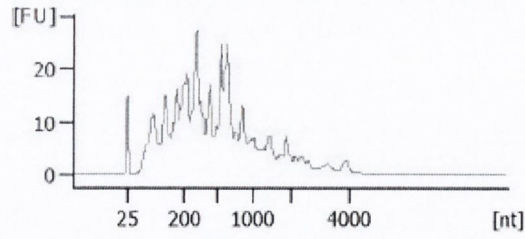| Position	UniGene	RefSeq	Symbol	Description	Gene Name
A01	Hs.525622	NM_005163	AKT1	V-akt murine thymoma viral oncogene homolog 1	AKT/PKB
A02	Hs.369675	NM_001146	ANGPT1	Angiopoietin 1	AGPT/AGPT
A03	Hs.553484	NM_001147	ANGPT2	Angiopoietin 2	AGPT2/ANG2
A04	Hs.552567	NM_001160	APAF1	Apoptotic peptidase activating factor 1	CED4
A05	Hs.367437	NM_000051	ATM	Ataxia telangiectasia mutated (includes complementation groups A, C and D)	AT1/ATA
A06	Hs.370254	NM_004322	BAD	BCL2-antagonist of cell death	BBC2/BCL2L8
A07	Hs.159428	NM_004324	BAX	BCL2-associated X protein	Bax zeta
A08	Hs.150749	NM_000633	BCL2	B-cell CLL/lymphoma 2	Bcl-2
A09	Hs.516966	NM_138578	BCL2L1	BCL2-like 1	BCL-XL/S
A10	Hs.194143	NM_007294	BRCA1	Breast cancer 1, early onset	BRCAI/BRCC1
A11	Hs.591630	NM_001228	CASP8	Caspase 8, apoptosis-related cysteine peptidase	CAP4/FLICE
A12	Hs.244723	NM_001238	CCNE1	Cyclin E1	CCNE
B01	Hs.437705	NM_001789	CDC25A	Cell division cycle 25 homolog A (S. pombe)	CDC25A2
B02	Hs.19192	NM_001798	CDK2	Cyclin-dependent kinase 2	p33(CDK2)
B03	Hs.95577	NM_000075	CDK4	Cyclin-dependent kinase 4	CMM3/PSK-J3
B04	Hs.370771	NM_000389	CDKN1A	Cyclin-dependent kinase inhibitor 1A (p21, Cip1)	CAP20/CDKN1
B05	Hs.512599	NM_000077	CDKN2A	Cyclin-dependent kinase inhibitor 2A (melanoma, p16, inhibits CDK4)	ARF/CDK4I
B06	Hs.390736	NM_003879	CFLAR	CASP8 and FADD-like apoptosis regulator	CASH/CASP8AP1
B07	Hs.291363	NM_007194	CHEK2	CHK2 checkpoint homolog (S. pombe)	CDS1/CHK2
B08	Hs.517356	NM_030582	COL18A1	Collagen, type XVIII, alpha 1	KNO
B09	Hs.96055	NM_005225	E2F1	E2F transcription factor 1	E2F-1/RBBP3
B10	Hs.446352	NM_004448	ERBB2	V-erb-b2 erythroblastic leukemia viral oncogene homolog 2, neuro/glioblastoma derived oncogene homolog (avian)	HER-2/HER-2
B11	Hs.652288	NM_005239	ETS2	V-Ets erythroblastosis virus E26 oncogene homolog 2 (avian)	c-Ets2
B12	Hs.244139	NM_000043	FAS	Fas (TNF receptor superfamily, member 6)	ALPS1A/APO-1
C01	Hs.533683	NM_000141	FGFR2	Fibroblast growth factor receptor 2 (bacteria-expressed kinase, keratinocyte growth factor receptor, craniofacial dysostosis 1, Crouzon syndrome, Pfeiffer syndrome, Jackson-Weiss syndrome)	BEK/BFR-1
C02	Hs.25647	NM_005252	FOS	V-fos FBJ murine osteosarcoma viral oncogene homolog	c-fos
C03	Hs.90708	NM_006144	GZMA	Granzyme A (granzyme 1, cytotoxic T-lymphocyte-associated serine esterase 3)	CTLA3/HFSP
C04	Hs.90753	NM_006410	HTATIP2	HIV-1 Tat interactive protein 2, 30kDa	CC3/TIP30
C05	Hs.37026	NM_024013	IFNA1	Interferon, alpha 1	IFL/IFN
C06	Hs.93177	NM_002176	IFNB1	Interferon, beta 1, fibroblast	IFB/IFF
C07	Hs.160562	NM_000618	IGF1	Insulin-like growth factor 1 (somatomedin C)	IGFI
C08	Hs.624	NM_000584	IL8	Interleukin 8	3-10C/AMCF-I
C09	Hs.652204	NM_181501	ITGA1	Integrin, alpha 1	CD49a/VLA1
C10	Hs.482077	NM_002203	ITGA2	Integrin, alpha 2 (CD49B, alpha 2 subunit of VLA-2 receptor)	BR/CD49B
C11	Hs.265829	NM_002204	ITGA3	Integrin, alpha 3 (antigen CD49C, alpha 3 subunit of VLA-3 receptor)	CD49C/GAP-B3
C12	Hs.440955	NM_000885	ITGA4	Integrin, alpha 4 (antigen CD49D, alpha 4 subunit of VLA-4 receptor)	CD49D/IA4
D01	Hs.436873	NM_002210	ITGAV	Integrin, alpha V (vitronectin receptor, alpha polypeptide, antigen CD51)	CD51/MSK8
D02	Hs.643813	NM_002211	ITGB1	Integrin, beta 1 (fibronectin receptor, beta polypeptide, antigen CD29 includes MDF2, MSK12)	CD29/FNRB
D03	Hs.218040	NM_000212	ITGB3	Integrin, beta 3 (platelet glycoprotein IIIa, antigen CD61)	CD61/GP3A
D04	Hs.536663	NM_002213	ITGB5	Integrin, beta 5	FLJ26658
D05	Hs.525704	NM_002228	JUN	Jun oncogene	AP1/c-Jun
D06	Hs.145442	NM_002755	MAP2K1	Mitogen-activated protein kinase kinase 1	MAPKK1/MEK1
D07	Hs.599039	NM_006500	MCAM	Melanoma cell adhesion molecule	CD146/MUC18
D08	Hs.567303	NM_002392	MDM2	Mdm2, transformed 3T3 cell double minute 2, p53 binding protein (mouse)	HDMX/hdm2
D09	Hs.132966	NM_000245	MET	Met proto-oncogene (hepatocyte growth factor receptor)	HGFR/RCCP2
D10	Hs.83169	NM_002421	MMP1	Matrix metallopeptidase 1 (interstitial collagenase)	CLG/CLGN
D11	Hs.513617	NM_004530	MMP2	Matrix metallopeptidase 2 (gelatinase A, 72kDa gelatinase, 72kDa type IV collagenase)	CLG4/CLG4A
D12	Hs.297413	NM_004994	MMP9	Matrix metallopeptidase 9 (gelatinase B, 92kDa gelatinase, 92kDa type IV collagenase)	CLG4B/GELB
E01	Hs.525629	NM_004689	MTA1	Metastasis associated 1	Mta-1
E02	Hs.173043	NM_004739	MTA2	Metastasis associated 1 family, member 2	DKFZp686F2281/MTA1L1
E03	Hs.336994	NM_014751	MTSS1	Metastasis suppressor 1	MIM/MIMA
E04	Hs.202453	NM_002467	MYC	V-myc myelocytomatosis viral oncogene homolog (avian)	c-Myc
E05	Hs.431926	NM_003998	NFKB1	Nuclear factor of kappa light polypeptide gene enhancer in B-cells 1 (p105)	DKFZp686C01211/EBP-1
E06	Hs.81328	NM_020529	NFKBIA	Nuclear factor of kappa light polypeptide gene enhancer in B-cells inhibitor,	IKBA/MAD-3
E07	Hs.118638	NM_000269	NME1	Non-metastatic cells 1, protein (NM23A) expressed in	AWD/GAAD
E08	Hs.9235	NM_005009	NME4	Non-metastatic cells 4, protein expressed in	NM23H4/nm23-H4
E09	Hs.645488	NM_002607	PDGFA	Platelet-derived growth factor alpha polypeptide	PDGF-A/PDGF1
E10	Hs.1976	NM_002608	PDGFB	Platelet-derived growth factor beta polypeptide (simian sarcoma viral (v-sis) oncogene homolog)	PDGF2/SIS
E11	Hs.132225	NM_181504	PIK3R1	Phosphoinositide-3-kinase, regulatory subunit 1 (p85 alpha)	GRB1/p85-ALPHA
E12	Hs.77274	NM_002658	PLAU	Plasminogen activator, urokinase	ATF/UPA
F01	Hs.466871	NM_002659	PLAUR	Plasminogen activator, urokinase receptor	CD87/UPAR
F02	Hs.409965	NM_002687	PNN	Pinin, desmosome associated protein	DRS/SDK3
F03	Hs.159130	NM_002880	RAF1	V-raf-1 murine leukemia viral oncogene homolog 1	CRAF/Raf-1
F04	Hs.408528	NM_000321	RB1	Retinoblastoma 1 (including osteosarcoma)	OSRC/RB
F05	Hs.81256	NM_002961	S100A4	S100 calcium binding protein A4	18A2/42A
F06	Hs.55279	NM_002639	SERPINB5	Serpin peptidase inhibitor, clade B (ovalbumin), member 5	PI5/maspin
F07	Hs.414795	NM_000602	SERPINE1	Serpin peptidase inhibitor, clade E (nexin, plasminogen activator inhibitor type 1), member 1	PAI/PAI-1
F08	Hs.349470	NM_003087	SNCG	Synuclein, gamma (breast cancer-specific protein 1)	BCSG1/SR
F09	Hs.371720	NM_003177	SYK	Spleen tyrosine kinase	Syk
F10	Hs.89640	NM_000459	TEK	TEK tyrosine kinase, endothelial (venous malformations, multiple cutaneous and mucosal)	CD202B/TIE-2
F11	Hs.492203	NM_198253	TERT	Telomerase reverse transcriptase	EST2/TCS1
F12	Hs.645227	NM_000660	TGFB1	Transforming growth factor, beta 1	CED/DPD1
G01	Hs.494622	NM_004612	TGFBR1	Transforming growth factor, beta receptor I (activin A receptor type II-like kinase, 53kDa)	AAT5/ACVRLK4
G02	Hs.164226	NM_003246	THBS1	Thrombospondin 1	THBS/TSP
G03	Hs.522632	NM_003254	TIMP1	TIMP metallopeptidase inhibitor 1	CLGI/EPA
G04	Hs.644633	NM_000362	TIMP3	TIMP metallopeptidase inhibitor 3 (Sorsby fundus dystrophy, pseudoinflammatory)	HSMRK222/K222
G05	Hs.241570	NM_000594	TNF	Tumor necrosis factor (TNF superfamily, member 2)	DIF/TNF-alpha
G06	Hs.521456	NM_003842	TNFRSF10B	Tumor necrosis factor receptor superfamily, member 10b	CD262/DR5
G07	Hs.279594	NM_001065	TNFRSF1A	Tumor necrosis factor receptor superfamily, member 1A	CD120a/FPF
G08	Hs.462529	NM_003790	TNFRSF25	Tumor necrosis factor receptor superfamily, member 25	APO-3/DDR3
G09	Hs.408312	NM_000546	TP53	Tumor protein p53 (Li-Fraumeni syndrome)	LFS1/TRP53
G10	Hs.66744	NM_000474	TWIST1	Twist homolog 1 (acrocephalosyndactyly 3; Saethre-Chotzen syndrome) (Drosophila)	ACS3/BPES2
G11	Hs.563491	NM_017068	EPDR1	Ependymin related protein 1 (zebrafish)	EPDR/MERP-1
G12	Hs.73793	NM_003376	VEGFA	Vascular endothelial growth factor A	VEGF/VEGF-A
H01	Hs.534255	NM_004048	B2M	Beta-2-microglobulin	B2M
H02	Hs.412707	NM_000194	HPRT1	Hypoxanthine phosphoribosyltransferase 1 (Lesch-Nyhan syndrome)	HGPRT/HPRT
H03	Hs.546356	NM_012423	RPL13A	Ribosomal protein L13a	RPL13A
H04	Hs.544577	NM_002046	GAPDH	Glyceraldehyde-3-phosphate dehydrogenase	G3PD/GAPD
H05	Hs.520640	NM_001101	ACTB	Actin, beta	PS1TP5BP1
H06	N/A	SA_00105	HGDC	Human Genomic DNA Contamination	HIGX1A
H07	N/A	SA_00104	RTC	Reverse Transcription Control	RTC
H08	N/A	SA_00104	RTC	Reverse Transcription Control	RTC
H09	N/A	SA_00104	RTC	Reverse Transcription Control	RTC
H10	N/A	SA_00103	PPC	Positive PCR Control	PPC
H11	N/A	SA_00103	PPC	Positive PCR Control	PPC
H12	N/A	SA_00103	PPC	Positive PCR Control	PPC

RNA quantity and purity (measured by nanodrop) and integrity (measured by Agilent Bioanalyser) of whole adipose tissue samples for Affymetrix microarrays. All samples had 260/280 purity ratio > 2, a 260/230 ratio > 1.7, and an RNA integrity number (RIN) > 6.7.

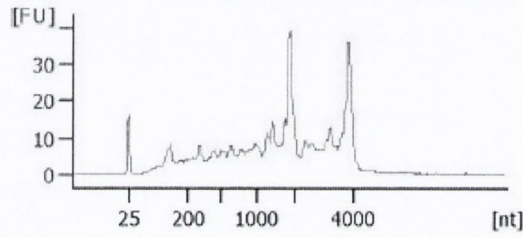| obese	sample	chip number	ng/ul	260/280	260/230	RIN
patient 1	whole adipose tissue	100837-01_1	135.4	2.12	1.87	7.6
patient 2	whole adipose tissue	100837-01_29	170.8	2.07	1.71	7
patient 3	whole adipose tissue	100837-03_3	100.1	2.11	1.87	8.2
patient 4	whole adipose tissue	100837-31_31	226.9	2.1	2.2	6.7
patient 5	whole adipose tissue	100837-05_5	124.7	2.06	1.75	8.1
patient 6	whole adipose tissue	100837-06_6	147.6	2.03	1.96	8.1
non obese						
patient 7	whole adipose tissue	100837-07_7	295.6	2.07	2.18	8.2
patient 8	whole adipose tissue	100837-08_8	210.9	2.09	2.1	8.6
patient 9	whole adipose tissue	100837-09_9	139.7	2.07	2.12	7.9
patient 10	whole adipose tissue	100837-10_10	292.5	2.07	2.11	8.3
patient 11	whole adipose tissue	100837-11_11	121.4	2.07	2.11	8.6
patient 12	whole adipose tissue	100837-12_12	131.6	2.08	2.12	7.8

RNA quantity and purity (measured by nanodrop) and integrity (measured by Agilent Bioanalyser) of co-cultured OE33 samples for Affymetrix microarrays. All samples had 260/280 purity ratio > 2, a 260/230 ratio > 1.7, and an RNA integrity number (RIN) > 6.7.

|	co-culture sample	chip number	ng/ul	260/280	260/230	RIN
patient 1	whole adipose tissue	100837-13_13	38.9	1.82	1.25	10
	adipocyte	100837-14_14	34.7	1.67	0.43	10
patient 2	whole adipose tissue	100837-15_15	66.3	1.98	1.15	10
	adipocyte	100837-16_16	26.2	1.89	0.44	10
patient 3	whole adipose tissue	100837-17_17	43	1.81	0.92	10
	adipocyte	100837-18_18	21.1	1.65	0.84	8.9
patient 4	whole adipose tissue	100837-19_19	55.1	1.67	0.64	9.3
	adipocyte	100837-20_20	52.7	1.72	1.34	10
patient 5	whole adipose tissue	100837-21_21	104.8	2.1	2.06	9.7
	adipocyte	100837-22_22	85.8	2.11	2.03	10
patient 6	whole adipose tissue	100837-23_23	71.8	2.05	1.84	10
	adipocyte	100837-32_32	60.5	2.13	2.11	9.9
	control media	100837-25_25	57.4	2.12	2.05	10
	control media	100837-34_34	65	2.04	0.83	9.9
	control media	100837-27_27	43.2	1.78	1.34	9.8
	control media	100837-28_28	42.9	1.77	1.62	10
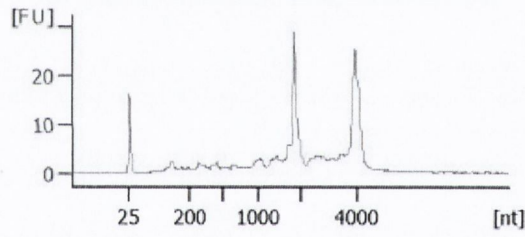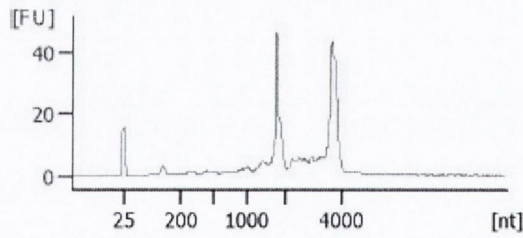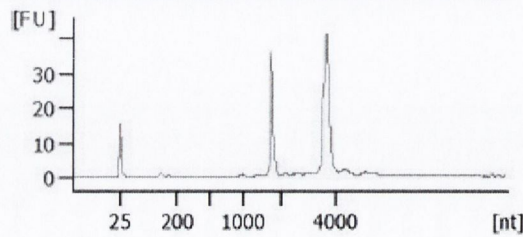
Electrophoretic trace diagrams of representative RNA samples showing RNA integrity. Only RNA samples with RIN > 6.7 were used on Affymetrix microarrays.
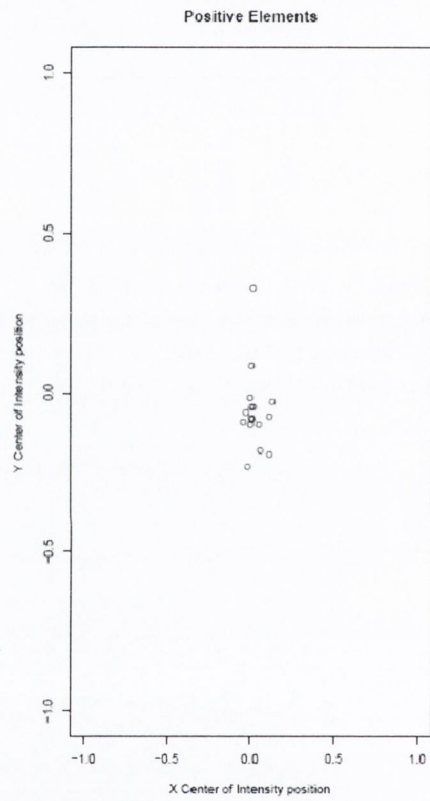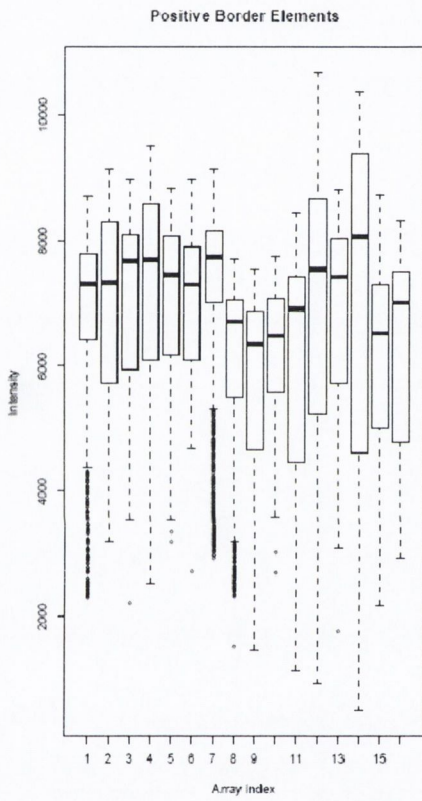
290
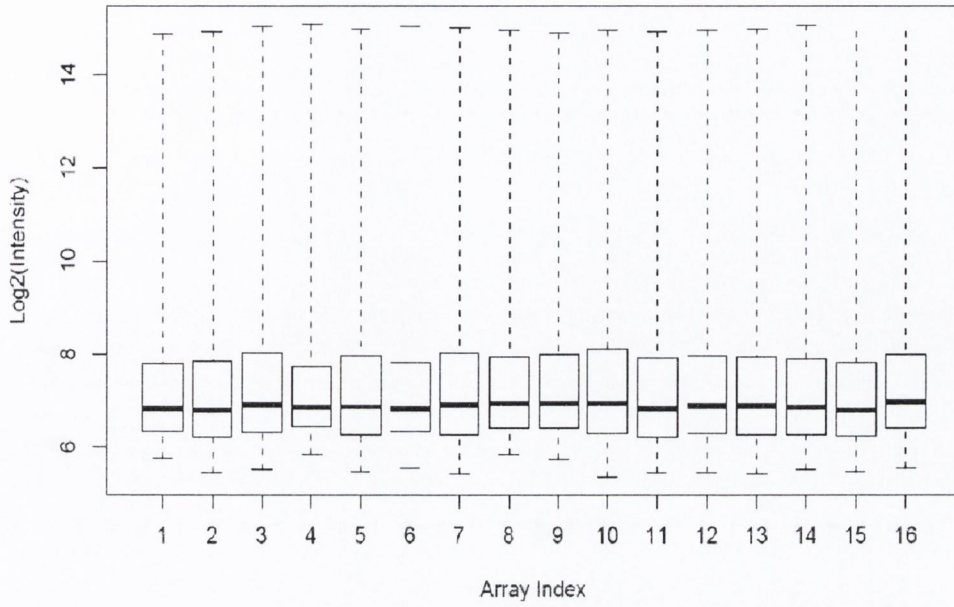
Overall signal intensity using calculated using predefined scripts and flexible programming with the R software environment for statistical computing and was found to be similar between microarrays (OE33 following co-culture with whole adipose tissue (samples 1 to 6), OE33 following co-culture with adipocytes (samples 7 to 12) and OE33 following culture with medium alone (samples 13 to 16)).
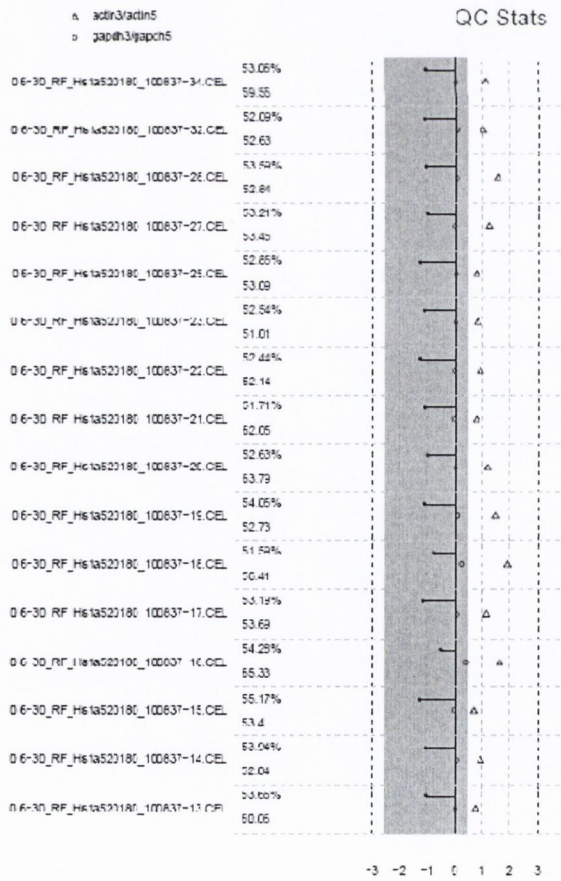

Internal control genes actin and GAPDH were measured using 3' and 5' probe sets, the ratio 3'/5' of each gene was calculated using predefined scripts and flexible programming with the R software environment for statistical computing and all arrays were found be fall within standard range.

Positive Border Elements

Positive Elements

Positive border elements for all arrays were measured using predefined scripts and flexible programming with the R software environment for statistical computing and found to fall within standard range.
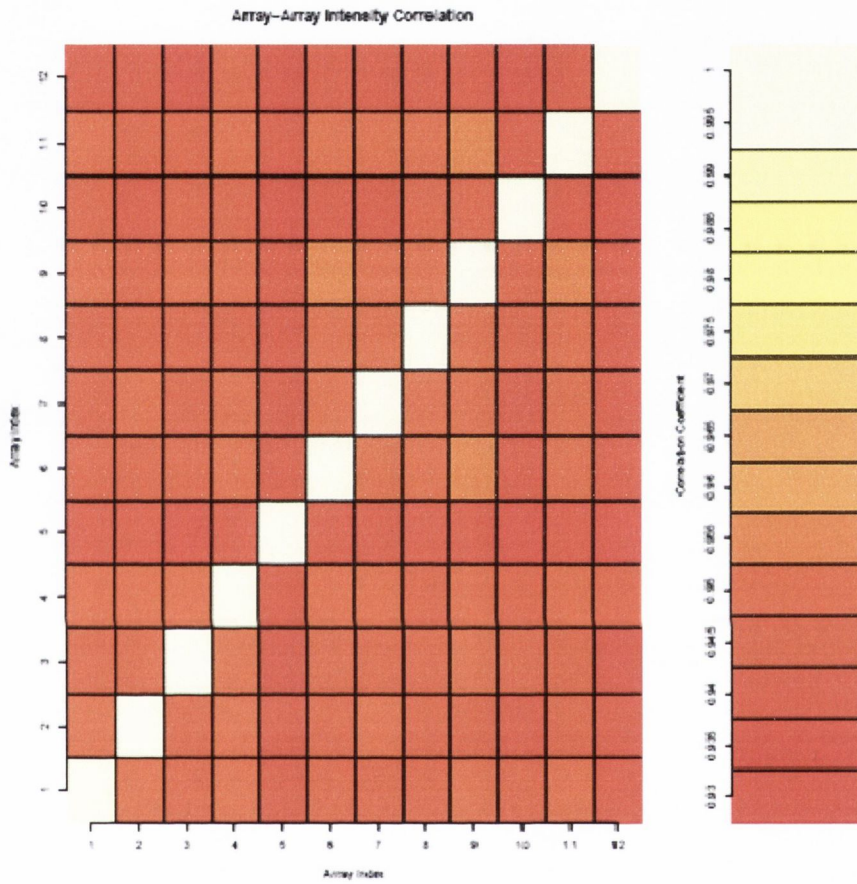
Correlation analysis between Affymetrix arrays examining whole adipose tissue from viscerally obese (Array Index 1 – 6) and non obese patients (Array Index 7 – 12) identified no outlier microarrays. All samples were therefore included in analysis.
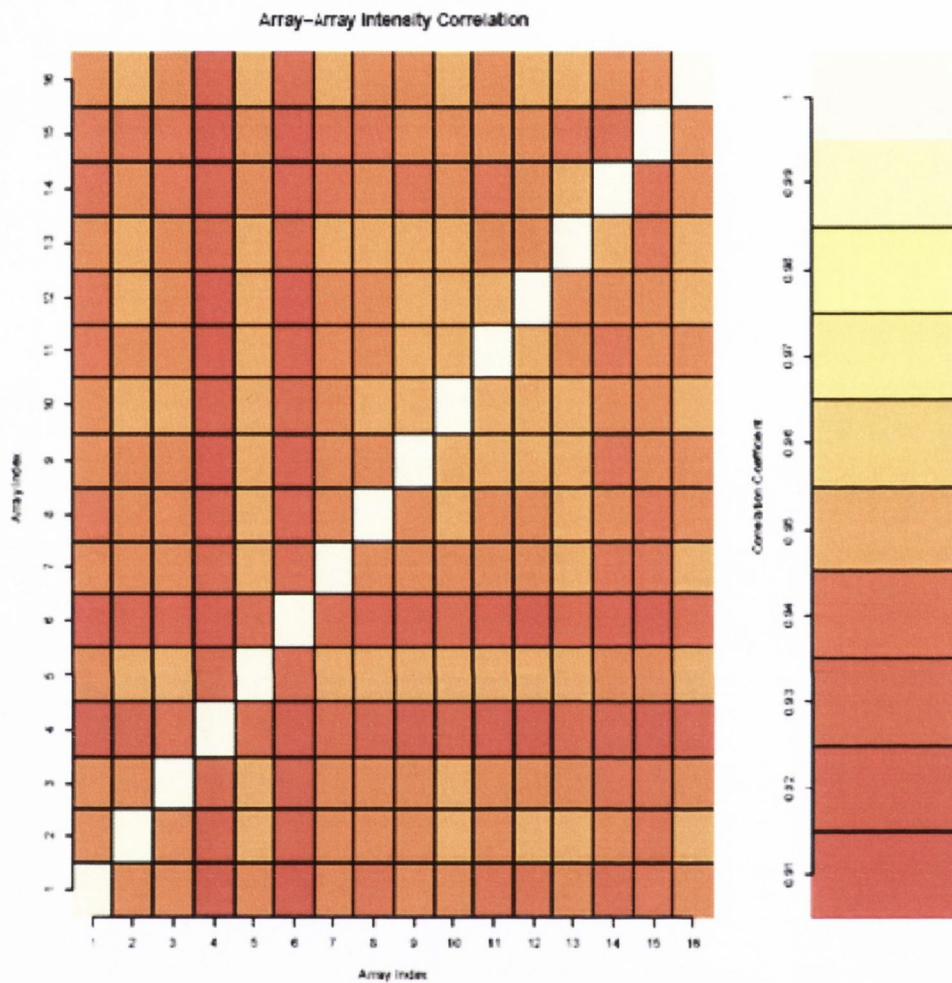
Correlation analysis between Affymetrix arrays examining OE33 oesophageal adenocarcinoma following co-culture with whole adipose tissue from viscerally obese OAD patients (Array Index 1 – 6), with adipocytes from matched patients (Array Index 7 – 12) and with control medium (Array Index 13 – 16). No outlier microarrays were identified and all samples were therefore included in analysis.